Volume 2, Number 1
January-February, 1961

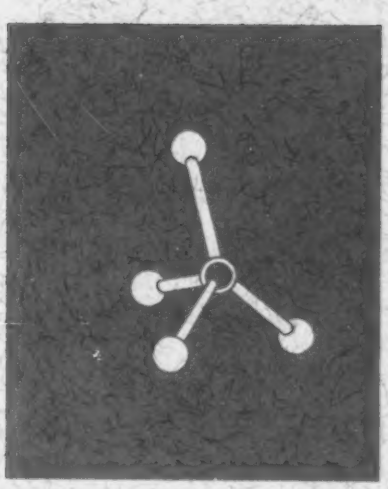

JOURNAL OF
STRUCTURAL CHEMISTRY

ЖУРНАЛ СТРУКТУРНОЙ ХИМИИ / ZHURNAL STRUKTURNOI KHIMII

TRANSLATED FROM RUSSIAN (c/b) CONSULTANTS BUREAU

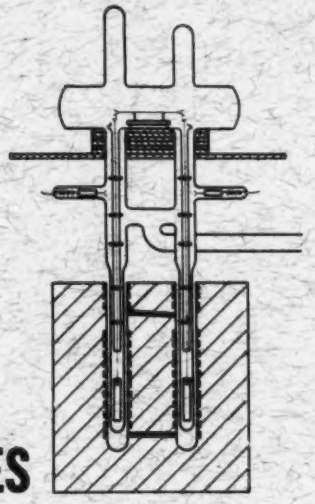

VOLUME I

VACUUM MICROBALANCE TECHNIQUES

Proceedings of the 1960 Conference Sponsored by
The Institute for Exploratory Research
U. S. Army Signal Research and Development Laboratory

Edited by
M. J. KATZ
U. S. Army Signal Research and Development Laboratory
Fort Monmouth, New Jersey

Introduction by
Thor N. Rhodin
Cornell University

The proceedings of this conference provide an authoritative introduction to the rapidly widening scope of microbalance methods which is not available elsewhere in a single publication.

The usefulness of microbalance techniques in the study of the properties of materials lies in their extreme sensitivity and versatility. This renders them particularly important in studies of properties of condensed systems. In addition to the historical use of microbalance techniques as a tool of microchemistry, they have, in recent years, found extensive application in the fields of metallurgy, physics, and chemistry. The uniqueness of the method results from the facility it provides in making a series of precise measurements of high sensitivity under carefully controlled conditions over a wide range of temperature and pressure.

This significant new volume contains papers in three major categories. The first group of reports deals with the general structural features and measuring capabilities of microbalances. In the second group, a sophisticated consideration and much needed evaluation of sources of spurious mass changes associated with microbalances is presented. The third group describes some of the most recent extensions in microbalance work to new research areas such as semiconductors, ultra-high vacuum, and high temperatures. These papers provide an interesting account of advances in the application of the microgravimetric method to three new and important fields of research on the behavior of materials.

170 pages **$6.50**

PLENUM PRESS, INC. 227 West 17th St., New York 11, N. Y.

ZHURNAL STRUKTURNOI KHIMII
EDITORIAL BOARD:

S. S. Batsanov *(Secretary)*
G. B. Bokii *(Editor)*
A. V. Nikolaev *(Acting Editor)*
B. V. Ptitsyn
O. Ya. Samoilov
Yu. T. Struchkov
Ya. K. Syrkin
V. V. Voevodskii
M. V. Vol'kenshtein

JOURNAL OF

STRUCTURAL CHEMISTRY

A translation of ZHURNAL STRUKTURNOI KHIMII,

a publication of the Academy of Sciences of the USSR

© 1961 CONSULTANTS BUREAU ENTERPRISES, INC.
227 West 17th Street, New York 11, N. Y.

Volume 2, Number 1 January-February, 1961

CONTENTS

	PAGE ENG.	PAGE RUSS.
Electron Diffraction Study of the Molecular Structure of ScF_3 in the Vapor State and Estimation of Scandium–Halogen Interactomic Distances in $ScCl_3$, $ScBr_3$, and ScI_3 Molecules. P. A. Akishin and V. A. Naumov	1	3
Structure of the Hydration Shell of the Co^{2+} Ion In Aqueous Solutions. S. N. Andreev, V. G. Khaldin, and E. V. Stroganov	4	7
Influence of Fluctuations on the Dielectric Properties of Solutions in Super-High Frequency Electromagnetic Fields. R. M. Kasimov, M. I. Shakhparonov, and A. Yu. Akhadov	9	13
Similarities and Differences of Crystal Structure of Internal Complex Compounds of Copper and Nickel. M. A. Porai-Koshits and P. M. Zorkii	15	20
X-Ray Investigation of the Normal Paraffin $C_{34}H_{70}$ under Pressures Up to 16 000 kg/cm^2. S. S. Kabalkina and Z. V. Troitskaya	22	27
X-Ray Investigation of the Systems $BaO-WO_3$, $BaO-MoO_3$, and $BaO-Ta_2O_5$. E. S. Zhmud' and E. P. Ostapchenko	27	33
Investigation of the Polymorphism of 1,8-Dinitronaphthalene. V. M. Kozhin	38	46
Calculation of the Ground States of Dibenzenechromium, the Cobalticinium Cations, and Chromocene by the Self-Consistent Molecular Orbital Method. E. M. Shustorovich and M. E. Dyatkina	40	49
Optical Activity of Amino Acids. M. V. Vol'kenshtein and M. P. Kruchek	49	59
Structure of the Molecules of Lithium and Sodium Metaborates in the Vapor State. P. A. Akishin and V. P. Spiridonov	53	63
Proton Relaxation in Aqueous Solutions of Diamagnetic Salts. V. M. Vdovenko, O. B. Stebunov, and V. A. Shcherbakov	55	64
Possible Existence of Body-Centered Boron Carbide and Silicon Oxycarbide Phases. V. A. Épel'baum, N. G. Sevast'yanov, B. F. Ormont, and M. A. Gurevich	57	65
The Crystal Structure of Euclase. V. V. Bakakin and V. M. Al'tshuller	59	66
Crystal Structure of 4,4'-Dichloroacenaphthene. G. L. Avoyan and Yu. T. Struchkov	61	67
Crystal Structure of 1,4,5,8-Tetrachloronaphthalene. M. A. Davydova and Yu. T. Struchkov	63	69
Crystal Structure of Trivalent Cobalt Acetylacetonate. L. M. Shkol'nikova and E. A. Shugam	66	72
REVIEWS		
Crystal Structures of Ternary Metallic Compounds. G. B. Bokii, B. K. Vul'f, and N. L. Smirnova	68	74
BIBLIOGRAPHY		
International Union of Crystallography. Commission on Crystal Structure Data. List of 1956 Publications Containing New Data on Crystal Structures	101	112

Annual Subscription: $80 **Single Issue: $20** **Single Article: $12.50**

Note: The sale of photostatic copies of any portion of this copyright translation is expressly prohibited by the copyright owners.

ELECTRON DIFFRACTION STUDY OF THE MOLECULAR STRUCTURE OF ScF_3 IN THE VAPOR STATE AND ESTIMATION OF SCANDIUM-HALOGEN INTERATOMIC DISTANCES IN $ScCl_3$, $ScBr_3$, AND ScI_3 MOLECULES

P. A. Akishin and V. A. Naumov

M. V. Lomonosov Moscow State University
Translated from Zhurnal Strukturnoi Khimii, Vol. 2, No. 1, pp. 3-6,
January-February 1961
Original article submitted March 17, 1960

The distance Sc–F = 1.91 ± 0.03 A in the plane trigonal ScF_3 molecule was determined by the sector photometric method. Interatomic distances in molecules of other scandium halides were estimated by comparison of this value with data for halides of other trivalent elements.

In communications [1-4] concerned with electron diffraction studies of the molecular structure of the halides of gallium, yttrium, lanthanum, and neodymium in the vapor state it was shown that all molecules of the MeX_3 type have plane symmetrical configuration. In the present investigation data were obtained, not previously reported in the literature, on the configuration and geometrical parameters of the scandium fluoride (ScF_3) molecule and Sc–X interatomic distances (where X = Cl, Br, I) were estimated for ScX_3 molecules of other scandium halides not studied previously.

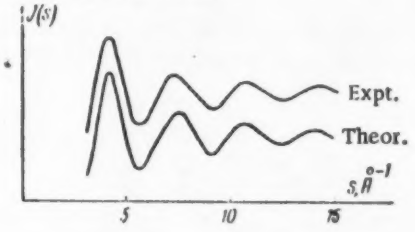

Fig. 1. Experimental and theoretical electron scattering intensity curves for the ScF_3 molecule.

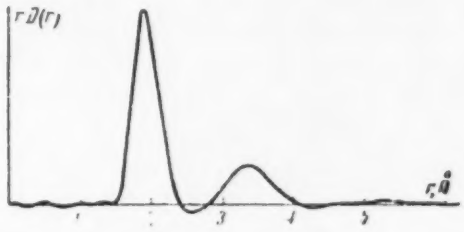

Fig. 2. Radial distribution curve for the ScF_3 molecule.

The investigation was carried out with the MGU electron-diffraction camera for investigation of the structure of gaseous molecules of compounds of low volatility [5] by the sector photometric technique. Ten series of electron diffraction patterns were obtained from scandium fluoride vapor with the use of the s^2 and s^3 sectors at accelerating voltages of 60 and 80 kv. The experimental photometric electron scattering intensity curve (Fig. 1) was interpreted by two methods: with the aid of a radial distribution curve and by selection of theoretical curves (trial and error); the methods are described in detail in earlier communications [6, 7].

The radial distribution curve rD(r) (Fig. 2) has two peaks, at 1.92 and 3.30 A, which may be regarded as structural. The presence of two peaks on the rD(r) curve indicates that scandium fluoride vapor consists of monometric ScF_3 molecules. In this case it is natural to assign the first peak to the Sc–F interatomic distance, and

the second to the F...F distance; the positions of the peaks on the rD(r) curves then correspond to a plane triangular structure of the ScF_3 molecule.

We used the effective root mean square atomic vibration amplitudes $l_{Sc-F} = 0.086$ and $l_{F...F} = 0.17$ A, found from the radial distribution curve for calculating the theoretical electron scattering intensity curve for the plane ScF_3 model, which gave quite satisfactory agreement with the experimental curve (Fig. 1, Table 1).

Thus, the results of the investigation established the plane symmetrical structure of the ScF_3 molecule in vapor form, with the parameters r(Sc − F) = 1.91 ± 0.03 A, ∠F − Sc − F = 120°.

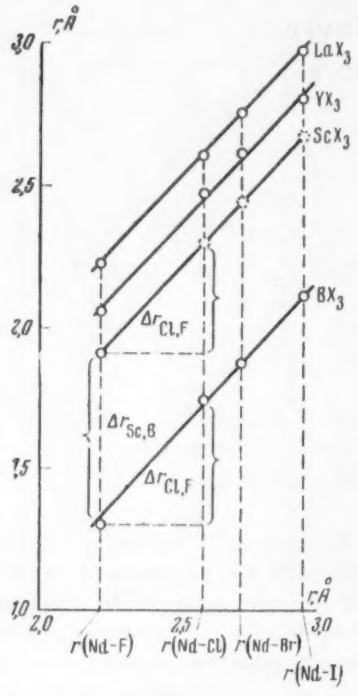

Fig. 3. Linear variation of Me−X interatomic distances in MeX_3 molecules of the same type.

Knowledge of the experimental value of the Sc−F interatomic distance makes it possible to estimate scandium−halogen distances in monomeric $ScCl_3$, $ScBr_3$, and ScI_3 molecules, not studied previously.* These estimates may be performed in two ways. First, using the values of r(Sc−F) and of the covalent radius of the fluorine atom, and also the electronegativities of the Sc and F atoms, we calculate the covalent radius of scandium from Schomaker and Stevenson's empirical equation [8]:

$$d_{AB} = r_A + r_B - 0{,}06\,|x_A - x_B|, \quad (1)$$

where d_{AB} is the interatomic distance, r_A and r_B are the covalent radii of A and B atoms, and x_A and x_B are their electronegativities. We then use the value found, r_{Sc} = 1.43 A, and tabulated data for the other quantities to find the Sc−X distances in ScX_3 molecules from Eq. (1).

The second method for estimating the interatomic distances is based on comparison of the molecular parameters in the similar molecules BX_3, YX_3, LaX_3, and NdX_3. If we take metal−halogen distances in molecules of the halides of any one element (for example, neodymium) as the abscissas and Me−X distances in molecules of halides of other elements (boron, yttrium, and lanthanum) as the ordinates, we obtain a group of approximately parallel straight lines (Fig. 3). Evidently, if r(Sc−F) is known it is easy to estimate by graphical extrapolation the interatomic Sc−X distances in the chloride, bromide, and iodide molecules (Fig. 3). On the other hand, the linear (additive) variation of interatomic distances in series of similar compounds (see [6, 9-12] for fuller details) can be represented by a system of equations of the form

$$r(Me_1 - X_i) - r(Me_2 - X_j) = \Delta r_{Me_1,Me_2} \quad (2)$$

and

$$r(Me_i - X_1) - r(Me_j - X_2) = \Delta r_{X_1,X_2}, \quad (2a)$$

where the subscripts i and j($i \neq j$) correspond to different pairs of elements, and the differences $\Delta r_{Me_1Me_2}$ and $\Delta r_{X_1,X_2}$, corresponding to the chosen pairs of elements (Me_1, Me_2) or (X_1, X_2) are virtually constant (for example, see Table 2).

For example, for estimating the interatomic distances in question, we have eq. (2a) and the data in Table 2:

$$r(Sc - Cl) = r(Sc - F) + \Delta r_{Cl,F} = 1{,}91 + 0{,}40 = 2{,}31\ Å,$$
$$r(Sc - Br) = r(Sc - F) + \Delta r_{Br,F} = 1{,}91 + 0{,}55 = 2{,}46\ Å,$$
$$r(Sc - I) = r(Sc - F) + \Delta r_{I,F} = 1{,}91 + 0{,}75 = 2{,}66\ Å.$$

*The literature contains no data on the presence of dimeric molecules in vapors of scandium halides. If their existence should be proved, the interatomic Sc−X distances given below must be assigned to external bonds of the "bridge" type [4].

TABLE 1. ScF_3 molecule; r_{theor} (Sc–F) = 1.91 A; ∠F–Sc–F = = 120°

Maximum	Minimum	I (s)	s_{theor}	s_{expt}	s_{theor}/s_{expt}	r_{expt}, A
1		+10,0	4,11	4,02	1,022	1,95
	2	— 6,2	5,55	5,70	0,974	1,86
2		+ 3,6	7,45	7,30	1,020	1,95
	3	— 3,2	8,98	9,02	0,996	1,90
3		+ 2,0	10,56	10,63	0,994	1,90
	4	— 1,5	12,34	12,36	0,998	1,91
4		+ 1,4	13,90	14,12	0,984	1,88
			Mean value		0,998	1,91
			Av. deviation		±0,013	±0,03

TABLE 2. Additivity of Interatomic Distances (A) in MeX_3 Molecules [Equation (2a)] from Experimental Data [1-4, 13]

Molecule	r (Me – F)	r (Me – Cl)	r (Me – Br)	r (Me – I)	$\Delta r_{Cl,F}$	$\Delta r_{Br,F}$	$\Delta r_{I,F}$
BX_3*	1,30	1,73	1,87	—	0,43	0,57	—
YX_3	2,04	2,47	2,63	2,80	0,43	0,59	0,76
LaX_3	2,22	2,60	2,75	2,98	0,38	0,53	0,76
NdX_3	2,22	2,58	2,72	2,94	0,36	0,50	0,72
Mean value					0,40± ±0,03	0,55± ±0,03	0,75± ±0,02

*Experimental data [13].

Thus, estimates of the Sc–X interatomic distances in $ScCl_3$, $ScBr_3$, and ScI_3 molecules, performed as described above, give the following average values:

$$r(Sc - Cl) = 2{,}32\ Å;\ r(Sc - Br) = 2{,}47 Å;\ r(Sc - I) = 2{,}68\ Å.$$

LITERATURE CITED

1. P. A. Akishin, V. A. Naumov, and V. M. Tatevskii, Kristallografiya 4, 194 (1959).
2. P. A. Akishin and V. A. Naumov, Nauchn. dokl. vyssh. shkoly (khimiya) 1, 5 (1959).
3. P. A. Akishin, V. A. Naumov, and V. M. Tatevskii, Nauchn. dokl. vyssh. shkoly (khimiya) 2, 229 (1959).
4. P. A. Akishin, V. A. Naumov, and V. M. Tatevskii, Vestn. Mosk. un-ta, Ser. mat., mekh., astr.,fiz., khim. 1, 229 (1959).
5. P. A. Akishin, M. I. Vinogradov, et al., Pribory i tekhnika éksperimenta 3, 70, 1958.
6. P. A. Akishin and V. P. Spiridonov, Kristallografiya 2, 475 (1957).
7. P. A. Akishin, N. G. Rambidi, and E. Z. Zasorin, Kristallografiya 4, 360 (1959).
8. V. Schomaker and D. P. Stevenson, J. Am. Chem. Soc. 63, 37 (1941).
9. V. P. Spiridonov, Candidate's Dissertation (Mosk. gos. un-t., 1958).
10. V. A. Naumov, Candidate's Dissertation (Mosk. gos. un-t., 1959).
11. M. Kh. Karapet'yants and Ling T'ing-chin, Zh. strukt. khimii 1, 277 (1960).
12. V. M. Tatevskii, V. P. Spiridonov, and P. A. Akishin, Dokl. AN SSSR (1961) (in press).
13. H. A. Levy and L. O. Brockway, J. Am. Chem. Soc. 59, 2085 (1937).

All abbreviations of periodicals in the above bibliography are letter-by-letter transliterations of the abbreviations as given in the original Russian journal. *Some or all of this periodical literature may well be available in English translation.* A complete list of the cover-to-cover English translations appears at the back of this issue.

STRUCTURE OF THE HYDRATION SHELL OF THE Co^{2+} ION IN AQUEOUS SOLUTIONS

S. N. Andreev, V. G. Khaldin,

and E. V. Stroganov

A. A. Zhdanov Leningrad State University

Translated from Zhurnal Strukturnoi Khimii, Vol. 2, No. 1, pp. 7-12,
January-February, 1961
Original article submitted February 29, 1960

The electron absorption spectra of single crystals of $Co(ClO_4)_2 \cdot 6H_2O$, $CoCl_2 \cdot 6H_2O$, $CoCl_2 \cdot 2H_2O$, Cs_2CoCl_4, $CoCl_2$, $CoBr_2$, and Cs_3CoBr_5 and absorption spectra of dilute aqueous solutions of Co(II) salts were investigated in the 240-1400 mμ region with natural and polarized radiation. The spectral measurements were taken as far as measurements of the absorption coefficients. It is shown that changes in the chemical nature and the spatial arrangement of the particles constituting the nearest environment of the Co^{z+} ion lead to well-defined changes in the absorption spectrum of the Co^{2+} cation. The pleochroism of all the crystals studied reduces to "absorption:" changes in the crystal orientation with respect to the vector $\vec{E}$ of the polarized ray only change the value of the absorption coefficient but do not alter the frequencies corresponding to the maxima of the absorption bands.

The electron absorption spectrum of Co^{z+} ions in dilute aqueous solutions of Co(II) salts is virtually identical with the absorption spectrum of the $Co(ClO_4)_2 \cdot 6H_2O$ crystal. The absorbing centers in the latter are $[Co(H_2O)_6]^{z+}$ ions of octahedral structure. The following conclusion is drawn: the nearest environment of the Co^{z+} ion in dilute aqueous solutions consists of six water molecules situated at the corners of a regular octahedron.

Despite the large number of publications concerned with the coordination numbers of ionic hydration [1 to 7], the problem cannot be regarded as finally solved. In our opinion considerable progress can be made in this field by studies of the electron spectra of ions in aqueous solutions. There have been few such investigations as yet [8-11].

In the present communication an attempt is made to elucidate the spatial configuration and number of water molecules constituting the nearest environment of the Co^{z+} ion in dilute aqueous solutions of cobalt salts.

The structure of the hydration shell of the Co^{z+} ion in dilute aqueous solutions may be established if it can be experimentally proved that 1) a change in the coordination number of this ion leads to significant changes in its electron spectrum; 2) changes in the chemical nature of substituents within the sphere, with the coordination number of the Co^{z+} ion unchanged, also alter the spectrum of the ion. It is also necessary to choose a complex compound of the Co^{z+} which has an electron spectrum analogous to the spectrum of the Co^{z+} ion in dilute aqueous solutions.

Investigations carried out by Katzin [12], Holmes [13], and Grum-Grzhimailo and Plyusnina [14] suggest that the problem may be solved by comparison of the electron absorption spectrum of Co^{z+} ions in aqueous solution with the spectra of various complex ions contained in crystal lattices of Co^{z+} salts and their crystal hydrates. Numerous literature data show that the electron absorption spectrum of dilute salt solutions always consists of two bands. The maxima of the absorption bands are at 512 mμ and 1240 mμ.

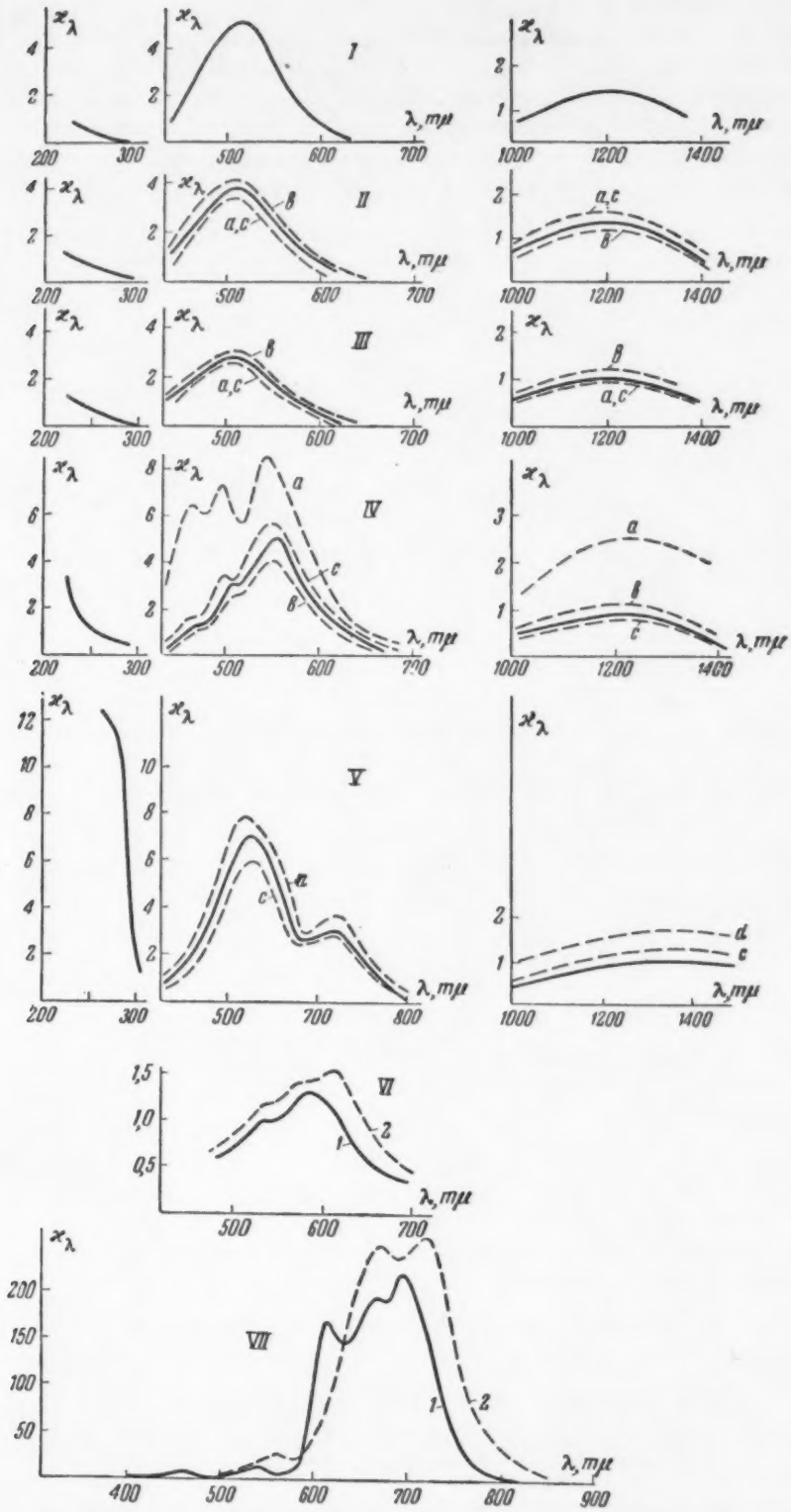

Fig. 1. Absorption curves of Co^{2+} ions in aqueous solutions and in salt crystals: I) Aqueous solutions of $CoCl_2$, $CoSO_4$, $Co(ClO_4)_2$, $Co(NO_3)_2$; II) $Co(ClO_4)_2 \cdot 6H_2O$ crystal; III) $CoSO_4 \cdot 7H_2O$ crystal; IV) $CoCl_2 \cdot 6H_2O$ crystal; V) $CoCl_2 \cdot 2H_2O$ crystal; VI) crystals of $CoCl_2$ (curve 1, crystal thickness 0.02 mm) and $CoBr_2$ (curve 2, crystal thickness 0.03 mm), ordinates – optical density D; VII) crystals of Cs_2CoCl_4 (curve 1) and Cs_3CoBr_5 (curve 2).

Our measurements of the optical density of aqueous $CoCl_2$, $Co(ClO_4)_2$, $CoSO_4$, $Co(NO_3)_2$ solutions in the 230-1350 mμ range show that the positions of these two maxima and the absorption coefficients do not depend either on the chemical nature of the anion (Fig. 1) or on the solution concentration if it does not exceed a certain value. In fairly concentrated $CoCl_2$ and $Co(NO_3)_2$ solutions, at concentrations above 2M for the first salt and 2,5 M for the second, the absorption bands are shifted, probably because of the entry of anions into the inner coordination sphere of the Co^{2+} ions. This fact suggests that the 512 mμ and 1240 mμ absorption bands belong to Co^{3+} ions, the nearest environment of which consists of water molecules only.

With the aid of x-ray structure data on Co(II) salts and their crystal hydrates it is possible to select a number of Co(II) complexes the spectra of which should be compared with the electron absorption spectrum of the ion in aqueous solution.

The structures of these complexes are shown in Fig. 2.

Ions of type (a) enter the crystal structure of $Co(ClO_4)_2 \cdot 6H_2O$ [15] and, according to our preliminary x-ray data, also form the structure of $CoSO_4 \cdot 7H_2O$.

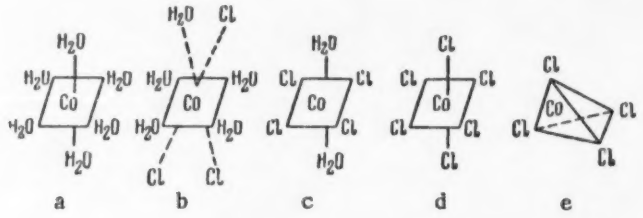

Fig. 2. Nearest environment of the Co^{2+} ion in crystals of: a) $Co(ClO_4)_2 \cdot 6H_2O$ and $CoSO_4 \cdot 7H_2O$; b) $CoCl_2 \cdot 6H_2O$, c) $CoCl_2 \cdot 2H_2O$; d) $CoCl_2$; e) Cs_2CoCl_4.

Type (b) complexes form the crystal structure of $CoCl_2 \cdot 6H_2O$ [16]. In these complex compounds two Cl ions and two H_2O molecules compete for a place near the Co^{2+} ion and occupy almost equivalent positions.

Ions of type (c) and (d) join into multinucleate complexes and form the "thread" crystal structure of $CoCl_2 \cdot 2H_2O$ [17] and the layer structure of $CoCl_2$ [18].

Type (e) ions for the crystal structure of Cs_2CoCl_4 [19].

Our x-ray structure analysis of $CoBr_2$ and Cs_3CoBr_5 suggests that the structure of $CoBr_2$ is analogous to the structure of $CoCl_2$; the nearest environment of the Co^{2+} ions in the Cs_3CoBr_5 crystal consists four Cl^- ions in the form of a tetrahedron.

Large single crystals (from 5 to 30 g in weight) of $Co(ClO_4)_2 \cdot 6H_2O$, $CoSO_4 \cdot 7H_2O$, $CoCl_2 \cdot 6H_2O$ were grown from solutions of the corresponding salts by the planetary rotation method [20]. Single crystals of $CoCl_2 \cdot 2H_2O$, in the form of inclined four-sided prisms, were grown by the static method from saturated aqueous solution at 63°. The largest $CoCl_2 \cdot 2H_2O$ crystals were 10 × 10 × 40 mm. The same method was used for growing Cs_2CoCl_4 and Cs_3CoBr_5 crystals at 20°.

The densities of $Co(ClO_4)_2 \cdot 6H_2O$(2.17 g/cc), $CoCl_2 \cdot 2H_2O$(2.20 g/cc), Cs_2CoCl_4(3.25 g/cc), and Cs_3CoBr_5 (4.03 g/cc), not given in the reference literature, were determined by the pycnometer method.

Plates cut from single crystals were used for investigation of the absorption spectra of the above-named compounds. The plates were ground with a mixture of emery and petrolatum, and polished with a mixture of petrolatum and rouge. The plate thickness varied from 0.01 to 0.7 mm.

We did not succeed in obtaining single crystals of $CoCl_2$ and $CoBr_2$. The absorption spectra of small $CoCl_2$ and $CoBr_2$ crystals were therefore measured with a microspectrophotometer kindly provided by M. V. Sevast'yanova.

The optical densities of the remaining specimens were measured in the 230-1400 mμ range with the SF-11 spectrophotometer. The absorption coeeficients $\varkappa\lambda$ [21] calculated per gram-ion of Co^{2+} from the equation

$I_\lambda = I_{0\lambda} \cdot 10^{-\varkappa_2 Cd}$, where $I_{0\lambda}$ – is the intensity of the incident light beam; I_λ is the intensity of the light beam emerging from the crystal; C is the concentration of Co^{2+} ions in g-ions/1000 cc, and d is the crystal thickness.

The absorption curves for the crystals, measured with natural radiation, are shown in Fig. 1 as continuous lines. The following conclusions may be drawn from a comparison of the absorption spectrum of Co^{2+} ions in aqueous solution and the spectra of Co^{2+} ions in the structure of $CoCl_2$, $CoBr_2$, Cs_2CoCl_2, Cs_3CoBr_5 and crystalline hydrated cobalt salts:

1. With an unchanged coordination number of the Co^{2+} ion, replacement of H_2O molecules by halogen ions leads to sharp changes in the electron spectrum of Co^{2+} ions.

2. With unchanged chemical nature of the particles constituting the nearest environment of the Co^{2+} ion change of the coordination number of the cobalt ion from six to four results in a radical change in the electron spectrum of the Co^{2+} ion. The spectra of the tetrahedral complexes $CoCl_4$ and $CoBr_4$ differ sharply from the spectra of the octahedral complexes $CoCl_6$ and $CoBr_6$; there is also a large difference between the spectra of CoO_4 tetrahedrons in the spinel structure [22] and $Co(H_2O)_6$ octahedrons.

3. The spectrum of the Co^{2+} ion in aqueous solution is identical by the number of absorption bands and by the frequencies corresponding to the absorption maxima with the spectrum of the octahedral $Co(H_2O)_6^{2+}$ ion in the crystal structure of the crystal hydrates $Co(ClO_4)_2 \cdot 6H_2O$ and $CoSO_4 \cdot 7H_2O$. The absorption coefficient of the Co^{2+} ion in aqueous solution is somewhat greater than that of the $Co(H_2O)_6^{2+}$ ion in crystal hydrates.

However, it cannot be conclusively claimed from the above that the nearest environment of the Co^{2+} ion in dilute aqueous solutions of Co(II) salts comprises six water molecules forming an octahedron. All the crystals studied belong to the middle and lowest classes: $Co(ClO_4) \cdot 6H_2O$ must be assigned to the hexagonal and $CoCl_2 \cdot$ $\cdot 6H_2O$, $CoCl_2 \cdot 2H_2O$ and $CoSO_4 \cdot 7H_2O$ to the monoclinic system. Because of the pleochroism of crystals of this type their absorption curves measured with natural radiation may be of random character.

We therefore studied the absorption spectra of the same crystal hydrates in the 400-1350 mμ region with polarized radiation. This series of measurements was performed with the SF-11 spectrophotometer; the polarizer was a Frank-Ritter prism. Plates cut from the crystals were orientated in the instrument in such a way that one of the optic axes of the crystal coincided with the direction of the vector $\vec{E}$ of the polarized beam. The absorption curves corresponding to different crystal orientations are shown by dash lines in Fig. 1 (curves a – the vector $\vec{E}$ is parallel to the [100] axis, curves b and c – to the [010] and [001] axes respectively).

These results show that the "pleochroism" of our crystals reduces to mere "absorption" [23]; a change of crystal orientation relative to the plane of vibrations of the polarized beam does not give rise to new frequencies in the absorption spectra. Investigation of the color of $CoCl_2$ and Cs_2CoCl_4 with the polarization microscope makes it possible to extend this conclusion to these two substances.

Thus, investigation of the electron absorption spectra of Co^{2+} ions in aqueous solution and of crystalline Co(II) complexes shows that the absorption spectrum and therefore the nearest environment of the Co^{2+} ion in dilute aqueous solutions coincide with those of the octahedral $Co(H_2O)_6^{2+}$ ion. The nearest environment of the Co^{2+} ion in dilute aqueous solutions consists of six water molecules at the corners of a tetrahedron. It must be pointed out that this refers only to the nearest environment of the Co^{2+} ion in aqueous solution and does not exclude the possibility of very pronounced interaction between the $Co(H_2O)_6^{2+}$ and the whole bulk of the solvent. Calculation of the heat of hydration of this aquo ion, carried out by Yatsimirskii [24] and ourselves in the case of $Co(H_2O)_6^{2+} \cdot 6H_2O$, shows that interaction of the $Co(H_2O)_6^{2+}$ ion with water is accompanied by a considerable exothermic effect.

It is our pleasant duty to offer our deep gratitude to K. P. Mishchenko for valuable critical comments.

SUMMARY

1. The electron absorption spectrum of Co^{2+} ions in aqueous solutions was investigated in the 230-1350 mμ region.

2. The electron absorption spectra of the following crystals were investigated with natural radiation in the 230-1350 mμ regions: $Co(ClO_4)_2 \cdot 6H_2O$, $CoSO_4 \cdot 7H_2O$, $CoCl_2 \cdot 6H_2O$, $CoCl_2 \cdot 2H_2O$, $CoCl_2$, $CoBr_2$, Cs_2CoCl_4, $CsCoBr_5$. Investigation of the same crystals with polarized radiation showed that their "pleochroism" reduces to "absorption."

3. Changes in the chemical nature of the particles surrounding the Co^{2+} ion and changes of the coordination number of this ion lead to pronounced changes in the electron absorption spectrum of the Co^{2+} ion.

4. This observation, and also the fact that the electron absorption spectrum of the Co^{2+} ion hydrated in aqueous solution coincides with the spectrum of the octahedral $Co(H_2O)_6^{2+}$ ion in the structure of crystal hydrates, suggests that the nearest environment of the Co^{2+} ion in dilute aqueous solutions consists of six water molecules forming a regular octahedron.

LITERATURE CITED

1. A. F. Kapustinskii, Zh. fiz. khim. 30, 548 (1956); 32, 1648 (1958).
2. K. P. Mishchenko, Zh. fiz. khim. 26, 1736 (1952).
3. O. Ya. Samilov, Structure of Aqueous Electrolyte Solutions and Ion-Hydration [in Russian] (Izd. AN SSSR, Moscow, 1957).
4. J. D. Bernal and R. H. Fowler, J. Chem. Phys. 1, 515 (1933).
5. A. M. Azzam, Z. Elektrochem. 58, 889 (1954).
6. E. Darmois, Mem. sci. phys. (Paris) 48, No. 1 (1946).
7. J. O'M. Bockris, Modern Aspects of Electrochemistry [Russian translation] (IL, Moscow, 1958).
8. K. P. Mishchenko and I. S. Pominov, Zh. fiz. khim. 31, 2026 (1957).
9. A. K. Babko and M. M. Tananaiko, Ukr. khim. zh. 24, 298 (1958).
10. A. Zaidel' and V. Rotshtein, Dokl. AN SSSR 57, 587 (1947).
11. V. Rotshtein, Dokl. AN SSSR 71, 335 (1950).
12. L. J. Katzin and E. Gebert, J. Am. Chem. Soc. 72, 5455 (1950).
13. O. G. Holmes and D. McClure, J. Chem. Phys. 26, 1686 (1957).
14. S. V. Grum-Grzhimailo and I. I. Plyusnina, Kristallografiya 3, 175 (1958).
15. A. F. West, Z. Krist. 91, 480 (1936).
16. E. V. Stroganov, I. I. Kozhina, and S. N. Andreev, Vestn. Leningr. un-ta 10, 109 (1958).
17. B. K. Vainshtein, Dokl. AN SSSR 68, 301 (1949).
18. B. F. Ormont, Structures of Inorganic Compounds [in Russian] (GTTI, Moscow-Leningrad, 1950).
19. H. M. Powell and A. F. Wells, J. Chem. Soc. 359 (1935).
20. O. M. Ansheles, V. B. Tatarskii, and A. S. Shternberg, Rapid Growing of Homogeneous Crystals from Solutions [in Russian] (Lenizdat, 1945).
21. GOST 7601-55.
22. R. Hill and O. Hovell, Phil. Mag. 48, 833 (1924).
23. V. B. Tatarskii, Crystal Optics [In Russian] (Izd. Leningr. un-ta, 1945).
24. K. B. Yatsimirskii, Thermochemistry of Complex Compounds [In Russian] (Izd. AN SSSR, Moscow, 1951).
25. S. N. Andreev, V. G. Khaldin, and E. V. Stroganov, Zh. obshchei khimii 29, 1798 (1959).

All abbreviations of periodicals in the above bibliography are letter-by-letter transliterations of the abbreviations as given in the original Russian journal. *Some or all of this periodical literature may well be available in English translation.* A complete list of the cover-to-cover English translations appears at the back of this issue.

INFLUENCE OF FLUCTUATIONS ON THE DIELECTRIC PROPERTIES OF SOLUTIONS IN SUPER-HIGH FREQUENCY ELECTROMAGNETIC FIELDS

R. M. Kasimov, M. I. Shakhparonov,

and Ya. Yu. Akhadov

M. V. Lomonosov Moscow State University

Translated from Zhurnal Strukturnoi Khimii, Vol. 2, No. 1, pp. 13-19,
January-February, 1961
Original article submitted February 3, 1960

The influence of fluctuations on the dielectric properties of solutions with weak orientation of the molecular dipoles is examined. Equations are derived for the relationships between the mean local and effective or macroscopic values of the dielectric constant in the frequency range where dispersion of electromagnetic waves occurs. Measurements of dielectric constant and loss in acetone–benzene solutions at $\lambda = 3.21$ cm and $\lambda = 8.15$ mm, performed over a wide range of concentrations and temperatures, are in agreement with theory.

It was shown earlier [1, 2] that the difference between the macroscopic or effective dielectric constant ε and the mean local value $\bar{\varepsilon}$ depends on fluctuations of the dielectric constant which arise under the influence of thermal motion and intermolecular forces. The relationship, applicable to static electric fields, derived from the values of ε, $\bar{\varepsilon}$, and the mean square fluctuation $\overline{(\Delta\varepsilon)^2}$ was expressed, in the first approximation, by the equation

$$\bar{\varepsilon} - \varepsilon = \frac{\overline{(\Delta\varepsilon)^2}}{\varepsilon\left(2 + \dfrac{d\bar{\varepsilon}/dq_i}{d\varepsilon/dq_i}\right)}, \qquad (1)$$

where q_i is a certain parameter characterizing the state of the system (temperature, pressure, component concentrations). It was shown in [2] that similar equations can be used for the relationships between macroscopic and mean local values of the magnetic permeability μ, electrical condutivity σ, etc., in presence of static or low-frequency alternating electric and magnetic fields.

In this paper we analyze the influence of fluctuations on dielectric constant and loss for individual liquids and solutions in the range where dispersion of electromagnetic waves occurs.

§ 1

Consider a volume V of solutions consisting of $N_1, N_2, \ldots, N_m$ molecules of components 1,2,...m and located in an electromagnetic field of frequency f.

In the frequency range where the substance absorbs electromagnetic waves the dielectric properties of the system are usually expressed in terms of the complex value of the dielectric constant $\varepsilon = \varepsilon' - j\varepsilon''$; here the imaginary part ε'' is proportional to the energy of the field absorbed by the substance.

As the result of fluctuations at a certain time instant there exist in solution individual elements of the volume where the local dielectric constants ε'_l and losses ε''_l differ from their mean values. Here, in accordance with [1], the local values ε'_l and ε''_l are taken to mean the values of ε' and ε'' which the whole solution would have if the nature of molecular distribution and orientation as a whole were the same as in the selected volume element. The values of ε'_l and ε''_l fluctuate near the mean local values $\bar{\varepsilon}'$ and $\bar{\varepsilon}''$ of the dielectric constant and loss. In the general case the latter are connected by a certain functional relationship $\varepsilon' = \gamma(\varepsilon'')$; then ε'_l and ε''_l are not statistically independent quantities and a definite value of ε'_l always corresponds to each value of ε''_l.

We assume that the probability distribution of ε'_l and ε''_l about their mean values is Gaussian.* Then the probability that ε'_l and ε''_l may exist simultaneously in a certain volume dV is determined by the expression:

$$dW_l = \frac{1}{\sqrt{2\pi(\varepsilon'_l - \bar{\varepsilon}')^2}} \exp\left[-\frac{(\varepsilon'_l - \bar{\varepsilon}')^2}{2(\varepsilon'_l - \bar{\varepsilon}')^2}\right] d\varepsilon'_l = \frac{1}{\sqrt{2\pi(\varepsilon''_l - \bar{\varepsilon}'')^2}} \exp \times \times \left[-\frac{(\varepsilon''_l - \bar{\varepsilon}'')^2}{2(\varepsilon''_l - \bar{\varepsilon}'')^2}\right] d\varepsilon''_l \tag{2}$$

Extending the integral equation derived in [1, 2] to the case of an alternating electric field, we have

$$\int \frac{dW_l}{\varepsilon_l + 2\varepsilon} = \frac{1}{3\varepsilon}. \tag{3}$$

Using Equation (2) and the expression for ε, we resolve Eq. (3) into its imaginary and real parts:

$$\left.\begin{aligned} \frac{1}{\sqrt{2\pi(\varepsilon'_l - \bar{\varepsilon}')^2}} \int_{\varepsilon'_{\min}}^{\varepsilon'_{\max}} \frac{(\varepsilon'_l + 2\varepsilon')}{(\varepsilon'_l + 2\varepsilon')^2 + (\varepsilon''_l + 2\varepsilon'')^2} \cdot \exp\left[-\frac{(\varepsilon'_l - \bar{\varepsilon}')^2}{2(\varepsilon'_l - \bar{\varepsilon}')^2}\right] d\varepsilon'_l = \frac{\varepsilon'}{3[(\varepsilon')^2 - (\varepsilon'')^2]}, \\ \frac{1}{\sqrt{2\pi(\varepsilon'_l - \bar{\varepsilon}')^2}} \int_{\varepsilon'_{\min}}^{\varepsilon'_{\max}} \frac{(\varepsilon''_l + 2\varepsilon'')}{(\varepsilon''_l + 2\varepsilon')^2 + (\varepsilon''_l + 2\varepsilon'')^2} \cdot \exp\left[-\frac{(\varepsilon'_l - \bar{\varepsilon}')^2}{2(\varepsilon'_l - \bar{\varepsilon}')^2}\right] d\varepsilon'_l = \frac{\varepsilon''}{3[(\varepsilon')^2 + (\varepsilon'')^2]} \end{aligned}\right\} \tag{4}$$

Transforming Eq. (4), we have:

$$\left.\begin{aligned} \sqrt{\frac{A}{l}} I_1 &= (1 + B^2) \frac{\varepsilon'}{3[(\varepsilon')^2 + (\varepsilon'')^2]} \\ \sqrt{\frac{A}{l}} I_2 &= B \frac{\varepsilon''}{3[(\varepsilon')^2 + (\varepsilon'')^2]} - B^2 \frac{\varepsilon'}{3[(\varepsilon')^2 + (\varepsilon'')^2]} \end{aligned}\right\}, \tag{5}$$

where

$$A = \frac{1}{2(\Delta\varepsilon)^2}; \quad \overline{(\Delta\varepsilon)^2} = \overline{(\varepsilon'_l - \bar{\varepsilon}')^2}; \quad B = \frac{d\bar{\varepsilon}''/d_{q_l}}{d\bar{\varepsilon}'/d_{q_l}};$$

$$I_1 = \int_{\varepsilon'_{\min}}^{\varepsilon'_{\max}} \frac{(\varepsilon'_l + 2\varepsilon') \cdot \exp\left[-A(\varepsilon'_l - \bar{\varepsilon}')^2\right]}{(\varepsilon'_l + 2\varepsilon')^2 + 2\alpha(\varepsilon'_l + 2\varepsilon') + \beta^2} d\varepsilon'_l;$$

*In small elements of the volume there may be deviations from a Gaussian distribution of fluctuations of ε'_l and ε''_l. However, as was shown in [2], the theoretical results still remain valid in such a case.

$$I_2 = \int_{\varepsilon'_{\min}}^{\varepsilon'_{\max}} \frac{\exp[-A(\varepsilon'_A - \varepsilon')^2]}{(\varepsilon' + 2\varepsilon')^2 + 2\alpha(\varepsilon' + 2\varepsilon') + \beta^2} d\varepsilon'.$$

Here

$$\alpha = \frac{B}{1+B^2}[(\bar{\varepsilon}'' + 2\varepsilon'') - B(\bar{\varepsilon}' + 2\varepsilon')];$$
$$\beta^2 = \frac{1}{1+B^2}[(\bar{\varepsilon}'' + 2\varepsilon'') - B(\bar{\varepsilon}' + 2\varepsilon')]^2.$$

After rearrangements similar to those given in [1] we have

$$\left.\begin{aligned} \bar{\varepsilon}' - \varepsilon' &= \frac{\overline{(\Delta\varepsilon)^2}}{[(\varepsilon')^2 + (\varepsilon'')^2]^2(1+R^2)} \cdot \frac{\varepsilon'(P_1Q_1 - P_2Q_2) - \varepsilon''(P_1Q_2 + P_2Q_1)}{d\bar{\varepsilon}'/dq_i + 2d\varepsilon'/dq_i}, \\ \bar{\varepsilon}'' - \varepsilon'' &= \frac{\overline{(\Delta\varepsilon)^2}}{[(\varepsilon')^2 + (\varepsilon'')^2]^2 \cdot (1+R^2)} \cdot \frac{\varepsilon'(P_1Q_2 + P_2Q_1) + \varepsilon''(P_1Q_1 - P_2Q_2)}{d\bar{\varepsilon}'/dq_i + 2d\varepsilon'/dq_i} \end{aligned}\right\}. \quad (6)$$

Here

$$R = \frac{d\bar{\varepsilon}''/dq_i + 2d\varepsilon''/dq_i}{d\bar{\varepsilon}'/dq_i + 2d\varepsilon'/dq_i};$$
$$P_1 = [(\varepsilon')^2 + (\varepsilon'')^2]\, d\varepsilon'/dq_i + 2\varepsilon'\varepsilon''\, d\varepsilon''/dq_i;$$
$$P_2 = [(\varepsilon')^2 - (\varepsilon'')^2]\, d\varepsilon''/dq_i - 2\varepsilon'\varepsilon''\, d\varepsilon'/dq_i;$$
$$Q_1 = (1 - B^2) + 2BR;$$
$$Q_2 = 2B - (1 - B^2)R.$$

In derivation of Equations (6) terms containing the factor dA/dq_i were small enough to reject.

In the particular case when the conditions $d\bar{\varepsilon}'/dq_i = d\bar{\varepsilon}'/dq_i$* and $d\bar{\varepsilon}/dq_i = d\bar{\varepsilon}''/dq_i$ hold Equations (6) are simplified and are written as follows:

$$\bar{\varepsilon}' - \varepsilon' = \frac{\overline{(\Delta\varepsilon)^2}}{3[(\varepsilon')^2 + (\varepsilon'')^2]}\left[\varepsilon'(1 - B^2) + 2B\varepsilon''\right], \quad (7)$$

$$\bar{\varepsilon}'' - \varepsilon'' = \frac{\overline{(\Delta\varepsilon)^2}}{3[(\varepsilon')^2 + (\varepsilon'')^2]}\left[2B\varepsilon' - \varepsilon''(1 - B^2)\right]. \quad (8)$$

At low frequencies there are no losses in solution ($\varepsilon'' = 0$); then

$$\bar{\varepsilon}' - \varepsilon' = \frac{\overline{(\Delta\varepsilon)^2}}{3\varepsilon}$$

which coincides with Equation (2−27) in [1].

Eliminating the meansquare fluctuation $\overline{(\Delta\varepsilon)^2}$ from Eq. (7) and (8) we have

$$\frac{\bar{\varepsilon}'' - \varepsilon''}{\bar{\varepsilon}' - \varepsilon'} = \frac{2B\varepsilon' - \varepsilon''(1 - B^2)}{\varepsilon'(1 - B^2) + 2B\varepsilon''}. \quad (9)$$

This last expression is the most convenient for semiquantitative estimates of the influence of fluctuations on dielectric properties of a system.

---

* As in the original Russian.

In the general case fluctuations of dielectric constant $\overline{(\Delta\varepsilon)^2}$ are induced by fluctuations of concentration, of density, etc. If the temperature of the solution is far from the critical point the influence of density fluctuations on ε' and ε'' may be disregarded. Fluctuations of concentration are large in solutions the properties of which exhibit considerable positive deviations from ideal behavior. For such solutions it is sufficient to consider the influence only of concentration fluctuations on ε' and ε''. In the simplest case of a binary solution we have:

$$\overline{(\Delta\varepsilon)^2} \simeq \left(\frac{\partial\bar{\varepsilon}'}{\partial c}\right)^2 \overline{(\Delta c)^2}. \tag{10}$$

Taking the concentration c of the second component as the parameter of the system in Eq. (7) and (8), and using (10), we transform these equations into

$$\bar{\varepsilon}' - \varepsilon' = \frac{\overline{(\Delta c)^2}}{3[(\varepsilon')^2 + (\varepsilon'')^2]}\left\{\varepsilon'\left[\left(\frac{\partial\bar{\varepsilon}'}{\partial c}\right)^2 - \left(\frac{\partial\varepsilon''}{\partial c}\right)^2\right] + 2\varepsilon''\frac{\partial\bar{\varepsilon}'}{\partial c}\cdot\frac{\partial\bar{\varepsilon}''}{\partial c}\right\}, \tag{11}$$

$$\bar{\varepsilon}'' - \varepsilon'' = \frac{\overline{(\Delta c)^2}}{3[(\varepsilon')^2 + (\varepsilon'')^2]}\left\{2\varepsilon'\frac{\partial\bar{\varepsilon}'}{\partial c}\cdot\frac{\partial\bar{\varepsilon}''}{\partial c} - \varepsilon''\left[\left(\frac{\partial\bar{\varepsilon}'}{\partial c}\right)^2 - \left(\frac{\partial\varepsilon''}{\partial c}\right)^2\right]\right\} \tag{12}$$

Equations (11) and (12) are derived for the conditions $\frac{\partial\bar{\varepsilon}'}{\partial c} = \frac{\partial\varepsilon'}{\partial c}$ and $\frac{\partial\bar{\varepsilon}''}{\partial c} = \frac{\partial\varepsilon''}{\partial c}$, each of which holds strictly at one concentration, usually in the region $\varphi = 0.5$, where φ is the concentration of one of the components expressed in volume fractions. These conditions are often satisfied with an adequate degree of approximation in the range $\varphi = 0.5 \pm 0.1$. At other concentrations Equations (6) should be used.

The values of $\bar{\varepsilon}'$ and $\bar{\varepsilon}''$, characterizing the mean local dielectric properties of a solution, can be calculated if the corresponding values ε'_{0i} and ε''_{0i} for the pure components are known. The macroscopic dielectric properties of the pure components are close to their mean local properties. Therefore, if the volume of the solution is the sum of the volumes of the components, $\bar{\varepsilon}'$ and $\bar{\varepsilon}''$ for the solution, with a sufficient degree of accuracy [1], are obtained additively from ε'_{0i} and ε''_{0i}.

$$\bar{\varepsilon}' = \sum_i \varepsilon'_{0i}\varphi_i \; ; \quad \bar{\varepsilon}'' = \sum_i \varepsilon''_{0i}\varphi_i \; . \tag{13}$$

It must be stressed that Eq. (13) can be used for calculating the mean local values of the dielectric constant and loss for a solution which are independent of existing positive deviations from Raoult's law. The values of $\bar{\varepsilon}'$ and ε'' calculated from Eq. (13) can be used in Eq. (11) and (12) for calculation of ε' and ε'', since values of $\overline{(\Delta c)^2}$ can be found from analogous measurements at other frequencies, including optical.

For experimental verification of the above we measured the dielectric constants and losses of binary acetone–benzene solution at two wave lengths ($\lambda = 3.21$ cm and 8.15 mm) between -10 and $+40°$. The measurements were performed by the waveguide method described in [3]. The degree of accuracy was 1% in measurements at $\lambda = 3.21$ cm and 2% in measurements at $\lambda = 8.15$ mm.

The dielectric properties of acetone at low frequencies conform fairly well to the Onsager theory. It may be assumed that short-range orientational order in acetone is weak. It is to be expected that in a solution of acetone in benzene (a nonpolar solvent) there is virtually no predominant mutual orientation of the polar molecules. In this case the observed deviations of ε' and ε'' of the solutions from additivity are due almost entirely to the influence of fluctuations. If this is so, then Eqs. (7-9, 11, 12) should quantitatively represent the experiment data.

In Fig. 1 and 2 the dielectric constants and losses are plotted against the solution concentration at two wave lengths at 20°. The degree of deviation of the macroscopic dielectric constant and loss from the mean values decreases with increase of frequency for ε' and increases for ε''. The greatest deviation for ε'' is found at approximately the frequencies corresponding to maximum absorption of radio waves by the solution. This relationship is shown more clearly in Fig. 3, which gives the dependence of macroscopic and mean local values of ε' and ε'' on frequency at 20° and $\varphi = 0.5$, calculated from Eqs. (11-13). Although Eqs. (11-13) do not contain the frequency relationships of ε', ε'', $\bar{\varepsilon}'$ and $\bar{\varepsilon}''$ in explicit form, these can be derived with the aid of values of ε'_{0i} and ε''_{0i}

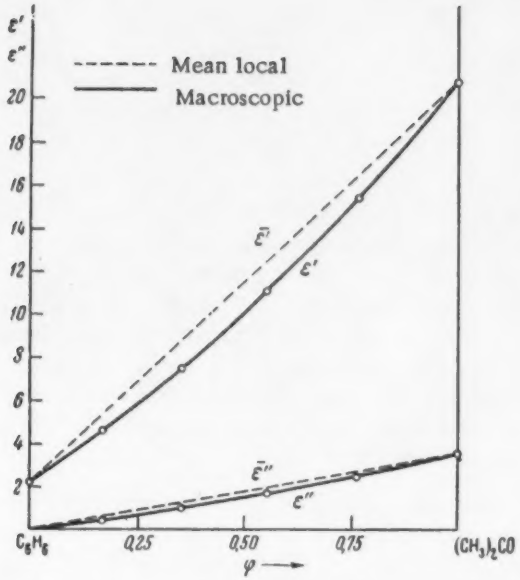

Fig. 1. Variations of the dielectric constant and loss of acetone–benzene solution with the concentration φ, expressed in volume fractions, at λ = 3.21 cm and t = 20°.

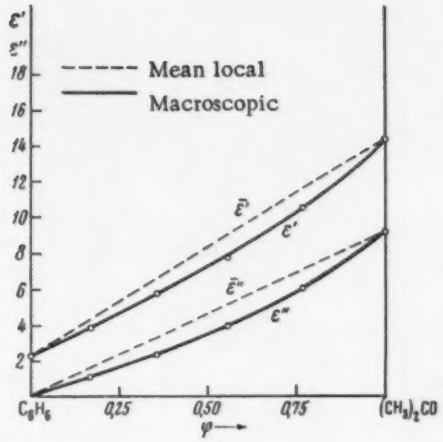

Fig. 2. Variations of the dielectric constant and loss of acetone–benzene solution with the concentration φ, expressed in volume fractions, at λ = 8.15 mm and t = 20°.

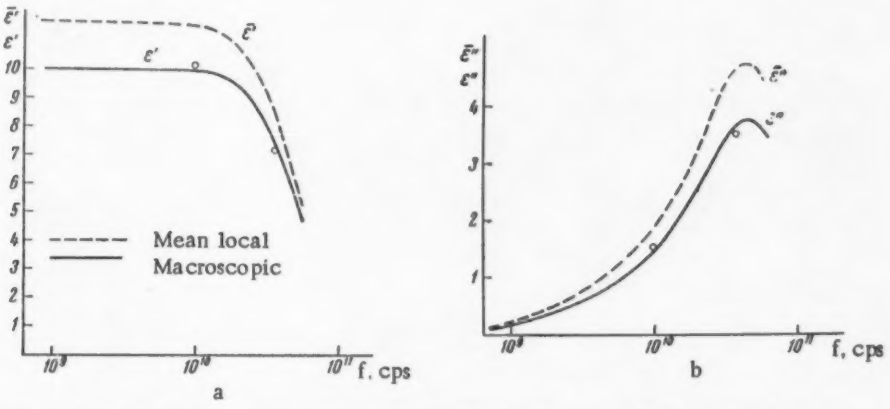

Fig. 3. Variations of the macroscopic and mean values with frequency at t = 20°: a) Dielectric constant; b) dielectric loss.

Differences	λ = 3.21 cm		λ = 8.15 mm	
	calc.	exptl.	calc.	exptl.
$\delta\varepsilon'$	1.60	1.40	0.86	1.17
$\delta\varepsilon'$	0.38	0.22	0.98	1.12

determined experimentally at different frequencies. The values obtained by Drude [4] for ε of acetone–benzene solutions and the values of ε' and ε'' for pure acetone determined by Calderwood and Smyth [5] were also used in the calculations. The corresponding differences $\delta\varepsilon' = \bar{\varepsilon}' - \varepsilon'$ and $\delta\varepsilon'' = \bar{\varepsilon}'' - \varepsilon''$, at φ = 0.5, are given in the table together with experimental values of these differences. It may be noted that the discrepancies between the calculated and experimental values of $\delta\varepsilon'$ and $\delta\varepsilon''$ are within the limits of experimental error, since we are comparing the differences and not the absolute values of ε' and ε''.

For analysis of the effect of temperature on the difference between the macroscopic and mean local values of ε' and ε'' we modify Eq. (9). Since these differences $\delta\varepsilon'$ and $\delta\varepsilon''$ are small by comparison with ε' and ε'' in the first approximation we can use, instead of the macroscopic values of ε' and ε'' in the right-hand side of Eq. (9), their mean local values calculated from Eq. (13). We then have, after transformation:

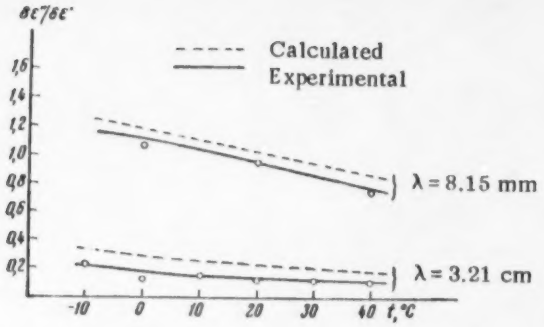

Fig. 4. Variations of the ratio $\delta\varepsilon''/\delta\varepsilon'$ with temperature at $\lambda = 3.21$ cm and 8.15 mm

where

$$\delta\varepsilon''/\delta\varepsilon' = \operatorname{tg}(2\psi - \delta),$$
$$\operatorname{tg}\psi = \frac{d\bar{\varepsilon}''/d\varphi}{d\bar{\varepsilon}'/d\varphi}, \qquad (14)$$
$$\operatorname{tg}\delta = \bar{\varepsilon}''/\bar{\varepsilon}'.$$

The dependence of $\delta\varepsilon''/\delta\varepsilon'$ on temperature calculated from Eq. (14) for two wave lengths is given in Fig. 4. In the first approximation we may assume that rise of temperature diminishes the angles ψ and δ equally. Therefore, according to (14), rise of temperature must also decrease the ratio $\delta\varepsilon''/\delta\varepsilon'$. This is confirmed both by the calculated and by the experimental curves in Fig. 4. It should be noted that the experimental values of the macroscopic ε' and ε'' agree to within 2–5% with the theoretical values calculated from Eqs. (7) and (8).

Thus it follows from all the foregoing that consideration of fluctuations of dielectric constant in the form presented here gives an acceptable explanation of the effects of frequency and temperature on the difference between the macroscopic and mean local dielectric constants and losses in acetone–benzene solutions and in certain other solutions with weak orientation of the molecular dipoles.

SUMMARY

1. Equations are derived for the influence of fluctuations on dielectric constant and loss in individual liquids and solutions in the region of dispersion of electromagnetic waves.

2. Equations are derived for the relationship between mean local and macroscopic or effective values of ε' and ε''.

3. Measurements of ε' and ε'' in acetone–benzene solutions at $\lambda = 3.21$ cm and 8.15 mm, performed over wide ranges of concentration and temperature, are in quantitative agreement with theory.

LITERATURE CITED

1. M. I. Shakhparonov, Zh. fiz. khim. 34, 1478 (1960).
2. M. I. Shakhparonov, Zh. fiz. khim. 35, 5 (1961).
3. J. P. Poley, Appl. Sci. Research B 4, 5, 337 (1955).
4. P. Drude, Z. Physik. Chem. 23, 267 (1897).
5. J. H. Calderwood and C. P. Smyth, J. Am. Chem. Soc. 78, 5, 1295 (1956).

All abbreviations of periodicals in the above bibliography are letter-by-letter transliterations of the abbreviations as given in the original Russian journal. *Some or all of this periodical literature may well be available in English translation.* A complete list of the cover-to-cover English translations appears at the back of this issue.

SIMILARITIES AND DIFFERENCES OF CRYSTAL STRUCTURE OF INTERNAL COMPLEX COMPOUNDS OF COPPER AND NICKEL

M. A. Porai-Koshits and P. M. Zorkii

M. V. Lomonosov Moscow State University
Translated from Zhurnal Strukturnoi Khimii, Vol. 2,
No. 1, pp. 20-26, January-February, 1961
Original article submitted March 5, 1960

It is shown that two facts usually established without much difficulty at the first stages of structure analysis—similarity (or difference) of crystal structures of corresponding internal complex compounds of copper and nickel, and the location of the metal atoms at the centers (or outside the centers) of symmetry of the crystals—can be used for drawing valuable conclusions about the molecular structure of these compounds. It can be predicted theroretically that if crystals of corresponding compounds are not isostructural then in at least one of them the complex is of nonplanar structure; this is confirmed by experimental data. In cases when the metal atom is linked with four O atoms or four S atoms the crystals of corresponding copper and nickel compounds are not isostructural, but copper complexes have planar structure in the first case, and nickel complexes in the second. Diamagnetic compounds of nickel, where the metal atom is linked to two N atoms and two O atoms, usually form crystals isostructural with crystals of the corresponding copper compounds in the case of planar trans-configuration, and nonisostructural in the case of enforced cis-configuration.

In a recent survey [1] on x-ray structural investigations of crystals of internal complex compounds (ICC) Shugam and Shkol'nikova note that corresponding compounds of copper and nickel are often nonisostructural although both metals form square planar complexes. They consider that the difference between the structure of copper and nickel compounds is that copper atoms in the crystals occupy general positions, whereas nickel atoms occupy special positions at the centers of symmetry. Shugam and Shkol'nikova attribute the location of copper atoms in general positions to greater or lesser deviations of the copper complexes from a planar structure.

Kitaigorodskii [2] showed that centrosymmetric molecules in crystals should be located at the centers of symmetry. It is true that several examples of crystallization of substances with centrosymmetric molecules in noncentrosymmetric space groups have been described in the literature [3], but Kitaigorodskii's doubts concerning the accuracy of these data seem justified [4]. In any event, it must be acknowledged that Kitaigorodskii's rule is valid for the vast majority of known structures. Therefore if the metal atom in an ICC is outside the center of symmetry it may be assumed that the molecule of this compound is noncentrosymmetric.*

The centrosymmetric character of an ICC molecule may be disturbed in various ways. The most probable of these ways are: 1) if the complex attains cis-configuration while retaining a planar configuration of the atoms in the central group, including the metal atom and the atoms joined to it chemically; 2) if the metal atom deviates from the plane containing the other atoms of the central group (pyramidal configuration); 3) if the atoms joined chemically to the metal are in nonplanar configuration. Experimental data available at this time show that the first possibility is realized only when the molecule cannot, because of its structure, assume the trans-

*Here and subsequently we consider only ICC of fourfold coordination, nonelectrolytes, with molecules consisting of one metal atom and two similar bidentate ligands or one tetradentate ligand.

configuration. This may be the case when a tetradentate ligand with a fairly rigid structure is involved in complex formation; an example is provided by salicylalethylenediaminates:

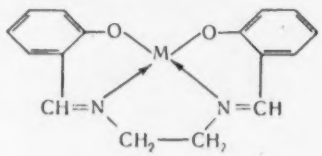

Bivalent copper and nickel very often do not form compounds of the same composition outside the ICC class. However, in so far as such compounds are formed their crystals are generally isostructural or have similar structures. The following examples may be mentioned: MLi_2N, M_2P, M_3P, M_5Sb_2, $4MO \cdot Fe_2O_3$, anhydrous and hydrate halides and sulfates, $[M(NH_3)_6]Br_2$, $[M(NH_3)_6]I_2$[5], $CsMCl_3$[6,7], $K_2Pb[M(NO_2)_6]$[5,8], where M = Cu or Ni.

In the ICC class corresponding compounds of copper and nickel are nearly always formed, but very often they are not isostructural. Bivalent copper and nickel ions are very similar to each other in size and electronic structure; it is therefore unlikely that packing differences between molecules of similar structure can be responsible for the fact that their corresponding ICC are not isostructural. Therefore in this case a difference of crystal structure indicates a difference of molecular structure, and primarily a difference in the structure of the central atomic group. The latter cannot undergo any significant changes if the center of symmetry is retained. Therefore, if corresponding copper and nickel ICC are not isostructural, it may be assumed with a high degree of probability that at least one of them has noncentrosymmetric molecules.

It follows from the foregoing that two facts usually established without much difficulty at the first stages of structure analysis—similarity (or difference) of crystal structures of corresponding copper and nickel compounds, and the location of the metal atoms at the centers (or outside the centers) of symmetry of the crystals—can be used for drawing conclusions about the structure of ICC molecules. Correlation and extension of such information is therefore of interest.

Comparison of such data with the results of magnetic investigations, which in themselves cannot lead to definite conclusions in many cases [9], is also useful for establishing the principles of structure of nickel ICC.

In the present investigation we used literature data and our own experimental data determined by electron and x-ray diffraction methods. The method used for the electron-diffraction work is described elsewhere [10]. The x-ray patterns were obtained by the powder method with copper radiation; x-ray oscillation patterns were obtained in some cases.

The results of our work show that for the class of copper and nickel ICC as a whole (regardless of the nature of the atoms surrounding the metal atom) it cannot be asserted, as is done by Shugam and Shkol'nikova [1], that a nonplanar structure is characteristic of copper complexes in contrast to nickel. With this approach it is also impossible to deduce how far the nonisostructural character of corresponding copper and nickel ICC is typical. We, therefore, classify these substances by the composition of the nearest environment of the metal atom, distinguishing five groups: M−4O, M − 4S, M − 4N, 2O(trans), M − 2N, 2O (cis).

Compounds of the M−4O Group (Table 1). In this group the Cu atoms are at the centers of symmetry, which indicates a planar structure of the copper complexes. Several nickel compounds in this group have been found to be paramagnetic (salicylaldehydate [11, 12], acetylacetonate [11], complex with o-hydroxyacetophenone [12], etc.); but the conclusion drawn from this, that the Ni atom bonds are tetrahedral [13], is questionable [9]. The isostructural character of Ni and Zn acetylacetonates and salicylaldehydates is not convincing evidence of the tetrahedral structure of these nickel complexes either [14, 15]. Bullen [16] and Lyle et al. [17] showed that in crystals of the latter two Ni compounds (and consequently of the analogous Zn compounds) the metal atoms are not at the centers of symmetry; trimers with very short metal−metal distances (2.72 and 2.88 A in the case of Ni acetylacetonate) are formed in this case. Consequently, specific interaction between the metal atoms is not excluded here. In any event, it may be assumed that corresponding ICC of Cu and Ni in this group form nonisostructural crystals. In fact, the two known examples support this view.

Compounds of the M−4S Group (Table 2). All the substances of this group for which we have structure data are characterized by four-membered metal cycles and not five- or six-membered as in the other compounds under consideration. It may be noted that formation of four-membered metal cycles, which is never observed with carboxylic acids, is quite usual if the O atoms of the carboxyl group are replaced by S atoms.

TABLE 1. Compounds of the M–4O Group*

Substances	Isostructural	Position of metal atom		Literature
		Cu	Ni	
Acetylacetonates	No	c	n	[16], [53] [54], [55]
Acetylacetoesterates	–	c	–	[56]
Benzoylacetonates	–	c	–	[53]
Salicylaldehydates	No	c	n	[15], [17], [38]
Tropolonates	–	c	–	[57]

*In this and the subsequent tables the presence of isostructural modifications is indicated by "Yes" and absence by "No;" centrosymmetric positions of the metal atoms are indicated by "c" and noncentrosymmetric by "n."

TABLE 2. Compounds of the M–4S Group

Substances	Isostructural	Position of metal atom		Literature
		Cu	Ni	
Diethyldithiocarbamates	No	n	c	[25]
n-Dipropyldithiocarbamates	No	n	c	[23], [24], [26]
Diethyldithiophosphates	–	–	c	[58]

TABLE 3. Compounds of the M–4N Group

Substances	Isostructural	Position of metal atom		Literature
		Cu	Ni	
α-Pyrrolaliminates	–	c	–	[38]
Dimethylglyoximates	No	n	c	[28], [29] [30], [31], [32]
Methylethylglyoximates	Yes	n	n	[33]
Phthalocyanines	Yes	c	c	[59]
Analog of Ni phthalocyanine	–	–	c	[60]

The numerous nickel compounds belonging to this group are diamagnetic (anthate [18, 19], diethyldithiophosphate [20], dithiocarbamate [18], and many others [18, 20, 21, 22]). This indicates that the nickel complexes have planar structure. In fact the very few structure investigations which have been performed show that in crystals of these ICC the Ni atoms occupy the centers of symmetry. However, the two Cu compounds which have been studied (diethyldithiocarbamate and n-dipropyldithiocarbamate) form crystals which are not isostructural with the crystals of the corresponding Ni compounds, and in this group, in contrast to the M–4O group, the Cu atoms occupy general positions [23, 24, 25]. It was shown recently [26] that this is due to the nonplanar configuration of

the atoms in the cental group. The structure of Pb diethyldithiocarbamate [27] is analogous. Here the Pb atom occupies the vertex of a tetragonal pyramid with four S atoms at its base.

Compounds of the M−4N Group (Table 3). Here the situation is very complicated and definite conclusions cannot be drawn from the few available examples. The dimethylgloximates of Cu and Ni are not isostructural; whereas the Ni atoms are at the center of symmetry [28, 29, 30] (like Pd and Pt atoms in the corresponding isostructural dimethylglyoximates [29, 30]), indicating a planar structure of the complex, the Cu atoms occupy general positions and, forming Cu−O intermolecular bonds, are at the centers of tetragonal pyramids [31, 32]. On the other hand, Cu and Ni methylethylglyoximates are isostructural. According to Cox [33], both these substances crystallize in the noncentrosymmetric space group $P2_12_12$. By Kitaigorodskii's rule [2, 4], this is possible only if the molecules are noncentrosymmetric. The Ni compounds of this group are usually diamagnetic.

Compounds of the M−2N, 2O(trans) Group (Table 4). Of the information at our disposal, data on this group are the most extensive. This group includes the majority of the substances investigated by us. With the exception of salicylaldoximates, corresponding compounds of Ni and Cu are isostructural in all known cases and in the majority of cases both the Cu atoms and the Ni atoms are at the centers of symmetry. In the two known modifications of the diamagnetic [11, 19, 34] Ni salicylaldoximate the metal atoms are at the centers of symmetry [35, 36], and in the crystals of the corresponding copper compound they are in noncentrosymmetric positions [37]. Modifications with both centrosymmetric and noncentrosymmetric positions of the metal atoms are known in the case of Cu salicylbutyliminate (our data) and of Cu salicylmethyliminate [38]. The literature data on the isostructural character Cu and Ni salicylalmethyliminates are contradictory [38, 63, 64].

It is significant that in this group we have diamagnetic nickel complexes [12, 16, 39, 40, 41] in all known cases where corresponding ICC are isostructural. At the same time, several internal Ni complexes of this group have been shown to be paramagnetic (the o-aminobenzoate [41], one modification of salicylalmethyliminate [42], 5-bromosalicylalanilinate [41], and others [44, 45, 46, 47]). The structure of these paramagnetic compounds has not been elucidated. The explanation of the paramagnetism of one modification of salicylalmethyliminate, based on the assumption of specific interaction between Ni and O atoms [43], meets a number of difficulties [10]. It is quite possible that the paramagnetic nickel ICC of this group will prove to be nonisostructural with the corresponding copper compounds.

The available structure data indicate a similarity of crystal structure between corresponding nickel and palladium ICC of this group (salicylaliminates [48], salicylaldoximates [37], and 5-chlorosalicylaldoximates [49]).

Compounds of the M−2N, 2O (cis) Group. It was stated earlier that a cis-configuration in ICC of Cu and Ni has been found only in cases when the structure of the molecule itself excludes the possibility of trans-configuration. Obviously the metal atoms in these compounds cannot be located at the centers of symmetry. The salicylalethylenediaminates and salicylal-o-phenylenediaminates of Cu and Ni proved to be nonisostructural [38]; this is confirmed by our data. The nonisostructural character of Ni and Cu resacetophenoneethylenediaminates was demonstrated by x-ray diffraction, and that of the corresponding salicylalhexamethylenediaminates by electron diffraction.* The existing information is therefore in favor of the view that the copper and nickel complexes of this group are diamagnetic (salicylalethylenediaminate [11, 29, 50], 5-bromosalicylalethylenediaminate [41], resactophenoneethylenediaminates [41] and salicylalisopropylenediaminate [12, 51]); this indicates that the metal atom bonds are planar.

The data discussed above are, obviously, far from complete and our conclusions are therefore tentative. It is seen that much remains obscure in the stereochemistry of four-coordinates copper and nickel ICC; it is difficult to account for many of the observed facts. Two points are of special interest. The first is that the resemblance between copper and nickel ICC crystals is much less than in the case of ordinary noncyclic compounds. This is possibly due to the considerably more covalent character of the metal bonds in ICC, so that the presence of an additional electron in copper plays an important part. The second point relates to the difference in behavior between paramagnetic and diamagnetic nickel ICC. As yet there is no satisfactory explanation of the paramagnetism of a number of such ICC. We may note that the explanation of the paramagnetism put forward by Sacconi et al. [52], based on the assumption that external d-orbits are utilized in bond formation (hybridization of $4s4p^24d$) is not confirmed by structure data. With bonding of this type the complexes should have planar square structure characterized by the presence of a center of symmetry; however, the paramagnetic nickel salicylaldehydate and acetylacetonate form crystals with the metal atoms in noncentrosymmetric positions.

*Because of the length of the hexamethylene chain these complexes may also have trans-configuration.

TABLE 4. Compounds of the M−2N, 2O (trans) Group*

Substances	Isostructure	Position of metal atom		Literature
		Cu	Ni	
α-Aminobutyrates	–	c	–	[61]
Salicylaliminates	Yes	c	c	e [38], [48], [62]
5-Bromosalicylaliminates	Yes	c	c	e
4-Methylsalicylaliminates	Yes	c	c	e
o-Hydroxyacetophenoneiminates	Yes	–	–	e
Salicylalmethyliminates	?	c, n	c	[38], [63], [64]
Salicylalethyliminates	Yes	–	–	e
Salicylalbutyliminates	Yes	c, n	n	e, o
Salicylalanilinates	–	c	–	[38]
Salicylaldoximates	No	n	c	[35], [36], [37]
5-Chlorosalicylaldoximates	–	–	c	[49]
β-Hydroxy-α-naphthadehydemethyliminates	–	c	–	[38]
Acetylacetoneiminates	Yes	n	n	o

*The symbols "e" and "o" refer to our results obtained from electron-diffraction or x-ray oscillation patterns.

SUMMARY

1. It can be predicted theoretically that if crystals of corresponding copper and nickel internal complexes are not isostructural then in at least one of them the metal atoms are not at the centers of symmetry (the complex is nonplanar). This is confirmed by experimental data.

2. The existing (somewhat limited) experimental data show that in the M−4O and M−4S groups the corresponding copper and nickel compounds are not isostructural, but in the first of these groups copper atoms and in the second nickel atoms are at the centers of symmetry.

3. Diamagnetic nickel compounds of the M−N,2O group (trans) usually form crystals isostructural with the crystals of the corresponding copper compounds, and in most cases the metal atoms are at the centers of symmetry. However, several exceptions are known. In known cases in the M−→N,2O(cis) group corresponding copper and nickel compounds are not isostructural.

4. Because of the paucity of structure data on crystals of compounds in the M−4N group, no definite conclusions can be drawn. Cases of similarity as well as sharp difference between the structures of corresponding internal copper and nickel complexes are known.

LITERATURE CITED

1. E. A. Shugam and L. M. Shkol'nikova, Usp. khimii 28, 889 (1959).
2. A. I. Kitaigorodskii, Organic Crystal Chemistry [in Russian] (Izd. AN SSSR, Moscow, 1955).
3. F. H. Herbstein and F. R. L. Schoening, Acta Cryst. 10, 657 (1957).
4. A. I. Kitaigorodskii, Kristallografiya 3, 391 (1958).
5. Landolt-Börnstein, Atom- und Molecularphysik (Berlin, 1955) Part 4.
6. A. F. Wells, J. Chem. Soc., 1662 (1947).
7. G. N. Tishchenko, Trudy Inst. kristallografii 11, 93 (1955).
8. L. Cavalca, M. Nardelli, and D. Grezioli, Gazz. chim. ital. 86, 104 (1956).
9. M. A. Porai-Koshits, Zh. neorgan. khimii 4, 730 (1959).
10. G. N. Tishchenko, P. M. Zorkii, and M. A. Porai-Koshits, Zh. strukt. khimii (1961) (in press).
11. D. P. Mellor and D. P. Craig, J. Proc. Roy. Soc. N. S. Wales 74, 475 (1940).
12. H. S. Frenk, M. Z. Magel, and E. Sheffield, J. Am. Chem. Soc. 64, 1924 (1942).
13. L. Pauling. J. Am. Chem. Soc. 54, 994 (1932).
14. S. Shibata, Bull. Chem. Soc. Japan 30, 842 (1957).
15. D. H. Curtiss, F. K. C. Lyle, and E. C. Lingafelter, Acta Cryst. 5, 388 (1952).
16. G. J. Bullen, Nature 177, 537 (1956).
17. F. K. C. Lyle, B. Morosin, and E. C. Lingafelter, Acta Cryst. 12, 938 (1959).
18. L. Cambi and L. Szegö, Ber. 64, 2591 (1931).
19. J. B. Willis and D. P. Mellor, J. Am. Chem. Soc. 69, 1237 (1947).
20. L. Malatesta and R. Pizzoti, Chim. e ind. (Milan) 27, 6 (1945).
21. L. Cambi and C. Coriselli, Gazz. chim. ital. 66, 81 (1936).
22. L. Malatesta, Gazz. chim. ital. 67, 738 (1937).
23. J. G. Peyronel, Z. Krist. 103, 139, 157 (1940).
24. J. G. Peyronel, Gazz. chim. ital. 73, 89 (1943).
25. E. A. Shugam and L. M. Shkol'nikova, Kristallografiya 3, 749 (1958).
26. J. G. Peyronel and A. Pignedoli, Ricerca sci. 29, 1505 (1959).
27. Z. V. Zvonkova, G. S. Zhadanov, and N. P. Ramnev, Kristallografiya 1, 514 (1956).
28. L. E. Godycki and R. E. Rundle, J. Chem. Phys. 19, 1205 (1951).
29. L. E. Godycki and R. E. Rundle, Acta Cryst. 6, 487 (1953).
30. D. E. Williams, G. Wohlaner, and R. E. Rundle, J. Am. Chem. Soc. 81, 755 (1959).
31. E. Frasson, R. Zanetti, R. Bardi, S. Bezzi, and G. Ciacometti, J. Inorg. and Nuclear Chem. 8, 452 (1958).
32. E. Frasson, R. Bardi, and S. Bessi, Acta Cryst. 12, 201 (1959).
33. E. G. Cox, E. Sharratt, W. Wardlaw, and K. C. Webster, J. Chem. Soc., 129 (1936).
34. Z. Malatesta, Gazz. chim. ital. 68, 319 (1938).
35. E. A. Shugam, Trudy Vses. n.-i. inst. khim. reaktivov 22, 53 (1958).
36. L. L. Merrit, C. Guare, and A. E. Lessor, Acta Cryst. 9, 253 (1956).
37. E. G. Cox, F. W. Pinkard, W. Wardlaw, and K. C. Webster, J. Chem. Soc., 459 (1935).
38. M. Stackelberg. Z. anorg. Chem. 253, 136 (1947).
39. W. Klemm and K. H. Raddatz, Z. anorg. u. algem. Chem. 250, 207 (1942).
40. J. N. Tyson and S. C. Adams, J. Am. Chem. Soc. 62, 1228 (1940).
41. V. V. Zelentsov, I. A. Savich, and V. B. Evdokimov, Nauchn. dokl. vyssh. shkoly, Khimiya i khim. tekhnologiya, 672 (1958).
42. S. E. Livingstone, J. Chem. Soc., 1042 (1956).
43. C. M. Harris, S. L. Lenzer, and R. L. Martin, Austral. J. Chem. 11, 331 (1958).
44. M. Calvin and D. H. Barkelew, J. Am. Chem. Soc. 68, 2267 (1946).
45. L. Sacconi, J. Am. Chem. Soc. 74, 4503 (1952).
46. L. Sacconi, J. Am. Chem. Soc. 76, 3400 (1954).
47. A. K. Mukherjee and P. Ray, J. Ind. Chem. Soc. 32, 604, 633 (1955).
48. S. H. Simonsen and C. E. Pfluger, Acta Cryst. 10, 471 (1957).
49. S. H. Simonsen and C. E. Pfluger, Acta Cryst. 10, 536 (1957).

50. I. Lifschitz and K. M. Dijkema, Rec. trav. chim. Pays Bas 60, 581 (1941).
51. D. P. Mellor, J. Proc. Roy. Soc. N. S. Wales 75, 157 (1941).
52. L. Sacconi and P. Paoletti, J. Am. Chem. Soc. 79, 4062 (1957).
53. E. G. Cox and K. C. Webster, J. Chem. Soc., 731 (1935).
54. E. A. Shugam, Dokl. AN SSSR 81, 853 (1951).
55. H. Kojama, Y. Saito, and H. Kuroja, J. Inst. Politech., Osaka City Univ. 4, 43 (1953).
56. E. A. Shugam, Zh. fiz. khimii 28, 643 (1954).
57. J. M. Robertson, J. Chem. Soc. 1222 (1951).
58. É. A. Gilinskaya and M. A. Porai-Koshits, Kristallografiya 4, 241 (1959).
59. J. M. Robertson and J. Woodward, J. Chem. Soc. 219 (1937), 36 (1940).
60. J. Speakmen, Acta Cryst. 6, 784 (1953).
61. A. J. Stosick, J. Am. Chem. Soc. 67, 362 (1945).
62. J. M. Stewart and E. C. Lingafelter, Acta Cryst. 12, 842 (1959).
63. E. Frasson and L. Sacconi, J. Inorg. and Nuclear Chem. 8, 443 (1958).
64. E. Frasson, C. Panattoni, and L. Sacconi, H. Phys. Chem. 63, 1908 (1959).

All abbreviations of periodicals in the above bibliography are letter-by-letter transliterations of the abbreviations as given in the original Russian journal. *Some or all of this periodical literature may well be available in English translation.* A complete list of the cover-to-cover English translations appears at the back of this issue.

X-RAY INVESTIGATION OF THE NORMAL PARAFFIN $C_{34}H_{70}$ UNDER PRESSURES UP TO 16000 kg/cm²

S. S. Kabalkina and Z. V. Troitskaya

Institute of High-Pressure Physics, Academy of Sciences, USSR
Translated from Zhurnal Strukturnoi Khimii, Vol. 2, No. 1,
pp. 27-32, January-February, 1961
Original article submitted February 3, 1960

The compressibility and phase transitions between the rhombic and triclinic modifications of the normal paraffin $C_{34}H_{70}$ under high pressures have been studied by the x-ray method. The kinetics of the phase transition was studied and the activation energy determined. Conditions influencing polymorphic transitions under high pressures in the paraffins n-$C_{30}H_{62}$, n-$C_{32}H_{66}$, and n-$C_{34}H_{70}$ have been determined.

The structure of the normal paraffin n-$C_{34}H_{70}$ under high pressures was investigated with the x-ray camera described in [1]. The paraffin sample 0.4-0.5 mm in diameter was placed in the channel of the beryllium cone. Pressure was transmitted to the sample by means of ligroin through a lithium partition 0.3-0.5 mm thick (the partition protects the sample from ligroin). The pressure in the ligroin was measured with a manganin manometer to within ±100 kg/cm². A sharp-focus tube with a copper anode was used; the cassette diameter was 86 mm. Figure 1 shows four x-ray patterns of n-$C_{34}H_{70}$ taken on the same film under different pressures P: a) 1 kg/cm² (before compression); b) 7100 kg/cm²; c) 12300 kg/cm²; d) 1 kg/cm² (after release of pressure). The x-ray pattern a corresponds to the rhombic modification [only the (110) and (200) lines of the R-modification are present], while b, c, and d represent mixtures of the rhombic and triclinic modifications (in addition to the "rhombic" lines these patterns contain lines characteristic of triclinic paraffins; see Table 1).

Fig. 1. X-ray patterns of n-$C_{34}H_{70}$.

TABLE 1. Interplanar Spacings for the Strongest Reflections of the R, T, and R + T Modifications

Modification	Paraffin	P, kg/cm²	Interplanar spacing, A				
T	n-$C_{20}H_{42}$	1	4,54		3,79		3,58
R	n-$C_{34}H_{70}$	1		4,12		3,73	
R + T	"	14000	4,21	3,84	3,59	3,43	3,18
R + T	"	1 (after release)	4,54	4,12	3,86	3,72	3,56

TABLE 2. Linear Compressibilities on n-$C_{34}H_{70}$ Along the a and b Directions

P, kg/cm²	expt. Δa/a, %	calc. Δa/a, %	expt. Δb/b, %	calc. Δb/b, %	P, kg/cm²	expt. Δa/a, %	calc. Δa/a, %	expt. Δb/b, %	calc. Δb/b, %
3200	2,2	2,2	1,8	2,1	11400	6,0	6,6	5,4	6,1
4900	3,2	3,3	3,0	3,1	12600	6,8	7,1	6,5	6,5
6400	4,2	4,2	3,5	3,9	13400	7,4	7,4	6,0	6,7
7300	4,6	4,6	4,4	4,3	13900	7,9	7,6	6,8	6,8
8100	5,6	5,1	4,5	4,7	14500	8,0	7,8	6,7	7,0
8300	5,2	5,2	4,8	4,8	15200	7,1	8,0	7,4	7,2
9500	5,7	5,8	5,6	5,3	16300	7,4	8,2	7,1	7,4

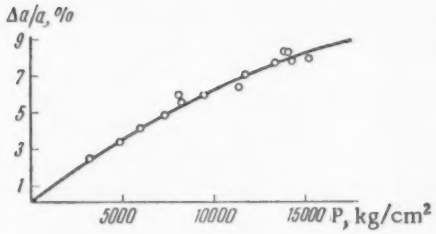

Fig. 2. Dependence of the linear compressibility Δa/a of n-$C_{34}H_{70}$ on pressure.

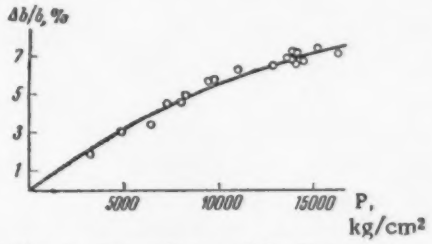

Fig. 3. Dependence of the linear compressibility Δb/b of n-$C_{34}H_{70}$ on pressure.

Thus, a polymorphic transition of n-$C_{34}H_{70}$, accompanied by partial conversion of the crystals from the rhombic into the triclinic modification, was detected under high pressures at room temperature; this transition is virtually irreversible at room temperature (in x-ray pattern d of Fig. 1, after release of pressure, only the lines of the triclinic phase are retained).

Investigation of the Rhombic Modification of n-$C_{34}H_{70}$ at Pressures up to 16000 kg/cm²

The x-ray patterns of n-$C_{34}H_{70}$ make it possible to determine the constants a and b of the R-modification under various pressures, and thus to estimate the compressibilities Δa/a and Δb/b. The calculations were based on the effective radius of the camera determined for each x-ray pattern from the photograph obtained at atmospheric pressure before compression of the sample. The linear compressibilities of n-$C_{34}H_{70}$ at various P are given in Table 2. The relationships between Δa/a and Δb/b and P may be represented analytically by second degree polynomials the coefficients of which were found by the method of least squares:

$$\Delta a/a = 74 \cdot 10^{-7} \; P - 140 \cdot 10^{-12} \; P^2,$$
$$\Delta b/b = 70 \cdot 10^{-7} \; P - 150 \cdot 10^{-12} \; P^2.$$

The calculated values of Δa/a and Δb/b are given in Table 2. The average deviation between the experimental and calculated values of Δa/a and Δb/b is 7-8%, and the maximum deviation is 15%. Graphical plots of the above-mentioned polynomials and the experimental points are given in Fig. 2 and 3.

It is important to note that the linear compressibility of the n-$C_{34}H_{70}$ crystal, like the compressibility of n-$C_{30}H_{62}$ and n-$C_{32}H_{66}$ [2] is approximately 10% greater in direction a than in direction b. At the same time, anisotropy of thermal expansion of paraffins in the a and b directions has been reported [3, 4] (the coefficient of thermal expansion in the a direction is 3,5-4 times the coefficient of expansion in the b direction).

Distances between nearest hydrogen atoms of neighboring molecules at pressures up to 16000 kg/cm² are given in Table 3. The table is based on geometrical analysis with the aid of the following parameters: C – H

TABLE 3. Shortest H...H Intermolecular Distances (in A) in $n\text{-}C_{34}H_{70}$ Crystals under High Pressures (for symbols, see [7])

Atoms	Pressure, kg/cm²						
	3000	6100	8000	10700	12000	13400	15500
$H_1...H_3$	2,40	2,30	2,25	2,23	2,20	2,18	2,16
$H_2...H_4$	2,83	2,72	2,68	2,64	2,67	2,63	2,61
$H_2...H_5$	2,41	2,30	2,24	2,21	2,19	2,20	2,14

TABLE 4. Concentration of T-Phase in Same Sample at Different Pressures

P, kg/cm²	C_T, %
5200	10
9800	20
14500	50

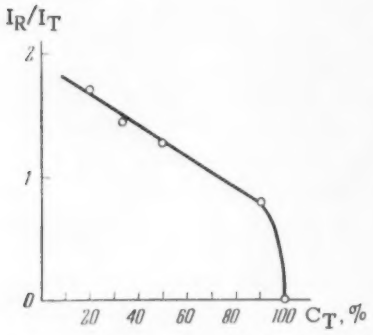

Fig. 4. Variation of I_R/I_T with the concentration of the T-phase (C_T, %) in R + T mixtures.

1.12 A [5] and C – C 1.53 A, distance between two consecutive nonvalence-bonded carbon atoms in the chain 2.54 A, $\varphi b = 41.2°, \varepsilon = 112°$ [6].

The R ⇌ T Polymorphic Transition in $n\text{-}C_{34}H_{70}$

As already stated, the transition from the rhombic to the monoclinic modification is not complete in the pressure range studied. We used quantitative phase analysis for estimating the amount of triclinic phase formed at any given pressure. Mixtures of the paraffins $n\text{-}C_{20}H_{42}$ and $n\text{-}C_{34}H_{70}$ of the following composition were prepared by fusion: 1) 20% + 80%; 2) 34% + + 66%; 3) 50% + 50%; 4) 90% + 10%. By photometric analysis of the x-ray patterns of the mixtures with the MF-4 microphotometer we determined the variations of the relative intensity of the two lines for the R- and T-modifications, I_R/I_T, with the concentration of the T-phase (C_T%); this relationship is plotted in Fig. 4 [I_R is the intensity of the (110) line of the R-modification, I_T is the intensity of the T-phase line of d = 3.56 A]. The curve was plotted from five points, for 20, 34, 50, 90, and 100% of the T-phase. The intensity of each line was estimated from the height of the maximum, which was more accurate in this case than estimation from the area of the whole maximum (maxima of neighboring lines overlap owing to their proximity). The relationship in Fig. 4 makes it possible to estimate the amount of T-phase formed in the transition. The results show that the transition begins at P = 5000 kg/cm². The amount of T-phase in the sample increases with increasing pressure.

Data on the T-phase contents of the same sample under different pressures are given in Table 4.

It was found from a large number of experiments that an average of about 40% of the triclinic modification is formed at P = 12000 kg/cm², and about 50% at P = 14000 kg/cm². In some instances the amount of the T-phase in the samples reached 65% at pressures of 6000-8000 kg/cm².

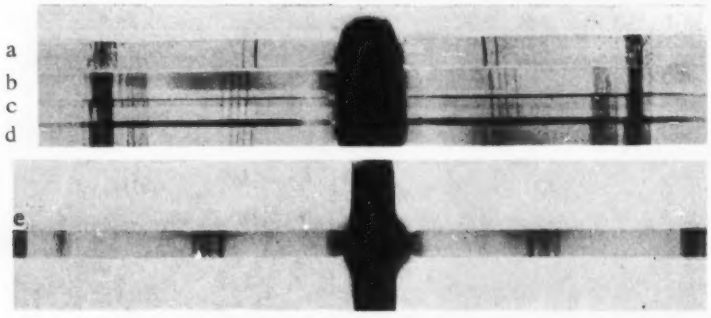

Fig. 5. X-ray patterns of $n\text{-}C_{34}H_{70}$. Cassette diameter 86 mm for patterns a, b, c, and d; 114 mm for e. CuKα radiation.

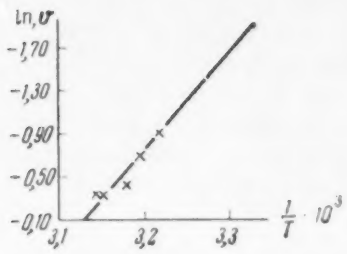

Fig. 6. Variation of ln v with 1/T.

The Residual Effect and Activation Energy of the T→R Transition in n-$C_{34}H_{70}$.

The R→T transition of n-$C_{34}H_{70}$ is virtually irreversible at room temperature. Figure 5 shows x-ray patterns of the same sample of n-$C_{34}H_{70}$: a) 1 kg/cm² (before compression); b) 5700 kg/cm², C_T = 58%; c) 7500 kg/cm², C_T = 66%; d) 1 kg/cm² (after release of pressure), C_T = 65%; e) 1 kg/cm², C_T = 65% (the x-ray pattern e was taken a month and a half after d). Therefore after the pressure has been released the sample consists, for an indefinitely long time, of a mixture of the R- and T-modifications of the same composition as the sample under pressure; consequently the rate of the T→R transition at room temperature is virtually zero. The fact that the R- and T-modifications can exist simultaneously indicates that their free energies are similar. However, the T-phase is not stable under atmospheric pressure; it disappears on heating. This effect was utilized in determination of the activation energy of the T→R transition. Suppose that after exposure to high pressure a sample contains C_1 of the T-phase at room temperature T_1 °K; at temperature ($T_2 > T_1$) the amount of T-phase in it decreases in unit time to C_2: the rate of the phase transition at T_2 is $v = 1 - C_2/C_1$. It is known that $v \propto \exp(-U/RT)$, where U is the activation energy of a polymorphic transition.

Having determined v at different temperatures experimentally, we estimated the activation energy U for n-$C_{34}H_{70}$ from the slope of the ln v = f(1/T) line, equal to U/R (Fig. 6). The value found was U = 16 ± 4 kcal/mole. For determination of v−T data, samples containing mixtures of the T-and R-modifications (as the result of previous action of high pressure) were annealed for half an hour in a thermostat (the annealing temperature was recorded to within ± 0.5°); the concentration of the T-phase of the sample before and after annealing was found by photometric analysis of the x-ray patterns.

Conditions Favoring the R → T Transition in n-$C_{30}H_{62}$, n-$C_{32}H_{66}$, and n-$C_{34}H_{70}$

It is interesting to compare the results obtained under high pressures for the paraffins n-$C_{30}H_{62}$, n-$C_{32}H_{66}$, and n-$C_{34}H_{70}$. The R → T phase transition was detected in n-$C_{30}H_{62}$ and n-$C_{32}H_{66}$ under quasihydrostatic pressure; under hydrostatic pressures up to 14000 kg/cm² only lines of the R-modification are present in the x-ray patterns of n-$C_{30}H_{62}$ and n-$C_{32}H_{66}$ [2]. The results of high-pressure investigations of n-$C_{30}H_{62}$, n-$C_{32}H_{66}$, and n-$C_{34}H_{70}$ appear different at first sight. However, different x-ray cameras were used in investigations of these substances. It is possible that differences in the behavior of n-$C_{30}H_{62}$, n-$C_{32}H_{66}$, and n-$C_{34}H_{70}$ may be explained by differences in the character of the pressure acting on the sample during the experiment. To test this hypothesis, we carried out an additional investigation of n-$C_{30}H_{62}$ and n-$C_{32}H_{66}$ under high pressure in the x-ray camera used in the present investigation (the n-$C_{30}H_{62}$ and n-$C_{32}H_{66}$ samples were the same as in [2]). Figure 7 shows four x-ray patterns of n-$C_{30}H_{62}$ taken on the same film in this camera: a) 1 kg/cm², b) 10800 kg/cm², c) 9900 kg/cm², and d) 1 kg/cm²

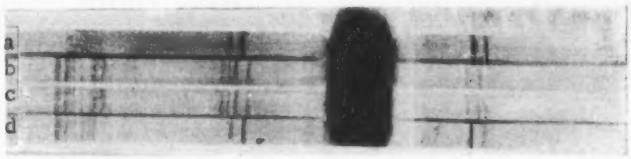

Fig. 7. X-ray patterns of n-$C_{30}H_{62}$. Cassette diameter 86 mm, CuKα radiation.

Fig. 8. X-ray patterns of n-$C_{32}H_{66}$. Cassette diameter 86 mm, CuKα radiation.

(after release of pressure). Figure 8 shows analogous patterns of n-$C_{32}H_{66}$ taken with the same camera: a) 1 kg per cm^2 (before compression); b) 8700 kg/cm^2; c) 1 kg/cm^2 (after release of pressure). The x-ray patterns of n-$C_{30}H_{62}$ and n-$C_{32}H_{66}$ correspond to the R-modification at 1 kg/cm^2 (patterns 7a, 7d, 8a, and 8c), and to mixtures of the R- and T-modifications at high pressures (patterns 7b, 7c, and 8b). Thus, high-pressure R→T transitions in n-$C_{30}H_{62}$, n-$C_{32}H_{66}$, and n-$C_{34}H_{70}$, characterized by partial conversion of the rhombic into the triclinic modifications, have been detected. This has demonstrated once again that the R→T transition in n-$C_{30}H_{62}$ and n-$C_{32}H_{66}$ depends on the character of the pressure exerted on the sample.

In the camera used in this investigation the sample is subjected to stresses from the walls of the plastically deformed beryllium in addition to the hydrostatic pressure. Therefore, the pressure exerted on the sample is not purely hydrostatic, which favors appearance of the T-phase. In contrast to the R→T transition in n-$C_{34}H_{70}$, the corresponding transitions in n-$C_{30}H_{62}$ and n-$C_{32}H_{66}$ are reversible; on release of pressure the T-phase vanishes completely (T-phase lines are absent in patterns 7d and 8b). The cause of this difference has not been established. It may be a consequence of differences in the purity of the samples. It is also possible that the residual effect in n-$C_{34}H_{70}$ is associated with the fact that the potential barrier of the T→R transition is increased with increasing number of carbon atoms in the paraffin molecule. It would therefore be interesting to study n-$C_{36}H_{74}$ under high pressure.

In conclusion, the authors must thank Corresponding Member of the Academy of Sciences USSR L. F. Vereshchagin for his interest and discussion of the results, and V. G. Gorshkov for help in the experimental work.

LITERATURE CITED

1. S. S. Kabalkina and L. F. Vereshchagin, Dokl. AN SSSR 131, 2, 300 (1960).
2. S. S. Kabalkina, Dokl. AN SSSR 125, 114 (1959).
3. A. Müller, Proc. Roy. Soc. (London) A 127, 417 (1930).
4. Yu. V. Mnyukh, Zh. fiz. khimii 33, 7, 1638 (1959).
5. B. K. Vainshtein, A. I. Lobachev, and M. M. Stasova, Kristallografiya 3, 452 (1958).
6. P. W. Teare, Acta Cryst. 12, 294 (1959).
7. A. I. Kitaigorodskii and Yu. V. Mnyukh, Dokl. AN SSSR 121, 2, 291 (1958).

All abbreviations of periodicals in the above bibliography are letter-by-letter transliterations of the abbreviations as given in the original Russian journal. *Some or all of this periodical literature may well be available in English translation.* A complete list of the cover-to-cover English translations appears at the back of this issue.

X-RAY INVESTIGATION OF THE SYSTEMS $BaO - WO_3$, $BaO - MoO_3$ and $BaO - Ta_2O_5$

E. S. Zhmud' and E. P. Ostapchenko

Translated from Zhurnal Strukturnoi Khimii, Vol. 2, No. 1,
pp. 33-45, January-February, 1961
Original article submitted February 28, 1959

In specimens in the $BaO - WO_3$ system heated for 2 hr in air at 1200° formation of the following barium tungstates was established by x-ray diffraction: $BaO \cdot WO_3$ (tetragonal structure; a = 5.56, c = 12.76 A), $2BaO \cdot WO_3$ (structure not interpreted), and $3BaO \cdot WO_3$ (pseudocubic face-centered structure; a = 8.16 A).

In the system $BaO - MoO_3$ (in specimens heated under the same conditions)the barium molybdates $BaO \cdot MoO_3$, $2BaO_3 \cdot MoO_3$ and $3BaO \cdot MoO_3$ are formed; these are fully isostructural with tungstates of the corresponding compositions. However, only the molybdate $BaO \cdot MoO_3$ was detected in the one-phase state.

Investigation of the system $BaO - Ta_2O_5$ (specimens heated in hydrogen) showed that, in accordance with the heating temperature, the following barium tantalates may be obtained: $5BaO \cdot Ta_2O_5$ (1000-1300°), $4BaO \cdot Ta_2O_5$ (1400-1500°) and $7BaO \cdot 7Ta_2O_5$ (1200-1300°). Formation of tantalates $BaO \cdot Ta_2O_5$ and $3BaO \cdot 7Ta_2O_5$ (or probably $BaO \cdot 2.5Ta_2O_5$) was also observed, but these could not be obtained as single phases at heating temperatues up to 1500°.

INTRODUCTION

Impregnated and pressed cathodes have been developed in recent years and are now being used fairly widely as thermionic emitters. The active materials in these cathodes are barium compounds such as $3BaO \cdot WO_3$, $3BaO \cdot Al_2O_3$, etc., usually made by sintering of mixtures of barium carbonate with oxides of various metals (W, Mo, Ta, Al, Zr, Th,etc.) in air or hydrogen at temperatures of the order of 1200°. It should be noted that some of these compounds, as for example $3BaO \cdot WO_3$, were obtained comparatively recently [1, 2] in investigations of oxide and L-cathodes. Previously only the compounds $BaWO_4$ in the system $BaO - WO_3$ and $BaMO_4$ in the system $BaO - MoO_3$ were known; information about compounds formed in the system $BaO - Ta_2O_5$ is restricted to references to aqueous barium meta-and hexatantalates [3].

Investigation of systems consisting of barium oxide and oxides of metals such as W, Mo, Ta, Nb, Ti, Th, Zr, V, Hf, etc. is of considerable interest for cathode electronics at the present time, both with regard to the possible formation of new compounds with high barium oxide contents, and with regard to the conditions for their formation. It is also important to study the structures of the compounds formed and to correlate their structural and emissive properties.

The systems investigated in the present work:

$$BaO - WO_3, \quad BaO - MoO_3 \text{ and } BaO - Ta_2O_5$$

were studied mainly by the x-ray diffraction method, which gives the most objective data on the phase composition of the compounds formed and makes it possible to establish their structure.

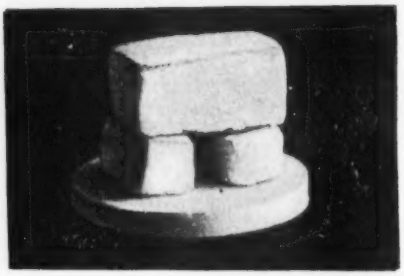

Fig. 1. Specimen on a ceramic disk before heating.

EXPERIMENTAL

Specimens for the Investigation. For preparation of the specimens, mixtures of barium carbonate with the appropriate metal oxide were heated in air or in some instances in hydrogen. It was assumed that the compounds were formed in these systems in accordance with the reaction

$$n\mathrm{BaCO_3} + m\mathrm{Me_xO_y} \rightarrow n\mathrm{BaO} \cdot m\mathrm{Me_xO_y} + n\mathrm{CO_2},$$

where $\mathrm{Me_xO_y} = \mathrm{WO_3}$, $\mathrm{MoO_3}$, $\mathrm{Ta_2O_5}$.

The composition of the specimens used are given in Tables 2, 5, and 6.

The starting materials were first mixed in a jasper mortar in the dry state, and then with addition of alcohol. As the alcohol evaporated, the mixture turned into a claylike mass which was molded in the shape of small bricks. These specimens were placed on disks made from alundum or steatite ceramics; in most cases the specimens which were to be investigated further were stood on supports made from the same mixture as the specimen, so that there was virtually no risk of products formed by reactions of the specimen with the ceramic material contaminating the specimen (Fig. 1). Specimens of all the systems were heated in air in a muffle furnace for 2 hours at definite temperatures; the temperature was usually raised at the rate of 100°/hr and the specimens were cooled with the furnace.

Specimens of the BaO – WO_3 system were heated in air at 1200° (specimens of certain compositions were also heated at lower temperatures).

All specimens of the BaO – MoO_3 system were heated in air at 1200, 1000, 800, and 500°. The heating temperature was lowered from 1200° to 500° because compositions of high MoO_3 contents were almost completely volatilized even at 800°.

Specimens of the system BaO – Ta_2O_5 were heated in air at 1100, 1200, and 1300° , and in hydrogen at temperatures from 900 to 1600° in 100° steps. The reason for this wide temperature range was that the reaction products in the specimens (especially with high Ta_2O_5 contents) consisted of several phases with similar interplanar spacings; in some cases reliable identification of the composition of the specimnes was almost impossible because of this.

All the specimens of any one batch were heated simultaneously in order that errors in determinations of the phase composition due to probable fluctuations of the furnace temperature could be avoided.

The phase composition of the specimens was determined by x-ray diffraction with copper radiation. The x-ray patterns were obtained with cameras of the RKD type (diameter 57.3 mm; sample diameter 0.6 mm) in the URS-55 and URS-70 instruments, and also in the URS-50I instrument with ionization recording of the diffraction pattern.

TABLE 1. Interplanar Spacings and Relative Intensities of X-ray Diffraction Lines of the WO_3 Used in This Investigation

Line No.	I	d (Å)	Line No.	I	d (Å)	Line No.	I	d (Å)	Line No.	I	d (Å)
1	100	3,87	9	90	2,63	17	19	1,92	25	16	1,56
2	97	3,78	10	9	2,53	18	16	1,89	26	38	1,64
3	91	3,67	11	24	2,18	19	49	1,83	27	6	1,56
4	31	3,37	12	29	2,16	20	31	1,81	28	46	1,54
5	29	3,13	13	7	2,04	21	24	1,80	29	12	1,52
6	31	3,10	14	10	2,02	22	25	1,71	30	20	1,50
7	61	2,70	15	8	2,00	23	25	1,69	31	24	1,49
8	47	2,68	16	9	1,97	24	21	1,68	32	6	1,47

TABLE 2. Results for Specimens in the System $BaO - WO_3$, Heated in Air at 1200°

$BaCO_3$:WO_3 (molar %)		External appearance		X-ray phase analysis	
		fusion of specimen	color	phase composition	notes
90:10 83.34:16.66 80:20	9:1 5:1 4:1		outer (dense) layer white; inner, gray	$3BaO \cdot WO_3 + BaCO_3$	Amount of $BaCO_3$ in the reaction product increases with the amount of $BaCO_3$ in the original mixture.
75:25	3:1			$3BaO \cdot WO_3$	
70:30	7:3	did not melt		$3BaO \cdot WO_3 + 2BaO \cdot WO_3$	Intensity of the strongest $3BaO \cdot WO_3$ line about double the intensity of the strongest $2BaO \cdot WO_3$ line
66.67:33.33	2:1		white	$2BaO \cdot WO_3$	
60:40	3:2			$BaO \cdot WO_3 + 2BaO \cdot WO_3$	The strongest $BaO \cdot WO_3$ and $2BaO \cdot WO_3$ lines of approximately equal intensity
50:50	1:1			$BaO \cdot WO_3$	
40:60	2:3	Melted; converted into congealed "drop"; did not separate from ceramic material	pale beige (spongy)	$BaO \cdot WO_3 + BaO \cdot 2WO_3$	$BaO \cdot WO_3$ largely predominant; presence of $BaO \cdot \cdot 2WO_3$ indicated only by a change in the intensity of one $BaO \cdot WO_3$ line coinciding with the strongest $BaO \cdot 2WO_3$
33.33:66.67 30:70	1:2	melted and percolated through ceramic			
20:80	1:4	slight surface fusion; spongy piece remained; did not separate from ceramic	greenish	$WO_3 + BaO \cdot 2WO_3$	Intensity distribution of the WO_3 lines differs somewhat from original; second phase gives very weak lines
10:90	1:9	did not melt			

Fig. 2. Diffractograms of the original substances and barium tungstates (abscissa – 2 Θ, ordinate – relative intensity): 1) $BaCO_3$, 2) $3\,BaO \cdot WO_3$, 3) $2BaO \cdot WO_3$, 4) $BaO \cdot WO_3$, 5) $BaO \cdot 2WO_3$, 6) WO_3

The specimens for investigation in the URS-50I instrument were made by pressing of the powder to be studied into a special aluminum support. The counter speed was 2°/min and the speed of the recorder chart was 2 cm/min.

X-ray phase analysis of barium carbonate, which was one of the initial components in all three systems, gave values of the interplanar spacings which completely agreed with literature data [4]. The interplanar spacings of the tungsten trioxide used in the work (Table 1) differed from the literature data.

Molybdenum trioxide was prepared by calcination of ammonium molybdate $(NH_4)_2MoO_4$ in air at 600°. The interplanar spacings of the MoO_3 were close to the values given in tables.

The original tantalum pentoxide was prepared by calcination of tantalum powder in air at 600°. Its interplanar spacings coincided completely with the values given for the low-temperature β-form of Ta_2O_5 [5]. When heated for 2 hr in hydrogen at 1400° and higher, tantalum pentoxide is completely converted into the low-temperature form (α-Ta_2O_5).

The System $BaO - WO_3$. The results of x-ray phase analysis of specimens in the system $BaO - WO_3$ together with the results of external visual inspection of these specimens are given in Table 2. It should be noted that in this and subsequent tables of the same type the sequence in which the phases are recorded is determined by the intensity of the strongest line of each phase; i.e., the first phase recorded is the one with the highest intensity of the strongest line.

It is clear from this table that one-phase products in the system $BaO - WO_3$ are formed (under the temperature conditions studied) at molar $BaCO_3 \cdot WO_3$ ratios of 1:1, 2:1,

TABLE 3. Interplanar Spacings and Relative Intensities of X-ray Diffraction Lines of Barium Tungstates

$BaO \cdot WO_3$			$2BaO \cdot WO_3$						$3BaO \cdot WO_3$		
Line No.	I	d (Å)	Line No.	I	d (Å)	Line No.	I	d (Å)	Line No.	I	d (Å)
1	100	3,34	1	44	3,50	17	9	1,89	1	100	3,05
2	33	3,17	2	17	3,32	18	26	1,84	2	5	2,58
3	44	2,78	3	100	3,16	19	35	1,76	3	29	2,15
4	68	2,09	4	87	3,07	20	14	1,74	4	38	1,76
5	18	$1,97_4$	5	62	2,97	21	33	1,71	5	7	1,65
6	35	$1,85_6$	6	46	2,84	22	22	1,68	6	13	1,52
7	47	$1,69_9$	7	44	2,72	23	24	1,66	7	7	1,46
8	37	$1,67_3$	8	31	2,64	24	21	1,63	8	12	$1,36_2$
9	16	$1,57_8$	9	22	2,40	25	15	1,59	9	2	$1,31_6$
10	13	$1,37_2$	10	17	2,26	26	11	1,55	10	3	$1,27_0$
11	27	$1,35_2$	11	25	2,21	27	4	$1,49_4$	11	4	$1,23_9$
12	14	$1,28_9$	12	22	2,18	28	15	$1,45_9$	12	3	$1,20_4$
13	8	$1,25_0$	13	49	2,10	29	32	$1,43_6$	13	7	$1,15_4$
14	14	$1,23_6$	14	10	2,07	30	8	$1,39_5$	14	3	$1,12_2$
15	7	$1,20_6$	15	40	1,95	31	14	$1,36_0$			
16	14	$1,16_3$	16	9	1,91	32	13	$1,32_7$			

TABLE 4. Results for Specimens in the System $BaO-MoO_3$, Heated in Air

$BaCO_2$:MoO_2 (molar %)		Phase composition of specimens heated in air for 2 hours at:			
		500 °C*	800 °C**	1000 °C***	1200 °C****
90 : 10	9 : 1	$BaCO_3$+$BaO \cdot MoO_3$+trace MoO_3	$BaCO_3$+$BaO \cdot MoO_3$	$BaCO_3$ + $2BaO \cdot MoO_3$ + + trace $3BaO \cdot MoO_3$	$BaCO_3$+$3BaO \cdot MoO_3$+ + (?) trace $BaO \cdot MoO_3$ + (?)
83,34 : 16,66	5 : 1	$BaCO_3$+$BaO \cdot MoO_3$+MoO_3			$3BaO \cdot MoO_3$+(?) $BaO \cdot MoO_3$ + +(?) trace $2BaO \cdot MoO_3$+$BaCO_3$+(?)
80 : 20	4 : 1				$3BaO \cdot MoO_3$ + (?) $BaO \cdot MoO_3$+ +$BaCO_3$+(?) trace $2BaO \cdot MoO_3$+(?)
75 : 25	3 : 1			$BaCO_3$ + $2BaO \cdot MoO_3$ + + trace $3BaO \cdot MoO_3$+ $BaO \cdot MoO_3$	$2BaO \cdot MoO_3$+(?) $BaCO_3$+ +(?) $BaO \cdot MoO_3$
70 : 30	7 : 3		$BaO \cdot MoO_3$+BaC_3O	$BaO \cdot MoO_3$ + $2BaO \cdot MoO_3$ + + (?) trace $BaCO_3$	$BaO \cdot MoO_3$+$2BaO \cdot MoO_3$+(?) $BaCO_3$
66,67 : 33,33	2 : 1			$2BaO \cdot MoO_3$+$BaO \cdot MoO_3$+(?)$BaCO_3$	$BaO \cdot MoO_3$+$2BaO \cdot MoO_3$+ + (?) trace $BaCO_3$
60 : 40	3 : 2	$BaO \cdot MoO_3$ + MoO_3 + $BaCO_3$		$BaO \cdot MoO_3$ + $2BaO \cdot MoO_3$	$BaO \cdot MoO_3$ + $2BaO \cdot MoO_3$
50 : 50	1 : 1	$BaO \cdot MoO_3$+MoO_3+$BaCO_3$+ + (?) trace $BaO \cdot 2MoO_3$	$BaO \cdot 2MoO_3$	$BaO \cdot MoO_3$	$BaO \cdot MoO_3$
40 : 60	2 : 3	$BaO \cdot MoO_3$ + MoO_3+$BaCO_3$ + + (?) $BaO \cdot 2MoO_3$	$BaO \cdot MoO_3$+$BaO \cdot 2MoO_3$	$BaO \cdot MoO_3$+ trace $BaO \cdot 2MoO_3$	$BaO \cdot MoO_3$+ (?) trace $BaO \cdot 2MoO_3$
33,33 : 66,67	1 : 2			$BaO \cdot MoO_3$ + $BaO \cdot 2MoO_3$ + (?)	
30 : 70	3 : 7	MoO_3+$BaO \cdot MoO_3$+(?)$BaO \cdot 2MoO_3$+ +$BaCO_3$			specimen volatilized
20 : 80	1 : 4		specimen volatilized	specimen volatilized	
10 : 90	1 : 9	MoO_3+$BaO \cdot MoO_3$+$BaCO_3$+ + (?) $BaO \cdot 2MoO_3$			

*Temperature raised during about 4 hours; cooling with furnace.

**Temperature raised during about 5 hours; cooling with furnace.

*** Temperature raised during about 6 hours; cooling with furnace.

**** Temperature raised at 100°/hour, cooling with furnace.

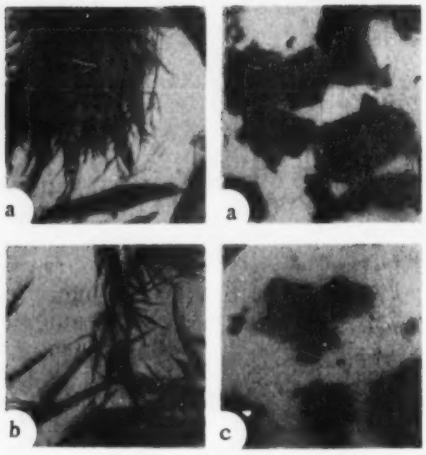

Fig. 3. Electron micrographs of barium tungstates (× 6700): a) $BaO \cdot WO_3$, b) $2BaO \cdot WO_3$, c) $3BaO \cdot WO_3$.

and 3:1. Interpretation of the x-ray patterns of these specimens confirmed the formation of the known barium tungstates $BaO \cdot WO_3$ (at 1:1 ratio) and $3BaO \cdot WO_3$ (at 3:1 ratio) [6]. The diffractograms of these tungstates are given in Fig. 2, and Table 3 gives the interplanar spacings. The $BaO \cdot WO_3$ lattice is tetragonal, with the constant a = 5.56, c = 12.76 A. The $3BaO \cdot WO_3$ lattice is pseudocubic, face centered, with a = 8.61 A [7]. The interplanar spacings for the compound $2BaO \cdot WO_3$ formed at $BaCO_3$: WO_3 = 2:1 initial ratio, are also given in Fig. 3. The structure of this compound has not been fully interpreted.

With more than three molecules of barium carbonate per molecule of tungsten trioxide in the original mixture the solid-phase reaction results in the formation of the "triple" tungstate $3BaO \cdot WO_3$ and a considerable amount of barium carbonate remains unchanged. Increase of the time of heating at 1200° from 2 to 5 hr does not lead to any other results.

At $BaCO_3$:WO_3 ratios of 7:3 and 6:4 mixtures of two phases are formed: $3BaO \cdot WO_3$ and $2BaO \cdot WO_3$ in the former case, and $BaO \cdot WO_3$ and $2BaO \cdot WO_3$ in the latter.

Specimens with $BaCO_3$:WO_3 ratios of 1:2 and 3:7, heated at 1200°, melted completely and "percolated" through the ceramic support. When specimens of the same compositions were heated in air at 1000° they also melted, but the melt did not "percolate" through the ceramic material because it solidified after cooling, and could not be detached from the ceramic material. These specimens were kept on the ceramic material for x-ray phase analysis. The diffractogram of the solidified melt is given in Fig. 2 (curve 5). It must be pointed out that the surface of the solidified melt was rather uneven (spongy), so that its x-ray pattern may have been somewhat imperfect.

When the temperature at which specimens of these compositions were heated was lowered it was found that they melt at 940-950°; the specimen of 1:2 composition melted more actively than the specimen of 3:7 composition, which suggested that in this case a one-phase reaction product of the formula $BaO \cdot 2WO_3$ is formed. Faint lines corresponding to this compound were found in x-ray patterns of the heated specimens with component ratios of 4:6, 1:4, and 1:9, the principal phase in the first of these was barium tungstate $BaO \cdot WO_3$, and in the two others WO_3.

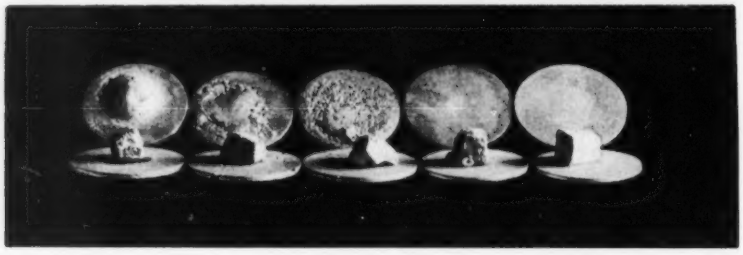

Fig. 4. Specimens in the $BaO - MoO_3$ system, heated in air at 1000°. Specimens containing 80 and 90% MoO_3 (top row, right) volatilized almost completely; specimens of 2:3, 1:2 and 3:7 composition (top left) contained a phase melting at 1000°; specimens 9:1, 4:1, 3:1, 7:3 and 1:1 composition (bottom row, left to right) retained the "brick" shape.

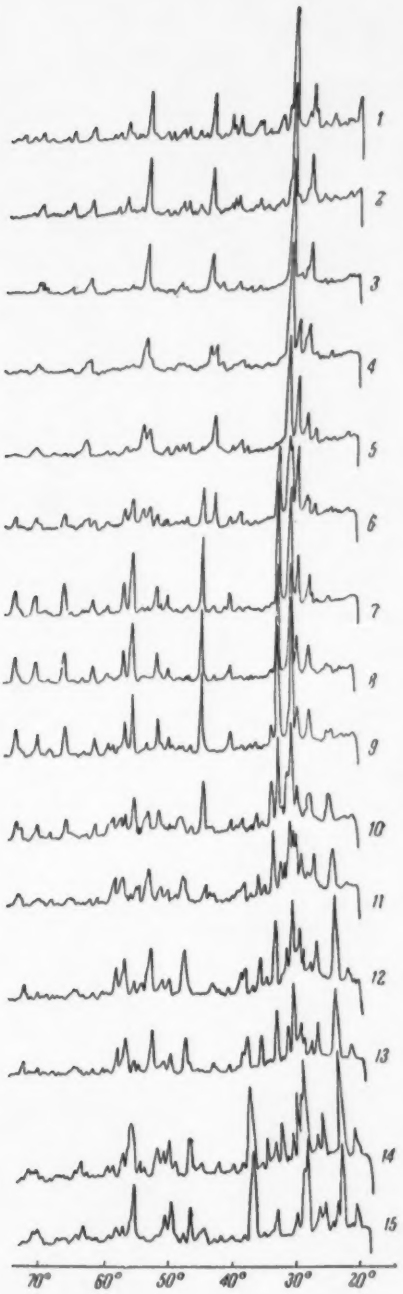

Fig. 5. Diffractograms of specimens in the system $BaO-Ta_2O_5$, heated in hydrogen at 1200°. Composition of specimens ($BaCO_3$:Ta_2O_5): 1) 9:1; 2) 7:1; 3) 5:1; 4) 4.5:1; 5) 4:1; 6) 3:1; 7) 7:3; 8) 2:1; 9) 3:2; 10) 1:1; 11) 2:3; 12) 3:7, 13) 1:4; 14) 1:9; 15) Ta_2O_5

The formation of a compound with such a low melting point in the system $BaO - WO_3$ is of definite interest; accordingly, preliminary experiments on the formation and behavior of this compound were carried out. It was found that when a specimen of 1:2 composition is held in the furnace for several minutes at 950° the melt begins to "boil". If it is removed quickly from the furnace it hardens rapidly and becomes greenish (if removed immediately after formation of the melt) or yellowish (if held in the furnace at 950° for some time). If the specimen is taken out of the furnace before complete fusion a small region of a pale lettuce color, with a smooth surface, remained on the ceramic material in the center of the specimen. X-ray phase analysis of such a specimen showed that in addition to the newly formed compound $BaO \cdot 2WO_3$ the tungstate $BaO \cdot WO_3$ and free tungsten oxide are present. When the heating temperature was lowered to 930, 900, and 850° it was found that at these temperatures the tungstate $BaO \cdot WO_3$ is formed in specimens of 1:2 composition and a considerable amount of unchanged tungsten trioxide remains.

For elucidation of the processes taking place at these temperatures a mixture of $BaO \cdot WO_3$ and WO_3 in 1:1 molar ratio was specially prepared (the tungstate $BaO \cdot WO_3$ was made by heating of $BaCO_3 + WO_3$ mixture at 1200°); when this mixture was heated at 940-950° the same results were obtained as with $BaCO_3 + 2WO_3$. These results show that the mixture of $BaO \cdot WO_3 + WO_3$ which is formed in $BaCO_3 + 2WO_3$ specimens at temperatures below 850° melts with formation of a compound to which the formula was ascribed.

The kinetics of formation of various barium tungstates in the system $BaO - WO_3$ was not studied specially in this investigation, but a number of experiments showed that formation of $BaO \cdot WO_3$ goes to completion even at 850° (in 2 hr). At the same temperature the tungstate $2BaO \cdot WO_3$ appears in $2BaCO_3 + WO_3$ mixture, but the tungstate $BaO \cdot WO_3$ and unconverted barium carbonate are also found in the specimen. In the mixture $3BaCO_3 + WO_3$ at 850° the tungstates $BaO \cdot WO_3$ and $2BaO \cdot WO_3$ are formed (unchanged $BaCO_3$ also remains), while traces of the tungstate $3BaO \cdot WO_3$ appear only after this mixture has been heated for 2 hr at 950°. Thus it may be supposed that the tungstate $2BaO \cdot WO_3$ is formed during further heating of the mixture of $BaO \cdot WO_3$ formed with $BaCO_3$, while the tungstate $3BaO \cdot WO_3$ is formed when a mixture of $2BaO \cdot WO_3$ with $BaCO_3$ is heated.

The x-ray phase analysis of these three barium tungstates was repeated after they had been kept for a long time (about 5 months) in air at room temperature; it was found that their structure remained without change.

Electron micrographs of barium tungstate, obtained with the ÉM-3 instrument, showed (Fig. 3) that the crystals of the tungstate tungstate $3BaO \cdot WO_3$ in contrast to the tungstates $2BaO \cdot WO_3$ and $BaO \cdot WO_3$ are of specific acicular form.

The System $BaO - MoO_3$. The results of x-ray phase analysis of specimens in the system $BaO - MoO_3$, heated at various temperatures, are given in Table 4.

The following conclusions may be drawn from this table.

TABLE 5. Results for Specimens in the System $BaO - Ta_2O_5$, Heated in Hydrogen

$BaCO_3$: : Ta_2O_5	Phase composition of specimens heated in hydrogen for 2 hours at:				
	1000°C	1100°C	1300°C	1500° C	1600°C
9 : 1					
7 : 1	$5BaO \cdot Ta_2O_5$ + (?)	$5BaO \cdot Ta_2O_5$ + (?)	$5BaO \cdot Ta_2O_5$ + (?)	$5BaO \cdot Ta_2O_5$ + (?)	$5BaO \cdot Ta_2O_5$ + (?)
5 : 1	$5BaO \cdot Ta_2O_5$	$5BaO \cdot Ta_2O_5$	$5BaO \cdot Ta_2O_5$	$5BaO \cdot Ta_2O_5$ + + trace $4BaO \cdot Ta_2O_5$	$5BaO \cdot Ta_2O_5$ + $4BaO \cdot Ta_2O_5$
4,5 : 1	$5BaO \cdot Ta_2O_5$ + + trace $7BaO \cdot 3Ta_2O_5$	$5BaO \cdot Ta_2O_5$ + + trace $4BaO \cdot Ta_2O_5$	$5BaO \cdot Ta_2O_5$ + $4BaO \cdot Ta_2O_5$	$4BaO \cdot Ta_2O_5$ + + $5BaO \cdot Ta_2O_5$	$4BaO \cdot Ta_2O_5$ + $5BaO \cdot Ta_2O_5$
4 : 1		$5BaO \cdot Ta_2O_5$ + $4BaO \cdot Ta_2O_5$	$4BaO \cdot Ta_2O_5$ + + trace $5BaO \cdot Ta_2O_5$	$4BaO \cdot Ta_2O_5$	$4BaO \cdot Ta_2O_5$ + $7BaO \cdot 3Ta_2O_5$
3 : 1		$4BaO \cdot Ta_2O_5$ + $7BaO \cdot 3Ta_2O_5$ + + trace $5BaO \cdot Ta_2O_5$	$4BaO \cdot Ta_2O_5$ + $7BaO \cdot 3Ta_2O_5$	$7BaO \cdot 3Ta_2O_5$ + + $4BaO \cdot Ta_2O_5$	$7BaO \cdot 3Ta_2O_5$ + $4BaO \cdot Ta_2O_5$
7 : 3	$5BaO \cdot Ta_2O_5$ + $7BaO \cdot 3Ta_2O_5$ + + trace $BaO \cdot Ta_2O_5$	$7BaO \cdot 3Ta_2O_5$ + $4BaO \cdot Ta_2O_5$	$7BaO \cdot 3Ta_2O_5$	$7BaO \cdot 3Ta_2O_5$ + + $3BaO \cdot 7Ta_2O_5$	$7BaO \cdot 3Ta_2O_5$ + $3BaO \cdot 7Ta_2O_5$
2 : 1	$7BaO \cdot 3Ta_2O_5$ + $5BaO \cdot Ta_2O_5$ + + trace $BaO \cdot Ta_2O_5$ + + trace β-Ta_2O_5		$7BaO \cdot 3Ta_2O_5$ + $3BaO \cdot 7Ta_2O_5$		
3 : 2	$7BaO \cdot 3Ta_2O_5$ + trace $BaO \cdot Ta_2O_5$ + trace β-Ta_2O_5	$7BaO \cdot 3Ta_2O_5$ + + trace $3BaO \cdot 7Ta_2O_5$ + + trace β-Ta_2O_5			$3BaO \cdot 7Ta_2O_5$ + $7BaO \cdot 3Ta_2O_5$ + $BaO \cdot Ta_2O_5$
1 : 1	$7BaO \cdot 3Ta_2O_5$ + $BaO \cdot Ta_2O_5$ + + β-Ta_2O_5	$7BaO \cdot 3Ta_2O_5$ + + $3BaO \cdot 7Ta_2O_5$ + β-Ta_2O_5	$7BaO \cdot 3Ta_2O_5$ + $3BaO \cdot 7Ta_2O_5$ + $BaO \cdot Ta_2O_5$	$3BaO \cdot 7Ta_2O_5$ + + $BaO \cdot Ta_2O_5$ + + trace $7BaO \cdot 3Ta_2O_5$	$3BaO \cdot 7Ta_2O_5$ + $BaO \cdot Ta_2O_5$ + + trace $7BaO \cdot 3Ta_2O_5$
2 : 3	$7BaO \cdot 3Ta_2O_5$ + β-Ta_2O_5 + + $BaO \cdot Ta_2O_5$	$7BaO \cdot 3Ta_2O_5$ + + $3BaO \cdot 7Ta_2O_5$ + + trace $BaO \cdot Ta_2O_5$ + β-Ta_2O_5	$3BaO \cdot 7Ta_2O_5$ + $BaO \cdot Ta_2O_5$ + + $7BaO \cdot 3Ta_2O_5$ + trace β-Ta_2O_5		$3BaO \cdot 7Ta_2O_5$ + $BaO \cdot Ta_2O_5$ + + trace α-Ta_2O_5 + + trace $7BaO \cdot 3Ta_2O_5$
3 : 7	β-Ta_2O_5 + $BaO \cdot Ta_2O_5$ + + $7BaO \cdot 3Ta_2O_5$	$3BaO \cdot 7Ta_2O_5$ + β-Ta_2O_5 + + $7BaO \cdot 3Ta_2O_5$ + $BaO \cdot Ta_2O_5$	$3BaO \cdot 7Ta_2O_5$ + β-Ta_2O_5 + + trace α-Ta_2O_5 + $7BaO \cdot 3Ta_2O_5$ + trace $BaO \cdot Ta_2O_5$	$3BaO \cdot 7Ta_2O_5$ + (?)	$3BaO \cdot 7Ta_2O_5$ + $BaO \cdot Ta_2O_5$ + + trace α-Ta_2O_5
1 : 4		β-Ta_2O_5 + $3BaO \cdot 7Ta_2O_5$ + + $BaO \cdot Ta_2O_5$	$3BaO \cdot 7Ta_2O_5$ + β-Ta_2O_5 + + α-Ta_2O_5 + trace $7BaO \cdot 3Ta_2O_5$ + trace $BaO \cdot Ta_2O_5$	$3BaO \cdot 7Ta_2O_5$ + α-Ta_2O_5	$3BaO \cdot 7Ta_2O_5$ + α-Ta_2O_5 + + $BaO \cdot Ta_2O_5$
1 : 9	β-Ta_2O_5 + $BaO \cdot Ta_2O_5$	β-Ta_2O_5 + $3BaO \cdot 7Ta_2O_5$	β-Ta_2O_5 + α-Ta_2O_5 + + $3BaO \cdot 7Ta_2O_5$ + (?)	α-Ta_2O_5 + + trace $3BaO \cdot 7Ta_2O_5$	α-Ta_2O_5 + $3BaO \cdot 7Ta_2O_6$
0 : 1	β-Ta_2O_5	β-Ta_2O_5	β-Ta_2O_5 + α-Ta_2O_5	α-Ta_2O_5	α-Ta_2O_5

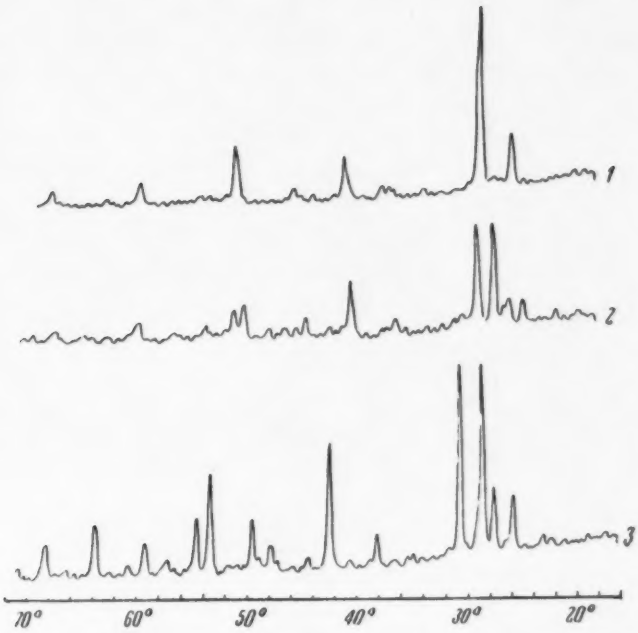

Fig. 6. Diffractograms of barium tantalates: 1) $5BaO \cdot Ta_2O_5$; 2) $4BaO \cdot Ta_2O_5$; 3) $7BaO \cdot 3Ta_2O_5$

TABLE 6. Relative (Visual)* Line Intensities and Interplanar Spacings of Barium Tantalates

Line No.	$7BaO \cdot 3Ta_2O_5$		$4BaO \cdot Ta_2O_5$		$5BaO \cdot Ta_2O_5$	
	I	d (A)	I	d (A)	I	d (A)
1	v.s	3.07	s.	3.18	v.s.	3.01
2	s.	2.89	s.	3.03	s.	2.12
3	s.	2.10	s.	2.20	v.w.	2.01
4	s.	1.82	s.	1.78	s.	1.92
5	s.	1.71	s.	1.75	v. s.	1.74
6	m.	1.67	m.	1.68	v. w.	1.57
7	s.	1.54	v.w.	1.62	m.	1.51
8	s.	1.44_2	w.	1.59	m.	1.36_9
9	s.	1.35_7	s.	1.52	m.	1.34_7
10	s.	1.30_8	s.	1.36_9	w.	1.22_8
11	s.	1.19_1	m.	1.32_1 1.30_9	m.	1.13
12	m.	1.13_2	m.	1.27_7		
13	s.	1.10_3	s.	1.25_0		
14	s.	1.09_1				

*s. = strong; m. = moderate; w. = weak; v. = very.

1. In specimens with predominant molybdenum trioxide contents (and at 500° also in the specimen containing 50% MoO_3) a compound is formed to which, by analogy with tungstates, the formula $BaO \cdot 2MoO_3$ may be ascribed. It should be noted that specimens with $BaCO_3$:MoO_3 ratios of 1:2 and 3:7 (heated at 800 and 1000°) externally resemble the corresponding specimens in the $BaO - WO_3$ system heated at above 940° (Fig. 4). However, in contrast to the $BaO - WO_3$ system, this compound was not obtained as the single phase in any of our molybdate specimens.

2. The molybdate $BaO \cdot MoO_3$ obtained as the single phase when specimens of 1:1 composition were heated at 800° and higher, is formed even at 500°; however, at that temperature the reaction is not completed within 2 hours whatever the component ratio may be, and original substances ($BaCO_3$ and MoO_3) are present in all the heated specimens.

3. The molybdate $2BaO \cdot MoO_3$ is formed after the specimens have been heated at 1000 and 1200°; specimens heated at 500 or 800° do not contain this compound.

4. The molybdate is present as traces in the products of the reaction at 1000°; therefore, this molybdate begins to form at or near this temperature. Specimens heated at 1200° contain considerable amounts of $3BaO \cdot MoO_3$.

5. Barium molybdate $BaO \cdot MoO_3$ was obtained as a single phase, whereas the molybdates $2BaO \cdot MoO_3$ and $3BaO \cdot MoO_3$ were obtained only in mixtures with other phases ($BaO \cdot MoO_3$, $BaCO_3$).

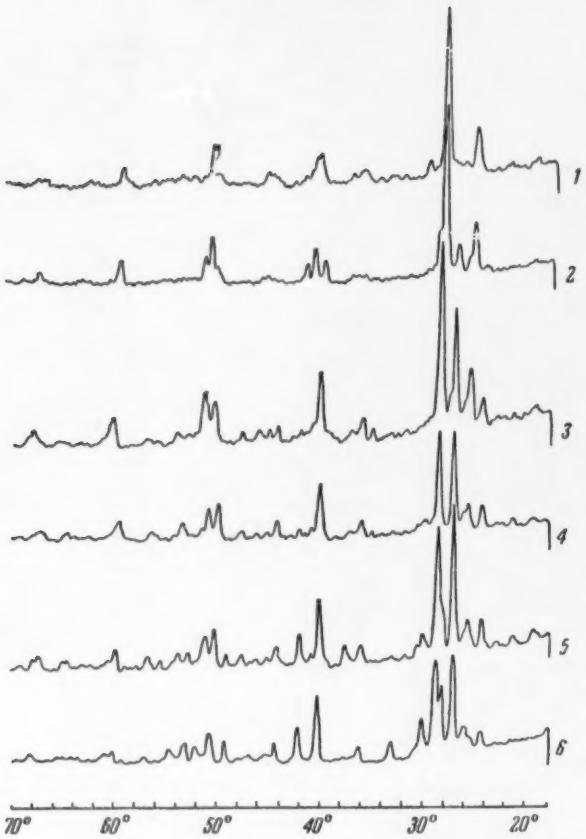

Fig. 7. Diffractograms of a specimen of $4BaCO_3 + Ta_2O_5$, heated in hydrogen at various temperatures: 1) 1000° ($5BaO \cdot Ta_2O_5$ + trace $7BaO \cdot 3Ta_2O_5$); 2) 1100° ($5BaO \cdot Ta_2O_5 + 4BaO \cdot Ta_2O_5$); 3) 1200° ($4BaO \cdot Ta_2O_5 + 5BaO \cdot Ta_2O_5$); 4) 1400° ($4BaO \cdot Ta_2O_5$); 5) 1600° ($4BaO \cdot Ta_2O_5 + 7BaO \cdot 3Ta_2O_5$) 6) 1700° ($4BaO \cdot Ta_2O_5 + 7BaO \cdot 3Ta_2O_5$)

Attempts were accordingly made to obtain molybdates of higher barium contents; for this, a mixture of the molybdate $BaO \cdot MoO_3$ and barium carbonate was heated in air (2 hr at 1200°); the specimens were in the form of small bricks. At the molar ratio $BaO \cdot MoO_3:BaCO_3 = 1:1$ the molybdate $2BaO \cdot MoO_3$ was obtained. However, it proved to be very unstable and was reconverted into the original mixture after 24 hr.

It should be noted that the x-ray patterns of $BaO \cdot MoO_3$ and $BaO \cdot WO_3$ are almost completely indentical (the interplanar spacings and line intensities are similar). The structures of $2BaO \cdot MoO_3$ and $3BaO \cdot MoO_3$ are also similar to the structures of the tungstates $2BaO \cdot WO_3$ and $3BaO \cdot WO_3$ respectively.

The System $BaO - Ta_2O_5$. The results of x-ray phase analysis of specimens in the system $BaO - Ta_2O_5$ heated in hydrogen for 2 hr are given in Table 5.

When specimens in this system were heated at 900, 1200, and 1400° the results did not differ qualitatively from the results at 1000, 1300, 1500, respectively. Heating in air (1100, 1200, 1300°) gave almost the same results as heating in hydrogen at the corresponding temperatures.

The diffractograms of specimens in the system $BaO - Ta_2O_5$, heated in hydrogen at 1200°, are given in Fig. 5.

Table 5 shows that single-phase reaction products were obtained at $BaCO_3$: Ta_2O_5 ratios of 5:1 at 1000-1300°; 4:1 at 1400-1500°; and 7:3 at 1200-1300°.

Accordingly, the formulas $5BaO \cdot Ta_2O_5$, $4BaO \cdot Ta_2O_5$ and $7BaO \cdot 3Ta_2O_5$ respectively were ascribed to these compounds. The diffractograms of these compounds are shown in Fig. 6, and the interplanar spacings are given in Table 6.

The formulas $BaO \cdot Ta_2O_5$ and $3BaO \cdot 7Ta_2O_5$ were ascribed to the compounds which were predominantly formed at $BaCO_3$: Ta_2O_5 ratios of 1:1 and 3:7.

It should be noted that these compounds were not obtained as the single phases at the temperatures given.*

The barium tantalates $5BaO \cdot Ta_2O_5$, $7BaO \cdot 3Ta_2O_5$ and $BaO \cdot Ta_2O_5$ are formed at temperatures of the order of 900-1000°, and formation of $5BaO \cdot Ta_2O_5$ in the corresponding mixture is complete even at 1000°. Complete formation of the tantalate $7BaO \cdot 3Ta_2O_5$ under these conditions took place at 1300°. The tantalates $4BaO \cdot Ta_2O_5$ and $3BaO \cdot 7Ta_2O_5$ begin to appear only at 1100°. It is interesting to note that when a mixture of the composition $4BaCO_3 + Ta_2O_5$ is heated at 1500° the single phase $4BaO \cdot Ta_2O_5$ is formed; on further rise of the heating temperature two phases appear, probably as the result of partial reduction of barium oxide in hydrogen.

Fig. 7. shows the diffractograms of the reaction products in specimens of the composition $4BaCO_3 + Ta_2O_5$, heated at various temperatures. It follows from Table 5 that similar results are obtained in specimens of $5BaCO_3 + Ta_2O_5$ and $7BaCO_3 + 3Ta_2O_5$.

SUMMARY

1. Specimens of the system $BaO - WO_3$, heated in air at 1200°, contained the following barium tungstates: $BaO \cdot WO_3$, $2BaO \cdot WO_3$ and $3BaO \cdot WO_3$. At $BaCO_3$: WO_3 = 1:2 ratio in the same system a mixture of the composition $BaO \cdot WO_3 + WO_3$ is formed; this mixture melts at about 940° with formation of a compound of the probable formula $BaO \cdot 2WO_3$.

2. The main reaction product in the system $BaO - WO_3$ is the tungstate $BaO \cdot WO_3$, formation of which is complete after the appropriate mixture of the original components has been heated for 2 hr at 850°. All the tungstates are stable in air for a considerable time.

3. When specimens in the system $BaO - MoO_3$ are heated in air, three compounds are likewise formed by the solid-state reaction: $BaO \cdot MoO_3$, $2BaO \cdot MoO_3$ and $3BaO \cdot MoO_3$; however, only the molybdate $BaO \cdot MoO_3$ was obtained as a single phase, even at 1200°. The molybdate $2BaO \cdot MoO_3$ was obtained as the single phase when a mixture of $BaO \cdot MoO_3 + BaCO_3$ was heated in air at 1200°.

4. The main compound in the system $BaO - MoO_3$ is the molybdate $BaO \cdot MoO_3$. The structures of the barium molybdates $BaO \cdot MoO_3$, $2BaO \cdot MoO_3$, $3BaO \cdot MoO_3$ are quite similar to the structures of the corresponding tungstates.

5. When specimens of the $BaO - Ta_2O_5$ system are heated in hydrogen, five barium tantalates are formed to which the following formulas may be ascribed: $5BaO \cdot Ta_2O_5$, $4BaO \cdot Ta_2O_5$, $7BaO \cdot 3Ta_2O_5$, $BaO \cdot Ta_2O_5$ and $3BaO \cdot 7Ta_2O_5$. The compounds to which the formulas $7BaO \cdot 3Ta_2O_5$ and $3BaO \cdot 7Ta_2O_5$ are ascribed may in fact be the compounds $2.5\ BaO \cdot Ta_2O_5$ and $BaO \cdot 2.5\ Ta_2O_5$; the mixtures corresponding to the latter compositions had not been investigated.

The results obtained for the system $BaO - Ta_2O_5$ cannot be regarded as completely reliable at this time, because the specimens were heated in hydrogen; this may distort the true phase picture somewhat although almost the same results were obtained when the system was heated in air at 1100, 1200, and 1300°.

LITERATURE CITED

1. E. G. Steward and H. P. Rooksby, Nature 157, 548 (1946).
2. E. P. Ostapchenko, Dissertation (Gos. soyuzn. inst. Ministerstva radiotekhnicheskoi prom., 1954).
3. V. A. Pchelkin, A. F. Efimov, and A. V. Lapitskii, Zh. obshch. khimii 24, 1284, 1495 (1954).
4. A. I. Kitaigorodskii, X-Ray Structure Analysis of Microcrystalline and Amorphous Substances [in Russian] (Gostekhizdat, Moscow, 1952).
5. A. I. Zaslavskii, R. A. Zvinchuk, and A. G. Tutov, Dokl. AN SSSR 104, 3, 409 (1955).
6. R. C. Hughes, P. P. Coppola, and T. H. Evans, J. Appl. Phys. 23, 6, 635 (1952).
7. E. G. Steward and H. P. Rooksby, Acta Cryst. 4, 503 (1951).

* The reaction products at these temperatures in most cases consisted of several phases with close values for the interplanar spacings so that interpretation and identification of the x-ray patterns was difficult. Accordingly, the formulas $BaO \cdot Ta_2O_5$ and $3BaO \cdot 7Ta_2O_5$ are somewhat tentative.

INVESTIGATION OF THE POLYMORPHISM OF 1,8-DINITRONAPHTHALENE

V. M. Kozhin

Institute of Heteroorganic Compounds, Academy of Sciences, USSR
Translated from Zhurnal Strukturnoi Khimii, Vol. 2, No. 1, pp. 46-48,
January-February, 1961
Original article submitted March 6, 1960

The behavior of a single crystal of 1,8-dinitronaphthalene in the temperature range from −195 to + 170° was studied by means of microstructural and differential thermal analysis.

When single crystals of 1,8-dinitronaphthalene were grown from melts it was noticed [1] that they rapidly lost their transparency on cooling. We accordingly investigated 1,8-dinitronaphthalene 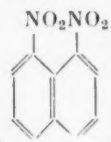 of m. p. 169° by means of microstructural and differential thermal analysis in the temperature range between −195 and +170°. A polarizing microscope with a universal stage [2] was used for this purpose; with this instrument it was possible to observe and photograph the phase transitions in this temperature range.

A Kurnakov pyrometer, calibrated against the melting points of standard substances, was used for measurements of the true phase-transition temperatures and photographic recording of ordinary and differential thermograms. Platinum and gold – palladium wires 0.2 mm in diameter were used for the microthermocouples. For ordinary recording the thermocouple junction was sealed directly in a single crystal of 1,8-dinitronaphthalene weighing 0.009 g (the test specimen), and the other end of the thermocouple for differential recording was sealed into a single crystal of anthracene also 0.009 g in weight (standard). The crystals were placed on a slide on the universal stage so that the specimens were in the field of vision of the polarizing microscope.

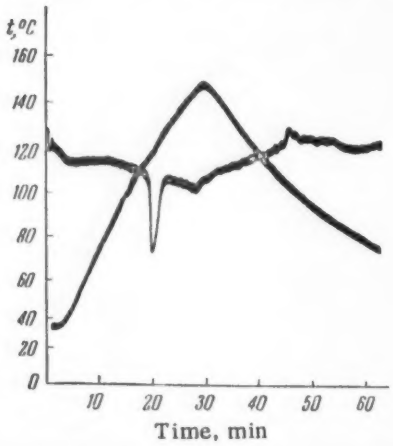

Fig. 1. Heating and cooling curves of a single crystal of 1,8-dinitronaphthalene.

The results revealed the existence of two interconvertible modifications of 1,8-dinitronaphthalene. The low-temperature rhombic form II [3], stable under normal conditions, is reversibly converted into form I at 118-120° (Fig. 1). Figure 2 shows a single crystal of 1,8-dinitronaphthalene in crossed nicols at 20° and at 118°, i.e., at the point where the phase transition begins. The differential heating and cooling curves show the II → I transition very distinctly, whereas the I → II transition is characterized by a weak extremal for the delayed exothermic effect. The extremal for the I → II transition was invariably recorded at 80-100° and not at 118° (Fig. 1). Thus, differential thermal analysis revealed a considerable shift (18-38°) of the temperature of the I → II phase transition relatively to that of the II → I transition. This temperature

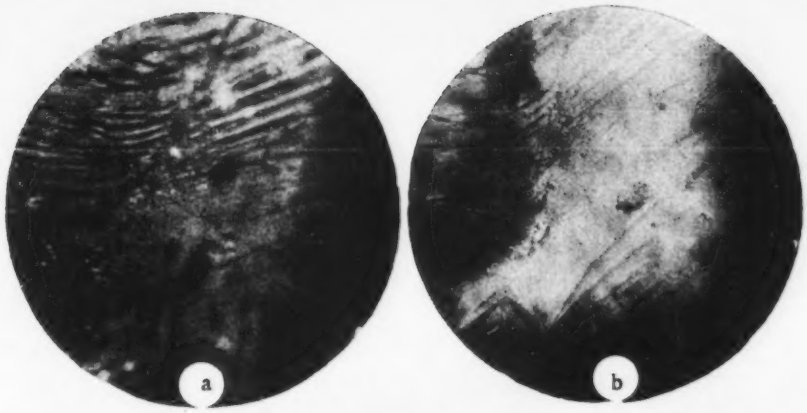

Fig. 2. a) Micrograph (×65) of a single crystal of 1,8-dinitronaphthalene (0.009 g) at 20° in polarized light; b) same at +118°. The bright field represents the start of the phase transition.

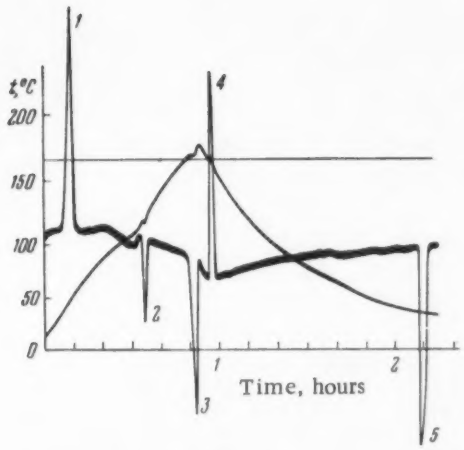

Fig. 3. Heating and cooling thermograms of 1,8-dinitronaphthalene and p-toluidine; 1) Fusion peak of p-toluidine; 2) phase transition peak of 1,8-dinitronaphthalene; 3 and 4) fusion and crystallization peaks of 1,8-dinitronaphthalene; 5) crystallization peak of p-toluidine.

hysteresis of the I ⇌ II phase transition is probably the consequence of the nonequilibrium character of the 1,8-dinitronaphthalene phase transition under these experimental conditions; as Ravich [4] points out, such hysteresis is a very typical effect in phase transitions in organic substances.

Quantitative determinations of the heats of phase transition and fusion of 1,8-dinitronaphthalene are of interest. These values were calculated from the formula:

$$Q_x/Q_e = M_x S_x/M_e S_e,$$

where Q is the heat of transition or fusion in kcal/mole; M is the molecular weight; S is the area of the peak on the differential thermogram curve; the subscripts x and e refer to the test substance and standard respectively.

The standard substances were p-toluidine (m.p. 42°, Q = 4.17 kcal/mole) and benzamide (m.p. 128°, Q = 4.90 kcal/mole). Comparison of the areas of the fusion peaks of the standard substances differentially recorded on the same thermogram showed that our values agree to within ±4% with the literature data (the sample weights were 0.042 g). A comparison of areas of the phase transition and fusion peaks of 1,8-dinitronaphthalene with those of the standard substances, performed by the same method, showed that the heat of phase transition of 1,8-dinitronaphthalene is 1.5 kcal per mole, and the heat of fusion is 5.3 kcal/mole. Figure 3 shows the thermograms of 1,8-dinitronaphthalene, and of p-toluidine used as standard (0.042 g samples).

In conclusion, it is my pleasant duty to thank the director of the laboratory, A. I. Kitaigorodskii, for his constant interest in the work.

LITERATURE CITED

1. A. I. Kitaigorodskii and R. M. Myasnikova, Dokl. AN SSSR 129, 2, 380 (1959).
2. V. A. Vol'nova, Proceedings of the Conference on Thermography [in Russian] (Izd. AN SSSR, Kazan', 1955) p. 121.
3. G. S. Zhdanov and M. M. Umanskii, Zh. fiz. khimii 21, 523 (1947).
4. G. B. Ravich and B. N. Egorov, Dokl. AN SSSR 122, 2, 250 (1958).

CALCULATION OF THE GROUND STATES OF DIBENZENECHROMIUM, THE COBALTICINIUM CATION, AND CHROMOCENE BY THE SELF-CONSISTENT MOLECULAR ORBITAL METHOD

E. M. Shustorovich and M. E. Dyatkina

M. V. Lomonosov Moscow Institute of the Fine Chemical Technology
N. S. Kurnakov Institute of General and Inorganic Chemistry,
Academy of Sciences, USSR
Translated from Zhurnal Strukturnoi Khimii, Vol. 2, No. 1, pp. 49-58,
January-February, 1961
Original article submitted February 14, 1960

The self-consistent molecular orbital method was used for calculating the ground states of dibenzenechromium $(C_6H_6)_2Cr$, the cobalticinium cation $(C_5H_5)_2Co^+$ and chromocene $(C_5H_5)_2Cr$. It was found that these complexes have the electron configurations $\ldots(e_{2g})^4(a'_{1g})^2$, $\ldots(a'_{1g})^2(e_{2g})^4$ and $\ldots(e_{2g})^3(a'_{1g})^1$ respectively [$\ldots$ represents $(a_{1g}\,a_{1u})^4(e_{1g}\,e_{1u})^8$]. The calculated ionization potential of $(C_5H_5)_2Cr$ is 4.82 ev, which is 70% of the experimental value (6.90 ev). It is predicted that the ionization potential of $(C_6H_6)_2Cr$ should be lower than those of $(C_5H_5)_2Cr$ and $(C_5H_5)_2Fe$. The electron density distributions were calculated: $Cr^{+1.5}(C_6H_6^{-0.75})_2$, $Co^{\sim 0.0}(C_5H_5^{+0.5})_2$ and $Cr^{+1.7}(C_5H_5^{-0.85})_2$. The energies of allowed one-electron transitions from the higher occupied a'_{1g} and e_{2g} levels have been calculated for $(C_5H_5)_2Fe$ and $(C_5H_5)_2Co^+$; the results are in good agreement with experimental spectroscopic data.

In the previous paper [1] we calculated the ground state of the ferrocene molecule by the self-consistent molecular orbital method (Roothaan's method [2]). In the present communication this calculation is extended to the isoelectronic cobalticinium cation, which differs from ferrocene by the presence of a positive charge. We then applied the same method to an aromatic metal complex containing benzene molecules (dibenzenechromium) instead of cyclopentadienyl rings. This compound differs from ferrocene in that the organic ligands do not have unpaired electrons, so that all the bonds between the metal and the rings are effected only by donor-acceptor or dative interaction. In addition, we performed similar calculations for a molecule which may be regarded as intermediate between ferrocene and dibenzenechromium, namely chromocene.

The first two of the systems studied, $(C_5H_5)_2Co^+$ and $(C_6H_6)_2Cr$ are, like ferrocene, diamagnetic, so that their singlet ground states were calculated in the same way as for ferrocene. The chromocene molecule in the ground state has two unpaired electrons. Therefore, the Roothaan method in its generalized form for radicals [3] was used to obtain self-consistency.

TABLE 1. Effective Charges in Slater Atomic Orbitals

Charge	Atom		
	C	Cr	Co+
ζ_{2p}	1,6	—	—
$\zeta_{4s,\ 4p}$	—	0,8	1,1
ζ_{3d}	—	1,6	2,2

The matrix elements for cobalticinium and chromocene were calculated from the formulas used for ferrocene. The distances Co – C 2.10 A, Cr – C 2.19 A (as in dibenzenechromium), C – C 1.43 A, and the effective atomic orbital charges of Co and Cr given in Table 1 were assumed. In the case of dibenzenechromium the ring molecular orbitals were written, by analogy with $(C_5H_5)_2M$, in the form of purely effective linear combinations of atomic 2_{p_z}-oribitals of C atoms for a six-membered ring with $\omega = \exp(2\pi i/6)$. The assignment of the ring orbitals and Cr atomic orbitals to the D_{6h} symmetry group was described earlier [4]. Since each benzene ring has six molecular orbitals, the total number of MO in dibenzenechromium

TABLE 2. S_{pg} Matrix Elements

S_{pq}	$(C_5H_5)_2Cr$	$(C_6H_6)_2Cr$	$(C_5H_5)_2Co^+$
$S(a_{1g}, 4s) = S_{12}$	0,239	0,242	0,443
$S(a_{1g}, 3d_{z^2}) = S_{13}$	0,083	—0,078	0,066
$S(a_{1u}, 4p_z) = S_{45}$	0,010	—0,081	0,209
$S(e_{1g}, 3d_{xz}) = S_{67} = S_{89}$	0,402	0,397	0,276
$S(e_{1u}, 4p_x) = S_{10,11} = S_{12,13}$	0,274	0,319	0,409
$S(e_{2g}, 3d_{x^2-y^2}) = S_{14,15} = S_{16,17}$	0,201	0,270	0,140

TABLE 3. H_{pg} Matrix Elements*

H_{pq}	$(C_5H_5)_2Cr$	$(C_6H_6)_2Cr$	$(C_5H_5)_2Co^+$
H_{11}	—3,7953	—4,1212	—4,6905
H_{12}	—0,0867	—0,0838	—0,1607
H_{22}	—3,3334	—3,7310	—5,1248
H_{33}	—4,4330	—4,8757	—6,7583
H_{44}	—3,7953	—4,1212	—4,6905
H_{45}	—0,0036	+0,0280	—0,0758
H_{55}	—3,5256	—3,8886	—5,2739
$H_{66} = H_{88}$	—3,6740	—4,0333	—4,5694
$H_{67} = H_{89}$	—0,1458	—0,1374	—0,1001
$H_{77} = H_{99}$	—4,4934	—5,0272	—6,7902
$H_{10,10} = H_{12,12}$	—3,6740	—4,0333	—4,5692
$H_{10,11} = H_{12,13}$	—0,0994	—0,1104	—0,1484
$H_{11,11} = H_{13,13}$	—3,2506	—3,7309	—5,0029
$H_{14,14} = H_{16,16}$	—3,4776	—3,8576	—4,3728
$H_{14,15} = H_{16,17}$	—0,0729	—0,0934	—0,0508
$H_{15,15} = H_{17,17}$	—4,2217	—4,7226	—6,6359
$H_{18,18} = H_{19,19}$	—3,4776	—3,8576	—4,3728

* All values are given in atomic units (1 at.u. = 27.21 ev).

is 21 (in distinction from 19 MO in complexes of the ferrocene type). The two additional orbitals relate to the b_{1g} and b_{2u} symmetry type and are strongly antibonding; they are high-level C_6H_6 orbitals without analogs among the Cr atomic orbitals; therefore they are of no interest in relation to the ground state of the molecule and we do not give the energies of these MO. The distances in dibenzenechromium were taken as: Cr − C 2.19 A and C − C 1.40 A.

The numerical values of the matrix elements for all three molecules are given above: S_{pq} in Table 2, H_{pq} in Table 3, and G_{pq} in Table 4. Table 5 gives the final forms of the self-consistent molecular orbitals and their energies.

In all cases (including ferrocene) the lowest bonding orbital is the orbital of a_{1g} symmetry, followed by the a_{1u} orbital. The highest occupied orbits in all cases are e_{2g} and a'_{1g} · either of these may be the highest in different molecules (e_{2g} in ferrocene and cobalticinium, and a'_{1g} in dibenzenechromium and chromocene). It is significant that the energies of the e_{2g} and a'_{1g} levels are similar, so that each molecule has really three quasidegenerate levels. This is in agreement with McConnell's experimental data on paramagnetic resonance of vanadicene [5] the three unpaired electrons of which are distributed over the e_{2g} and a'_{1g} levels.

TABLE 4a. G_{pq} Matrix Elements for the Cobalticinium Cation (p = line; q = column)*

1	2	3	4	5	6	7	8	9	10	11	12	13	14	15	16	17	18	19	
0,24290	0,24	0,27 —	0,24290 0,09932	0,27 —	0,24290 0,04308	0,27 —	0,24290 0,04308	0,27 —	0,24290 0,05242	0,24 —	0,24290 0,05242	0,24 —	0,24290 0,02348	0,26 —	0,24290 0,02348	0,26 —	0,24290 0,02303	0,24290 0,02303	1
	0,25247	0,31111	0,24	0,25247	0,24	0,31111	0,24	0,31111	0,24	0,25247	0,24	0,25247	0,24	0,31111	0,24	0,31111	0,24	0,24	2
		0,61939	0,27	0,32267	0,27	0,56214	0,27	0,56214	0,27	0,30533	0,27	0,30533	0,27	0,54795	0,27	0,54795	0,27	0,27	3
			0,24290	0,27 —	0,24290 0,05242	0,27 —	0,24290 0,05242	0,27 —	0,24290 0,04308	0,24 —	0,24290 0,04308	0,24 —	0,24290 0,04303	0,26 —	0,24290 0,02303	0,26 —	0,24290 0,02348	0,24290 0,02348	4
				0,27436	0,27	0,31690	0,27	0,31690	0,27	0,24153	0,27	0,24153	0,27	0,29954	0,27	0,29954	0,27	0,27	5
					0,25464	0,27 —	0,23116 0,01174	0,27 —	0,25464 0,11073	0,24 —	0,23116 0,01151	0,24 —	0,24290 0,03328	0,26 —	0,24290 0,03328	0,26 —	0,24290 0,03772	0,24290 0,03772	6
						0,61939	0,27	0,55268	0,27	0,31690	0,27	0,29954	0,27	0,55268	0,27	0,55268	0,27	0,27	7
							0,25464	0,27 —	0,23116 0,01151	0,24 —	0,25464 0,11073	0,24 —	0,24290 0,03328	0,26 —	0,24290 0,3328	0,26 —	0,24290 0,03772	0,24290 0,03772	8
								0,61939	0,27	0,29954	0,27	0,31690	0,27	0,55268	0,27	0,55268	0,27	0,27	9
									0,25464	0,24 —	0,23116 0,01174	0,24 —	0,24290 0,03772	0,26 —	0,24290 0,03772	0,26 —	0,24290 0,03328	0,24290 0,03328	10
										0,27436	0,24	0,24153	0,24	0,31690	0,24	0,31690	0,24	0,24	11
											0,25464	0,24 —	0,24290 0,03772	0,26 —	0,24290 0,03772	0,26 —	0,24290 0,03328	0,24290 0,03328	12
												0,27436	0,24	0,31690	0,24	0,31690	0,24	0,24	13
													0,26445	0,26 —	0,22136 0,02154	0,26 —	0,26445 0,12205	0,22436 0,02621	14
														0,61939	0,26	0,56687	0,26	0,26	15
															0,26445	0,26 —	0,22136 0,02621	0,26445 0,12205	16
																0,61939	0,26	0,26	17

*The number in space pq represents the value of the Coulomb integral $[\chi_p\chi_p/\chi_q\chi_q]$ (χ_p and χ_q are the atomic orbitals). In cases where in our chosen approximation the exchange integral $[\chi_p\chi_q/\chi_p\chi_q]$ is not zero its value is given under the value of the Coulomb integral. All values are in atomic units.

TABLE 4b. G_{pq} Matrix Elements for Chromocene*

1	2	3	4	5	6	7	8	9	10	11	12	13	14	15	16	17	18	19	
0,23827	0,208 —	0,260 —	0,23827 0,10396	0,233 —	0,23827 0,04345	0,266 —	0,23827 0,04345	0,266 —	0,23827 0,05205	0,206 —	0,23827 0,05205	0,206 —	0,23827 0,02344	0,239 —	0,23827 0,02344	0,239 —	0,23827 0,02306	0,23827 0,02306	1
	0,18362	0,22626	0,208	0,18362	0,208	0,22626	0,208	0,22626	0,208	0,18362	0,208	0,18362	0,208	0,22626	0,208	0,22626	0,208	0,208	2
		0,45046	0,260	0,23468	0,260	0,40883	0,260	0,40883	0,260	0,22205	0,260	0,22205	0,260	0,39851	0,260	0,39851	0,260	0,260	3
			0,23827	0,233 —	0,23827 0,05205	0,266 —	0,23827 0,05205	0,266 —	0,23827 0,04345	0,206 —	0,23827 0,04345	0,206 —	0,23827 0,02306	0,239 —	0,23827 0,02306	0,239 —	0,23827 0,02344	0,23827 0,02344	4
				0,19954	0,233	0,23047	0,233	0,23047	0,233	0,17566	0,233	0,17566	0,233	0,21784	0,233	0,21784	0,233	0,233	5
					0,25000	0,266 —	0,22654 0,01172	0,266 —	0,25000 0,11549	0,206 —	0,22654 0,01153	0,206 —	0,23827 0,03345	0,239 —	0,23827 0,03345	0,239 —	0,23827 0,03756	0,23827 0,03756	6
						0,4506	0,266	0,40195	0,266	0,23047	0,266	0,21784	0,266	0,40195	0,266	0,40195	0,266	0,266	7
							0,25000	0,266 —	0,22654 0,01153	0,206 —	0,25000 0,11549	0,206 —	0,23827 0,03345	0,239 —	0,23827 0,03345	0,239 —	0,23827 0,03756	0,23827 0,03756	8
								0,45046	0,266	0,21784	0,266	0,23047	0,266	0,40195	0,266	0,40195	0,266	0,266	9
									0,25000	0,206 —	0,22654 0,01172	0,206 —	0,23827 0,03756	0,239 —	0,23827 0,03756	0,239 —	0,23827 0,03345	0,23827 0,03345	10
										0,19954	0,206	0,17566	0,206	0,23047	0,206	0,23047	0,206	0,206	11
											0,25000	0,206 —	0,23827 0,03756	0,239 —	0,23827 0,03756	0,239 —	0,23827 0,03345	0,23827 0,03345	12
												0,19954	0,206	0,23047	0,206	0,23047	0,206	0,206	13
													0,26000	0,239 —	0,21654 0,02172	0,239 —	0,26000 0,12998	0,21654 0,02602	14
														0,45046	0,239	0,41227	0,239	0,239	15
															0,26000	0,239 —	0,21654 0,02602	0,26000 0,12998	16
																0,45046	0,239	0,239	17

*See footnote to Table 4a.

TABLE 4c. G_{pq} Matrix Elements for Dibenzenechromium*

1	2	3	4	5	6	7	8	9	10	11	12	13	14	15	16	17	18	19	
0,22736	0,21	0,25	0,22736 0,08701	0,22	0,22736 0,04127	0,27	0,22736 0,04127	0,27	0,22736 0,05336	0,21	0,22736 0,05336	0,21	0,22736 0,02292	0,24	0,22736 0,02292	0,24	0,22736 0,02195	0,22736 0,02195	1
	0,18362	0,22626	0,21	0,18362	0,21	0,22626	0,21	0,22626	0,21	0,18362	0,21	0,18362	0,21	0,22626	0,21	0,22626	0,21	0,21	2
		0,45046	0,25	0,23468	0,25	0,40883	0,25	0,40883	0,25	0,22205	0,25	0,22205	0,25	0,39851	0,25	0,39851	0,25	0,25	3
			0,22736	0,22	0,22736 0,05336	0,27	0,22736 0,05336	0,27	0,22736 0,04127	0,21	0,22736 0,04127	0,21	0,22736 0,02195	0,24	0,22736 0,02195	0,24	0,22736 0,02292	0,22736 0,02292	4
				0,19954	0,22	0,23047	0,22	0,23047	0,22	0,17566	0,22	0,17566	0,22	0,21784	0,22	0,21784	0,22	0,22	5
					0,23882	0,27	0,21590 0,01146	0,27	0,23882 0,09798	0,21	0,21590 0,01098	0,21	0,22736 0,02869	0,24	0,22736 0,02869	0,24	0,22736 0,03507	0,22736 0,03507	6
						0,45046	0,27	0,40195	0,27	0,23047	0,27	0,21784	0,27	0,40195	0,27	0,40195	0,27	0,27	7
							0,23882	0,27	0,21590 0,01098	0,21	0,23882 0,09798	0,21	0,22736 0,02869	0,24	0,22736 0,02869	0,24	0,22736 0,03507	0,22736 0,03507	8
								0,45046	0,27	0,21784	0,27	0,23047	0,27	0,40195	0,27	0,40195	0,27	0,27	9
									0,23882	0,21	0,21590 0,01146	0,21	0,22736 0,03507	0,24	0,22736 0,03507	0,24	0,22736 0,02869	0,22736 0,02869	10
										0,19954	0,21	0,17566	0,21	0,23047	0,22	0,23047	0,21	0,21	11
											0,23882	0,21	0,22736 0,03507	0,24	0,22736 0,03507	0,24	0,22736 0,02869	0,22736 0,02869	12
												0,19954	0,21	0,23047	0,21	0,23047	0,21	0,21	13
													0,23882	0,24	0,21590 0,01146	0,24	0,23882 0,09798	0,21590 0,01098	14
														0,45046	0,24	0,41227	0,24	0,24	15
															0,23882	0,24	0,21590 0,01098	0,23882 0,09798	16
																0,45046	0,24	0,24	17

*See footnote to Table 4a.

TABLE 5. Molecular Orbitals of Complexes and MO Energies

Symmetry	Molecule	Bonding MO		Antibonding MO
		form of orbital	energy (ev)	energy (ev)
a_{1g}	$Co(C_5H_5)_2^+$	$0,79a_{1g} + 0,62s$	−20,84	−5,33
	$Cr(C_5H_5)_2$	$0,97a_{1g} + 0,25s$	−13,71	+1,74
	$Cr(C_6H_6)_2$	$0,98a_{1g} + 0,22s$	−13,31	+3,21
a'_{1g}	$Co(C_5H_5)_2^+$	d_{z^2}	−13,20	—
	$(Cr\,C_5H_5)_2$	d_{z^2}	− 4,82	—
	$Cr(C_6H_6)_2$	d_{z^2}	− 4,19	—
a_{1u}	$Co(C_5H_5)_2^+$	$0,91a_{1u} + 0,41p_z$	−18,04	−5,20
	$Cr(C_5H_5)_2$	$0,99a_{1u} + 0,06p_z$	−13,12	+3,73
	$Cr(C_6H_6)_2$	$0,99a_{1u} + 0,062p_z$	−12,73	+2,15
e_{1u}	$Co(C_5H_5)_2^+$	$0,77e_{1u} + 0,64p_x$	−16,65	−1,96
	$Cr(C_5H_5)_2$	$0,94e_{1u} + 0,35p_x$	−9,82	+4,05
	$Cr(C_6H_6)_2$	$0,94e_{1u} + 0,36p_x$	−10,72	+3,84
e_{1g}	$Co(C_5H_5)_2^+$	$0,90e_{1g} + 0,44d_{xz}$	−14,20	+0,19
	$Cr(C_5H_5)_2$	$0,92e_{1g} + 0,39d_{xz}$	−10,56	+7,94
	$Cr(C_6H_6)_2$	$0,96e_{1g} + 0,30d_{xz}$	−10,61	+10,12
e_{2g}	$Co(C_5H_5)_2^+$	$0,32e_{2g} + 0,95d_{xy}$	−11,13	+0,57
	$Cr(C_5H_5)_2$	$0,55e_{2g} + 0,83d_{xy}$	−5,22	+5,88
	$Cr(C_6H_6)_2$	$0,78e_{2g} + 0,63d_{xy}$	−4,76	+6,97
e_{2u}	$Co(C_5H_5)_2^+$	e_{2u}	—	−0,27
	$Cr(C_5H_5)_2$	e_{2u}	—	+4,00
	$Cr(C_6H_6)_2$	e_{2u}	—	+2,19

TABLE 6. Ionization Potentials of $(C_5H_5)_2M$ (ev)

Potential	$(C_5H_5)_2Fe$	$(C_5H_5)_2Cr$
Calculated	6.39	4.82
Experimental	7.05	6.90

The total energy of a molecule comprises a number of terms, including the total electron energy determined by the electron distribution over the MO, the nuclear repulsion energy, and the energy of excitation of the atoms to the valence states. The last two factors are destabilizing. The closeness of the energies of the highest occupied MO suggests that the difference between the energies of molecular states differing in electron distribution over the e_{2g} and a'_{1g} orbits should be small. This indicates that the selection of a molecular state of a definite multiplet character, i.e., number of unpaired electrons in the molecule is determined, as we supposed earlier [6] by the energy difference between the initial valence states rather than by the electron energy of the molecular states.*

*Unfortunately, this hypothesis cannot be proved by direct calculation. Even in complete calculations by the Roothaan method the energy difference between states differing in multiplet character is indistinct [7]. A reliable evaluation of this difference is even less likely in our approximation because of the rough assumptions in calculations of the matrix elements of electron–electron interaction. Nevertheless, we consider that this difference is either small or has the same sign as the energy difference between the valence states leading to molecular states of the given multiplet character.

TABLE 7. Electron Density Distribution

Compound	Effective charges (in atomic units)				Dipole moments (in D)	
	on central atom	on both rings	on one ring	on each C atom	metal–C bonds	metal–ring
$(C_6H_6)_2Cr$	+1,470	−1,470	−0,735	−0,122	1,30	5,90
$(C_5H_5)_2Fe$	+0,682	−0,682	−0,341	−0,068	0,57	2,64
$(C_5H_5)_2Cr$	+1,700	−1,700	−0,850	−0,170	1,80	7,40
$(C_5H_5)_2Co^+$	−0,118	+1,118	+0,559	+0,112		

TABLE 8. Allowed Transitions

One-electron transition $\varphi_i \rightarrow \varphi_a$	Excited states of the molecules		Allowed transitions
	orbital degeneration*	Symmetry of states**	
$e_{2g} \rightarrow e'_{1u}$	4	$E_{1u} + E_{2u}$	$^1A_{1g} \rightarrow {}^{1,3}E_{1u}$
$e_{2g} \rightarrow e_{2u}$	4	$A_{1u} + A_{2u} + E_{1u}$	$^1A_{1g} \rightarrow {}^{1,3}A_{1u}\,{}^{1,3}E_{1u}$
$a'_{1g} \rightarrow a'_{1u}$	1	A_{1u}	$^1A_{1g} \rightarrow {}^{1,3}A_{1u}$
$a'_{1g} \rightarrow e'_{1u}$	2	E_{1u}	$^1A_{1g} \rightarrow {}^{1,3}E_{1u}$

*Electron–electron interaction not taken into account.

**With electron–electron interaction taken into account.

The energies of the highest occupied MO of the complexes, taken with the plus sign, are the first ionization potentials of the molecules. These values are compared in Table 6 with the experimental values of the potentials for ferrocene and chromocene.

It is seen that the calculated values are close in order of magnitude to the experimental but lower than the latter; the divergence increases appreciably as we pass from ferrocene to chromocene, probably because of the greater calculation error for molecular radicals in our approximation. The relatively satisfactory agreement suggests that the ionization potentials of the dibenzenechromium molecule and cobalticinium cation should be close to the calculated values of 4.19 and 11.13 ev respectively. Even without attaching any great significance to these absolute values we may assume that the energy of removal of an electron from the dibenzenechromium molecule should be less than for the other aromatic complexes considered here. The higher value for $(C_5H_5)_2Co^+$ is also to be expected, since this refers to the removal of the second electron.

A number of conclusions can also be drawn from the form of the MO (see Table 5). The AO coefficients in the MO of the complexes give the effective charges on the individual atoms in the molecules, given in Table 7.

It is seen that the coefficients of the central atoms AO in bonding MO are smaller than those of the MO of the rings in nearly every case. This means that in all neutral molecules the metal atom carries a positive charge, i.e., electrons are attracted from the metal toward the rings with an increase of the π-electron density at the carbon atoms. This conclusion is at variance with the usual idea that in molecules of transition-element compounds the most important role belongs to donor–acceptor bonds with transfer of electrons from the ligands to the central atom. Our results indicate that, in addition to electron transfer from ligands in donor–acceptor bonds, reverse transfer of electrons from the central atom to the rings, corresponding to formation of dative bonds, is also important. In molecules of bis-cyclopentadienyl compound another important fact is that bonds of the e_{1g} type, formed by unpaired electrons of the rings and central atoms, are appreciably polar, with the positive end of the dipole at the metal atom. However, in the case of dibenzenechromium, where no such bonds exist, the

metal atom also carried a considerable positive charge, which in this case originated only from the dative bonds. It should also be noted that displacement of electrons from the metal to the rings was greatest in chromocene, somewhat less in dibenzenechromium, even less in ferrocene, while in the cobalticinium cation it was overbalanced by displacement of electrons in the reverse direction, so that in this last system the metal is either almost neutral or bears a small negative charge. We consider that this sequence reflects the relative roles of donor–acceptor and dative bonds in the respective molecules. Apparently in chromium compounds the role of dative bonds is very large and donor–acceptor bonds are of relatively little significance, while in ferrocene there is a great increase in the role of donor–acceptor bonds, causing displacement of electrons from the ligands to the metal; this is no longer compensated by the dative bonds and is counterbalanced only because of the high polarity of bonds of the e_{1g} type. Because of the presence both of e_{2g} dative bonds and e_{1g} polar covalent bonds in chromocene the positive charge of the central atom in the molecule is highest in this compound, exceeding the charge on the metal atom in dibenzenechromium, where only dative bonds are present (the e_{1g} bonds in dibenzenechromium are also of the donor–acceptor type and thus lead to displacement of electrons from the ligand to the metal). The charge on the metal atom in chromocene reaches the value of +1.70. This result is consistent with the chemical properties of chromocene. It is known from chemical data that chromocene differs strongly from typically covalent bis-cyclopentadienyl compounds and approximates to the ionic $Mn^{2+}(C_5H_5^-)_2$, as is shown by the instantaneous metathetical reaction with $FeCl_2$ (with a 70% yield of ferrocene), hydrolysis by acids, electrical conductivity, etc. This view is also confirmed by investigations of the infrared spectra of $(C_5H_5)_2Mn$ and $(C_5H_5)_2Cr$, which have considerable similarities. At the same time, the charges on the Cr atoms in $(C_5H_5)_2Cr$ and $(C_6H_6)_2Cr$ are fairly similar, which is in agreement with the small dipole moment (between 0 and 0.4D) of the mixed $(C_6H_6)Cr(C_5H_5)$ complex [8].

It follows from Table 7 that in the cobalticinium cation $(C_5H_5)_2Co^+$, which is isoelectronic with ferrocene $(C_5H_5)_2Fe$, the central atom is almost neutral and the entire positive charge is therefore distributed between the cobalticinium in electrophilic substitution reactions, despite its high stability [9, 10].

In the ground singlet state of the isoelectronic molecules $(C_5H_5)_2Fe$ and $(C_5H_5)_2Co^+$ 18 electrons completely fill the 9 MO $(a_{1g})^2 (a_{1u})^2 (e_{1u})^4 (e_{1g})^4 (a'_{1g})^2 (e_{2g})^4$, so that the resultant electron state of the whole molecule has $^1A_{1g}$ symmetry and the remaining 10 MO (a''_{1g}, a''_{1u}, e''_{1g}, e'_{1g}, e''_{2g}, e_{2u}) remain free. Of the excited states of these molecules we considered only those which arise in excitation of one electron from the higher filled levels a'_{1g} and e_{2g}. The selection rules for these transitions were derived with the aid of the group theory. The allowed transitions are those given in Table 8 [with D_{5d} molecular symmetry the electric moment vector components refer to the concepts $a_{1u}(M_Z)$ and $e_{1u}(M_X, M_Y)$ not given].

It follows from Table 8 that there are 10 allowed transitions (to five singlet and five triplet states), and configurational interaction should play a significant role even in these one-electron transitions, so that exact calculations of the transition energies are impossible because of the crude assumptions made in calculations of the electron–electron interaction matrix. However, we may attempt to estimate the position of the absorption bands by considering the "center of gravity" of the transitions. This can be illustrated by the calculation of the first excited states of benzene, performed by Goeppert-Mayer and Sklar [11]. In the case of benzene the excited state corresponding to the $e_1 \rightarrow e_2$ one-electron transition is resolved into eight levels: $^{1,3}B_{1u} + {}^{1,3}B_{2u} + {}^{1,3}E_{1u}$ (four singlet and four triplet). The wave functions of the doubly degenerate triplet level $^3E_{1u}$ can still be represented by one determinant and not by their linear combination. Therefore, the energy of the $^3E_{1u}$ level can be calculated with the aid of formulas analogous to those used in calculation of transitions between undegenerate MO. If the energy of this excited state is represented by $^3E_{1u}$ the energies of the other two triplet levels can be expressed as

$$^3B_{1u} = {}^3E_{1u} - \xi$$

and

$$^3B_{2u} = {}^3E_{1u} + \xi,$$

where ξ is a certain integral; i.e., the $^3E_{1u}$ level can be regarded as the center of gravity of all three triplet states. We estimated the positions of these "centers of gravity" of the triplet states for $(C_5H_5)_2Fe$ and $(C_5H_5)_2Co^+$ for transfer of electrons from the e_{2g} orbit to the e''_{1u} and e_{2u} orbits. The values found were 0.8 and 2.8 ev respectively for ferrocene, and 1.4 and 4.0 ev for cobalticinium.

Earlier we found the energies of one-electron transitions $a'_{1g} \rightarrow a'_{1u}({}^1A_{1g} \rightarrow {}^{1,3}A_{1u})$ and $a'_{1g} \rightarrow e'_{1u}({}^1A_{1g} \rightarrow {}^{1,3}E_{1u})$ for ferrocene [1]; the values were 1.0 and 2.5 ev respectively. The energy of the $a'_{1g} \rightarrow e'_{1u}$ transition for cobalticinium was found to be 3.3 ev.

The uv spectra of crystals of these compounds contain bands corresponding to transitions with energies of 2.88, 3.81, and 4.96 ev (ferrocene), and 3.10, 4.00, and 4.77 ev cobalticinium cation). We do not attach any significance to the accidental numerical agreement (2.8 and 2.88 ev; 4.0 and 4.00 ev), but we consider that the closeness of the orders of magnitude and the predicted shift of the bands in the short-wave direction in the transition from $(C_5H_5)_2Fe$ to $(C_5H_5)_2Co^+$ are important.

The authors thank S. N. Dobryakov for help in the calculations of the self-consistent MO of dibenzenechromium.

LITERATURE CITED

1. E. M. Shustorovich and M. E. Dyatkina, Zh. strukt. khimii 1, 1, 109 (1960).
2. C. C. Roothaan, Rev. Mod. Phys. 23, 69 (1951).
3. J. A. Pople and R. K. Nesbet, J. Chem. Phys. 22, 571 (1954).
4. M. E. Dyatkina, Izv. AM SSSR. Otd. khim. n. , 1027 (1959).
5. H. McConnell, W. W. Borterfield, and R. E. Robertson, J. Chem. Phys. 30, 442 (1959).
6. E. M. Shustorovich and M. E. Dyatkina, Zh. neorgan. khimii 3, 2721 (1958); M. E. Dyatkina and E. M. Shustorovich, Zh. neorgan. khimii 4, 402 (1959); E. M. Shustorovich and M. E. Dyatkina, Zh. neorgan. khimii 4, 553 (1959).
7. R. G. Parr and R. S. Mulliken, J. Chem. Phys. 18, 1338 (1950).
8. E. O. Fischer and S. Schreiner, Chem. Ber. 92, 938 (1959).
9. A. N. Nesmeyanov, Reports of the 8th Mendeleev Congress [in Russian] (Izd. AN SSSR, Moscow, 1959) p. 27.
10. G. Wilkinson, J. Am. Chem. Soc. 74, 6148 (1952).
11. M. Goeppert-Mayer and A. Sklar, J. Chem. Phys. 6, 645 (1938).
12. S. Yamada, A. Nakahara, and R. Tsuchida, J. Chem. Phys. 22, 1620 (1954); Bull. Chem. Soc. Japan 28, 465 (1955).

All abbreviations of periodicals in the above bibliography are letter-by-letter transliterations of the abbreviations as given in the original Russian journal. *Some or all of this periodical literature may well be available in English translation.* A complete list of the cover-to-cover English translations appears at the back of this issue.

OPTICAL ACTIVITY OF AMINO ACIDS

M. V. Vol'kenshtein and M. P. Kruchek

A. I. Gertsen Leningrad Pedagogic Institute

Translated from Zhurnal Strukturnoi Khimii, Vol. 2, No. 1,
pp. 59-62, January-February, 1961
Original article submitted February 7, 1960

The polarizability theory was used for calculating changes in the optical activity of two amino acids, alanine and valine, when they pass from the dipolar ion to the cationic form. The results are in agreement with experimental data and make it possible to interpret the observed fact that the above-named transition is accompanied by a change of molecular rotation by a positive value.

Asymmetry of natural amino acids is a very important physicochemical and biological property. The optical activity of amino acids is determined by their structure and depends very much on the nature of the solvent. In an acid medium the dipolar amino acid ion is converted into a cation:

$$H_3\overset{+}{N} - CHCRCOO^{-} \rightarrow H_3\overset{+}{N} - CHCRCOOH.$$

The molecular rotation alters by a positive value in this conversion for all amino acids present in proteins. Clough [1, 2], who established this relationship, concluded from it that all amino acids have the same stereochemical structure. The fact that the relationship between molecular rotation and pH of the medium is the same for a number of different amino acids [3, 4] provides further evidence for this view. The purpose of the present work is to examine the Clough relationship theoretically.

By the quantum mechanical theory, molecular rotation is expressed by the formula [5]:

$$[M]_\nu = \frac{288\pi^2 N_A \nu^2}{c^2} \cdot \frac{n_\nu^2 + 2}{3} g_\nu , \qquad (1)$$

where N_A is the Avogadro number; ν is the frequency of the incident light; n_ν is the refractive index of the medium; c is the velocity of light; g_ν is the mean gyration of the active substance

$$g_\nu = \frac{c}{3\pi h} \sum_n \frac{\dot{I}_m(\vec{p}_{0n}\vec{m}_{n0})}{\nu_{n0}^2 - \nu^2} . \qquad (2)$$

p_{0n}, m_{n0} are the matrix elements of the electric and magnetic dipole moments; $\dot{I}_m$ is the imaginary part of the expression.

If a molecule is represented as a combination of separate groups in which electron transitions are localized, the gyration may be represented as [6]

$$g = g^{(0)} + g^{(1)} + \sum_i g^{(i)} , \qquad (3)$$

where i is the index of the group, $g^{(i)}$ is the internal gyration of the group; the term $g^{(1)}$ is expressed in terms of the matrix elements of the electric dipole of one group, and of the magnetic dipole of the other; finally, the

polarization term $g^{(0)}$ is determined by the polarizabilities and geometrical configuration of the groups. The term $g^{(1)}$ is small and may be disregarded [6, 7]; the expression for $g^{(0)}$ was derived by the quantum mechanical method by Kirkwood [6] and one of us [5, 8]. Internal gyrations $g^{(i)}$ have been calculated in a number of papers by the quantum mechanical method on the basis of the so-called one-electron model [9]. The calculations were performed for several simple compounds [10, 11, 12]. In these papers the polarization effect, characterized by $g^{(0)}$, was not considered and gyration was identified with $g^{(1)}$ belonging to the single chromophore group. The resultant agreement between theory and experiment is not very convincing, as the calculation results depend very much on the form of the approximate wave functions [13].

In our examination of the Clough relationship we performed the appropriate calculations for the amino acid chromophores (carboxyl groups) with wave functions in the form of LCAO (Slater functions [14] being taken as AO) and found a value for $g^{(1)}$ two orders of magnitude lower than the experimental values of g. Therefore in the subsequent calculations we restrict ourselves to the polarization term $g^{(0)}$.

Let us consider the change of $g^{(0)}$ in the conversion of an α-amino acid from the dipolar into the cationic form. In the first approximation of the polarizability theory $g^{(0)}$ for groups with axially symmetric polarizability tensors is of the form [5, 6, 8]:

$$g^{(0)} = -\frac{2\pi}{3\lambda}\sum_{k>l}\frac{1}{R_{kl}^3}(\alpha_{k\parallel}-\alpha_{k\perp})(\alpha_{l\parallel}-\alpha_{l\perp})(\vec{R}_{kl}\cdot[\vec{l}\vec{k}])\left\{\frac{3}{R_{kl}^2}(\vec{R}_{kl}\vec{k})(\vec{R}_{kl}\vec{l})-(\vec{k}\,\vec{l})\right\}, \tag{4}$$

where $\vec{R}_{kl}=\vec{R}_k-\vec{R}_l$; $\vec{R}_k$, $\vec{R}_l$ are the radius vectors of the k-th and l-th bond or group; $\alpha_{l\parallel}$, $\alpha_{l\perp}$ are the polarizabilities of the l-th group along and across its axis of symmetry; $\vec{k}$, $\vec{l}$ are the single group along and across the axis of symmetry of the $\underline{k}$ and $\underline{l}$ groups.

Molecular rotation for the sodium D line is obtained from (1) and (4) in the form:

$$[M]_D = 7{,}73\left(\frac{n^2+2}{n}\right)_D g_D\cdot 10^{20}. \tag{5}$$

The absolute configuration of α-amino acids is known [15] and is shown in Fig. 1. The N, O', O" atoms and the C atom of the carboxyl group lie in the same plane.

When an amino acid passes from the dipolar into the cationic form the following change occurs:

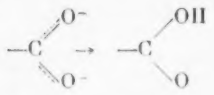

Assume that the hydrogen atom is linked to the O' oxygen atom in the cation. Then the gyration difference between the cation and the dipolar ion is represented by the formula:

$$\begin{aligned}\Delta g &= g_{C=O''} + g_{C-O'} + g_{O'-H} - g_{C\cdots O''} - \\ &- g_{C\cdots O'} = (g_{C=O''} - g_{C\cdots O''}) + (g_{C-O'} - g_{C\cdots O'}) + g_{O'-H}.\end{aligned} \tag{6}$$

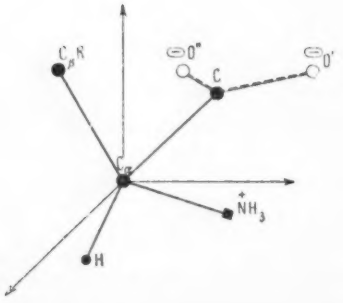

Fig. 1.

The right-hand side contains gyrations of the individual bonds in the hydroxyl group, determined by interactions with the other bonds in the molecule. We disregard interactions with C−H bonds, as their anisotropy is low. For aliphatic amino acids expression (6) has the form:

$$\begin{aligned}\Delta g = (\alpha_{\parallel}-\alpha_{\perp})_{C-C}\Big\{&[(\alpha_{\parallel}-\alpha_{\perp})_{C=O} - \\ &-(\alpha_{\parallel}-\alpha_{\perp})_{C\cdots O}]G_{O''-C} + \\ &[(\alpha_{\parallel}-\alpha_{\perp})_{C-O}-(\alpha_{\parallel}-\alpha_{\perp})_{C\cdots O}]G_{O'-C} + \\ &+(\alpha_{\parallel}-\alpha_{\perp})_{O'H}G_{O'H}\Big\}\cdot\left(-\frac{2\pi}{3\lambda_D}\right),\end{aligned} \tag{7}$$

where G_k is the geometric factor [4]:

$$G_k = \sum_{l\ k}\frac{1}{R_{kl}^3}(\vec{R}_{kl}[\vec{l}\vec{k}])\left\{\frac{3}{R_{kl}^2}(\vec{R}_{kl}\vec{l})(\vec{R}_{kl}\vec{k})-(\vec{k}\,\vec{l})\right\}. \tag{8}$$

G_k includes all bonds except those coplanar with the carboxyl group. We assume standard values for the distances and angles (C−C 1.54 A; C−H 1.08 A; C−O 1.25 A, tetrahedral angles with the exception of the O'CO" angle, which is taken to be 120°). We assume that the polarizabilities of the "sesqui" C $\cdots$ O$^-$ bond are equal to the arithmetic mean of the corresponding polarizabilities of the C=O and C−O bonds.

$$\alpha_{\parallel C\cdots O} = \frac{1}{2}(\alpha_{\parallel C=O} + \alpha_{\parallel C-O});\ \alpha_{\perp C\cdots O} = \frac{1}{2}(\alpha_{\perp C=O} + \alpha_{\perp C-O}). \tag{9}$$

Then

$$\Delta g = -\frac{\pi}{3\lambda_D}\Delta\alpha_{C-C} \times \times \{(\Delta\alpha_{C\cdots O} - \Delta\alpha_{C-O})(G_{O'-C} - G_{O''-C}) + 2\Delta\alpha_{O-H}G_{O'-H}\}. \tag{10}$$

Polarizability anisotropy of the C=O and C−O bonds was calculated by Vuks [16] in accordance with the Denbigh valence-optical scheme [17, 18]. According to Vuks, $\Delta\alpha_{C-C} = 1{,}43\cdot10^{-24}$ cm^3, $\Delta\alpha_{C=O} = 1{,}11\cdot10^{-24}$ cm^3. The method used by Vuks for C−C and C−H bonds gave the following values for C−O and O−H bonds (with the aid of data for CH_3OH and H_2O):

$$\alpha_{\parallel C-O} = 1{,}55\cdot10^{-24},\ \alpha_{\perp C-O} = 0{,}08\cdot10^{-24},\ \Delta\alpha_{C-O} = 1{,}47\cdot10^{-24},$$
$$\alpha_{\parallel O-H} = 0{,}9\cdot10^{-24},\ \alpha_{\perp O-H} = 0{,}66\cdot10^{-24},\ \Delta\alpha_{O-H} = 0{,}24\cdot10^{-24}\ \text{cm}^3.$$

The values for the C=O bond are effective values, as the π-bond does not have axial symmetry.

Values of Δg were calculated for the simplest aliphatic α-amino acids $H_2NCH(CH_3)COOH$ alanine and valine $H_2NCH[CH(CH_3)_2]COOH$.

The three conformations shown in Fig. 2 are possible for valine:

I) Of the two C_β−C bonds one is parallel to the C_α−H bond and the other to the C_α−N bond;

II) One C_β−C bond is parallel to the C_α−N bond and the other to the C_α−C bond;

III) One C_β−C bond is parallel to the C_α−C bond and the other to the C_α−H bond.

The hydrogen atom of the carboxyl group is assumed to lie in the plane of the latter, with the O−H bond at an angle of 90° to the C−O bond.

We also performed calculations for cations in which the H atom is linked to O" and not O'. In this case:

$$\Delta g = -\frac{\pi}{3\lambda}\Delta\alpha_{C-C} \times \times \{(\Delta\alpha_{C=O} - \Delta\alpha_{C-O})(G_{O'-C} - G_{O''-C}) + 2\Delta\alpha_{O-H}G_{O''-H}\}. \tag{11}$$

The calculations gave the following values (in cm$^3\cdot10^{14}$):

	$G_{O'-C}$	$G_{O''-C}$	$G_{O'-H}$	$G_{O''-H}$
Alanine	−8.26	10.95	5.87	−1.33
Valine	I−13.34	11.47	4.26	−3.81
	II −5.88	7.57	3.78	1.17
	III −8.85	10.73	5.33	−4.99

The corresponding differences between the molecular rotations ΔM of the cation and dipolar ion (in degrees · cm^3 · dm^{-1}) are:

	CO"(O'H) Configuration	CO'(O"H) Configuration	Exptl. [19]
Alanine	23.00	−34.7	10.7
Valine	I 37.8	−39.0	26.2
	II 17.5	−30.0	
	III 22.2	−24.7	

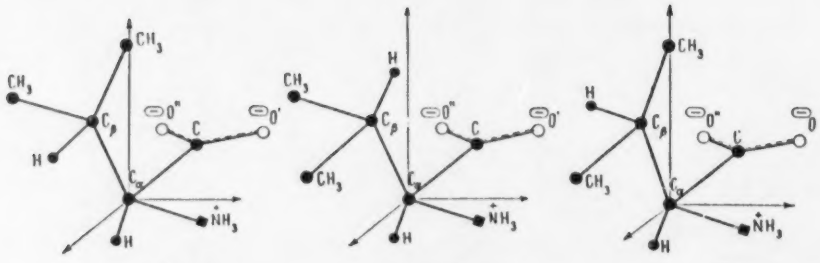

I II III

Fig. 2.

The agreement between calculation and experiment for the CO"(O'H) configuration and for valine conformation I is quite satisfactory. Attachment of hydrogen to the O' atom, which is nearer to N^+ than O" (see Fig. 1), also is more probable on other grounds. In fact, N^+ must have a certain polarizing effect on the $C\begin{matrix}O\\ \diagdown\\ \diagup\\ O+\end{matrix}$ group, attracting the negative charge toward the O' oxygen, and in consequence a proton can be added more easily to the latter. It is evident from the calculations that similar agreement should be found for other amino acids. Despite the number of assumptions made, it may be taken as established that the polarizability theory explains the relationships observed for optical activity of amino acids.

LITERATURE CITED

1. G. W. Clough, J. Chem. Soc. 107, 1509 (1915).
2. G. W. Clough, J. Chem. Soc. 113, 526 (1918).
3. O. Lutz and B. Jirgensons, Ber. 63, 448 (1930).
4. O. Lutz and B. Jirgensons, Ber. 64, 1221 (1931).
5. M. V. Vol'kenshtein, Molecular Optics [in Russian] (GTTI, Moscow-Leningrad, 1951).
6. J. Kirkwood, J. Chem. Phys. 5, 479 (1937).
7. H. Murakami, J. Chem. Phys. 27, 1231 (1957).
8. M. V. Vol'kenshtein, Dokl. AN SSSR 71, 447 (1950); Izv. AN SSSR, Ser. fiz. 17, 574 (1953).
9. E. Condon, W. Altar, and H. Eyring, J. Chem. Phys. 5, 753 (1937).
10. E. Gorin, J. Walter, and H. Eyring, J. Chem. Phys. 6, 824 (1938).
11. E. Gorin, W. Kautzmann, and J. Walter, J. Chem. Phys. 7, 327 (1939).
12. W. Kautzmann, J. Walter, and H. Eyring, Chem. Rev. 26, 339 (1940).
13. M. V. Vol'kenshtein and M. P. Kruchek, Optika i spektroskopiya, 5 (1960).
14. J. L. Onsley, Rev. Mod. Phys. 31, 30 (1959).
15. R. Slater, Phys. Rev. 36, 57 (1930).
16. M. F. Vuks, Optika i spektroskopiya 2, 494 (1957).
17. K. G. Denbigh, Trans. Faraday Soc. 36, 936 (1940).
18. M. V. Vol'kenshtein, Configuration Statistics of Polymer Chains [in Russian] (Izd. AN SSSR, Moscow, 1959) Section 42.
19. A. Neuberger, "Stereochemistry of amino acids," in Collection: Protein Chemistry [Russian translation] (GIIL, 1952) Vol. 2.

All abbreviations of periodicals in the above bibliography are letter-by-letter transliterations of the abbreviations as given in the original Russian journal. *Some or all of this periodical literature may well be available in English translation.* A complete list of the cover-to-cover English translations appears at the back of this issue.

BRIEF COMMUNICATIONS

STRUCTURE OF THE MOLECULES OF LITHIUM AND SODIUM METABORATES IN THE VAPOR STATE

P. A. Akishin and V. P. Spiridonov

M. V. Lomonosov Moscow State University
Translated from Zhurnal Strukturnoi Khimii, Vol. 2, No. 1, p. 63,
January-February, 1961
Original article submitted March 30, 1960

In this brief communication we present preliminary results of an electron diffraction study of $LiBO_2$ and $NaBO_2$ molecules in the vapor state.

The samples of lithium and sodium metaborates, prepared as described in [1], were remelted and deaerated for a long time under vacuum. The substances were evaporated from a molybdenum ampoule at 1200-1500°. An instrument designed for high-temperature work [2] was used for obtaining the electron diffraction patterns of the vapors. The electron diffraction patterns of the metaborate vapors showed an intensity distribution of the scattered electrons with characteristic alternation of strong (even) and weak (odd) rings, very similar to the alternation on the electron diffraction patterns of boron oxide [3] and boron sulfide [4] vapors studied by us earlier. Comparison of the values of s_{exptl} for the electron diffraction patterns of B_2O_3 [3], $LiBO_2$, and $NaBO_2$ vapors (see table) shows that they agree within the limits of experimental error. It is therefore natural to assume the presence of a common structural unit in the molecules of B_2O_3, $LiBO_2$, and $NaBO_2$. This may evidently be the linear group O − B = = O, which makes the main contribution to the intensity function of electron scattering by these molecules.

We interpreted the electron diffraction patterns by the methods of radial distribution and consecutive approximations (trial and error) on the assumption that the vapors of the compounds contain monomeric $LiBO_2$ and $NaBO_2$ molecules. The following values were found for the parameters: r (B—O) = 1,36 Å, r(B = O) = 1,20 Å, r(Li — O) = 1,82 Å, r (Na — O) = 2,14 Å, $\angle$Li — O — B ≅ $\angle$Na—O—B ≅ 90°—105°. However, the assumption that lithium and sodium metaborate vapors contain $LiBO_2$ or $NaBO_2$ molecules requires experimental confirmation by an idependent method.

A mass spectrum study of the composition of lithium and sodium metaborate vapors has been carried out in our laboratory [5]; the results will complete the study of their molecular structure.

Comparison of Values of s_{exptl} for Electron Diffraction Patterns of Boron Oxide and the Metaborates of Lithium and Sodium in Vapor Form

Max.	Min.	B_2O_3	$LiBO_2$	$NaBO_2$	Max.	Min.	B_2O_3	$LiBO_2$	$NaBO_2$
2		5,57	5,46	(5,91)	4		10,46	10,35	10,33
	3	6,84	6,79	6,97		5	11,81	11,73	11,68
3		7,85	7,85	7,73	5		12,98	12,74	12,81
	4	9,20	9,16	9,12		6	14,11	14,03	14,11
					6		15,29	15,13	15,26

LITERATURE CITED

1. G. Brauer, Handbook of Preparative Inorganic Chemistry [Russian translation] (IL, Moscow, 1956).
2. P. A. Akishin, M. I. Vinogradov, K. D. Danilov, N. P. Levkin, E. N. Martinson, N. G. Rambidi, and V. P. Spiridonov, Pribory i tekhnika éksperimenta 3, 70 (1958).
3. P. A. Akishin and V. P. Spiridonov, Dokl. AN SSSR 131, 3, 557 (1960).
4. P. A. Akishin and V. P. Spiridonov, Dokl. AN SSSR 129, 6, 1377 (1959).
5. P. A. Akishin, L. N. Gorokhov, and Yu. S. Khodeev, Zh. strukt. khimii 2, 2 (1961).

All abbreviations of periodicals in the above bibliography are letter-by-letter transliterations of the abbreviations as given in the original Russian journal. *Some or all of this periodical literature may well be available in English translation.* A complete list of the cover-to-cover English translations appears at the back of this issue.

PROTON RELAXATION IN AQUEOUS SOLUTIONS OF DIAMAGNETIC SALTS

V. SOLUTIONS OF URANYL SALTS

V. M. Vdovenko, O. B. Stebunov,

and V. A. Shcherbakov

V. G. Khlopin Radium Institute, Academy of Sciences, USSR, Leningrad

Translated from Zhurnal Strukturnoi Khimii, Vol. 2, No. 1, pp. 64-65, January-February, 1961
Original article submitted January 7, 1960

Investigation of uranyl salt solutions is of considerable interest for further development of our earlier work [1]. It is important not only because additional information on the nature and hydration of this ion can be obtained, but also in relation to certain problems touched upon earlier.

The method used did not differ substantially from that described in the first communication of this series. The UO_4 obtained by precipitation from aqueous uranyl nitrate solution with hydrogen peroxide in the cold was dissolved in the appropriate acid. A certain excess of acid was maintained in order to prevent hydrolysis (solution pH about 0). The concentration was checked by permanganate titration, except in the case of hydrochloric acid solutions when the gravimetric method was used. The experimental results are presented in the figure and table. The τ_c^i/τ_c^0 ratios were calculated by the method described in Communication II. The diagram shows that the effect of the uranyl ion on the proton relaxation time ($1/T_1$) depends on the nature of the anion. This is shown by the magnitudes of the molar relaxation shifts ΔM, and even more clearly by the value of τ_c^i/τ_c^0 (see table). Whereas this last value is approximately the same for chloride as for nitrate solutions, it is considerably higher for perchlorate and sulfate solutions. It is interesting to note the correlation between the shifts and τ_c^i/τ_c^0 ratios for the uranyl ion and the ionic radii of the anions which are given in the table.

The main conclusion to be drawn from the results is that the degree of covalency of the $U-OH_2$ bonds does not remain constant but varies in accordance with the nature of the anion present in the solution. It is not convincing, from the point of view of the tendency of these anions to form complexes with uranyl, to attribute the observed effect to formation of ion–anion covalent bonds, as the stability of the complexes formed by these anions increases in the sequence $ClO_4^- < Cl^-, NO_3^- \ll SO_4^{2-}$ [2,3], and sulfate (and not perchlorate) is the only anion in this series which could possibly form covalent bonds with uranyl. The increase of the molar shift ΔM and the τ_c^i/τ_c^0 ratio for ions of large radius suggests competition between two processes in this case: hydration and complex formation of the uranyl ion. However, the measured values probably reflect the degree of deformation of the hydration shell of the central ion by a given anion and not its ability to form complexes with uranyl. This hypothesis obviously requires additional experimental confirmation.

Salt	Δ_M ($\pm$0,5), arbitrary units	Anion radius, A	τ_c^i/τ_c^0
$UO_2(ClO_4)_2$	68,0	2,36	42,2
UO_2SO_4	56,0	2,06	34,5
$UO_2(NO_3)_2$	40,0	1,89	25,1
UO_2Cl_2	38,5	1,81	25,2

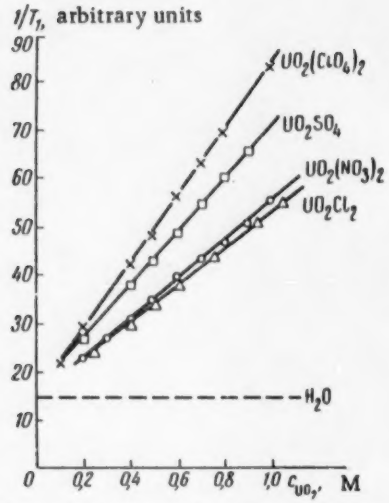

Variation of the time of proton relaxation in uranyl salt solutions. The signal of Mn^{2+} solution of $4.02 \cdot 10^{-4}$ M concentration was taken as 100.

Another aspect of the observed effect is significant. The probable competition between water and the anion in interaction with uranyl has a considerable influence on τ_C^i/τ_C^0 for a given ion; i.e., whereas these values can be determined with good confidence for alkali metals and halide ions, the determination is difficult for ions which enter into convalent interaction with water. Since uranyl forms bonds of a considerable degree of covalency with water, this has a most pronounced effect on its value of τ_C^i/τ_C^0.

LITERATURE CITED

1. V. M. Vdovenko and V. A. Shcherbakov, Zhur. Strukt. khim. 1, 1, 28 (1960).
2. G. T. Seaborg and J. J. Katz (editors), Actinide Elements [Russian translation] (IL, Moscow, 1955).
3. I. I. Lipilina, Uranyl and Its Compounds [in Russian] (Izd. AN SSSR, Moscow, 1959).

All abbreviations of periodicals in the above bibliography are letter-by-letter transliterations of the abbreviations as given in the original Russian journal. *Some or all of this periodical literature may well be available in English translation.* A complete list of the cover-to-cover English translations appears at the back of this issue.

POSSIBLE EXISTENCE OF BODY-CENTERED BORON CARBIDE AND SILICON OXYCARBIDE PHASES

V. A. Épel'baum, N. G. Sevast'yanov,

B. F. Ormont, and M. A. Gurevich

L. Ya. Karpov Physicochemical Scientific Research Institute
Translated from Zhurnal Strukturnoi Khimii, Vo. 2, No. 1,
p. 65, January-February, 1961
Original article submitted January 21, 1960

It was reported in [1] that the x-ray patterns of boron carbide contain lines corresponding to a cubic body-centered phase (with an identity period of about 3.16 kx), which was named the β-phase. The composition of this phase was not determined; in view of the fact that the intensity of its reflections was very high for all the samples, in some cases even higher than the intensity of the reflections of the main α-phase, it was to be assumed that this phase belongs to the boron–carbon system. Of course, it was difficult to exclude the possible presence of impurities in its composition, despite the fact that measures (treatment with hydrofluoric and other acids, etc.) were taken to remove them.

It was found later [2] that lines of the same phase are given by samples with the most diverse boron and carbon contents. It was therefore impossible for us to determine the position of the phase on the boron-carbon phase diagram; this gave rise to doubts concerning the composition of the phase, and then led to further experimental verification (see below) although, as was reported in [2], spectrum analysis did not reveal any appreciable impurities.

In 1958 Samsonov [3, 4] reported that he, jointly with Zhuravlev, discovered this phase in boron carbide as long ago as 1952-1953, but that it is in reality silicon oxycarbide. Despite the categorical character of Samsonov's statement, we consider that this fact required careful verification because of the practical importance of silicon oxycarbide and the theoretical significance of Samsonov and Zhuravlev's discovery. Up to now only the cubic carbide (and oxycarbide) of silicon was known, with only a face-centered cell of the sphalerite type. The system of lines in the x-ray pattern given by this system is entirely different from that given by the cubic body-centered cell. Therefore, Samsonov really claimed that he discovered a new silicon oxycarbide phase with a cubic body-centered lattice and an identity period of 3.16 kx.

We must point out that a cubic body-centered lattice of period 3.16 kx leads to definite crystal-chemical difficulties both in the case of boron carbide and in the case of silicon oxycarbide, because the interatomic distance $d = a\sqrt{3/2} = 2.85$ kx is greater than the sum of the radii of the atoms involved, and to account for this it is necessary to assume the existence either of structural units containing impurity atoms or of complex structural units giving a corresponding system of reflections. We concluded from this that the system of reflections corresponding to the cubic body-centered boron carbide cell is parasitic and is due to the presence of an extraneous phase in the sample.

Our exhaustive verifications showed that this contamination must be attributed to tungsten introduced with the wire used in filling the capillary with the sample for the x-ray investigation. Although it may seem strange at first sight that the amount of impurities introduced into the sample in this manner would give lines of even greater intensity than the lines of the principal phase [1], such an effect is quite probable, and was observed in [2], because of the great difference between the reflecting power of tungsten as compared with boron, silicon, and carbon.

It is likely that the cubic body-centered silicon oxycarbide phase discovered by Samsonov and Zhuravlev [3] in 1952 is of similar origin.

LITERATURE CITED

1. V. A. Épel'baum, M. A. Gurevich, and B. F. Ormont, Zh. neorgan. khimii 1, 2149 (1956).
2. V. A. Épel'baum, M. A. Gurevich, and B. F. Ormont, Zh. neorgan. khimii 4, 1938 (1959).
3. G. V. Samsonov, Zh. fiz. khimii 32, 2424 (1958).
4. G. V. Samsonov, Ukr. khim. zh. 24, 6, 659 (1958).

All abbreviations of periodicals in the above bibliography are letter-by-letter transliterations of the abbreviations as given in the original Russian journal. *Some or all of this periodical literature may well be available in English translation.* A complete list of the cover-to-cover English translations appears at the back of this issue.

THE CRYSTAL STRUCTURE OF EUCLASE

V. V. Bakakin and V. M. Al'tshuller

Institute of Inorganic Chemistry, Siberian Division, Academy of Sciences USSR, Novosibirsk

Translated from Zhurnal Strukturnoi Khimii, Vol. 2, No. 1, pp. 66-67, January-February, 1961
Original article submitted October 20, 1960

The crystal structure of euclase $AlBeSiO_4(OH)$ was determined by the trial method by Biscoe and Warren [1] in 1933; their paper contains a number of errors. Here we discuss only the most serious of these errors. One of the projections of the structure, chosen for the most graphic representation of the structure motif, is so arbitrary that it does not agree with the values of the atomic coordinates, especially for OH and Be, given later. Moreover, the coordinates as given lead to a different structure motif, which gives rise to certain doubts but is nevertheless given by the authors, who evidently did not notice the contradictions on the neighboring projection. Later publications on the structure of euclase either give the atomic coordinates from [1] without indication of the structure

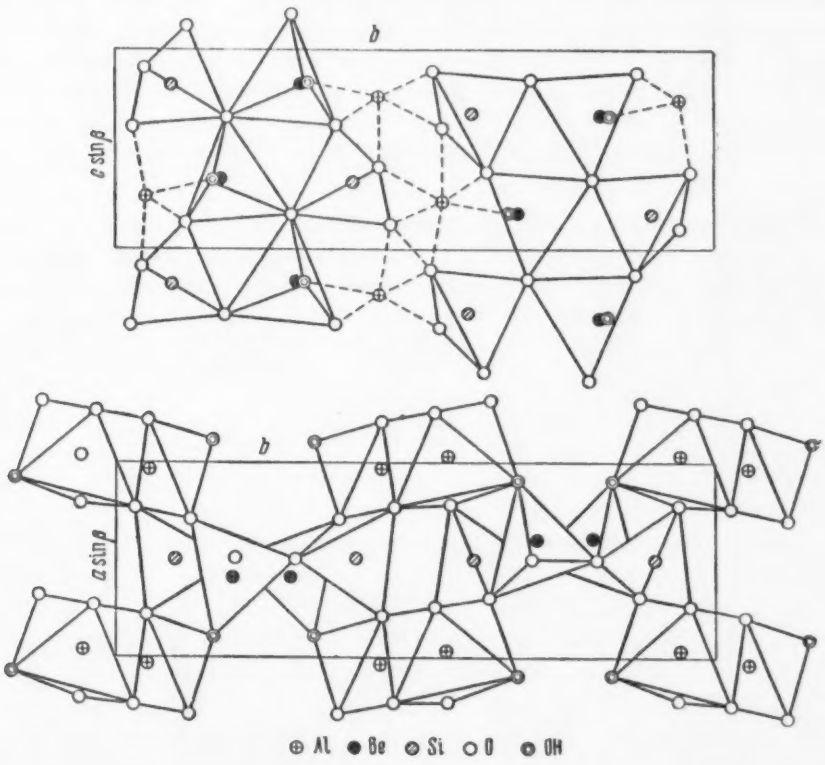

Projections of euclase structure.

Coordinates of Basal Atoms in Euclase Structure

	Data from [1]			Our data				Data from [1]			Our data		
	x	y	z	x	y	z		x	y	z	x	y	z
Al	0,97	0,440	0,25	0,03	0,445	0,247	O_{II}	0,74	0,030	0,17	0,78	0,053	0,101
Si	0,47	0,097	0,15	0,47	0,099	0,175	O_{III}	0,54	0,190	0,37	0,47	0,199	0,339
Be	0,50	0,306	0,48	0,53	0,300	0,164	O_{IV}	0,22	0,360	0,39	0,30	0,375	0,383
O_I	0,22	0,050	0,39	0,24	0,034	0,386	OH	0,78	0,330	0,19	0,87	0,332	0,164

motif [2, 3], or schematic descriptions of the structure without use of numerical characteristics [4, 5]; i.e., the incompatible data appear separately.

Preliminary results of a determination of the crystal structure of euclase by direct x-ray structural methods [6, 7] are given below. Fragments of large euclase crystals, obtained from the Mineralogical Museum of the Academy of Sciences, USSR, were used for the investifation. The constants of the monoclinic cell coincided, within the limits of accuracy with those given in [1]: a = 4.63, b = 14.27, c = 4.76 A, $\beta = 100°15'$, Z = 4, Fedorov group $C_{2h}^5 = P2_1/c$. A range of F_{hk0} and F_{hkl} was obtained with the KFOR x-ray goniometer with Mo radiation (the intensities were assessed visually from density ratings). The divergence coefficients (R) calculated from these values and from the coordinates [1] were 0.57 and 0.51 respectively; this confirmed our decision to use direct methods which do not require any arbitrary assumptions for the structure determinations.

The individual structure amplitudes, F_{0kl}, were found for 111 reflections after correction to an absolute scale by the Wilson and Vainshtein methods and introduction of an artificial temperature factor ($B = 1\ A^2$). The Harker–Kasper inequalities were used for determining the signs of 46 amplitudes which comprised (after verification by statistical equations) the basic groups from which the signs of 47 more amplitudes were determined by a purely statistical method. The 93 F_{0kl} to which signs had been allotted (83% of all the reflections of the zone) were used for constructing the $\sigma(yz)$ electron density projection which clearly showed peaks corresponding to all the atoms in the formula with the exception of Be. The value of R for this projection was 0.23 ($\sin\theta/\lambda \leq 1.05$, $F \neq 0$). Analysis of a second $\sigma(yz)$ projection, constructed with all the F_{0kl} taken into account, showed that the maximum initially ascribed to the OH group corresponds to overlapping OH and Be, and therefore, additional data are required for precise determination of their coordinates. An attempt at an analogous solution of the xy projection by direct methods was not successful, and at this stage of the investigation the x coordinates are estimated roughly, from crystal-chemical considerations.

The coordinates found for the basal atoms of the euclase structure are given in the table, with the coordinates from [1] also given for comparison. All the atoms are in general positions, and the structure is characterized by 24 independent parameters. The figure shows projections of the structure onto the yz and xy planes, which reflect its main characteristics most fully. The structure parameters are being determined more precisely.

LITERATURE CITED

1. J. Biscoe and B. E. Warren, Z. Krist. 86, 292 (1933).
2. R. W. G. Wyckoff, The Structure of Crystals (New York, 1935).
3. Strukturbericht (Leipzig, 1937) Vol. 3.
4. W. L. Bragg, Atomic Structure of Minerals (New York, 1937).
5. N. V. Belov, Mineralogical Collection of the Lvov Geological Society [in Russian] (1950) Vol. 4, pp. 29-32.
6. N. V. Belov and I. M. Rumanova, Trudy Inst. kristallografii 9, 103 (1954).
7. P. V. Pavlov and N. V. Belov, Kristallografiya 4, 324 (1959).

CRYSTAL STRUCTURE OF 4,4'-DICHLOROACENAPHTHENE

G. L. Avoyan and Yu. T. Struchkov

Institute of Heteroorganic Compounds, Academy of Sciences, USSR
Translated from Zhurnal Strukturnoi Khimmi, Vo. 2, No. 1, pp. 67-69,
January-February,1960
Original article submitted October 24, 1960

In a series of systematic investigations [1] of the structure of substances with considerable steric hindrances in the molecules ("overcrowded molecules") we determined completely the structure of 4,4'-dichloroacenaphthene. Its crystals belong to the C_{2h}^6 – C2/c space group with four molecules in the cell, which accordingly occupy special positions on the two-fold axes (a special position at the centers of symmetry is incompatible with the symmetry of the molecule itself). The constants of the unit cell are: $a = 15.37_5 \pm 0.01_2$, $b = 9.45_4 \pm 0.00_3$, $c = 7.47_5 \pm 0.01_2$A, $\beta = 118°25' \pm 15'$. An approximate model of the structure was found from projections of the interatomic function and electron density onto the ab face of the cell, and z coordinates were determined approximately by geometrical analysis of the molecular packing. The coordinates were determined more precisely by calculation of a three-dimensional electron density series (two approximations) from 600 structure amplitudes (taken with molybdenum radiation). The final values for the coordinates of symmetrically independent atoms are given in the table.

The precision in determinations of the atomic coordinates, estimated from Vainshtein's formulas [2], is Cl ± 0.002, C ± 0.008 A. This leads to errors of ± 0.01 A and ± 45' respectively in determinations of bond lengths and valence angles. The high degree of precision is also indicated by the fact that three of the four symmetrically independent hydrogen atoms were revealed (H_7^2 was not revealed); the average C–H bond length is 1.09 ± 0.11 A. The confidence factor for all reflections (including zero) is $R_{hkl} = 14\%$, and the temperature factor $B = 2.9$ A^2.

The structure of the molecule is shown in the figure (literature data [3] for acenaphthene itself are also given for comparison). Numbers with asterisks indicate the heights of the electron density maxima in electrons/A^3, and the numbers in parentheses represent the distances, in A, between the atoms and the median plane of the molecule, drawn through the C_2, C_3, C_5, and C_6 atoms. With the exception of C_1–C_7, the bond lengths in the ace-

Atom	x	y	z	Atom	x	y	z
Cl	0,1093	0,2200	0,2894	H_2	$0,22_6$	$0,72_6$	$0,32_3$
C_1	0,080	0,699	0,273		(0,228)*	(0,693)	(0,320)
C_2	0,164	0,632	0,296	H_3	$0,22_5$	$0,44_6$	$0,28_2$
C_3	0,168	0,482	0,301		(0,236)	(0,430)	(0,329)
C_4	0,089	0,402	0,279	H_7^1	$0,11_2$	$0,89_5$	$0,37_1$
C_5	0	0,464	1/4		(0,103)	(0,903)	(0,395)
				H_7^2			
C_6	0	0,614	1/4		(0,050)	(0,895)	(0,124)
C_7	0,052	0,848	0,259				

*Coordinates of the hydrogen atoms calculated with the usual assumptions (C–H=1.08 A, H–C–C'=–H–C–C'), are given in parentheses.

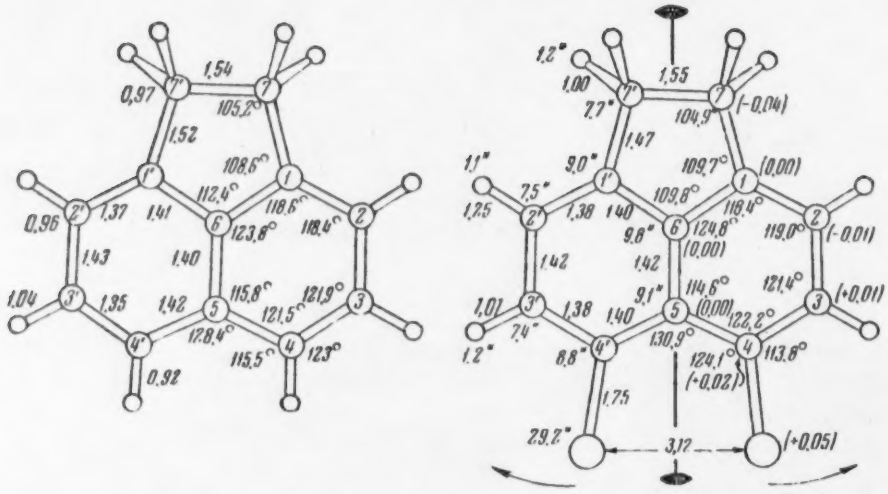

naphthene and 4,4'-dichloroacenaphthene molecules almost coincide; the observed differences may be attributed to the chemical influence of the chlorine atoms on the nucleus. On the other hand, because of the significant steric hindrance between the chlorine atoms, the valence angles in the two molecules differ considerably. The chlorine atoms repel each other and thus subject the molecule to the effect of a couple (arrows in the figure) which should, for example, increase the $C_4-C_5-C_4'$, C_5-C_4-Cl valence angles and decrease the $Cl-C_4-C_3$, $C_1-C_6-C'_1$ angles. This is fully confirmed by experimental results. As the result of these distortions of the valence angles the Cl . . . Cl distance increases from 2.77 A (with undistorted valence angles in the acenaphthene nucleus and with equal Cl–C–C external valence angles) to 3.12 A, but still remains appreciably less than double the intermolecular chlorine radius, 3.60 A. Moreover, because of the steric hindrance the molecule ceases to to be planar; one chlorine atom rises above and the other sinks below the median plane of the nucleus. The planar character of the nucleus itself is disturbed. However, the deviation from planarity is not large; this shows that deviation of a bond from its ideal direction in the plane of the nucleus occurs more easily than deflection from that plane. This difference is quite understandable if it is taken into account that the conjugation energy is diminished if the planar character of an aromatic system is disturbed (see, for example, [4]).

We are at present conducting x-ray structural investigations of crystals of other halogen-substituted acenapthenes, namely 4,4'-dibromoacenaphthene and 4-chloro-4'-bromoacenaphthene. The first of these is isomorphous with the 4,4'-dichloro derivative; the second forms triclinic crystals: space group $C_1^1-P\bar{1}$ with two molecules in the cell. The cell constants are: a = 9.11; b = 7.78; c = 8.49 A; $\alpha = 109.2°$; $\beta = 65.0°$; $\gamma = 99.0°$. Because of the large intermolecular radius of bromine, the molecules of these compounds are characterized by greater steric hindrances and therefore differ more than the dichloro derivative from the conformation of the acenaphthene molecule.

Experimental data on the molecular conformations of halogenated acenaphthenes, and also of other "overloaded" halogenated derivatives studied by us (in particular, 1,8-dihalonaphthalenes) make it possible to determine more precisely the curve for Van der Waals interaction of the halogen atoms and thereby to modify the results of theoretical calculations in conformation analysis [5]. The authors thank Prof. A. I. Kitaigorodskii for his interest in this work.

LITERATURE CITED

1. Yu. T. Struchkov et al., Series of articles on "Steric hindrance and molecular conformation" in Izv. AN SSSR, OKhN, e. g., 1, 105 (1960) and subsequent issues.
2. B. K. Vainshtein, Zh. éksperim. i teor. fiziki 27, 44 (1954).
3. H. W. W. Ehrlich, Acta Cryst. 10, 699 (1957).
4. C. A. Coulson and S. Senet, J. Chem. Soc., 1813 (1955).
5. A. J. Kitaygorodsky, Tetrahedron 9, 183 (1960).

CRYSTAL STRUCTURE OF 1, 4, 5, 8- TETRACHLORONAPHTHALENE

M. A. Davydova and Yu. T. Struchkov

Institute of Heteroorganic Compounds, Academy of Sciences, USSR
Translated from Zhurnal Strukturnoi Khimii, Vol. 2, No. 1, pp. 69-71,
January-February, 1961
Original article submitted October 24, 1960

This paper describes a part of our systematic investigation of the structure of aromatic molecules with large steric hindrances [1]; in particular, of halogenated naphthalene and acenaphthene [2, 3]. The purpose of this investigation is to determine the conformations of spatially stressed molecules and to determine more precisely the curves for the energy of interaction of atoms not linked by valence bonds [4, 5].

The crystals of 1, 4, 5, 8-tetrachloronaphthalene belong to the Pccn space group with four molecules in the cell, which should therefore be in special positions with symmetry $\bar{1}$ or 2. Our values for the cell constants coincide with those given in [6]: a = 9.45 ± 0.03; b = 15.20 ± 0.02; c = 7.07 ± 0.03 A. The approximate model of the structure, found from the xy projections of the interatomic function and electron density, showed that the molecules are in a special position on the dCad axes. These data themselves suggest that the molecule is nonplanar. In fact, a planar molecule has mmm self symmetry; on the other hand, a configuration which is nonplanar because of steric hindrance should have 222 symmetry. By the close-packing theory [7] in the former case the molecule should be on a center of symmetry; in the second case it should occupy a general position or lie on a two-fold axis.

The approximate values of the $\underline{z}$ coordinates of the chlorine atom were found from sections of the three-dimensional interatomic function $1/2, 1/2, \underline{z}$ and $2x_{Cl}, 2y_{Cl}, \underline{z}$ (two sections) which showed clearly that the molecule is not planar. Refinement of the structure was effected by calculation of two approximations of the three-dimensional electron density series (taken with molybdenum radiation; 350 nonzero reflections). The final values of the coordinates of symmetrically independent atoms in one molecule are given in the table, where the more natural structural numbering of the atoms is used, and not chemical numbering (see figure).

Atom	Experimental			Average*		
	x	y	z	x	y	z
Cl_1	0,1706	0,0280	0,1236	0,1702	0,0276	0,1236
Cl_2	0,5775	0,3530	0,1751	0,5770	0,3527	0,1751
C_1	0,260$_6$	0,127$_2$	0,145$_8$	0,2624	0,1264	0,1444
C_2	0,407$_9$	0,115$_1$	0,147$_0$	0,4080	0,1139	0,1448
C_3	0,501$_8$	0,188$_2$	0,156$_9$	0,5010	0,1882	0,1539
C_4	0,447$_4$	0,272$_0$	0,155$_7$	0,4457	0,2728	0,1543
C_5	0,297$_9$	0,287$_4$	0,149$_4$	0,2971	0,2877	0,1494
H_2				0,451	0,048	0,138
H_3				0,614	0,179	0,161

*The coordinates of the hydrogen atoms were calculated with the usual assumptions: C–H = 1.08A, the C'CH and C"CH angles are equal, and C, C', C", and H atoms are in the same plane.

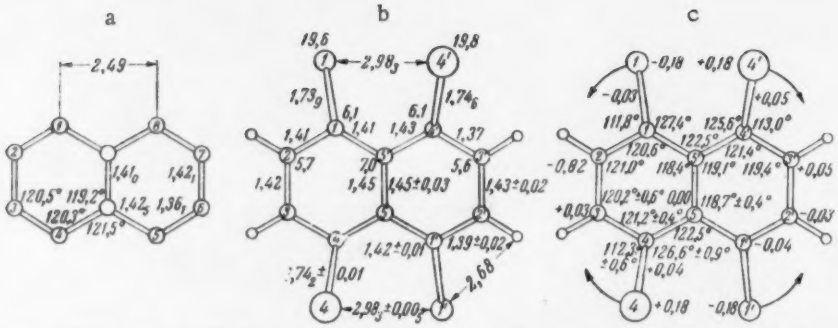

a) Structure of the naphthalene molecule according to [8]; atoms numbered in accordance with the chemical nomenclature; b) bond lengths (A) and heights of electron density maxima (el./A^3) in the structure of tetrachloronaphthalene; experimental values above and average values below; structural numbering of atoms; c) valence angles and distances (in A) of atoms from the median plane in the tetrachloronaphthalene molecule.

Since the symmetry of the molecule itself is 222, and the symmetry in the crystal is 2, i.e., lower, the accuracy of the calculations can be estimated from the scatter of the values for chemically equivalent but structurally different bonds, angles, and atoms. This comparison (see figure) shows that the errors are: for interatomic distances Cl−Cl ± 0.006, C−Cl ± 0.01−0.02, C−C ± 0.03 A; for valence angles ±1°; for distances from the median plane of the molecule ± 0.005 A for Cl atoms and ± 0.02 A for C atoms; ± 0.1 electron/A^3 for the heights of the electron density maxima. However, deviations of the chemically equivalent valence angles and of distances of the atoms from the median plane may be due to the influence of the force field of the crystal as well as to errors in the investigation. A similar estimate of the accuracy of the results is given by B. K. Vainshtein's formula with the parameters characteristic of this structure: $B = 3.7A^2$, $s_{max} = 0.60\ A^{-1}$, R = 15% (including zero reflections, hydrogen atoms disregarded). In addition to the experimental values, the table also gives average values for the coordinates calculated on the assumption of 222 symmetry for the molecule itself; these were used for calculating the average values in the figure.

The geometrical parameters found for the molecule are given in the figure, with data for naphthalene [8] shown for comparison. The lengths of the $C_5-C'_5$ and C_1-C_2 bonds are greater than in naphthalene, while the differences of the other bond lengths do not exceed the error limits (Fig. b). Changes of the valence angles in the naphthalene nucleus are also close to the experimental error, yet these changes coincide in sign with the deformations to be expected as the result of steric hindrances. These hindrances are due mainly to repulsion between neighboring chlorine atoms, the distance between which in a plane model with ideal valence angles (Fig. a) is anomalously small: 2.49 A instead of the equilibrium value of 3.6 A. Because of these hindrances the molecule is, as it were, subjected to the action of two couples (arrows in Fig. c) which push neighboring chlorine atoms apart. This should result in deformation not only of the CCCl valence angles but, although to a lesser extent, of the angles in the naphthalene nucleus itself (since conformational distortions spread over the whole molecule, rapidly diminishing with the distance from the site of their origin). In fact, the CCCl angles are deformed by 6-8°, and the angles in the nucleus by 0.5-1°, and in full agreement with our hypothesis the 1−5'−4' and 2−1−5' angles are increased while the 1−5'−5 and 1−2−3 angles are decreased. In addition to these deformations of the angles, the planarity of the molecule is disturbed appreciably (Fig. c). One of the causes of this disturbance is that the chlorine atoms, diverging in the plane of the molecule, approach the hydrogen atoms and repulsion arises between them (in the molecule in question the distance Cl...H = 2.68 A, which is less than the sum of the intermolecular radii, 3.0 A). Therefore, a further increase of the Cl...Cl distance owing to divergence of the chlorine atoms in the plane is apparently disadvantageous, and the increase is effected by emergence of these atoms from the plane of the molecule alternately upward and downward. It is probable that the hydrogen atoms which were not detected experimentally undergo analogous displacement, i.e., the arrangement of the peripheral atoms (chlorine and hydrogen) is similar to the arrangement of carbon atoms in the chair conformation of cyclohexane. In leaving the plane the peripheral atoms "draw" with them carbon atoms from the nucleus, which also loses its planar character (the disturbance is of the same character as in the trans-conformation of decalin); however, this

disturbance is small and close to the experimental error. It follows that steric hindrances are not localized in some restricted part of the molecule but are spread over the whole molecule by distortion of the valence angles, and in the case of aromatic systems the benzene rings have a tendency to adopt a conformation of the cyclohexane chair type. Because of these deformations the Cl····Cl distance in the molecule in question is increased from 2.49 to 2.98 A. It is still less than double the intermolecular radius for chlorine, 3.6 A (the atom compression–angle deformation compromise is operative here).

It is interesting to compare the conformations of 1,4,5,8-tetrachloronaphthalene and 4,4'-dichloroacenaphthene [3] molecules. In the former case the $Cl_1 \ldots Cl'_4$ and $Cl_4 \ldots Cl'_1$ steric hindrances (transmitted over the molecule through the hydrogen atoms) balance each other in the plane of the molecule. In the second molecule the CH_2-CH_2 bridge, which "draws together" the carbon atoms in the peri-positions, distorts the valence angles in the naphthalene nucleus in the same direction as does repulsion of the chlorine atoms. In full agreement with our hypotheses, the Cl . . . Cl distances and distortions of the valence angles were less, and disturbance of planarity greater, in the tetrachloronaphthalene molecule than in the dichloroacenaphthene molecule.

It will be very interesting to compare these two structures with the structures of peri-substituted naphthalenes which we are now investigating:

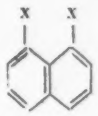

$X = CH_3$, Cl, Br, I

The crystals of 1,8-dichloro- (I) and 1,8-dibromonaphthalene (II) are isostructural and belong to the $P2_1/a$ space group with four molecules in the cell:

	I	II
a, Å	11,10	11,13
b, Å	10,65	10,90
c, Å	7,77	8,09
β	109°	108°

The data for (I) coincide with those given in [9]. In addition, another modification of (I) exists, with the same space group but with eight molecules in the cell. The crystals of 1,8-diiodonaphthalene are triclinic; space group $P\bar{1}$ with six molecules in the cell; the short period is approximately the same as for the other 1,8-dihalonaphthalenes.

In conclusion, the authors thank A. I. Kitaigorodskii for his interest in the work, and V. A. Koptyug for providing the samples for investigation.

LITERATURE CITED

1. Yu. T. Struchkov et al., Izv. AN SSSR, OKhN, 1, 105 (1960); 2, 322 (1960) and subequent communications in this series.
2. A. I. Kitaigorodskii, Yu. T. Struchkov, G. L. Avoyan, and M. A. Davydova, Dokl. AN SSSR 136, 3, 607 (1961).
3. G. L. Avoyan and Yu. T. Struchkov, Zh. strukt. khimii 2, 1, 67 (1961).
4. A. I. Kitaigorodskii, Tetrahedron 9, 183 (1960).
5. A. I. Kitaigorodskii, Dokl. AN SSSR (1961) (in press).
6. G. Gafner and F. H. Herbstein, Acta Cryst. 13, 702 (1960).
7. A. I. Kitaigorodskii, Organic Crystal Chemistry [in Russian] (Izd. AN SSSR, Moscow, 1955).
8. D. W. J. Cruickshank, Acta Cryst. 10, 504 (1957).
9. G. A. Gol'der, G. S. Zhdanov, M. M. Umanskii, and V. P. Glushkova, Zh. fiz. khimii 25, 1259 (1952).

CRYSTAL STRUCTURE OF TRIVALENT COBALT ACETYLACETONATE

L. M. Shkol'nikova and E. A. Shugam

All-Union Scientific Research Institute of Chemical Reagents
Translated from Zhurnal Strukturnoi Khimii, Vol. 2, No. 1,
pp. 72-73, January-February, 1961
Original article submitted January 26, 1960

The crystal and molecular structures of internal complexes of acetylacetone with various metals have been investigated for a number of years in the x-ray structure analysis laboratory of the Institute of Chemical Reagents. The acetylacetonates of aluminum, chromium, and cobalt [1-4] have been fully investigated by the x-ray structural method, and these compounds have been conclusively shown to be isomorphous.

In 1958, when we had nearly completed the investigations of these acetylacetonates, Padmanabhan [5] published the results of an x-ray structural investigation of trivalent cobalt acetylacetonate crystals. The values of the lattice constants and the space group given in his paper coincide with our data. However, comparison of the structure factors for reflections of the $0k\ell$ and $h0\ell$ types showed that Padmanabhan's values do not agree with ours. Our values of the $F(h0\ell)$ and $F(0k\ell)$ structure factors for cobalt acetylacetonate are close to the corresponding values for chromium acetylacetonate; this is a necessary consequence of the isomorphism of these compounds.

The difference in the values of $F(h0\ell)$ may be attributed to the fact that Padmanabhan's choice of axes in indexing of the x-ray patterns was different from ours: our $F(h0\ell)$ values are close to the $F(\bar{h}0\ell)$ values given in his paper, and vice versa; this suggests that Padmanabhan chose the reverse positive direction of the $\underline{x}$ axis. However, this suggestion cannot explain the observed differences for reflections of the $(0k\ell)$ type.

The coordinates of the cobalt atom, found from the Patterson projection, are x = 0.260, y = 0.160, z = 0.240, according to Padmanabhan, while our values are x = 0.230, y = 0.256, z = 0.211. The difference between the values of $\underline{y}$ is the most noteworthy. To verify Padmanabhan's determination of this coordinate we calculated the P(0vw) Patterson function projection from his experimental data; the result is shown in Fig. 1. This projection lacks the peak corresponding to the value y = 0.16 for the coordinate (marked by a cross). For comparison, we calculated the P(0vw) projection from our data. The resultant projection of the interatomic function (Fig. 2) confirms that our results are correct.

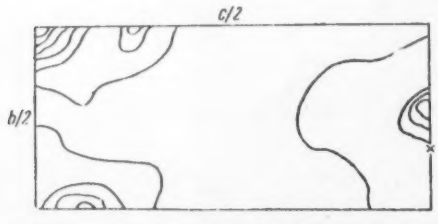

Fig. 1. bc projection of the P(Ovw) Patterson function from Padmanabhan's data.

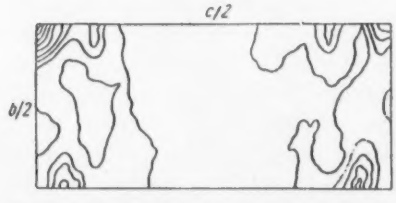

Fig. 2. bc projection of the P(Ovw) Patterson function from our data.

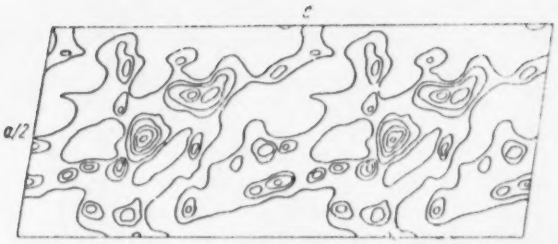

Fig. 3. Electron density projection p(x0z) from Padmanabhan's data (calculated by the authors).

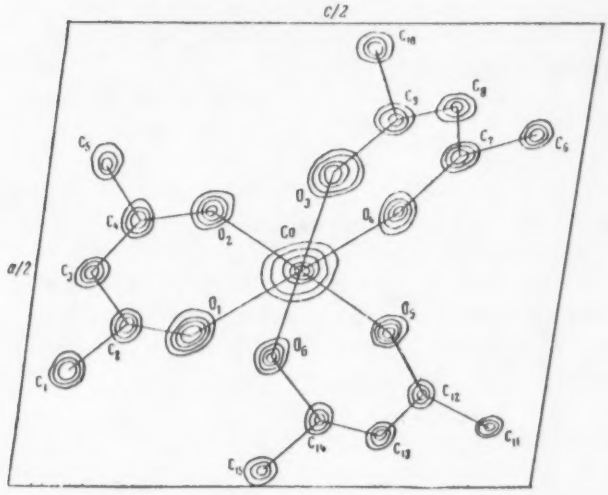

Fig. 4. ac projection of the structure of Co(III) acetylacetonate, based on Padmanabhan's data.

We also used Padmanabhan's data to calculate the electron density projection $\rho(x0z)$. The resultant distribution of the electron density peaks in the projection (Fig. 3) does not correspond to the diagram of the atomic configuration given in Padmanabhan's paper (Fig. 4). It is clear from a comparison of Fig. 3 and 4 that the peaks in the $\rho(x0z)$ projection given by Padmanabhan coincide very roughly with the peaks of our calculated $\rho(x0z)$ projection, while some atoms do not have corresponding electron density peaks at all. In addition, the $\rho(x0z)$ projection contains many false peaks, which can never be the case if the signs of all or most of the structure amplitudes are determined correctly.

The theoretical values of the structure amplitudes calculated from the atomic coordinates given in [5] do not confirm the corresponding values given by Padmanabhan [5], although in most cases they agree in sign. Calculation of the deviation coefficient, based on our values of F_{theor} and Padmanabhans's values of F_{exptl} gave R = 68%, whereas the value R = 18% is given in his paper.

Projections of the molecule onto the three coordinate planes, based on Padmanabhan's values of the coordinates, showed that the acetylacetone rings are completely distorted in all three projections. The values of valence angles for some atoms are impossible in real molecules. It is surprising that, despite all these contradictions in Padmanabhan's paper, he gives quite reasonable values for the interatomic distances and valence angles, close to those found by us, although the arrangement of the molecules in the crystal and their orientation with respect to the crystallographic axes diverge completely from our data. We are unable to account for this.

Padmanabhan's paper does not describe the whole course of the structure determination, but only the initial and final stages: calculation of the P(0vw) Patterson series from which the y and z coordinates of the cobalt atom were determined, and calculation of the electron density projection $\rho(x0z)$ whereby the coordinates of all the atoms could be determined. We repeated both these calculations, but obtained different results. The author does not describe the intermediate stages of the x-ray structure investigation.

Our detailed analysis of the investigation of the structure of trivalent cobalt acetylacetonate [5] showed with certainty that the atomic coordinates given by Padmanabhan are erroneous.

LITERATURE CITED

1. E. A. Shugam and L. M. Shkol'nikova, Kristallografiya 1, 4, 478 (1956).
2. L. M. Shkol'nikova, Kristallografiya 4, 3, 419 (1959).
3. L. M. Shkol'nikova and E. A. Shugam, Kristallografiya 5, 1, 32 (1960).
4. E. A. Shugam and L. M. Shkol'nikova, Dokl. AN SSSR 133, 2, 387 (1960).
5. V. M. Padmanabhan, Proc. Indian Acad. Sci. 47, 5, 329 (1958).

REVIEWS

CRYSTAL STRUCTURES OF TERNARY METALLIC COMPOUNDS

G. B. Bokii, B. K. Vul'f, and N. L. Smirnova

Institute of Inorganic Chemistry, Siberian Division, Academy
of Sciences USSR, Novosibirsk
N. E. Zhukovskii Air Force Engineering Academy
M. V. Lomonosov Moscow State University
Translated from Zhurnal Strukturnoi Khimii, Vol. 2, No. 1,
pp. 74-111, January-February, 1961
Original article submitted February 14, 1960

Ternary metallic compounds have been classified by their crystal structures for the first time. The system is based on principles of structural and chemical similarities between these compounds. Similar structural types are considered together as derivatives of certain simple structures. The data in this paper can be utilized in further development of the theory of the structure of multicomponent metallic phases, and are intended as reference material for a wide circle of specialists working in the fields of crystallography, crystal chemistry, and metal science.

CONTENTS

Introduction

List of compounds by structural types

a) Class ABC

I. Order of ternary compounds with structures based on those of pure metals with superstructures.

1. Copper family
2. Family of magnesium and multilayer hexagonal closest packings
3. α-Iron family
4. α-Manganese family
5. β-Manganese family
6. β-Uranium family

II. Order of ternary compounds with structures based on those of binary compounds with superstructures

1. Family of Laves phases
2. Family of other binary compounds

III. Order of true ternary intermetallic compounds

Subclass of silicides and borides

I. Order of ternary silicides and borides with structural types base on those of binary compounds with superstructures

II. Order of true ternary silicides and borides

b) Class ABX

Subclass of interstitial phases (carbides or nitrides)

I. Order in which the atoms of both metals are distributed statistically or with a superstructure in the positions of the atoms in the structural types of pure metals with the closest packing

II. Order of interstitial phases with structures based on those of binary compounds with superstructures

Subclass of other chemical compounds

I. Order of ternary compounds with structures based on those of binary compounds with superstructures

1. The ZnS (sphalerite) family

2. The CsCl – CaF_2 family and superstructures
3. The Fe_2As family
4. Family of other structural types
c) Class AXY
I. Order of interstitial phases
II. Order of carbonitrides
III. Order of ternary compounds with the structure of binary compounds
Ternary compounds with incompletely established structures
Cubic system
Hexagonal system
Tertagonal system
Rhombic system
Monoclinic system
Triclinic system
Undetermined system
Index of ternary metallic compounds
Literature cited

INTRODUCTION

Metallic compounds, i.e., compounds of metals with each other (intermetallic compounds) or compounds of metals with nonmetals, which retain metallic properties (such as carbides, silicides, nitrides, borides, etc.), are of undoubted theroretical interest and of great practical importance, as they are formed in many technical alloys.

The group of binary metallic compounds has been studied in detail; the structure, properties, and conditions for their formation in alloys are known for most of them. Several publications [1, 2] deal with the systematics of binary metallic compounds based on distinctions of their crystal structures. The first classification based on this principle is given in [1], where the position of metallic compounds among saltlike, organic, and other substances is also shown. Some of the most important metallic compounds are described in [3].

Many alloys contain, in addition to binary metallic compounds, the more complex ternary metallic compounds; interest in these has grown recently in relation to searches for new industrial alloys, based on studies of phase diagrams of three and more components.

The ternary metallic phases formed in such systems have a great diversity of structure and properties. An attempt has been made [4] to subdivide them into simpler types. This classification, based on a comparison of the location and extent of the homogeneous regions in ternary phase diagrams, to some extent reflects the conditions of chemical interaction of the components and is a further development of N. S. Kurnakov's [5] classification of metallic phases. Of the eight types of ternary metallic phases (Fig. 1), the last two should be classified as ternary metallic compounds. They are characterized by homogeneous regions limited on all sides and are phases which differ from the metals constituting the ternary system and from the binary compounds formed in that system by their own type of crystal structure and specific properties. The remaining ternary metallic phases, which are solid solutions based on one of the components in the diagram or on a binary compound (metallide solutions), cannot be regarded as independent ternary compounds and are therefore not considered in this review; the exceptions are the few phases of these types with a superstructure. In some instances it has not been established whether a given phase is a ternary compound or a metallide solution; such phases are considered below with appropriate comments.

Data on the structure of certain ternary metallic compounds are to be found in the well-known reference works Strukturbericht and Structure Reports. Fuller information on the subject is given in Pearson's handbook [6] where ternary and binary metallic compounds are described together and are not classified by structural types.

Palatnik and Finkel' [7] attempted to find the general structural relationships between certain ternary metallic compounds by classification, in accordance with structural characteristics, into electronic compounds, interstitial phases, Laves phases, nickel arsenide phases, and sigma-phases with the β-uranium lattice.

Special mention must be made of the numerous publications by P. I. Kripyakevich and his co-authors, concerned with determination and analysis of crystal structures of metallic compounds. In particular, an excellent

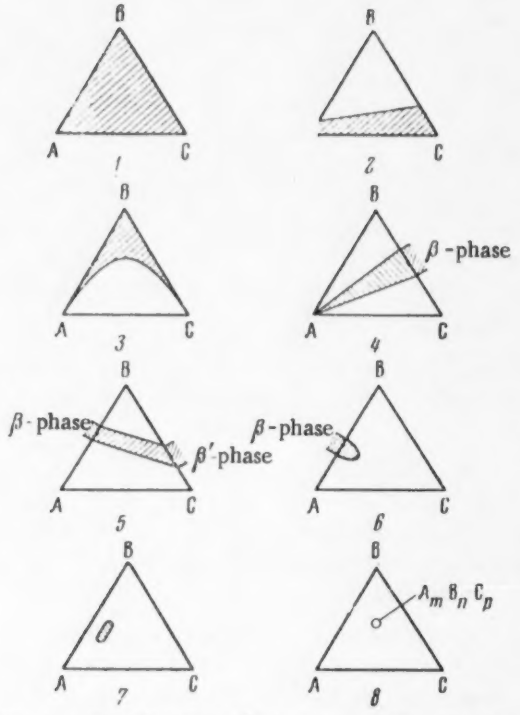

Fig. 1. Classification of ternary metallic phases: 1) continuous three component solid solutions; 2) continuous solid solutions of two components, with limited participation of a third component; 3) limited ternary solid solutions based on one component; 4) continuous solid solutions of one of the components with a binary metallic compound; 5) continuous mutual solid solutions of pairs of binary metallic compounds; 6) limited solid solutions based on a binary metallic compound; 7) ternary metallic compounds with limited homogeneity regions; 8) ternary metallic compounds which do not form solid solutions.

analysis of these structures regarded as packings of coordination polyhedra is presented by P. I. Kripyakevich in his dissertation [8] and in the paper [9]. Therefore, structural problems directly associated with coordination numbers are not considered in detail in the present review.

A general classification of ternary metallic compounds by the types of their crystal structures (interpreted up to 1957) was first given in [10]; however, the lattice constants and atomic coordinates are not given in this publication. Moreover, these data are now far from complete, because during recent years there have been many publications reporting determinations of crystal structures of new ternary metallic compounds and refinement of earlier results.

In this article we present classified data on crystal structures of ternary metallic compounds, with detailed characterization, completely covering all the literature up to 1960.

In this review ternary metallic compounds are arranged by structural types. The choice of the arrangement of the structural types presented certain difficulties. It is known that classification based on coordination numbers is widely used at the present time, since this principle gives the fullest characterization of the spatial relationships of the atoms in the crystal structure and to some extent reflects the character of interatomic bonding. Moreover, there are relatively few coordination numbers and they can be determined quite easily.

However, the coordination principle does not give a classification of structural types by their genetic characteristics; i.e., it cannot be used for considering individual structural groups in the light of a common structure. An attempt is therefore made in the present review to unify a number of structural types, which are presented as derivatives of certain very simple structures formed as the result of ordering, with or without removal of part of the atoms. This concept is a further development of the ideas of N. V. Belov [3], who showed that very many structural types can be reduced to closest packing with vacancies filled in different ways. We discovered a similar relationship between structural types among certain ternary metallic compounds. In addition, we attempted to emphasize the similarity of individual motifs in the simplest and more complex structures, and also the similarity found between their superstructure types.

Thus, the proposed classification is based on principles of chemical and structural similarities of ternary metallic compounds.

The ternary metallic compounds can be divided into three main classes:

a) The ABC class, comprising the intermetallic compounds, i.e., compounds consisting of metals of all the a subgroups of the periodic system, the first three b subgroups, and certain semimetals lying below the diagonal boundary drawn from boron to astatine. These semimetals are of intermediate character and can therefore play different roles in different structural types, so that compounds containing them may occur in different classes.

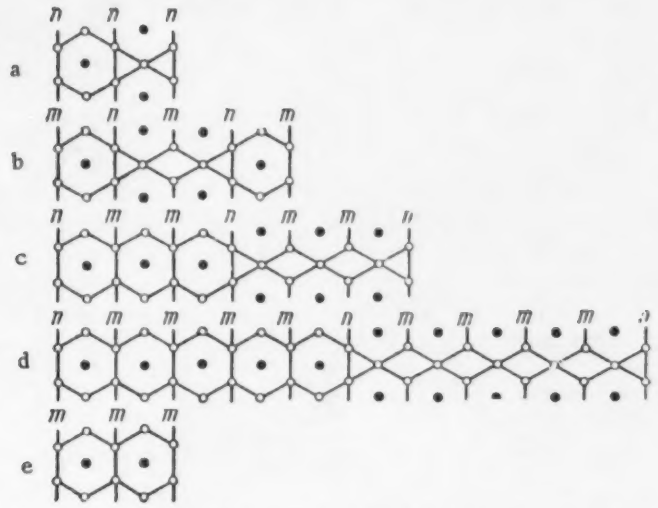

Fig. 2. Some types of band combination in closest packings.

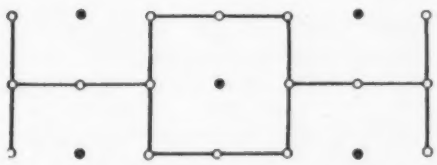

●–(Ga, Zn) ₂ o–Au

Fig. 3. Position of (Ga, Zn) ₂ and Au atoms in the $Au_5(Zn_2,Ga)$.

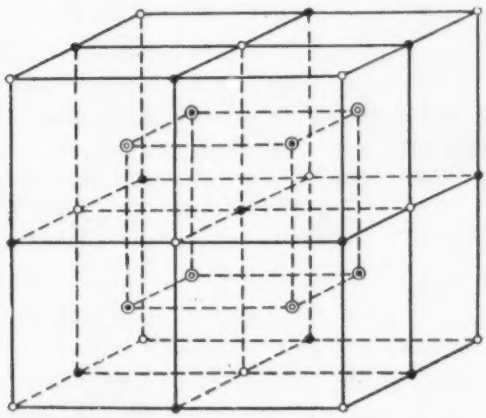

Fig. 4. Superstructure of α-Fe type.

b) The ABX class, in which one of the elements (X) is above this diagonal boundary and is therefore an organogen, and only the other two elements are metals; this group includes such compounds as phosphides.

c) The AXY class, with two organogen elements (X and Y) and one metal.

Compounds containing elements located on the diagonal boundary are the most difficult to classify.

We have put the great majority of the silicides in class "a" if normal intermetallic compounds crystallize in this structural type together with the silicides. If the presence of silicon leads to distinct structural types, they are considered separately in the appropriate subclasses.

A very small number of silicides is placed in class "b," which is often characterized by special structural types with low coordination numbers, such as ZnS or CaF_2. The carbide structural types, together with some nitrides which are interstitial phases, are considered as a subclass of this class. These structures are often characterized by closest packing of the metal atoms, which accounts for their formal similarity to class "a" structures.

It follows from the above that the arrangement of ternary metallic compounds by classes and subclasses is primarily based on chemical characteristics. Within the classes or subclasses the ternary compounds are grouped in orders, which differ significantly from each other by structural characteristics. Finally, in each order there may be families, which combine similar structural types which differ either by distortion of the crystal structure or by the nature of the superstructure.

Ternary metallic compounds with incompletely established structures are classified by their crystal systems in separate table.

No.	Compound	Lattice constants a, Å	Literature	No.	Compound	Lattice constants a, Å	Literature
No. 1	$Ca_2(Tl_3, Sn_3)$*	4,767	[15]	No.3	$Ca_2(Sn_3, Pb_3)$	4,825	[15]
No. 2	$Ca_2(Tl_3, Pb_3)$	4,856	[15]	No.4	$Fe(Pt_2, Cu)$	3,825	[16]

*This compound should be represented by the formula $Ca(Tl, Sn)_3$, as the Tl and Sn atoms correspond to the Cu atoms in Cu_3Au and are evidently distributed statistically. However, to make it easier to use the literature, we retain the formulas as written in the original papers, with the statistically distributed atoms in parentheses and separated by commas. This formulation gives some indication of the composition of the composition of the compound.

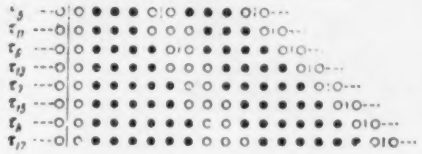

Fig. 5. Alternation of metal atoms and vacancies in τ-(Al – Cu – Ni) phases.

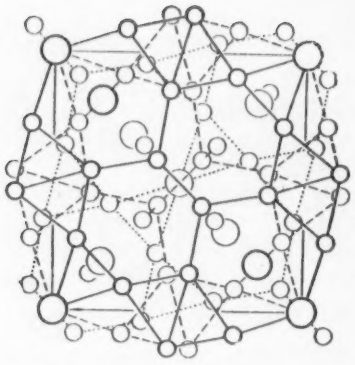

Fig. 6. Structure of χ-(Cr – Mo – Fe) phases.

The crystal system,* Fedorov space group (F. gr.), number of formula units in the unit cell (Z), and position of the atoms (with lattice constants) are stated for each structural type, and the general characteristics of the structure are given. In cases of well-known structural types of elements or binary compounds the positions of the atoms and descriptions of the structure are not given, only references to the corresponding literature sources ([1], [3], etc.)being given; if the atomic coordinates are given in these sources, they are not detailed here. Complex cubic structures of metallic compounds are not described from the point of view of their formation from networks (polygons), because such analysis has been performed in detail by Kasper, Frank, and others [11, 12].

The compounds in a given structural type are listed next. For each compound we give the serial number in the classification, the composition in atomic percentages or the stoichiometric formula (sometimes both), the lattice characteristics (distances,** axis ratios, angles), and literature references.

If different authors give different structural characteristics for a given ternary metallic compound, the most reliable and complete data are given together with all literature references to the compound. References to sources containing the most complete data are given in semibold type in such cases. Low-temperature and high-temperature modifications are indicates as l.t. and h.t. respectively.

The ternary metallic compounds within each structural type are usually given in an order corresponding to the positions of their constituent elements in the groups of the expanded form of the periodic system; if the elements are in the same group, then the compounds are given in order of increasing atomic numbers of the elements. However, in some instances there are deviations from this rule, because it is preferable to present structurally analogous elements of a ternary compound and of a compound which is a representative of a given structural type in the same sequence.

*The following abbreviations are used: C. = cubic; H. = hexagonal; T. = tetragonal; R. = rhombic; M. = monclinic; Tr. = triclinic.

**If no units are given, the lattice constants in the original publication and in our list are given in kx.

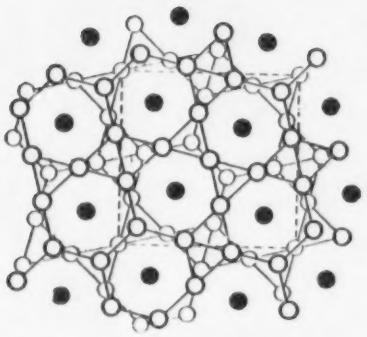

Fig. 7. Structure of σ-phase.

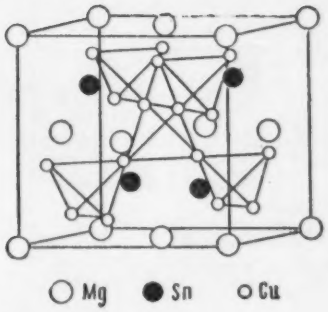

Fig. 8. Structure of $MgSnCu_4$.

The appended illustrations in some cases give a clearer picture of the common character of the structural types, and in others, explain the positions of the atoms in certain complex crystal structures of ternary metallic compounds. Diagrams of well-known structures of metals and binary compounds (Mg, Au, $CrSi_2$, Ta_3B_4, Laves phases, etc.) are not given; only references to general handbooks [1, 3] and other sources containing such diagrams are indicated.

At the end of the review there is an index in which all the ternary metallic compounds are arranged in alphabetical order of the elements and the number of each compound in the list of structural types is given.

The authors certainly admit that the proposed system for classification of ternary metallic compounds by crystal structures is subject to possible corrections and improvements, and thank readers in advance for their comments. The authors offer their sincere thanks to P. I. Kripyakevich for his thorough examination of the manuscript and for a number of valuable comments.

LIST OF COMPOUNDS BY STRUCTURAL TYPES

A) CLASS ABC

I. ORDER OF TERNARY COMPOUNDS WITH STRUCTURES BASED ON THOSE OF PURE METALS WITH SUPERSTRUCTURES

1. Copper Family

Superstructures in the Cu_3Au structural type. C.; F. gr. Pm3m; Z = 1. [1], p. 279.

According to [13] and [14], each type of superstructure in closest packings of the AB_3 type can be characterized uniquely by:

1) type of closest packing; 2) type of combination of the bands of atomic hexagons in the closely packed layer.

Cu_3Au has closest packing of the ABC type, band combination n (Fig. 2a), CC superposition of cube-octahedron layers.

Structural Type $Au_{62.5}Zn_{29.5}Ga_8[Au_5(Zn_2,Ga)]$

R.; F.gr. Z = 4. [1], p. 282.

$Au_{(1)}$ 8(*f*) : $x = 0{,}105$; $y = 0{,}784$; $z = 0$. $Au_{(2)}$ 8(*f*) : $x = 0{,}23$; $y = 0$; $z = 1/4$.
$Au_{(3)}$ 4(*b*). $(Zn, Ga)_{(1)}$ 8(*i*) : $x = 0{,}108$; $y = 0{,}29$; $z = 0$. $(Zn, Ga)_{(2)}$4(*a*).

Cubic closest packing with superstructure. If the difference of $Au_{(1,2,3)}$ and $(Zn, Ga)_{(2)}$ and a certain displacement of the atoms are disregarded, the structure should be assigned to the $TiAl_3$ type; ABC packing; band combination m (Fig. 2e), CC superposition of cube-octahedron layers.

The $(Zn, Ga)_{(2)}$ atoms are located in layers which in $TiAl_3$ are perpendicular to the fourfold axis and consist only of Al atoms. The $(Zn, Ga)_{(2)}$ and Au atoms (in 1:3 ratio) are in an ordered arrangement in these layers (Fig. 3) and in both the first and the second coordination spheres are surrounded only by Au atoms within the layer.

No. 5. $Au_5(Zn_2, Ga)$ $a = 10,924$ $b = 5,462$ $c = 8,068$ [17]

Structural Type $ZrAl_3$

T; F. gr. 14/mmm; Z = 4. [1], p. 282; [3], p. 195.

ABC closest packing; band combination nm (Fig. 2b); CCC'C' superposition of cube-octahedron layers.

No. 6. Pt (Cu, Zn_2) $a = 3,84_8$ $c = 14,5_0$ $c/a = 3,76_8$ [18]

Structural Type $Au_{75}Zn_{18}Ga_7[Au_3(Zn_{2/3}, Ga_{1/3})]$

T.; F. gr. 14/mcm; Z = 12.

Au 16(*l*). Au 8(*f*) : $z = 0,080$. Au 8(*h*) : $x = 0,190$; $y = 0,31$; $z = 0$.
Au 4(*b*). Zn, Ga 8(*g*) : $x = 0,5$; $y = 0$; $z = 0,089$. Zn, Ga 4(*a*).

Distorted cubic closest packing of Au, Zn, Ga atoms. The Zn, Ga atoms in cube-octahedrons of Au atoms. Band alternation nnm in layer, CCCC'C'C' alternation of cube-octahedron layers.

No. 7. $Au_3(Zn_{2/3}, Ga_{1/3})$ $a = 5,580$ $c = 25,16$ [17]

Structural Type $Au_{62,5}Zn_{35}Ga_{2,5}[Au_5(Zn_{2,8}, Ga_{0,2})]$.

Distorted cubic closest packing. $(Zn, Ga)_I$ atoms in cube-octahedrons of Au and $(Zn, Ga)_{(II)}$. Band alternation nnnnm in layer, CCCCCC'C'C'C'C' alternation of cube-octahedron layers. The $(Zn, Ga)_{II}$ and Au atoms in ordered positions, as $(Zn, Ga)_{(2)}$ and $Au_{1,2,3}$ in Au_5Zn_2Ga.

No. 8. $Au_5(Zn_{2,8}, Ga_{0,2})$ [17]

2. Family of Magnesium and Multilayer Hexagonal Closest Packings

Structural Type Mg

H.; F. gr. C6/mmc; Z = 2. [1], pp. 99 and 226.

	a	*c*	*c/a*	
No. 9. $MnCu_2Sn$, l.t.	2,73	4,34	1,59	[19]
No. 10. $FeCu_2Sn$, l.t.	2,73	4,34	1,59	[19]
No. 11. RuOsIr				[20]
No. 12. Cd (Mg, Al)$_2$	3,12	5,09	1,63	[20a]

Structural Type Ni_3Ti

H.; F. gr. C6/mmc; Z = 4. [1], p. 287.

ABAC closest packing; band combination n (Fig. 2a); CC superposition of cube-octahedron layers.

No. 13. $Au_{82,5}Cd_{10}In_{7.5}^{**}$ $a = 5,791$ $c = 9,522$ $c/a = 1,644_3$ [21,22]

Structure Type $Au_{75}Cd_{2.5}In_{22.5}$

R. ABAC closest packing; band combination mmmmn (Fig. 2d); CC'CC'C superposition of cube-octahedron layers.

No. 14. $Au_{75}Cd_{2,5}In_{22,5}$ $a = 5,847$ $b = 50,91$ $c = 4,758$ [22]

Structural Type $Au_{78,7}Cd_{12,6}In_{8,7}$

R. ABABAC closest packing; band combination nm (Fig. 2b); CCC'C' superposition of cube-octahedron layers. Atoms somewhat displaced from ideal position.

No. 15. $Au_{78,7}Cd_{12,6}In_{8,7}$ $a = 5,802$ $b = 20,09$ $c = 14,340$ [21,22]

---

* ~ 7.5 % at. %

** According to [22], a solid solution of Cd in Au_7In.

Structural Type $Au_{75}Cd_{3.5}In_{21.5}$

R. ABABACAC closest packing; band combination mmn (Fig. 2c); CCC'CCC' superposition of cube-octahedron layers. Structure with rhombic distortion.

No. 16. $Au_{75}Cd_{3,5}In_{21,5}$ $a = 5,840$ $b = 30,34_4$ $c = 19,09_5$ [21,22]

Structural Type $Au_{75}Cd_{10}In_{15}$

M. ABABCBCAC closest packing; band combination mmn (Fig. 2c); CCC' superposition of cube-octahedron layers.

No. 17. $Au_{75}Cd_{10}In_{15}$ $a = 5,819$ $b = 30,32_4$ $c = 64,60_5$ $\alpha^* = 89,75°$ [21,22]

Structural Type $Au_{75}Cd_{12.5}In_{12.5}$

M. ABABCBCAC closest packing; band combination nm (Fig. 2b); CCC'C superposition of cube-octahedron layers. Atoms somewhat displaced from ideal position.

No. 18. $Au_{75}Cd_{12,5}In_{12.5}$ $a = 5,820$ $b = 20,10_8$ $c = 86,20_0$ $\alpha^* = 89,73°$ [21,22]

3. The α- Iron Family

Structural Type CsCl

C.; F. gr. Pm3m; Z = 1. [1], p. 349.

Figure 4 shows eight cells of the CsCl structure; the Cs atoms are at a and b, the Cl atoms at c and d.

	a	
No. 19. $Li_2(Hg_1, Tl_1)$	3,354	[23]
No. 20. β-Ti (Mo, Al)**		[24]
No. 21. β_3-$(Ti_1, Al_1)Ni_2$***		[25, 26]
No. 22. $(Mn_1, Si_1)Co_2$	2,827	[27, 28]
No. 23. T-$Cu_5(Zn_2, Al_3)$	2,920	[29, 30]

Structural Type $Au_2(Cu_1, Zn_1)$

R.; F. gr. Pcma; Z = ½.

Au 4(*h*) : $x = 0,136$; $z = 3/16$. Cu, Zn 4(*g*) : $x = 0,114$; $z = 11/16$.

Distorted CsCl.

No. 24. $Au_2(Cu_1, Zn_1)$ $a = 8,980$ $b = 2,886$ $c = 4,539$ [3] [3]

Apparently the Cu_2Au_3Zn phase with rhombic symmetry, found in [32], corresponds to this phase.

Structural Type Fe_3Al

C.; F. gr. Fm3m; Z = 4. [1], p. 428 (BiF_3).

The Fe atoms are at b, c, d; the Al atoms are at a (Fig. 4).

	a	
No. 25. β'-$(Mg, Ag)_3Sn$	6,60	[33]
No. 26. $(Ni, Cu)_3Sn$	5,946	[34]
No. 27. β-$(Ni, Cu)_3Sb$	5,857	[34]

Structural Type Cu_2AlMn

C.; F. gr. Fm3m; Z = 4.

The Cu atoms are in positions c and d; Al atoms are at a and Mn atoms at b (Fig. 4).

*In the original paper the special direction is called the a axis.

**Most probable composition is Ti_2MoAl.

***The Al and Ti atoms alternate in the cubes like Zn and Al in Cu_2ZnAl.

	a			a	
No. 28. Co_2MnGe	5,733	[28]	No. 37. Cu_2MnGa***		[41]
No. 29. Co_2MnSn	5,991	[35, 36, 37]	No. 38. Cu_2MnIn	6,1865 Å	[42]
No. 30. Ni_2MgSn	6,097	[34]	No. 39. Cu_2MnSn, l.t.	6,1608	[39, 43]
No. 31. Ni_2MgSb	6,050	[34]	No. 40. Cu_2FeSn, l.t.	5,92	[18]
No. 32. Ni_2TiAl	5,86	[25]	No. 41. Cu_2CoSn	5,97	[18]
No. 33. Ni_2MnGe*	5,69	[28]	No. 42. Cu_2NiSn	5,91	[18]
No. 34. Ni_2MnSn	6,045	[35, 36, 37]	No. 43. Cu_2InSn	6,1865—6,1881 Å	[42, 44]
No. 35. Ni_2MnSb**	6,001	[38]	No. 44. Zn_2CuAu	6,10	[31]
No. 36. Cu_2MnAl, h.t.	5,937	[39, 40]	No. 45. β^*-Zn_2AgAu	$6,2833_2$	[45, 46]

Structural Type NaTl

C.; F. gr. Fd3m; Z = 8. [1], p. 291.

Na atoms in positions a and d; Tl atoms at b and c (Fig. 4).

	a	
No. 46. Li_2MgZn	6,7 Å	[8, 47****]
No. 47. Li_2MgAl	6,7 Å	[48, 49, 50]

Structural Types of τ-(Cu – Ni – Al) Phases *****

The structures are intermediate between the NiAl and Ni_2Al_3 types. NiAl has structure of the CsCl type: the Ni atoms form a simple cubic structure in which all the close-packed networks, perpendicular to one of the threefold axes, are occupied by Ni atoms. In Ni_2Al_3 two such networks occupied by Ni atoms alternate with one vacant network.

In τ-phases the network alternation is more complex. Figure 5 shows alternation of Ni, Cu atoms (black circles) and vacancies (white circles) in the direction of the z axis for each τ-phase; the subscript with each phase symbol indicates the number of networks per period (marked off by vertical strokes).

Structural Type τ_5; H.; F. gr. $R\bar{3}m$; Z = 3*****

No. 48. $Al_5(Cu, Ni)_3$ $a = 8,7050$ Å $\alpha = 27°19'22"$ [51, 52]

hexagonal cell: $a = 4,111$; $c = 5,0250 \cdot 5$Å (composition: Al — 57, Cu — 37, Ni — 6 at. %)

Structural Type τ_{11}; H.; F. gr. $C\bar{3}m$; Z = 3.

No. 49. $Al_{11}(Cu, Ni)_6$ $a = 4,1141$ Å $c = 5,0263 \cdot 11$ Å [52]
(comp: Al — 57, Cu — 35, Ni — 8 at. %)

Structural Type τ_6; H.; F. gr. $C\bar{3}m$; Z = 3.

No. 50. $Al_6(Cu, Ni)_4$ $a = 4,1132$ Å $c = 5,0225 \cdot 6$ Å [52]
(comp: Al — 57, Cu — 34, Ni — 9 at. %)

Structural Type τ_{13}; H.; F. gr. $R\bar{3}m$; Z = 3.******

No. 51. $Al_{13}(Cu, Ni)_8$ $a = 21,8537$ Å $\alpha = 10°48'00"$ [52]

hexagonal cell: $a = 4,1133$; $c = 5,0133 \cdot 13$Å (composition: Al — 57, Cu — 32, Ni — 11at. %)

---

*Composition corresponds to nonhomogeneous microstructure.

**Homogeneity region includes the composition Ni(Mn, Sb), where the arrangement of the atoms corresponds to the As(Mg, Ag) structure (see p. 92).

***Assignment to Cu_2AlMn structural type not proved.

****Data on the cubic structure of Li_2MgZn not confirmed in [47].

*****The τ-(Cu_9Al_4Ni) phase was first discovered in 1938 [51]. In subsequent investigations [52 and others] the existence of different τ-phases was demonstrated (fuller details in text).

******Z given for hexagonal lattice.

Structural Type τ_7; H.; F. gr. $C\bar{3}m$; Z = 3.

No. 52. $Al_7(Cu, Ni)_5$ $a = 4,1062$ Å $c = 4,9912 \cdot 7$ Å [52]
(comp: Al — 61, Cu — 28, Ni — 11 at. %)

Structural Type τ_{15}; H.; F. gr. $C\bar{3}m$; Z = 3.

No. 53. $Al_{15}(Cu, Ni)_{10}$ $a = 4,0958$ Å $c = 4,9763 \cdot 15$ Å [52]
(comp: Al — 60, Cu — 28, Ni — 12 at. %)

Structural Type τ_8; H.; F. gr. $R\bar{3}m$; Z = 3.*

No. 54. $Al_8(Cu, Ni)_3$ $a = 13,4929$ Å $\alpha = 17°29'50"$ [52]
hexagonal cell: $a = 4,1045$; $c = 4,9812 \cdot 8$Å (composition: Al — 61, Cu — 27; Ni — 12%)

Structural Type τ_{17}; H.; F. gr. C3m; Z = 3.

No. 55. $Al_{17}(Cu, Ni)_{12}$ $a = 4,1014$ Å $c = 4,9705 \cdot 17$ Å [52]
(comp: Al — 61, Cu — 26, Ni — 13 at. %)

Structural Type T_1-Al_7Cu_4Ni

H.; F. gr.. $R\bar{3}m$; Z = 1.

$Al_{(1)}1(a)$. $Al_{(2)}2(c)$: $x = 0,1255$. $Al_{(3)}2(c)$: $x = 0,2515$. $Al_{(4)}2(c)$: $x = 0,3800$. $Al_{(5)}2(e)$.

12,5% vacant sites in Al positions. Al 12,5% vacant sites in Al positions
$(Cu, Ni)_{(1)}$ $2(c)$: x=0,1900 (15% vacant sites).
$(Cu, Ni)_{(2)}$ $2(c)$: x=0,3145 (32% vacant sites).
$(Cu, Ni)_{(3)}$ $2(c)$: x=0,4380.

According to [52], type T_1 corresponds to type τ_8, but in distinction from it also has vacant sites in positions of the Al atoms.

No. 56. T_1-Al_7Cu_4Ni $a = 13,53$ Å $\alpha = 17°27'$ hexagonal cell: a=4.105; c=39,97Å

Structural Type τ-(Cu_3Al_6Ni)

(See note on structural types of τ-(Cu — Ni — Al), phases, p. 76)

No. 57. $T' = Cu_{16}Zn_3Al_{21}$ ** [30, 54]

4. The α-Manganese Family

Structural Type of χ-phases (superstructure of α-manganese)

C.; F. gr. $I\bar{4}3m$; Z = 58. [1], p. 229.

Atom distribution in χ-(Cr—Mo—Fe): $Mo_{(1)}2(a)$. $Mo_{(2)}8(c)$. 15Fe + 9Cr 24(g). 21Fe + 3Cr 24(g).

Atom distribution in $TiCr_2Co_4$: Ti, Cr 2(a). Ti, Cr 8(c). Cr, Co 24(g). Co 24(g).

If we move from the vertices or the center of the cell we meet, for example in χ=(Cr — Mo — Fe), with the following sequence of polyhedrons: center [$Mo_{(1)}$], tetrahedron [$Mo_{(2)}$], Laves polyhedron (Fe + Cr), Laves polyhedron (Fe + Cr);*** For comparison with σ-and p-phases (see Fig. 7 and 12), the structure is represented in Fig. 6 in the form of networks of hexagons, triangles, and additional atoms.

		a	
No. 58.	χ - $Ti_8Cr_7Fe_{17}$	8,904	[55]
No. 59.	$TiCr_2Co_4$	8,82	[56]
No. 60.	χ - (Cr — Mo — Fe)	8,920Å	[57, 58, 59, 60, 61]
No. 61.	Cr_3Co_3Si	8,708	[62]
No. 62.	χ - (Cr — W — Fe)		[60, 61, 63]
No. 63.	χ - (Cr — Fe — Ni)	8,878 Å	[64]

*Z given for hexagonal lattice.
**One of the possible compositions of the T' phase is given.
*** As in the original Russian.

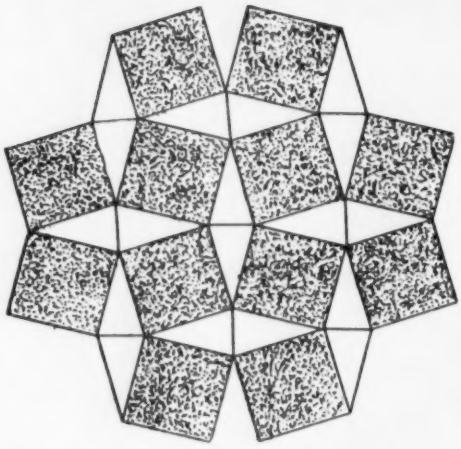

Fig. 9. Networks of Al atoms in the structures of Co_2Al_9 and $FeCu_2Al_7$.

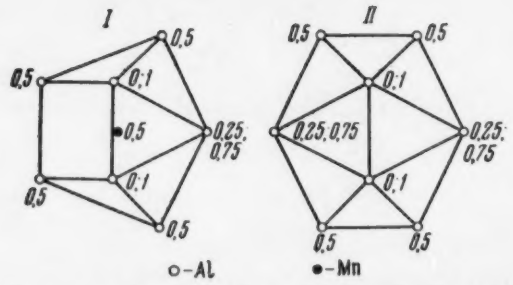

Fig. 10. Geometrical similarity between the icosahedron and the coordination polyhedron of Al atoms around the Mn atom in the $MnAl_6$ structure; I) coordination polyhedron; II) icosahedron (crystallographic).

5. The β-Manganese Family (Structural Type β-Mn)

C.; F. gr. $P4_32$ or $P4_132$; Z = 20. [1], p. 231.

	a	
No. 64. β^m - (W — Fe — C)*	6,395 A	[65, 66]
No. 65. β' - $Al_3Cu_{12}Sn$**		[67]
No. 66. $Cr_3Ni_5Si_2$	6,108	[62]
No. 67. $Ni_{15}Cu_{65}Ge_{20}$	6,260	[68]

6. The β-Uranium Family (Structural Type of σ-phases)

T.; F. gr. P4/mnm; Z = 30. Apparently superstructure of β-uranium. Atomic positions: 2(a). 4(f): x = 0.3981. 8(i_1): x = 0.4632; y = 0.1316. 8(i_2): x = 0.7376; y = 0.0653. 8(j): x = 0.1823; z = 0.2524. The distribution of the atoms is shown in Fig. 7.

	a	c	c/a	
No. 68. σ-(Cr — Mo — Fe)***	8,929 Å	4,640 Å	0,5196	[59, 69]
No. 69. Cr_8WNi_5	8,901 —8,945 Å	4,599 — —4,621 Å	0,5167 —0,5166	[70, 71]
No. 70. $Cr_{65}Ni_{25}Si_{10}$	8,769	4,561	0,529	[62]

II. ORDER OF TERNARY COMPOUNDS WITH STRUCTURES BASED ON THOSE OF BINARY COMPOUNDS WITH SUPERSTRUCTURES

1. Family of Laves Phases (Structural Type $MgCu_2$)

C.; F. gr. Fd3m; Z = 8. [1], p. 299

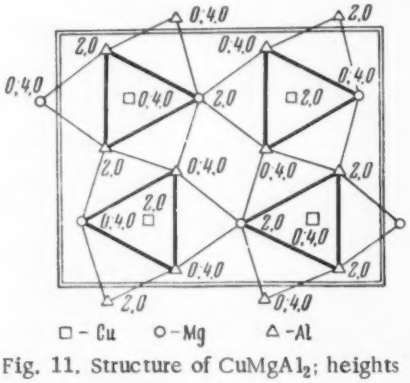

Fig. 11. Structure of $CuMgAl_2$; heights given to the nearest 0.1 A.

N. V. Belov [3] regards Laves phases as defective closest packings. From this point of view the $MgCu_2$ type is a cubic closest packing of Cu atoms with half the sites omitted. The Mg atoms occupy 1/8 of the tetrahedral voids. In contrast to Cu_3Au, formed from one type of AB_3 layers ($AuCu_3$, Fig. 2a), $MgCu_2$ is formed from alternating A'B'$_2$(IICu$_3$)* and A"B'$_2$(CuII$_3$). The A'B_3' layers are superposed on A"$B"_3$ layers like AB_3 layers in Cu_3Au.

	a	
No. 71. θ-Mg(Li_1, Zn_1)	7,427	[47,72]
No. 72. U'-Mg_3(Al_2, Cu_4)	7,01—7,12	[73,74]
No. 73. Mg($Co_{0,7}$, $Zn_{1,3}$)		[75]
No. 74. Mg(Ni, $Zn)_2$	6,909Å	[76]
No. 75. Mg($Ni_{1,8}$, $Si_{0,2}$)		[75]
No. 76. 7 =Mg(Cu_1, Zn_1)		[76,77]
No. 77. Mg($Ag_{0,8}$, $Zn_{1,2}$)		[75]

*If the carbon atoms are in the octahedral voids then this compound should be assigned to the $Fe_7Mo_{13}n_4$ structural type of the ABX class (p. 95).

**On the basis of the valence-electron concentration the authors of [7] consider the formula $Al_4Cu_{15}Sn$ as the more correct

***Possibly a metallide solution; investigation not completed.

****II represents a vacant site.

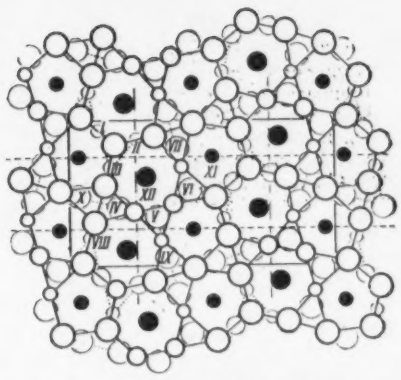

Fig. 12. Structure of the R-(Mo – Ni – Cr) phase. The Roman numerals are the number of the atoms (see text).

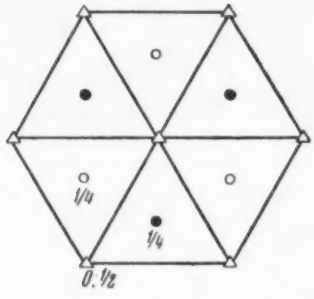

△-Zr ●-Be ○-Si

Fig. 13. Structure of BeSiZr. The numbers are heights in fractions of the unit cell.

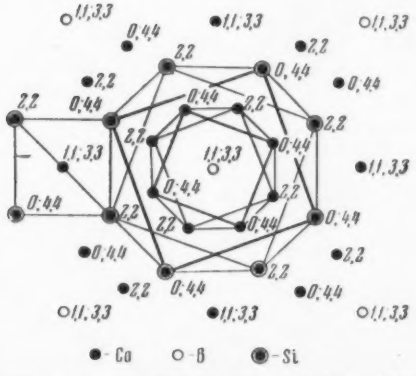

●-Co ○-B ◉-Si

Fig. 14. Structure of $Co_{4.7}Si_2B$, heights given to within 0.1 A.

No. 78. $Zr(V_{0.6}, Ni_{1.6})$	6,946	[8,28,78]
No. 79. $Zr(Cr_1,Ni_1)$ **		[28]
No. 80. $Zr(Mn_1, Ni_1)$	7,003—7,031	[8,28,78]
No. 81. $Ta(V_1, Cu_1)$	7,115Å	[70]
No. 82. $Ta(V_{1.5}, Mn_{0.5})$	7,008Å	[70]
No. 83. $Ta(Fe_1,Ni_1)$	6,717Å	[70]
No. 84. $U(Fe_1, Ni_1)$	7,054Å	[79]
No. 85. $Mn(Be_{1.2}, Co_{0.8})$	6,19	[8]
No. 86. $Mn_1(Cu_8,Sn_1)$ ***	6,9658Å	[80]
No. 87. $Cd(Cu_1, Zn_1)$	7,15	[75]

Structural Type $FeAl_2Be_{2.3}$

M.; F. gr. C2/m; Z = 2

2Fe 2(*a*). 2Be 2(*c*). 3Be 4(*f*). 4Al 4(*i*): $x = 0{,}3707$; $z = 0{,}1139$.

Superstructure of $MgCu_2$. $A'B'_3 = \Pi Cu_3$; $A''B''_3 = Fe\Pi_3$ (compare with Mg_2Cu_3Si). No. 88. $FeAl_2Be_{2.3}$ a=7,718A, b = 4,4554Å, c = 5,542Å, β = 124°32′ [81]

Structural Type $MgSnCu_4$

C.; F. gr. F43m; Z = 4.

Mg 4(a). Sn 4(b). Cu 16(c).

Superstructure of $MgCu_2$. The Mg and Sn atoms are distributed like Zn and S in sphalerite (Fig. 8).

No. 89. $MgSnCu_4$ a=7,030 [82,83]

Structural Type Cu_2AlBe_3

R.; F. gr. Pmma; Z = 2.

Al 2(*e*): $z = 7/8$. Cu 2(*f*): $z = 5/8$.
2 Cu + 6Be 2(*c*), 2(*b*), 4(*k*): $y = 1/4$; $z = 1/4$.

Superstructure of $MgCu_2$. The Al and Cu atoms are in the ordered positions of Mg. In the direction of one of the "former" fourfold axes two layers of Al atoms alternate with two layers of Cu atoms.

	a	b	c	
No. 90. δ1-(Cu,Al)(Cu_1,Be_3) *	4,499Å	4,499Å	6,362Å	[84]

Structural Type $MgZn_2$

H.; F. gr. $P6_3/mmc$; Z = 4. [1], p. 301; [3], p. 186.

The Zn atoms are at the positions of the ABAC (chch) closest packing with half the sites omitted. The Mg atoms occupy 1/8 of the tetrahedral voids. The $A'B'_3(\Pi Zn_3)$ layers of type h and $A''B''_3(Zn\,\Pi_3)$ layers of type c are formed as shown in Fig. 2a. The $A'B'_3$ layers are superposed on $A''B''_3$ layers like AB_3 layers in the Ni_3Ti type.

		a	c	c/a	
No. 91.	$Mg(Al_1, Cu_1)$, l.t.	5,119Å	8,39Å	1,639	[74]
No. 92.	$Mg(Al_{1.1}, Ag_{0.9})$				[75]
No. 93.	$Ca(Mg,Cd)_2$	6,06₂Å	9,83₂Å	1,621	[85]
No. 94.	$Ca(Mg_{0.02},Ag_{1.98})$	~5,71	~9,34	1,64	[85,86]
No. 95.	$Ca(Al,Ag)_2$				[75]
No. 96.	$Zr(V,Fe)_2$**				[87]

*Possibly a solid solution based on $ZrCr_2$.

**This formula represents one of the stoichiometric compositions found in [80], but does not correspond to the atom distribution in the Laves phase; it is more correct to represent this compound by the formula (Mn, Sn)(Cu, Sn)$_2$.

***With 15.45% Al and 11.7% Be by weight.

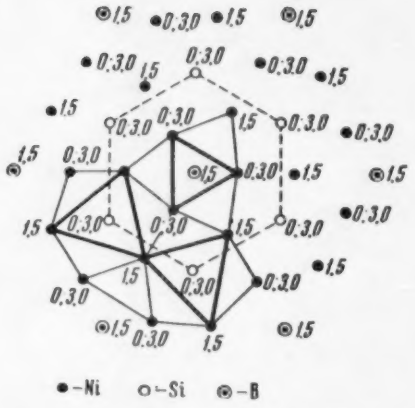

Fig. 15. Structure of Ni_6Si_2B; heights given to within 0,1 A.

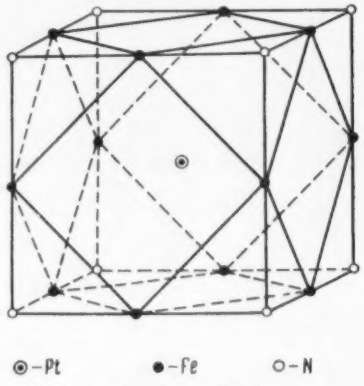

Fig. 16. Structure of $PtNFe_3$.

No. 97. $Zr(V, Co)_2$**				[87]
No. 98. $Zr(Cr,Co)_2$				[87]
No. 99. $Ta(Ti_1, Co_1)$	4,982Å	8,140Å	1,634	[70]
No. 100. $Ta(V_1, Co_1)$	4,893Å	7,909Å	1,616	[70]
No. 101. $Ta(V_1, Ni_1)$	4,848Å	7,909Å	1,631	[70]
No. 102. $Ta(V_{1,5}, Cu_{0,5})$	5,072Å	8,206Å	1,631	[70]
No. 103. $Ta(Cr_1, Ni_1)$	4,855Å	7,888Å	1,624	[70]
No. 104. $(Cr, Fe)Be_2$, h.t. **	4,37	6,98	1,60	[88]
No. 105. $(Mn_1, Co_1)Be_4$***	4,27	6,94	1,625	[8]
No. 106. $Mn(Mn_{0,125}, Co_{1,125} Si_{0,75})$ ****	4,738	7,452	1,572	[28,89]
No. 107. $Mn(Mn_{0,125}, Ni_{1,125}, Si_{0,75})$ ****	4,752	7,492	1,576	[28,89]
No. 108. $Fe(Ti_1Si_1)$******				[90]

Structural Type Mg_2Cu_3Si

H.; F. gr. C6/mmc; Z = 4.

Mg 4(*f*)*****. Si 2(*a*). Cu 6(*h*).

Superstructure of $MgZn_2$: $A'B'_3 = \Pi Cu_3$; $A''B''_3 = Si\Pi_3$.

No. 109. Mg_2Cu_3Si l.t. $a = 5,004$ $c = 7,872$ $c/a = 1,573$ [91,92]

Structural Type $MgNi_2$

H.; F. gr. $P6_3/mmc$; Z = 8. [1], p. 302 and [3], p. 186.

Closest packing ABCBACBC (cchccccchc) of Ni atoms with half the sites omitted. The Mg atoms occupy $^1/_8$ of the tetrahedral voids. The $A'B'_3(\Pi Ni_3)$ and $A''B''_3(Ni\Pi_3)$ layers are as in $MgZn_2$, with $A'B''_3$ of type c only.

	a	*c*	*c/a*	
No.110. $Mg(Li_{0,25}, Zn_{1,75})$*****	5,220	17,201	3,295	[47]
No.111. $Mg(Cu_1,Al_1)$ l.t.	5,080	16,57	3,262	[74]
No.112. $Mg_2(Cu_1, Zn_3)$	5,124Å	16,82Å	3,283	[75,76]
No.113. *V*-$Mg_2(Cu_1, Zn_4)$	5,11	16,55	3,24	[93]
No.114. $Mg_2(Cu_3, Si_1)$, l.t.	5,0	16,0	3,2	[75,91,92]
No.115. $Mg(Ag_{0,4}, Zn_{1,6})$				[75,94]
No.116. $U(Mn, Ni)_2$	4,9760	16,420	$3,300_0$	[95]
No.117. $U(Fe, Ni)_2$	$4,961_8$	$16,390_8$	$3,303_4$	[95]
No.118. $U(Co,Ni)_2$	$4,952_9$	$16,361_4$	$3,303_4$	[95]

2. Family of Other Binary Compounds

Structural Type NiAs – Ni_2In

H.; F. gr. C6/mmc; Z ~ 1.6 [1], p. 353.

No. 119. CoNiSn * $a = 4,087$ $c = 5,198$ $c/a = 1,272$ [36]

Structural Type MnGeNi

H.; F. gr. $P6_3/mmc$; Z = 2

Mn 2(*a*). Ge 2(*c*). Ni 2(*d*).

Superstructure of Ni_2In the same as for BeSiZr (see p. 86).

---

*Possible a metallide solution.

** $z_{(Mn_1, Co_1)} = 0,053$.

*** Mn 4(*f*) : $z = {}^1/_{16}$. 0,5Mn + 4,5Co(Ni) + 3Si 2(*a*)and 6(*h*) : $x = {}^5/_6$.

**** For coordinates, see $MgZn_2$.

***** $z_{Mg_{(1)}} = 0,094$; $z_{Mg_{(2)}} = 0,844$; $x_{(Li,Zn)_{(2)}} = 0,167$; $z_{(Li,Zn)_{(3)}} = 0,125$.

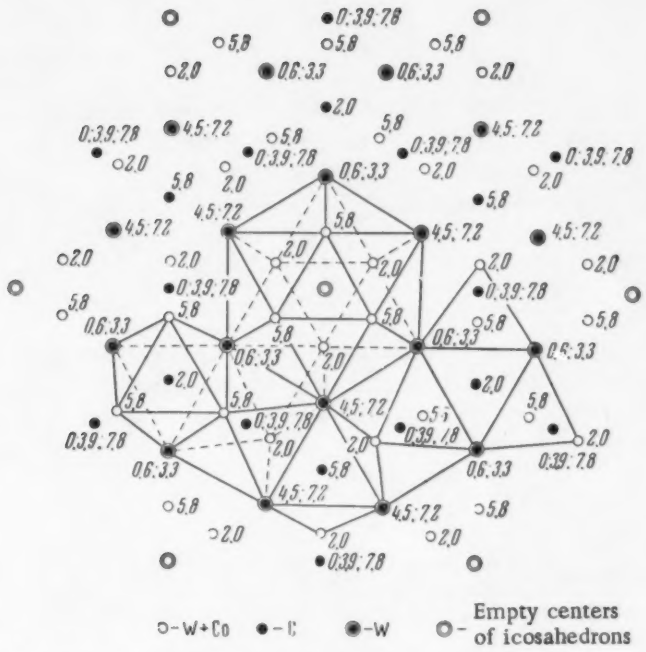

Fig. 17. Structure of $Co_3W_9C_4$; heights given to within 0.1 A.

		a	c	c/a	
No. 120.	FeGeMn	4,096	5,213	1,273	[36]
No. 121.	FeGeNi*	4,008	5,072	1,266	[36]
No. 122.	CoMnGe	4,034	5,241	1,299	[36]
No. 123.	CoFeGe *	3,970	5,018	1,264	[36]
No. 124.	CoNiSb **	3,987	5,158	1,294	[36]
No. 125.	NiMnGe	4,058	5,331	1,326	[36]

Structural Type CoSn

H.; F. gr. C6/mmm; Z = 3. [1], p. 308.

No. 126. $Fe_2(Ga_1, Ge_1)$ $a=5,00$ $c=4,035$ $c/a=0,807$ [18]

Structural Type Pt_2Sn_3

H.; F. gr. C6/mmc; Z = 2. [1], p. 312.

Very "flattened" ABCACB closest packing of Sn atoms. The tetrahedrons under the octahedron form a 7-point polyhedron with the latter. The Pt atoms fill all the octahedral voids except those between BC and CB layers. The Pt atom has another neighboring Pt atom in addition to seven neighboring Sn atoms. The eight Pt neighbors form a distorted cube.

No. 127. $Au_4(In_3,Sn_3)$ $a=4,49$ $c=13,08$ $c/a=2,91$ [96]

Structural Type Co_2Al_9

M.; F. gr. $P2_1/a$; Z = 2. [1], p. 307.

The structure consists of square networks alternating with the networks shown in Fig. 9 and formed from Al atoms. The Co atoms are located in the Thomson cubes formed between the different types of networks. The structure is allied to $FeCu_2Al_7$

No. 128. p-$(Fe,Ni)_2Al_9$ [97,98]

*Possibly a metallide solution.

**Z ~1.6. (1.5Co + 0.5Ni) 2(a). (1.5Sb + 0.5Ni) 2(c). 0.5Ni 2(d); possibly a metallide solution.

Structural Type $MnAl_6$

R.; F. gr. Cmcm; Z = 4.

Mn 4(c) : $y = 0{,}457$. $Al_{(1)}8(e) : x = 0{,}324$. $Al_{(2)}8(f) : y = 0{,}14$; $z = 0{,}10$. $Al_{(3)}8(g)$: : $x = 0{,}32$; $y = 0{,}284$.

The Mn atoms are in 10-point polyhedrons of Al atoms (Fig. 10). In Fig. 10 the 10-point polyhedron is compared schematically with the icosahedron. The numbers represented the heights of the atomic positions; the measurement unit is the distance between parallel edges of the icosahedron.

No. 129. $(Fe,Cu)(Cu,Al)^*_6$ $a=7{,}449$ $b=6{,}428$ $c=8{,}768$ [99,100]

Structural Type Co_2Al_5

H.; F. gr. C6/mmc; Z = 4. [1], p. 307.

The space is filled with Al and Co icosahedrons, Al 9-point polyhedrons (trigonal prism + 3 hemioctahedrons, empty Al octahedrons, and Al and Co tetrahedrons. The icosahedrons contain Al atoms, and the 9-point polyhedrons, Co atoms. The atoms contained in the Co icosahedrons composed of Co are themselves in icosahedrons formed by Al and Co (compare with $Co_3W_9C_4$).

No. 130. π-$Al_{10}(Fe_3,Ni_1)$ [97,98]

Structural Type Al_9Mn_3Si

H.; F. gr. $P6_3/mmc$; Z = 2.

$Al_{(1)}6(h) : x = 0{,}4578$. $Al_{(2)}12(k) : x = 0{,}2007$; $z = 0{,}933$. Mn $6(h) : x = 0{,}1199$. Si $2(a)$.

The structure is of the Co_2Al_5 but the 9-point polyhedrons formed by Al atoms are not occupied. The Si atoms are in icosahedrons formed by Mn and Al atoms, and the Mn atoms in their turn are distorted icosahedrons formed by Al and Mn atoms. If the Mn atoms are disregarded, the coordination polyhedron of Al atoms around the Mn atoms is a 9-point polyhedron very close to the coordination polyhedron of Mn atoms in $MnAl_6$.

No. 131. β-Al_9Mn_3Si $a=7{,}513$Å $c=7{,}745$Å $c/a=1{,}0308$ [101,102]

Structural Type WAl_{12}

C.; F. gr. Im3; Z = 2.

W $2(a)$. Al $24(g) : y = 0{,}184$; $z = 0{,}309$.

The WAl_{12} structure is the same as that of $CoAs_3$, but the W atoms are in icosahedrons and the octahedrons are empty.

No. 132. $(Cr,Mn)Al_{12}$ $a=7{,}505$Å [103]

Structural Type $Mg_2Cu_6Al_5$

C.; F. gr. Pm3; Z = 3.

$Cu_{(1)}12(k) : y = 0{,}243$; $z = 0{,}336$. $Cu_{(2)}6(e) : x = 0{,}225$. $Al_{(1)}8(i) : x = 0{,}215$. $Al_{(2)}6(g)$: : $x = 0{,}16$. $Al_{(3)}1(b)$. Mg $6(f) : x = 0{,}32$.

Superstructure of Mg_2Zn_{11}. The structure is made up of individual "bricks" which are themselves (Cu_3Au; β-W) of structural types, and of hexagonal antiprisms which also contain atoms. As in other complex cubic structures, the following sequence is found in the $Mg_2Cu_6Al_5$ structure starting from the center: (Cu) octahedron, (Al) cube, cube with truncated vertices, formed by two distorted (Cu) cube-octahedrons with somewhat twisted triangular faces, a distorted Fedorov (Mg and Al) cube-octahedron, (Al) cube.

No. 133. V-$Mg_2Cu_6Al_5^{**}$ $a=8{,}311$Å [73,104,105]

*Not definitely assigned to $MnAl_6$ type.

**According to [104], identical with the compound $Mg_3Cu_7Al_{10}$ found in [105]; however, according to [106], the alloy corresponding to the composition $Al_5Cu_6Mg_2$ is not a single phase.

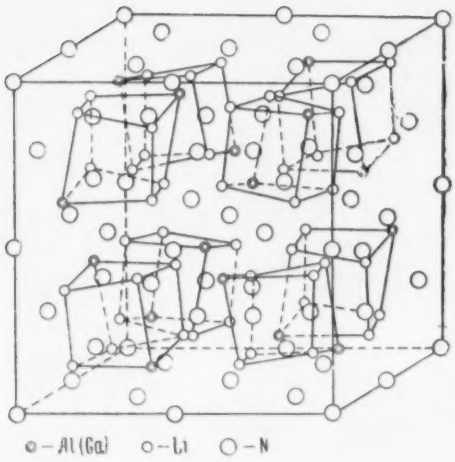

Fig. 18. Structure of Li_5GaN_2 (Li_3AlN_2).

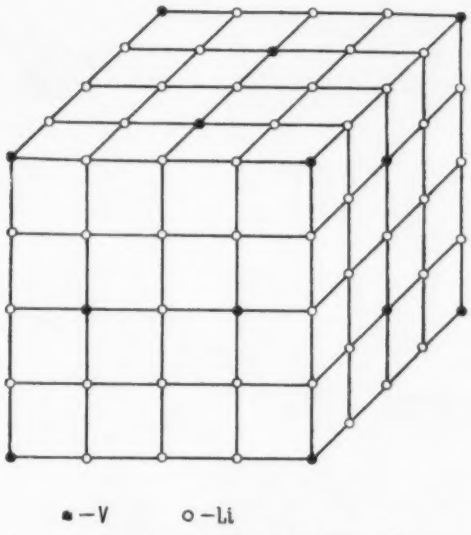

Fig. 19. Positions of V and Li atoms in the ternary compound Li_7VN_4.

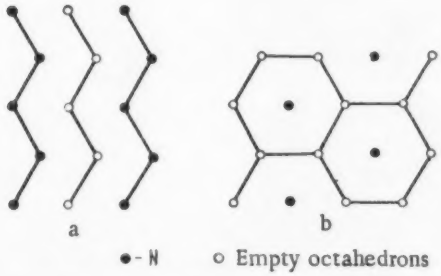

Fig. 20. Arrangements of N atoms in Fe – C – N phases.

III. ORDER OF TRUE TERNARY INTERMETALLIC COMPOUNDS

Structural Type $FeCu_2Al_7$

T.; F. gr. P4/mnc; Z = 4.

$Al_{(1)}4(e) : z = 0{,}134$. $Al_{(2)}8(g) : x = 0{,}165$.
$Al_{(3)}16(i) : x = 0{,}198$; $y = 0{,}420$; $z = 0{,}100$.
Cu $8(h) : x = 0{,}278$; $y = 0{,}088$. Fe $4(e) : z = 0{,}2992$. In the compound $CoCu_2Al_7$ the values of the coordinates are: 0.132; 0.153; 0.202; 0.420; 0.100; 0.272; 0.088; and 0.2970.

Two square networks of Al atoms, one above the other, form cubes in some of which Cu atoms are situated in an ordered arrangement. The two square networks alternate with one network of the type shown in Fig. 9. The Thomson cubes formed between networks of different types contain Fe atoms.

		a	*c*	*c/a*	
No. 134.	ω-$FeCu_2Al_7$	6,336Å	14,870Å	2,347	[100,107, 108]
No. 135.	$CoCu_2Al_7$	6,3047Å	14,756Å	2,341	[108,109]

Structural Type $CuMgAl_2$

R.; F. gr. C/mcm; Z = 4.
Al $8(f) : y = 0{,}355$; $z = 0{,}055$.
Cu $4(c) : x = 0{,}778$. Mg $4(c) : x = 0{,}072$.

The Cu atoms are in 9-point polyhedrons of Al and Mg atoms. The Al atoms form prisms, and the Mg atoms lie opposite the centers of the square faces of the prisms (Fig. 11). The 9-point polyhedrons are arranged as in $PuBr_3$. One of the edges of the $MgCuAl_2$ cell is almost equal to the edge of the $PuBr_3$ cell, but the other two are considerably less. Therefore, the $MgCuAl_2$ cannot be regarded as a superstructure of the $PuBr_3$ type.

No. 136. *S*-$CuMgAl_2$ a=4,00 b=9,27 c=7,14 [100,110,111]

R-phase Structural Type

R.; F. gr. Pbnm; A* = 56.

Atom No.	at. % Mo	Positions of atoms	*x*	*y*	*z*
I	35	4(*c*):	0,0737	0,1134	
II	20	4(*c*):	0,1363	0,2547	
III	0	4(*c*):	0,3257	0,1578	
IV	78	4(*c*):	0,6058	0,1819	
V	65	4(*c*):	0,6650	0,3253	
VI	100	4(*c*):	0,4746	0,4536	
VII	100	4(*c*):	0,1988	0,4047	
VIII	0	4(*c*):	0,8152	0,0780	
IX	78	4(*c*):	0,9383	0,3650	
X	100	4(*c*):	0,5202	0,0355	
XI	0	8(*d*):	0,2504	0,5375	0,9986
XII	52	8(*d*):	0,3868	0,2883	0,0008

Figure 12 shows that the structure consists of networks of joined hexagons, triangles, and pentagons. The networks are

* A is the number of atoms in the unit cell.

superposed with formation of antiprisms with atoms at their centers. All the atoms are situated in polyhedrons formed by triangular faces only (see [11, 12]).

No. 137. R-$Cr_{18}Mo_{12}Ni_{40}$ a=9,070Å b=16,983Å c=4,752Å [112,113]
No. 138. R-(Mo—Fe—Ni) [114]

Structural Type $Ni_4Mn_{11}Al_{60}$

R.; F. gr. Bbmm (Cmcm); Z = 2.

	x	y	z		x	y	z
Ni 8(g):	0,715	0,750	0,181	$Mn_{(3)}$ 8(f):	0,639	0,055	0
$Al_{(1)}$ 16(h):	0,553	0,935	0,188	$Mn_{(4)}$ 8(f):	0,913	0,068	0
$Al_{(2)}$ 16(h):	0,828	0,065	0,190	$Al_{(7)}$ 8(f):	0,637	0,853	0
$Al_{(3)}$ 16(h):	0,714	0,127	0,190	$Al_{(8)}$ 8(f):	0,738	0,938	0
$Al_{(4)}$ 8(g):	0,014	0,250	0,206	$Al_{(9)}$ 4(c):	0,813	0,750	0
$Al_{(5)}$ 16(h):	0,891	0,885	0,185	$Al_{(10)}$ 4(c):	0,797	0,250	0
$Al_{(6)}$ 8(g):	0,894	0,250	0,185	$Al_{(11)}$ 8(f):	0,538	0,122	0
$Mn_{(1)}$ 4(c):	0,542	0,750	0	$Al_{(12)}$ 4(c):	0,637	0,250	0
$Mn_{(2)}$ 4(c):	0,920	0,750	0	$Al_{(13)}$ 8(f):	0,988	0,897	0

The Ni atoms are in pentagonal antiprisms of Al atoms. The Al and Ni atoms above the pentagonal faces convert these coordination polyhedrons into icosahedrons. Some of the Mn atoms are in Al icosahedrons and in Al 9-point polyhedrons (three-sided prism with three additional atoms opposite the square faces or Thomson cube with an additional atom opposite one of the square faces). The remaining Mn atoms are in 10-point polyhedrons of Al atoms, same as for Mn in $MnAl_6$, but somewhat distorted. The tenth Al atom is somewhat further thant the other nine.

	a,Å	b,Å	c,Å	
No. 139. $Mn_3Cu_2Al_{20}$	24,2	12,5	7,72	[100,115,116]
No. 140. Mn_3ZnAl_{24}	25,1	24,8	30,3	[116,117]
No. 141. $Mn_{11}Ni_4Al_{60}$	23,8	12,5	7,55	[116,118]

Structural Type $Mg_{32}(Zn, Al)_{49}$

C.; F. gr. Im3; Z = 2.

Al 2(a). Zn, Al 24(g) : $y = 0,097$; $z = 0,157$.
Zn, Al 24(g) : $y = 0,195$; $z = 0,310$. Zn, Al 48(h) : $x = 0,160$;
$y = 0,190$; $z = 0,400$. Mg 16 (f) : $x = 0,185$. Mg 24(g) : $y = 0,300$;
$z = 0,115$. Mg 12(e): $x = 0,605$. Mg 12(e) : $x = 0,185$.

The structure is made up of icosahedrons formed by (Zn, Al) atoms with Al atoms in the centers, and Laves polyhedrons; the latter adjoin the triangular faces of the icosahedrons and are formed partly from (Zn, Al) atoms only and partly from Mg and (Zn, Al) atoms. All these Laves polyhedrons contain Mg atoms. In addition, there is another type of polyhedron; it is made up of three hexagons joined in pairs by parallel edges with an additional atom over one of the hexagons. These polyhedrons also contain Mg atoms.

	a, Å	
No. 142. T-$Mg_{32}(Cu,Al)_{49}$	14,26—14,33.	[73,100,119]
No. 143. T-$Mg_{32}(Zn,Al)_{49}$	14,16	[76,120,121]

Structural Type $Mg_3Cr_2Al_{18}$

C.; F. gr. Fd3m; Z = 8.

$Mg_{(1)}$8(b). $Mg_{(2)}$ 16(d). Cr16(c). $Al_{(1)}$48(f) : $x = 0,1407$.
$Al_{(2)}$96(g) : $x = 0,0666$; $z = 0,2998$.

The series of complex cubic structures are more or less similar if the minor cubes into which the unit cell can be divided are compared. Thus, the $Mg_3Cr_2Al_{18}$ structure consists of minor cubes of two types, alternating in staggered order. In minor cube I, starting from the center, we have: (Al) octahedron, (Cr) tetrahedron, distorted (Al) cube-octahedron, strongly distorted (Al) cube-octahedron, (Mg) cube. In minor cube II: Laves (Al) polyhedron, (Mg) tetrahedron, strongly distorted (Al) cubic cube-octahedron.

No. 144. E-$Mg_3Cr_2Al_{18}$ a=14,53Å [122,123]

I. ORDER OF TERNARY SILICIDES AND BORIDES WITH STRUCTURAL TYPES BASED ON THOSE OF BINARY COMPOUNDS WITH SUPERSTRUCTURES

Structural Type $CrSi_2$

H.; F. gr. $C6_22$; Z = 3. [1], p. 330.

	a	c	c/a	
No. 145. β-Cr(Al,Si)$_2$	4,496Å	6,377Å	1,418	[124,125]
No. 146. Mo($Al_{0,4}$,$Si_{1,6}$)	4,66$_5$	6,54$_5$	1,403	[126]
No. 147. W(Al,Si)$_2$	4,71$_7$	6,56$_9$	1,393	[126]

Structural Type $Cu_2Sb(Fe_2As)$

H.; F. gr. P4/nmm; Z = 2. [1]. p. 366.

In $Si_4(Na_{0,92}, Al_{1,07})$ the Na and Al atoms occupy statistically the position 2(c): z = 0.63, Si in 2(a) and 2(c): z = 0.21. The Na and Al atoms are in 9-point polyhedrons of Si atoms. The Si atoms from position 2(c) are also in 9-point polyhedrons of Si and Na, Al atoms.

No. 148. $Si_4(Na_{0,92}Al_{1,07})$ $a = 4,130$ $c = 7,400$ $c/a = 1,792$ [127,128 *]

Structural Type Fe_3C

R.; F. gr. Pbnm; Z = 4. [1], p. 338; [3], pp. 129 and 199.

No. 149. $Fe_3(Si,B)$ $a = 4,46—4,47$Å $b = 5,36—5,30$Å $c = 6,66—6,67$Å [129]

Structural Type FeSi

C.; F. gr. $P2_13$; Z = 4. [1], p. 328; [3], p. 57.

	a	x_{Me}	x_B	
No. 150. Co_4 (Ga_1, Ge_3)	4,63	0,138	—0,162	[31, 130]
No. 151. Rh_5 (Ga_1, Ge_4)	4,822	0,140	—0,160	[130]
No. 152. Ni_3 (Al_1, Si_1)	4,55	0,147$_5$	—0,160	[31, 130]
No. 153. Ni_7 (Ga_6, Ge_1)	4,46	0,14$_5$	—0,162	[31, 130]
No. 154. Pd_4 (Al_3, Si_1)	4,82	0,148	—0,157$_5$	[31, 130]
No. 155. Pd_5 (Al_4, Ge_1)	4,86			[130]

Structural Type CdI_2

H. F. gr. C6mc; Z = 2. [1], p. 372.

No. 156. Nb_2 (C, Si) $a = 3,117$ Å $c = 4,969$ Å $c/a = 1,594$ [131]

Structural Type U_3Si_2

T.; F. gr. P4/mbm; Z = 2. [1], p. 328.

The atoms in ternary compounds are probably in an ordered arrangement.

No. 157. (Mo_2Co) B_2 [132]
No. 158. (Mo_2Ni) B_2 [132]

Structural Type Mo_5SiB_2 (T - 2)

T.; F. gr. I4/mcm; Z = 4.

Mo_I 4(c). B 8(h) : $x = 0,375$. Si 4(a). Mo_{II} 16(l) : $x = 0,160$; $z = 0,143$.

---

*The authors of [128] found the composition $NaAlSi_{1,25-1,33}$ and consider that the substance reported in [127] was contaminated with silicon.

The structure is a combination of the U_3Si_2 and $CuAl_2$ types. Similar layers of Mo atoms lie one above the other, either turned or not turned. In the former case a layer of Thomson (Mo) cubes containing Si atoms and (Mo) tetrahedrons is formed; the next layer consists of (Mo) cubes with (Mo) atoms inside, and (Mo) trigonal prisms with B atoms inside.

		a	*c*	*c/a*	
No. 159.	$V_5(B_2Si)$				[133]
No. 160.	(Nb — B — Si)				[133]
No. 161.	(Ta — B — Si)				[133]
No. 162.	(Cr — B — Si)				[133]
No. 163.	$Mo_5(B_2Si)$	6,01	11,01	1,83	[133, 134*]
No. 164	$W_5(B_{1,5}Si_{1,5})$**	6,035	10,97	1,82	[133]
No. 165.	$Mn_5(B_2Si)$	5,61 Å	10,44 Å	1,86	[129]
No. 166.	$Fe_5(B_2Si)$	5,54 Å	10,32 Å	1,86	[129, 135, 136]

Structural Type BeSiZr

H.; F. gr. $P6_3/mmc$; Z = 2.

Zr2(a). Be2(c). Si2(d).

Formally this is the CoNiSb type, i. e., a superstructure of Ni_2In. However, as $c/a \approx 2$, the BeSiZr type is a superstructure of AlB_2. In each layer (Fig. 13) the Si and Be atoms are in trigonal prisms of Zr atoms. In each successive layer in the prisms Si atoms are above Be atoms, and Be atoms above Si atoms.

No. 167. BeSiZr $a = 3,71$ Å $c = 7,19$ Å $c/a = 1,94$ [137]

Structural Type Cr_2NiB_4

R.; F. gr. Immm; Z = 2. [1] p. 322 (for Ta_3Ba_4)

Superstructure of Cr_3B_4 type. The Cr and Ni atoms are apparently arranged in order. Each chain of Ni atoms is between two chains of Cr atoms.

		a	*b*	*c*	
No. 168.	$(Cr_2Ni)B_4$	6,05 Å	12,67 Å	5,96 Å	[138]
No. 169.	$(Mo_2Fe)B_4$				[132]
No. 170.	$(Mo_2Co)B_4$				[132]
No. 171.	$(Mo_2Ni)B_4$				[132]

Structural Type "Mn_5Si_3"

H.; F. gr. C6/mcm; Z = 2. [1], p. 329.

In $Mo_{5-x}Si_{3-y}C_{x+y}$ the distribution of the atoms is as follows: Mo, Si4(d). Mo6(g). Si, C6(g)

		a	*c*	*c/a*	
No. 172.	(Ti — Si — C)				[133]
No. 173.	(Zr — Si — B)				[133, 139]
No. 174.	(Zr — Si — C)				[133]
No. 175.	(Zr — Si — N)				[133, 139]
No. 176.	$V_{5-x}Si_{3-y}B_{x+y}$				[133, 139]
No. 177.	(V — Si — C)				[133, 139]
No. 178.	(V — Si — N)				[133, 139]
No. 179.	$Nb_{5-x}Si_{3-y}B_{x+y}$				[133, 139]
No. 180.	(Nb — Si — C)				[133, 139]
No. 181.	(Nd — Si — N)				[133]
No. 182.	$Ta_{5-x}Si_{3-y}B_{x+y}$				[133, 139]
No. 183.	$Ta_{5-x}Si_{3-y}C_{x+y}$	7,494 Å	5,242 Å	0,700	[131, 133, 139]

*The full structure determination is also given in [134].

** The order of Si and B is not definitely established.

No. 184. $Ta_{5-x}Si_{3-y}N_z$	7,05	4,72	0,670	[131, 133, 139]
No. 185. $Cr_{5-x}Si_{3-y}B_{x+y}$				[19, 140]
No. 186. $Cr_{5-x}Si_{3-y}C_{x+y}$	6,97$_9$ Å	4,76$_6$ Å	0,676	[133, 139, 141]
No. 187. $Mo_{5-x}Si_{3-y}C_{x+y}$	7,27	5,05—4,99	0,695—0,687	[133, 142]
No. 188. $W_{5-x}Si_{3-y}C_{x+y}$	7,18 Å	4,84 Å	0,675	[133, 141]

II. ORDER OF TRUE TERNARY SILICIDES AND BORIDES

Structural Type $Co_{4,7}Si_2B$

T.; F. gr. 14/mcm; Z = 4.

$16Co_{(1)}16(k) : x = 0,0757;\ y = 0,2036.$
$2,5—3Co_{(2)}\ 4(b).\ 8Si\ 8(h) : x = 0,162.\ 4B4(a).$

The Si and B atoms (Fig. 14) form a "very flattened" CuAl structure where B atoms play the part of Cu atoms, and Si, of Al atoms (compare Ni_6Si_2B). The $Co_{(2)}$ atoms statistically fill the tetrahedral voids (as in TlSe); they are contained in 6-point polyhedrons of Si and B atoms.

The latter have triangular faces only, and are parts of 8-point polyhedrons ([13], p. 206). The $Co_{(1)}$ atoms in their turn form columns of Thomson cubes which, strictly speaking, contain the B atoms. The Si atoms are situated in 9-point polyhedrons of Co atoms (Fig. 8).

No. 189. $Fe_{4,7}Si_2B$	$a = 8,82$ Å	$c = 4,34$ Å	$c/a = 0,492$	[129]
No. 190. $Co_{4,7}Si_2B$				[129]

Structural Type Ni_6Si_2B*

H.; F. gr. $P\bar{6}2m$; Z = 1.

$Ni_{(1)}3(f) : x = 0,247.\ Ni_{(2)}3(g) : x = 0,608.\ Si\ 2(c).\ B\ 1(b).$

The structure is characteristic of borides. The Ni atoms form three-sided prisms of two types. Some contain Ni atoms, other B and Si atoms. The Si and B atoms form a very "flattened" structure of the AlB_2 type. The Ni atoms are in 5-point polyhedrons and tetrahedrons of B and Si. If the Ni atoms are also taken into account, the coordination numbers of the Ni atoms are higher. This is seen in Fig. 15, which also shows 9-point polyhedrons (prisms and hemioctahedrons) containing Si and B atoms.

No. 191. Ni_6Si_2B	$a = 6,105$ Å	$c = 2,895$ Å	$c/a = 0,4742$	[143]

Structural Type $Al_{13}Cr_4Si_4$

C.; F. gr. $F\bar{4}3m$; Z = 4

$Al_{(1)}4(a).\ Al_{(2)}24(f) : x = 0,315.\ Al_{(3)}24(g) : x = 0,565.$
$Cr\ 16(e) : x = 0,342.\ Si\ 16(e) : x = 0,125.$

The structure is almost the same as in η-carbides. In minor cube I, starting from the center, we have: (Al) octahedron, distorted cubic (Al) cube-octahedron, (Al) tetrahedron; in minor cube II: (Co) tetrahedron, (Si) tetrahedron, distorted cubic (Al) cube-octahedron, (Al) tetrahedron.

No. 192. α-$Al_{13}Cr_4Si_4$ $a = 10,917$ Å

Structural Type $Cu_{16}Mg_6Si_7$

C.; F. gr. Fm3m; Z = 4.

$Si_{(1)}4(b).\ Si_{(2)}24(d).\ Mg\ 24(e) : x = 0,1824.$
$Cu_{(1)}32(f) : x = 0,1684.\ Cu_{(2)}32(f) : x = 0,3770$

*Related to Fe_2P.

All the minor cubes have the same structure. Starting from the center, we have: (Cu) tetrahedron, (Cu) tetrahedron, (Si) octahedron, distorted cubic (Mg) cube-octahedron, (Si) tetrahedron.

No. 193. $Cu_{16}Mg_6Si_7$ $a = 11{,}65$ Å [91, 145, 146, 147**]

B) CLASS ABX

SUBCLASS OF INTERSTITIAL PHASES (CARBIDES OR NITRIDES)

I. ORDER IN WHICH THE ATOMS OF BOTH METALS ARE DISTRIBUTED STATISTICALLY OR WITH A SUPERSTRUCTURE IN THE POSITION OF THE ATOMS IN THE STRUCTURAL TYPES OF PURE METALS WITH THE CLOSEST PACKING

Structural Type $CaTiO_3$ (cubic)

C.; F. gr. Pm3m; Z = 1 [3], p. 148.

Ca1(a). Ti1(b). O3(c).

The metal atoms in the ternary compounds occupy the positions of Ca and O atoms; they form a structure of the Cu_3Au type (p.). The carbon (nitrogen) atoms occupy 1/3 of the octahedral voids. The superstructure of the carbon (nitrogen) atoms and unoccupied octahedral voids also belongs to the Cu_3Au type (Fig. 16).

	a	
No. 194. MgC_xCo_3	3,81	[148, 149]
No. 195. K-$MgC_{0,15-1,25}Ni_3$	3,72—3,81	[148, 150]
No. 196. $NiNFe_3$	3,790 Å	[151]
No. 197. $PtNFe_3$	3,857 Å	[151]
No. 198. $ZnCMn_3$	3,923$_9$ Å	[148, 152]
No. 199. ZnC_xFe_3	3,80	[148]
No. 200. ZnC_xCo_3	3,72	[148]
No. 201. $ZnC_{0,7}Ni_3$	3,65	[148]
No. 202. $AlCMn_3$	3,868 Å	[148, 153]
No. 203. $AlC_{0,66}Fe_3$	3,75—3,77	[148, 154, 155]
No. 204. $AlC_{0,59}Co_3$	3,59	[148, 149]
No. 205. $AlC_{0,29}Ni_3$	3,61	[148, 149]
No. 206. $GaCMn_3$	3,876	[148, 156]
No. 207. InC_xMn_3	3,90—3,94	[157]
No. 208. InC_xFe_3	3,87	[157]
No. 209. $InC_{0,75}Co_3$	3,81—3,89	[157]
No. 210. $InC_{0,5}Ni_3$	3,77—3,79	[157]
No. 211. $GeCMn_3$	3,86—3,87*	[157]
No. 212. $GeC_{0,45}Fe_3$	3,65	[157]
No. 213. $GeC_{0,25}Co_3$	3,59—3,62	[157]
No. 214. GeC_xNi_3	3,57	[157]
No. 215. $SnC_{0,8}Mn_3$	3,98	[148, 158]
No. 216. SnC_xFe_3	3,85**	[148]
No. 217. $SnC_{0,7}Co_3$	3,77	[148]

Structural Type "$CaTiO_3$" (tetragonal)

T.; Z = 1.

* According to [147] the Mg atoms are arranged somewhat differently.

** When x = 1.

Tetragonally deformed type of cubic $CaTiO_3$.

No. 218. $ZnCMn_3$* $a = 3,921$ Å $c = 3,899$ Å $c/a = 0,9947$ [152]

Structural Type Ta_3MnN_4

H.; F. gr. $P6_3/mmc$; Z = 1.

1 Mn + 1Ta 2(*a*). Ta 2(*d*). N 4 (*f*): $z \sim 0,25$

The Ta and Mn form ABAC (chch) closest packing. The Ta atoms are in h-type layers, the Ta and Mn atoms are in c-type layers, and the N atoms are in the octahedral voids.

No. 219. Ta_3MnN_4 $a = 3,023$ Å $c = 10,49$ Å c/a 3,470 [159]

Structural Type Ta_2FeN_3

H.; F. gr. $\overline{P}62m$; Z = 4.

Ta 2(*e*) : $z = 0,25$. Ta 3(*f*) : $x = 0,333$. Ta 3(*g*) : $x = 0,667$. Fe 4(*h*) : $z = 0,25$.

The Ta and Fe atoms together form ABCB (hchc) closest packing. The close-packed layers of Ta atoms alternate with graphite layers of Fe atoms with Ta atoms in the centers of the rings. The Ta atoms form h-type layers. The Ta atoms from the c-type layers are one over the other. The N atoms are apparently in the octahedral voids.

	a, Å	*c*, Å	*c/a*	
No. 220. $Ta_2FeN_{2,60}$	5,156	10,31	2,000	[159]
No. 221. $Ta_2CoN_{2,5}$	5,161	10,30	1,996	[159]
No. 222. $Ta_2NiN_{2,45}$	5,168	10,36	2.005	[159]

Structural Type $Fe_7Mo_{13}N_4$

C.; F. gr. $P4_132$; Z = 1.

The Fe and Mn atoms form the β-Mn structure ([1], p. 320); the N atoms are in the octahedral voids [position 4(a)].

	a, Å	
No. 223. β^m - (Mn — Mo — N)		[65]
No. 224. β^m - $Fe_7Mo_{13}N_4$	6,6948—6,7020	[65]
No. 225. β^m - (Co — Mo — N)		[65]
No. 226. β^m - (Ni — Mo — N)		[65]

II. ORDER OF INTERSTITIAL PHASES WITH STRUCTURES BASED ON THOSE OF BINARY COMPOUNDS WITH SUPERSTRUCTURES.

Structural Type $Cr_{21}W_2C_6$

C.; F. gr. Fm3m; Z = 8. [3], p. 192.

$Cr_{(1)}$4(*a*). $Cr_{(2)}$48(*h*) : $x = 0,165$. $Cr_{(3)}$32(*f*) : $x = 0,385$. W 8(*c*). C 24(*e*) : $x = 0,275$.

(The parameters are given for $Cr_{23}C_6$; see [1], p. 339).

All the minor cubes are of the same structure. From the center we have: (W) center, (Cr) Laves polyhedron, (Cr) tetrahedron, (C) cube-octahedron, (Cr) tetrahedron.

No,227. $Cr_{21}W_2C_6$ [160]
No.228. $Fe_{21}Mo_2C_6$ [160]
No.229. $Fe_{21}W_2C_6$ [160]

*At −196°.

Structural Type MoC

H.; F. gr. C6m2; Z = 1. [1], p. 338.

Superstructure of AlB_2 type. The Mo atoms form a framework of trigonal prisms. The C atoms occupy half the prisms in the layer. In all the remaining prism layers occupied prisms are situated over other occupied prisms (compare with BeSiZr, Fig. 13).

		a	c, Å	c/a	
No. 230.	$Ti_{0,7}Co_{0,3}N$	2,94	2,90	0,99	[161]
No. 231.	$Ti_{0,7}Ni_{0,3}N$	2,94	2,89	0,985	[161]
No. 232.	$Mn_{0,8}C_{0,2}N$	2,84	2,79	0,985	[161]
No. 233.	$Mn_{0,8}Ni_{0,2}N$	2,84	2,78	0,98	[161]

Structural Type $Co_3W_9C_4$

H.; F. gr. $P6_3/mmc$; Z = 2.

$(3\,Co + 3W)_I\ 6(h) : x = 0{,}890.\ (3Co + 3W)_{II} 6(h) : x = 0{,}555.$
$\overline{W}\ \overline{12}(k)\quad x = 0{,}205;\ z = 0{,}075;\ C_1 2(c).\ C_{(2)} 6(g).$

The structure is of the Co_2Al_5 type. The W atoms occupy six points of 9-point polyhedrons (with C atoms inside), forming prisms. The icosahedrons of Co and W atoms are unoccupied. The octahedrons, joined by their vertices and forming chains, are occupied by C atoms. The octahedrons joined by their triangular faces are unoccupied (Fig. 17).

	a, Å	c/Å	c, a	
No. 234: (W — Mn — C)	7,756	7,756	1,000	[162]
No. 235. $(W_9Co_3C_4$	7,826	7,826	1,000	[163, 164]
No. 236. κ-$W_{16}Ni_3C$	7,8183	7,8180	1,000	[162, 165]

Structural Type $W_4CoC - A_4B_2C$ (η_2-carbide type)

C.; F. gr. Fd3m; Z = 16.

W 48(f) : $x = 0{,}194$ *. W 16(d). Co 32(e) : $x = -0{,}168$ *. C 16(c).

The W and Co atoms are arranged as Ti and Cu atoms respectively in the Ti_2Cu structural type. The minor cubes of the two types alternate as in NaCl. In cube I, starting from the center, we have: (W) octahedron, (C) tetrahedron, (Co) tetrahedron, distorted cubic (W) cube-octahedron; in cube II: (Co) tetrahedron, (W) tetrahedron, distorted cubic (W) cube-octahedron.

	a, Å	
No. 237. Mo_4Fe_2C	11,62	[167]
No. 238. Mo_4Co_2C	11,25	[167]
No. 239. Mo_4Ni_2C	11,25	[167]
No. 240. η_2-W_4Co_2C	11,215—11,218	[168, 169]
	11,210	from [169]
No. 241. θ-$W_6Co_3C_2$ **	11,25	[163]
No. 242. θ-W_6Ni_3C	11,217	[165]

Structural Type $(W_3Fe_3C - W_2Fe_4C) - (A_3B_3C - A_2B_4C)$ (η_1-carbide type)

C.; F. gr. Fm3m; Z = 16.

The atoms occupy the same positions as in η_2-carbide. The additional atoms are in the 16(d) positions and statistically in 48(f) positions. In the C_1 phase the C atoms additionally occupy the 8(a) position, and in the C_2 phase, only the 8(a) position.

*Parameters taken from [166].

**According to [169], the θ-phase corresponds to the formula W_4Co_2C.

		a	
No. 243.	Zr_3V_3C	12,12 Å	[167]
No. 244.	Nb_3Cr_3C	11,49 Å	[167]
No. 245.	Mo_3Mn_3C	11,13 Å	[167]
No. 246.	Mo_3Fe_3C **	11,09—11,12	[170]
No. 247.	Mo_3Co_3C		[167]
No. 248.	Mo_3Ni_3C	11,05 Å	[167]
No. 249.	η_1-Mo_3Fe_3N	11,065—11,095 Å	[65]
No. 250.	W_3Mn_3C	11,13 Å	[167]
No. 251.	C_1-W_2Fe_2C ***	11,050—11,125 Å	[166, 171]
No. 252.	W_3Fe_3C — W_2Fe_4C	11,04	[171, 172, 173]
No. 253.	C_2-W_6Fe_6C	10,93 Å	[166]
No. 254.	W_3Co_3C	11,01	[170, 174]
No. 255.	C_2-W_6Co_6C	10,914 Å	[168]
No. 256.	W_3Ni_3C	11,15	[170]
No. 257.	W_6Ni_3C	10,873 Å	[165]

SUBCLASS OF OTHER CHEMICAL COMPOUNDS

I. ORDER OF TERNARY COMPOUNDS WITH STRUCTURES BASED ON THOSE OF BINARY COMPOUNDS WITH SUPERSTRUCTURES

Structural Type ZnS (Wurtzite)

H.; F. gr. C6mc; Z = 2. [1], pp. 357, 105.

No.258. $(Be_1, Si_1)N_2$ $a = 2{,}87_2$ Å $c = 4{,}67_4$ Å $c/a = 1{,}62_7$ [176]

1. The ZnS (Sphalerite) Family

Structural Type ZnS (Sphalerite)

C.; F. gr. $F\bar{4}3m$; Z = 4. [1], p. 356.

In Fig. 4, Zn atoms in position a, S atoms in position d; positions b and c not occupied.

		a	
No. 259.	$(Ga_1, In_1)Sb_2$	6,34	[177]
No. 260.	$(Ga_1, In_2)Sb_3$	6,37	[177]

Structural Type $CuFeS_2$

T.; F. gr. $I\bar{4}2d$; Z = 2.

Cu 4(*a*). Fe 4(*b*). S 8(*d*) : $x = 0{,}27$.

$CuFeS_2$ is a superstructure of the sphalerite type, with the positions of the Zn atoms occupied by Fe and Cu atoms.

		a, Å	c, Å	c/a	
No.261.	$ZnGeP_2$	5,46	$10{,}7_6$	1,97	[178]
No.262.	$ZnGeAs_2$	5,64	$11{,}1_0$	1,967	[178]
No.263.	$CdGeAs_2$	5,942	$11{,}2_3$	1,889	[178]
No.264.	$CdSnAs_2$	6,092	$11{,}9_2$	1,957	[178]

2. The CsCl — CaF_2 Family and Superstructures

Structural Type CaF_2

C.; F. gr. Fm3M; Z = 4. [1], p. 366; [3], p. 165.

In Fig. 4, F atoms in positions d and c; Ca atoms in position a; position b not occupied.

		a	
No. 265.	$Co(Mn_1, Sb_1)$	5,888	[179]
No. 266.	T_B-$Cu_4(Li_1, Al_{7.5})$*	5,83 Å	[180]

*The arrangement of the C atoms is not clear; perhaps statistically in 8(a) and 16(c).

**The formula W_2Fe_4C is more probable; the atomic arrangement is different according to [171] and [175].

***When Cu atoms are in some excess they are distributed together with Al atoms; if deficient, vacant sites are left.

No. 267. N (Li_1, Mg_1)	4,970	[181]
No. 268. P_3(Li_5, Ti_1)	5,95	[182]
No. 269. P_4(Li_7, V_1)	$5,97_5$	[183]
No. 270. P_3(Li_5, Si_1)	5,842	[182]
No. 271. P_3(Li_5, Ge_1)	5,88	[182]
No. 272. As_3(Li_5, Ti_1)	6,13	[182]
No. 273. As_4(Li_7, V_1)	6,150	[183]
No. 274. As_3(Li_5, Si_1)	6,043	[182]
No. 275. As_3(Li_5, Ge_1)	6,08	[182]

Structural Type LiMgP

C.; F. gr. $F\bar{4}3m$; Z = 4.

P4(a). Mg4(c). xLi4(b). (4 − x) Li 4(d).

In Fig. 4, Li atoms in positions b and c; Mg atoms in position d; P atoms in position a.

	a	
No. 276. LiMgP	$6,01_1$	[184, 185]

Structural Type As(AgMg)

C.; F. gr. $F\bar{4}3m$; Z = 4.

As 4(a). Ag 4(c). Mg 4(d).

In Fig. 4, As atoms in position a; Ag atoms in position d; Mg atoms in position c; position b not occupied.

	a			a	
No. 277. Ni(MgSb)	6,036	[179]	No. 285. N(LiZn)	$4,87_7$	[181]
No. 288. Ni(MgBi)	6,154	[179]	No. 286. P(LiZn)	$5,76_8$	[184]
No. 279. Cu(MgSn)	6,214	[83, 186, 187]	No. 287. As(LiMg)	6,21	[192]
No. 280. Cu(MgSb)	6,152	[186, 188, 189]	No. 288. As(LiZn)	$5,91_2$	[184]
No. 281. Cu(MgBi)	6,256	[188]	No. 289. As(NaZn)	$5,90_0$	[191]
No. 282. Cu(MnSb)	6,054	[179]	No. 290. As(MgAg)	6,240	[188]
No. 283. Cu(CdSb)	$6,26_2$	[190]	No. 291. Sb(LiMg)	6,61	[192]
No. 284. Ag(ZnAs)	5,900	[191]	No. 292. Bi(LiMg)	6,75	[192]

Structural Type $N_2(Li_3Al)$

C.; F. gr. Ia3; Z = 16.

For $N_2(Li_3Al)$: $N_{(1)}8(a)$. $N_{(2)}24(d)$: $x = 0,205$. Al 16(c): $x = 0,115$. Li 48(e): $x = 0,160$; $y = 0,382$; $z = 0,110$.

For $N_2(Li_3Ga)$: $x_{N_{(2)}} = 0,215$; $x_{Ga} = 0,117$; $x_{Li} = 0,152$; $y_{Si} = 0,381$; $z_{Li} = 0,114$.

For $N_3(Li_5Ge)$: $x_{N_{(2)}} = 0,205$; $x_{10\%Ge+5\%Li} = 0,115$; $x_{Li} = z_{Li} = 0,125$; $y_{Li} = 0,375$.

Somewhat distorted superstructure of CaF_2 type. The Li and Al atoms are in the positions of F atoms and form a simple cubic structure. Each Al atoms has six neighboring Li atoms; each Li atom has two neighboring Al* atoms. The Li_3AlN_2 type (Fig. 18) in which the positions of the Al atoms are not occupied corresponds to the Mn_2O_3 type.

	a	
No. 293. $N_3(Li_5Ti)$	9,700 Å	[194]
No. 294. $N_2(Li_3Al)$	$9,46_1$	[195, 196]
No. 295. $N_2(Li_3Ga)$	$9,59_2$	[195, 196]
No. 296. $N_3(Li_5Si)$	9,436 Å	[194]
No. 297. $N_3(Li_5Ge)$	9,614 Å	[194]
No. 298. $P_2(Li_3Ga)$	11,74	[182]

Structural Type $As_2(Li_3Ga)$

T.; distorted $N_2(Li_3Al)$

No. 299. $As_2(Li_3Ga)$: $a = 11,94$ $c = 12,13$ $c/a = 1,016$ [182]

*This type of superstructure is not given in [193].

Structural Type $P_2(Li_3Al)$

R.; F. gr. Ibca; Z = 16.

P_I 8(*a*). P_{II}8(*c*). P_{III}8(*e*). Al16(*f*). Li_I 16(*f*). Li_{II}16(*f*). Li_{III}16(*f*).

Distorted $N_2(Li_3Al)$ type

		a, Å	*b*, Å	*c*, Å	
No. 300.	$P_2(Li_3Al)$	11,471	11,610	11,731	[197]
No. 301.	$As_2(Li_3Al)$	11,865	11,981	12,114	[197]

Structural Type $N_4(Li_7V)$

C.; F. gr. $P\bar{4}3n$; Z = 8.

V_I 2(*a*). V_{II} 6(*c*). N_I8(*e*): $x=0,120$.
N_{II}24(*i*): $x=y=3/8$; $z=1/8$. Li_I 6(*b*). Li_{II} 6(*d*).
Li_{III} 8(*e*): $x=1/4$. Li_{IV} 12(*f*): $x=1/4$.
Li_V 24(*i*): $x=y=1/4$; $z=0$.

Superstructure of GaF_2 type. The Li and V atoms in ordered positions of F atoms. Each N atom is in a cube of seven Li atoms and one V atom. Eight such cubes form one large cube of Li atoms with a V atom in the center. The relative positions of the large cubes are such that the V atoms form a structure of the β-W type (Fig. 19).

		a, Å	
No. 302.	$N_4(Li_7V)$	9,604	[198, 199]
No. 303.	$N_4(Li_7Mn)$	9,571	[198]

Structural Type $P_2(Li_3Mn)$

T.; F. gr. $P\bar{4}2m$; Z = 2.

P 4(n): x = 0.25; z = 0.26

Li_I 1(*a*). Li_{II}1(*d*). Li_{III} 2(*e*). (Li, Mn)$_I$ 1(*b*). (Li, Mn)$_{II}$1(*c*). (Li, Mn)$_{III}$ 2(*f*).

In Fig. 4, the Li atoms occupy points in the lower and upper face of the major cube; the Li, Mn atoms are in the median plane of the major cube; P atoms are in the upper face of the minor cube. The four corners of the lower face of this cube are unoccupied.

No. 304. $P_2(Li_3Mn)$ $a = 5,88_6$ Å $c = 5,98_3$ Å $c/a = 1,016$ [200]

3. The Fe_2As Family

Structural Type Cu(MgAs)

T.; F. gr. P4/nmm; Z = 2.

Cu2(a). Mg2(c): z = −0.250. As2(c): z = 0.335.

Superstructure of Cu_2Sb type; in Fig. 4 the As and Mg atoms are in positions a and b. The As atoms are displaced from the ideal position (the ideal is z = 0.375). The Cu atoms occupy the centers of the four top cubes. The centers of the four bottom cubes are unoccupied.

No. 305. Cu(MgAs) $a = 3,95_3$ $c = 6,22_3$ $c/a = 1,57_6$ [186, 188]

Structural Type MgAgSb

Somewhat distorted Cu(MgAs) type

No. 306. MgAgSb [188]

4. Family of Other Structural Types

Structural Type FeS_2 (pyrite).

C.; F. gr. Pa3; Z = 4. [1], p. 393.

CaF_2 type in which the S atoms are displaced from the cube centers with formation of S_2 dumb-bells along four nonintersecting threefold axes.

No. 307. $(Ni_{0,12}Pd_{0,88})As$ * [201]

Structural Type La_2O_2S

H.; F. gr. $C\bar{3}m$; Z = 1. [1], p. 404 (La_2O_2).

Superstructure of La_2O_3. Very flattened cubic ABC closest packing of O and S atoms. As in Pt_2Sn_3, the tetrahedrons in the incompleted layer join with octahedrons to form 7-point polyhedrons (cubes with one corner missing). The coordination number of the La atoms is 7; the type is close to Ni_2Al_3.

	a	c	c/a	
No. 308. $Mg(Mg, Zn)_2Sb_3$	4,573—4,372	7,229—7,151	1,581—1,636	[202]

Structural Type $CoAs_3$

C.; F. gr. Im3; Z = 8. [1], p. 396 and [63] p. 197.

No. 309. $(Fe, Co)As_3$ ** $a = 8,21$ Å [203]

CLASS AXY

I. ORDER OF INTERSTITIAL PHASES

Structural Type G-Fe_2N

R.; F. gr. Pbcn; Z = 4.

N 4(c) : $y = 1/8$. Fe 8(d) : $x = 1/4$; $y = 1/8$; $z = 1/4$.

Zigzag chains of occupied octahedrons alternate in a layer and neighboring layers with similar chains of unfilled octahedrons. The arrangement of N atoms is shown in Fig. 20a.

No. 310. G-Fe_2(C, N) $a = 4,836$—$4,851$ Å $b = 4,409$—$4,383$ Å $c = 2,761$—$2,750$ Å [204]

Structural Type ε-Fe_3N

H.; F. gr. $C6_32$; Z = 2.

N 2(c), Fe 6(h) · $x = 2/3$.

The Fe atoms are in hexagonal closest packing. Octahedrons with N atoms are in centers of rings in graphite layers of empty octahedrons. In the direction of the c axis the occupied octahedrons are one above the other (Fig. 20b).

No. 311. ε-Fe_{2-3}(C, N) $a = 3,885$—$3,983$ Å $c = 4,730$—$4,414$ Å $c/a = 1,217$—$1,109$ [204, 205]

No. 312. ε-Ni_3(C, N) [206]

Structural Type NaCl

C.; F. gr. Fm3m; Z = 4. [1]. pp. 103, 350.

In Fig. 4, Na atoms are in position a and Cl atoms in position b; positions c and d are unoccupied.

No. 313. U_2(C, N) $a = 4,93$ Å [207]

II. ORDER OF CARBONITRIDES

Structural Type Al_5C_3N

H.; F. gr. $P6_3mc$; Z = 2.

*Possibly this phase is not a ternary compound but a solid solution of palladium and nickel in the compound $PdAs_2$.

**Possibly a metallide solution.

$Al_{(1)}2(a)$: $z = 0,150$. $Al_{(2)}2(e)$: $z = 0,0445$. $Al_{(3)}2(b)$:
$z = 0,456$. $Al_{(4)}2(a)$: $z = 0,345$. $Al_{(5)}2(b)$: $z = 0,240$.
$C_{(1)}2(b)$: $z = 0,133$. $C_{(2)}2(a)$: $z = 0,0014$.
$C_{(3)}2(b)$: $z = 0,369$. N 2(a): $z = 0,250$.

The Al atoms are in 10-layer closest packing of the ABABACBCBC type. The octahedral voids between each pair of c-type layers contain C atoms. The paired tetrahedral voids in h-type layers contain N and C atoms; a layer of N atoms is between two layers of C atoms. The C and N atoms are slightly displaced from the paired tetrahedral voids into one of the tetrahedrons.

No. 314. Al_3C_2N $a = 3,280$ Å $c = 21,55$ Å $c/a = 6,575$ [208]

III. ORDER OF TERNARY COMPOUNDS WITH THE STRUCTURE OF BINARY COMPOUNDS

Structural Type $AuZn_3$

C.; F. gr. Pm3n; Z = 4.

$Au_{(1)}2(a)$. $Au_{(2)}6(c)$. Zn24(c): $y = 0,16_5$; $z = 0,30_9$.

The Au atoms form a β-W structure, some of the tetrahedral voids of which contain Zn atoms. The latter, in their turn, form icosahedrons and somewhat distorted cube-octahedrons containing Au atoms. The three-sided prisms of Zn atoms are empty. In this structural type the places of the Au atoms are occupied by As and Sb atoms.

No. 315*. $(As_1, Sb_1)Cu_6$ $a = 7,575$ [21, 209]

TERNARY COMPOUNDS OF INCOMPLETELY ESTABLISHED STRUCTURE

No.	Compound	Lattice constants	Notes	Literature
		Cubic system		
316	$LiMgAl_2$	$a = 20,2$ Å	Pseudocubic; tetragonal or rhombic distortion; isomorphous with $N_4(Li_7Ta)$	[48]
317	Li_7NbN_4			[199]
318	Li_7TaN_4		Pseudocubic with tetragonal or rhombic distortion; isomorphous with $N_4(Li_7Nb)$	[199]
319	$Be_5(Cr,Fe)$, l.t.	$a = 6,04$	Face-centered; decomposes on cooling	[88]
320	Q - $Mg_6Cu_3Al_7$	$a = 12,087$ Å	F.gr. $I\bar{4}3$; Z = 6	[210]
321	γ - $Al_2Cu_{12}Sn_x$**	$a = 17,75$—$17,78$	The γ-brass type; constant double that of binary phases	[67]
321a	(U,Nb)C	$a = 4,693$ Å	Face-centered	[234]
322	$U\,Ta_x\,C_y$	$a = 4,41$ Å	Face-centered	[211]
322a	G - $Ti_8Ni_{19}Si_6$	$a = 11,198$ Å	Z = 4; F.gr. Fm3m (possibly with subgroups)	[235]
323	$TiCu_x\,Al_y$	$a = 3,94$ Å (or 2·3,94 Å)		[212]
324	(Ti — Al — C)	$a = 11,20$	Constant for composition 10 wt.% Al, 1 wt.% C	[213]
325	ZrNiH	$a = 7,045$ Å	Similar to ZrNi; ZrNiH and $ZrNiH_3$ may possibly be the same phase	[214]
326	$ZrNiH_3$	$a = 7,40$ Å	Similar to ZrNi (see No. 325) pseudocubic cell	[214]
327	γ-(Mn — Ni — Cu)	$a = 3,71_0$ Å		[215]
328	Mn_2Cu_3Al	$a = 6,89$	Face-centered; Z = 4	[216]
329	c - (Mn — Al — Si)	$a = 12,625$	Approximate comp. $Mn_3Al_{12}Si$ Structural type α-(Fe-Al-Si)	[100]

*No. 316-368 are collected in the table.

**The authors of [7] consider the formula $Cu_{310}Al_{62}Sn_{44}$ to be more correct on the basis of valence-electron concentration.

No.	Compound	Lattice constants	Notes	Literature
330	c - (Fe — Al — Si)	$a = 12{,}523$	Another representation is α-$Fe_{1.5}Al_6Si$; structurally similar to $FeAl_3$ and $FeAl_7$	[100, 217, 218]
331	α_3 - (Fe — Al —Si)	$a = 16{,}00$	Constant for composition 35.3 wt.%Fe, 12.8 wt. % Si	[218]
332	T_2 - (Ni —Cu—Al)	$a = 14{,}6$ Å	Laue class m3m; according to [52] T_2 phase idential with τ_5	[53]
333	$Ni_{15}Cu_{60}Ge_{25}$ *	$a = 8{,}250$	Structure close to γ-brass type	[68]
		Hexagonal system		
334	T_1 - $LiCuAl_2$	$a = 4{,}97$ Å $c = 9{,}35$ Å $c/a = 1{,}88$	Constants for composition 52.8 wt. % Cu, 5.4 wt.% Li	[180]
335	$TiCu_w$ Al_z	$a = 5{,}05$ $c = 8{,}06$ $c/a = 1{,}596$	F.gr. P6/mmm (other subgroups possible)	[212]
336	(TiFe)V	$a = 4{,}88$ Å $c = 7{,}96$ Å $c/a = 1{,}63$		[219]
337	Mn_6CN			[204]
338	α - (Fe — Al — Si)	$a = 12{,}3$ Å $c = 26{,}2$ Å $c/a = 2{,}13$	F.gr. $P6_3/mmc$	[220]
339	α_2 - (Fe — Al— Si)	$a = 4{,}95$ $c = 7{,}07$ $c/a = 1{,}43$	Constants for composition 24.2 wt.% Fe, 11.3 wt.% Si	[218]
340	(Fe — Al — Si)	$a = 8{,}36$ Å $c = 14{,}58$ Å $c/a = 1{,}915$		[221]
341	(Fe — Si — N)	$a = 2{,}636$ Å $c = 4{,}316$ Å $c/a = 1{,}637$		[222]
342	$(Ni, Cu)_5Ge_2$	$a = 6{,}85$—$6{,}96$ * $c = 12{,}50$—$12{,}62$ * $c/a = 1{,}823$—$1{,}815$ *	Structural type Ni_5As_2	[68]
		Tetragonal system		
343	U - Mg_2Cu_2Al	$a = 5{,}71$ $c = 7{,}94$ $c/a = 1{,}39$	According to [110], this compound is in the (S+α) two-phase region, where S is ~ $MgCuAl_2$ and α is a solid Al(Mg, Cu) solution	[223, 224]
344	(Ti — Cu — Al)	$a = 3{,}55_8$ Å $c = 4{,}625$ Å $c/a = 1{,}30$	Body-centered	[225]
345	$FeCu_4Al_{12}$	$a = 6{,}32$ $c = 14{,}72$ $c/a = 2{,}29$	Constants for composition 38 wt.% Cu, 9 wt. % Fe F.gr. D^6_{4h}; Z = 2 According to [107], confirmed in [108], this composition is in the two-phase region. According to [100], the $Al_{12}Cu_4Fe$ structure is analogous to the Al_7Cu_2Fe structure	[226]
346	γ-$FeAl_4Si_2$	$a = 6{,}11$ $c = 9{,}46$ $c/a = 1{,}55$	Another representation is t-(Fe-Al-Si). According to [217], corresponds to the composition $Fe_{1,5}Al_{1\ 5}Si$	[100, 217, 221, 227]
347	Cu_2AuZn			[32]
		Rhombic system		
348	S'-$MgCuAl_2$	$a = 8{,}40$ Å $b = 5{,}66$ Å	After quenching and aging; constant c not given	[228]
349	$Mo_7B_7Al_6$	$a = 6{,}34$ $b = 7{,}03$ $c = 5{,}76$	Z = 1 Phase rich in Mn and Cu	[229]

* This composition corresponds to at least two phases, apparently with the gamma-brass structure.

** For valence-electron concentrations from 1.25 to 1.6 el./at. respectively

No.	Compound	Lattice constants	Notes	Literature
350	γ-(Mn — Cu —Al)	$a = 14,79$ $b = 12,60$ $c = 13,43$		[115]
351	T_2 - Mn_2ZnAl_6		F.gr. V_h^{13}	[117]
352	(Fe — Al — Si)	$a = 6,09$ Å $b = 9,96$ Å $c = 3,74$ Å		[221]
353	β'''-(Ni — Cu — Al)	$a = 4,22$ Å $b = 4,39$ Å $c = 5,32$ Å	Constants for composition: > 12 wt. % Al, ~ 4% Ni; nonequilibrium phase formed by quenching	[230]
354	CuAuZn			[32]
355	Cu_2Au_3Zn		According to [31], possibly $Au_2(Cu, Zn)$	[32]
356	$ZnPbP_{11}$	$a = 10,55$ $b = 12,69$ $c = 9,85$	F.gr. Pbnm or Pbn Z = 4	[231]
357	$CdPbP_{14}$	$a = 10,71$ $b = 12,80$ $c = 9,91$	F.gr. Pbnm; Pbn	[231]
358	$HgPbP_{11}$	$a = 10,69$ $b = 12,77$ $c = 9,91$	F.gr. Pbnm; Pbn	[231]
		Monoclinic system		
359	φ-$FeCu_{10}Al_{10}$		Allied to δ-(Ni_2Al_3)	[107]
360	($FeCoAs_4$)	$a = 5,25$ Å $b = 2,93$ Å $c = 5,97$ Å	F.gr. P 2/m; Z = 1	[232]
		Triclinic system		
361	(Fe — C — Si)	$a = 6,4$ Å $c = 9,6$ Å $c/a = 1,5$	For the composition ~ 14 at. % Si and ~ 4% Ni; nonequilibrium phase formed by quenching	[233]
362	(Fe — Al — Si)	$a = 6,88$ Å $b = 5,93$ Å $c = 4,32$ Å $\alpha = 104°45'$ $\beta = 130°40'$ $\gamma = 68°24'$		[221]
		Undetermined system		
363	N-(Cr — Mo — Fe)		By x-ray pattern similar to R-(Cr-Mo-Co)	[57, 236]
364	$(Cr, Co)_2Ti$		Laves phase; possibly with superstructure	[237]
365	$Mn_{12}Co_3Si_5$		Allied to σ-phases; comp. determined approximately	[28]
366	T-$(Fe, Ni)_{11}Zn_{89}$		May be structurally similar to δ-$Co_{11}Zn_{89}$	[238]
367	χ-$FeCu_{10}Al_{18}$		Allied to $FeCu_{10}Al_{10}$	[107]
368	β -, $FeAl_{4-5}Si$	$a = 6,18$ Å $c = 42,5$ Å	Another representation m-(Fe-Al-Si) Laue class 4/m, according to [100] $a_1 = a_2 = 6.11$; $a_3 = 41.4$; $a_2 = 91°$	[100, 217, 227, 239]

Compound	Serial No.	Compound	Serial No.	Compound	Serial No.
$(Ag, Al)_2Ca$	95	β'-$Al_3Cu_{12}Sn$	65	AuCuZn	354
$Ag_{0.9}Al_{1.1}Mg$	92	Al_yCu_xTi	323	$AuCuZn_2$	44
AgAsMg	290	Al_zCu_wTi	335	$AuCu_2Zn$	347
AgAsZn	284	(Al — Cu — Ti)	344	Au_2CuZn	24
β''-$AgAuZn_2$	45	T-$Al_3Cu_5Zn_2$	23	Au_3Cu_2Zn	355
$(Ag_{1.98}Mg_{0.02})Ca$	94	T'-$Al_3Cu_5Zn_2$	57	$Au_3Ga_{1/3}Zn_{2.3}$	7
AgMgSb	306	ρ-$Al_9(Fe, Ni)_2$	128	$Au_3Ga_{0.2}Zn_{2.8}$	8
β'-$(Ag, Mg)_3Sn$	25	π-$Al_{10}Fe_3Ni$	130	Au_3GaZn_3	5
$Ag_{0.4}MgZn_{1.6}$	115	γ-Al_4FeSi_2 •	346	$Au_4In_3Sn_3$	127
$Ag_{0.8}MgZn_{1.2}$	77	β-$Al_{4-5}FeSi$ ••	368	B_2CoMo_2	157
$AlAs_2Li_3$	301	α-$Al_6Fe_{1.5}Si$ •••	330	B_4CoMo_2	170
$Al_6B_7Mo_7$	349	α-(Al — Fe — Si)	338	$BCo_{4.7}Si_2$	190
δ_1-(Al — Be — Cu)	90	α_2-(Al — Fe — Si)	339	B_4Cr_2Ni	168
$Al_2Be_{2.3}Fe$	88	α_3-(Al — Fe — Si)	331	$B_{x+y}Cr_{5-x}Si_{3-y}$	185
AlC_xCo_3	204	(Al — Fe — Si)	340	(B — Cr — Si)	162
AlC_xFe_3	203	(Al — Fe — Si)	352	B_4FeMo_2	169
$AlCMn_3$	202	(Al — Fe — Si)	362	$BFe_{4.7}Si_2$	189
Al_5C_3N	314	Al_4GePd_5	155	B_2Fe_3Si	166
AlC_xNi_3	205	$AlLi_2Mg$	47	(B, Si) Fe_3	149
(Al — C — Ti)	324	Al_2LiMg	316	B_2Mn_5Si	165
$(Al, Mg)_2Cd$	12	$AlLi_3N_2$	294	B_2Mo_2Ni	158
Al_7CoCu_2	135	$AlLi_3P_2$	300	B_4Mo_2Ni	171
E-$Al_{18}Cr_2Mg_3$	144	T-$(Al, Zn)_{49}Mg_{32}$	143	B_2Mo_5Si	163
$Al_{12}(Cr, Mn)$	132	$Al_{60}Mn_{11}Ni_4$	141	$B_{x+y}Nb_{5-x}Si_{3-y}$	179
α-$Al_{13}Cr_4Si_4$	192	β-Al_9Mn_3Si	131	(B — Nb — Si)	160
β-$(Al, Si)_2Cr$	145	$Al_{12}Mn_3Si$ ••••	329	BNi_6Si_2	191
ω-Al_7Cu_2Fe	134	T_2-Al_6Mn_2Zn	351	$B_{x+y}Si_{3-y}Ta_{5-x}$	182
φ-$Al_{10}Cu_{10}Fe$	359	$Al_{24}Mn_5Zn$	140	(B — Si — Ta)	161
$Al_{13}Cu_4Fe$	345	$Al_{0.4}MoSi_{1.6}$	146	B_2SiV_5	159
χ-$Al_{18}Cu_{10}Fe$	367	β-(Al, Mo) Ti	20	$B_{x+y}Si_{3-y}V_{5-x}$	176
$(Al, Cu)_6(Cu, Fe)$	129	$AlNaSi_4$	148	$B_{1.5}Si_{1.5}W_5$	164
T_1-Al_2CuLi	334	$AlNi_2Si$	152	(B — Si — Zr)	173
T_B-$Al_{7.5}Cu_4Li$	266	$AlNi_2Ti$	32	$Be_{1.2}Co_{0.8}Mn$	85
AlCuMg, h.t.	111	β_2-$AlNi_2Ti$	21	Be_4CoMn	105
AlCuMg, l.t.	91	Al_3Pd_4Si	154	$Be_2(Cr, Fe)$	104
U-$AlCu_2Mg_2$	343	$(Al, Si)_2W$	147	$Be_5(Cr, Fe,)$ h.t.	319
S-Al_2CuMg	136	As_2CdGe	263	BeN_2Si	258
S'-Al_2CuMg	348	As_2CdSn	264	BeSiZr	167
U'-$Al_2Cu_6Mg_2$	72	$As_7(Co, Fe)$	309	BiCuMg	281
V-$Al_5Cu_6Mg_2$	133	As_4CoFe	360	BiLiMg	292
Q-$Al_7Cu_3Mg_6$	320	AsCuMg	305	BiMgNi	278
T-$(Al, Cu)_{49}Mg_{32}$	142	$AsCu_6Sb$	315	C_xCo_3Ge	213
$AlCu_2Mn$, h.t.	36	As_2GaLi_3	299	C_xCo_3In	209
$AlCu_3Mn_2$	328	As_3GeLi_5	275	C_xCo_3Mg	194
$Al_{20}Cu_2Mn_3$	139	As_2GeZn	262	CCo_2Mo_4	238
η-(Al — Cu — Mn)	350	AsLiMg	287	CCo_3Mo_3	247
$Al_5(Cu, Ni)_3$	48	As_3Li_5Si	274	C_xCo_3Sn	217
$Al_6(Cu, Ni)_4$	50	As_3Li_5Ti	272	η_2-CCo_2W_4	240
T_1-Al_7Cu_4Ni	56	As_4Li_7V	273	CCo_3W_3	254
$Al_7(Cu, Ni)_5$	52	AsLiZn	288	K_2-CCo_6W_6	255
$Al_8(Cu, Ni)_6$	54	AsNaZn	289	θ-$C_2Co_3W_6$	241
$Al_{11}(Cu, Ni)_6$	49	$AsNi_{0.12}Pd_{0.88}$	307	$C_4Co_3W_3$	235
$Al_{13}(Cu, Ni)_8$	51	$Au_{75}Cd_{2.5}In_{22.5}$	14	C_xCo_3Zn	200
$Al_{15}(Cu, Ni)_{10}$	53	$Au_{75}Cd_{3.5}In_{21.5}$	16	CCr_3Nb_3	244
$Al_{17}(Cu, Ni)_{12}$	55	$Au_{75}Cd_{10}In_{15}$	17	$C_{x+y}Cr_{5-x}Si_{3-y}$	186
β'''-(Al — Cu — Ni)	353	$Au_{75}Cd_{12.5}In_{12.5}$	18	$C_6Cr_{21}W_2$	227
T_2-(Al — Cu — Ni)	332	$Au_{78.7}Cd_{12.6}In_{8.7}$	15		
γ-$Al_2Cu_{12}Sn_2$	321	$Au_{82.5}Cd_{10}In_{7.5}$	13		

• ~t-(Al — Fe — Si).
•• ~m-(Al — Fe — Si)
••• ~c-(Al — Fe — Si)
•••• ~c-(Al — Mn — Si)

Compound	Serial No.	Compound	Serial No.	Compound	Serial No.
C_xFe_3Ge	212	$(Co,Cr)_3Zr$	98	CuTaV	81
C_xFe_3In	208	$CoCu_2Sn$	41	Fe_2GaGe	126
CFe_2Mo_4	237	CoFe Ge	123	FeGeMn	120
CFe_3Mo_3	246	Co_4GaGe_3	150	FeGeNi	121
$C_6Fe_{21}Mo_2$	228	CoGeMn	122	η_1 - Fe_3Mo_3N	249
G-(C, N) Fe_2	310	Co_2GeMn	28	β^m-$Fe_7Mo_{13}N_4$	224
ε-(C,N) Fe_{2-3}	311	$Co_{0,7}MgZn_{1,3}$	73	P-(Fe — Mo — Ni)	138
(C — Fe — Si)	361	$Co_{0,2}Mn_{0,8}N$	232	Fe_3NNi	196
CFe_3Sn	216	CoMnSb	265	Fe_3NPt	197
C_xFe_3Sn	216	Co_2MnSi	22	(Fe — N — Si)	341
K_1-CFe_2W_2	251	$Co_3Mn_{12}Si_5$	365	$FeN_{2,60}Ta_2$	220
CFe_3W_3	252	(Co — Mn — Si)	106	FeNiTa	83
CFe_4W_2	252	Co_2MnSn	29	FeNiU	84
K_2-CFe_6W_6	253	β^m - (Co — Mo — N)	225	$(Fe, Ni)_2U$	117
$C_6Fe_{21}W_2$	229	$CoN_{2,5}Ta_2$	221	T-$(Fe, Ni)_{11}Zn_{89}$	366
β^m-(C — Fe — W)	64	$Co_{0,3}NTi_{0,7}$	230	FeSiTi	108
C_xFe_3Zn	199	CoNiSb	124	FeTiV	336
$CGaMn_3$	206	CoNiSn	119	$(Fe, V)_2Zr$	96
$CGeMn_3$	211	$(Co, Ni)_2U$	118	Ga_6GeNi_7	153
C_xGeNi_3	214	CoTaTi	99	$GaGe_4Rb_5$	151
C_xInMn_3	207	CoTaV	100	$GaInSb_2$	259
C_xInNi_3	210	$(Co, V)_2Zr$	97	$GaIn_2Sb_3$	260
K-C_xMgNi_3	195	N-(Cr — Fe — Mo)	363	$GaLi_3N_2$	295
CMn_3Mo_3	245	σ-(Cr — Fe — Mo)	68	$GaLi_3P_2$	298
CMn_6N	337	χ-(Cr — Fe — Mo)	60	$GeLi_5N_3$	297
C_xMn_3Sn	215	χ-(Cr — Fe — Ni)	63	$GeLi_5P_3$	271
CMn_3W_3	250	χ-$Cr_7Fe_{17}Ti_5$	58	GeMnNi	125
(C — Mn — W)	234	χ-(Cr — Fe — W)	62	$GeMnNi_2$	33
CMn_3Zn	198	P-$Cr_{18}Mo_{42}Ni_{40}$	137	GeP_2Zn	261
CMn_3Zn *	218	$Cr_3Ni_2Si_2$	66	HNiZr	325
CMo_3Ni_3	248	$Cr_{65}Ni_{25}Si_{10}$	70	H_3NiZr	326
CMo_4Ni_2	239	CrNiTa	103	$HgLi_2Tl$	19
$C_{x+y}Mo_{5-x}Si_{3-y}$	187	Cr_4Ni_5W	69	$HgP_{14}Pb$	358
ε-(C, N) Ni_3	312	CrNiZr	79	IrOsRu	11
(C, N) U_2	313	Cu_2FeSn, h.t.	4	LiMgN	267
(C, Si) Nb_2	156	Cu_2FeSn, l.t.	40	LiMgP	276
(C — Nb — Si)	180	Cu_2GaMn	10	LiMgSb	291
C (Nb, U)	321	$\sim Cu_2Ge_2Ni_3$	37	$Li_{0,25}MgZn_{1,75}$	110
CNi_3W_3	256	$Cu_{60}Ge_{25}Ni_{15}$	342	0-LiMgZn	71
0-CNi_3W_6	242	$Cu_{65}Ge_{20}Ni_{15}$	333	Li_2MgZn	46
K-CNi_3W_{16}	236	Cu_2InMn	67	Li_7MnN_4	303
CNi_5W_6	257	Cu_2InSn	38	Li_3MnP_2	304
C_xNi_3Zn	201	CuMgSb	43	Li_7N_4Nb	317
$C_{x+y}Si_{3-y}Ta_{5-x}$	183	Cu_3Mg_2Si, h.t.	280	Li_5N_3Si	296
(C — Si — Zr)	172	Cu_3Mg_2Si, l.t.	114	Li_7N_4Ta	318
(C — Si — V)	177	$Cu_{16}Mg_6Si_7$	109	Li_5N_3Ti	293
$C_{x+y}Si_{3-y}W_{5-x}$	188	CuMgSn	193	Li_7N_4V	302
(C — Si — Zr)	174	Cu_4MgSn	279	LiNZn	285
C_yTa_xU	322	$CuMg_2Zn_3$	89	Li_5P_3Si	270
CV_3Zr_3	243	V-$CuMg_2Zn_4$	112	Li_5P_3Ti	268
$Ca(Cd, Mg)_2$	93	T-(Cu—Mg —Zn)	113	Li_7P_4V	269
$Ca_2Pb_3Sn_3$	3	γ-(Cu — Mn — Ni)	76	LiPZn	286
$Ca_2Pb_3Tl_3$	2	CuMnSb	327	MgNiSb	277
$Ca_2Sn_3Tl_3$	1	Cu_2MnSn, h.t.	282	$MgNi_2Sb$	31
CdCuSb	283	Cu_2MnSn, l.t.	39	$MgNi_{1,8}Si_{0,2}$	75
CdCuZn	87	Cu_8Mn_4Sn	9	$MgNi_2Sn$	30
$CdP_{14}Pb$	357	β-$(Cu, Ni)_3Sb$	86	Mg (Ni, Zn)$_2$	74
Co_2Cr_2Si	61	Cu_2NiSn	27	(Mg — Sb — Zn)	308
$(Co_4Cr)_2Ti$	59	$(Cu, Ni)_3Sn$	42	β^m-(Mn — Mo — N)	223
	364	$CuPtZn_2$	26	$Mn_{0,8}NNi_{0,2}$	233
		$Cu_{0,5}TaV_{1,5}$	6	MnN_4Ta_3	219
			102	$MnNi_2Sb$	35
				(Mn — Ni — Si)	107

* at − 196°

Compound	Serial No.	Compound	Serial No.	Compound	Serial No.
$MnNi_2Sn$	34	(N — Nb — Si)	181	(N — Si — Zr)	175
$(Mn, Ni)_2U$	116	$N_{2,45}NiTa_2$	222	$G\text{-}Ni_{13}Si_6Ti_8$	322
MnNiZr	80	$NNi_{0,3}Ti_{0,7}$	231	NiTaV	101
$Mn_{0,5}TaV_{3,5}$	82	$N_zSi_{3-y}Ta_{5-x}$	184	$Ni_{1,5}V_{0,5}Zr$	78
β^m-(Mo — N — Ni)	226	(N — Si — V)	178	$P_{14}PbZn$	356

LITERATURE CITED

1. G. B. Bokii, Introduction to Crystal Chemistry [in Russian] (Izd. MGU, 1954).
2. P. I. Kripyakevich, "Classified system of binary intermetallic phases" Izvest. Sektora Fiz.-Khim. Analiza IONKh Akad. Nauk SSSR, 24, 59 (1954).
3. N. V. Belov, Structure of Ionic Crystals and Metallic Phases [in Russian] (Izd. AN SSSR, Moscow, 1947).
4. B. K. Vul'f, "Classification of ternary metallic phases" Fizika Metallov i Metallovedenie, 3, 1, 97 (1956).
5. N. S. Kurnakov, Introduction to Physicochemical Analysis [in Russian] 4th Editions (Izd. AN SSSR, Moscow, 1940).
6. W. Pearson. A Handbook of Lattice Spacings and Structures of Metals and Alloys. (London, 1958).
7. L. S. Palatnik and V. A. Finkel', Kristallografiya, 3, 4, 467 (1958).
8. P. I. Kripyakevich, Candidate's Dissertation [in Russian] (L'vov State Univ., 1956).
9. P. I. Kripyakevich, Kristallografiya, 5, 1, 79 (1960).
10. B. K. Vul'f, Ternary Metallic Phases in Alloys [in Russian] (Izd. VVIA im. N. E. Zhukovskogo, 1959) No. 718.
11. J. Kasper. Acta crystallogr., 11, 3, 184 (1958).
12. F.Frank and J. Kasper. Acta crystallogr., 12, 7, 483 (1959).
13. N. L. Smirnova, Kristallografiya, 1, 2, 165 (1956).
14. N. L. Smirnova, Kristallografiya, 4, 1, 13 (1959).
15. A. Jandelli. R. S. Sem. Fac. Sci. Cagliari, 19, 133, (1951); C. A., 46, 3437 (1952).
16. E. S. Makarov, Izvest. Sektora Fiz.-Khim. Analiza, IONKh Akad. Nauk SSSR, 19, 463 (1949).
17. M. Wilkens and K. Schubert. Z. Metallk., 49, 12, 633 (1958).
18. K. Schubert, M. Balk, S. Bhan, H. Breimer, P. Esslinger, and E. Stolz. Naturwiss., 46, 23, 647 (1959).
19. A. P. Klyucharev, Zhur. Éksp. i Teoret. Fiz. 9, 1501 (1939).
20. S. Aoyama. Sci. Rep. Toh. Imp. Univ., (Vol. K. Honda), 527 (1936).
20a. K. Riederer. Z. Metallk., 30, 15 (1938).
21. K. Schubert, H. Breimer, W. Burkhardt, E. Günzel, R. Hauffler, H. Lukas, H. Vetter, J. Wegst, and M. Wilkens. Naturwissenschaften, 44, 7, 229 (1957).
22. J. Wegst and K. Schubert. Z. Metallk., 49, 10, 533 (1958).
23. E. Zintl and G. Brauer. Z. Phys. Chem., 20, 245 (1933).
24. H. Böhm and K. Löhberg. Z. Metallk., 49, 4, 173 (1958).
25. A. Taylor and R. Floyd. J. Inst. Metals., 81, 25 (1952).
26. A. Taylor. J. Metals, 8, 10, S. 2, 1356 (1956).
27. E. I. Gladyshevskii, P. I. Kripyakevich, and Yu. B. Kuz'ma, Fizika Metallov i Metallovedenie, 2, 3, 454 (1956).
28. E. E. Cherkashin, E. I. Gladyshevskii, P. I. Kripyakevich, and Yu. B. Kuz'ma, Zhur. Neorg. Khim. 3, 3, 650 (1954).
29. E. Gebhardt. Z. Metallk., 34, 9, 208 (1942).
30. W. Köster and K. Moeller. Z. Metallk., 33, 8/9, 278, 284 (1941).
31. K. Schubert, W. Burkhardt, P. Esslinger, E. Günzel, H. Meissner, W. Schütt, J. Wegst, and M. Wilkens. Naturwissenschaften, 43, 11, 248 (1956).
32. E. Raub and P. Walter. Z. Metallk., 41, 425 (1950).
33. G. Raynor and B. Frost. J. Inst. Metals., 75, 777 (1949).
34. P. Rahlfs. Metallwirt., 16, 640 (1937).
35. P. I. Kripyakevich, E. I. Gladyshevskii, and O. S. Zarechnyuk, Doklady Akad. Nauk SSSR, 95, 3, 525 (1954).
36. L. Castelliz. Monatsh. Chem. , 84, 4, 765 (1953).
37. P. I. Kripyakevich, E. I. Gladyshevskii, and O. S. Zarechnyuk, Nauk. Zap. L'vivsk. Univ., Ser. Khim. 34, 4, 98 (1955).
38. L. Castelliz. Monatsh. Chem., 82, 1059 (1951).
39. A. Bradley and J. Rodgers. Proc. Roy. Soc. A, 144, 340 (1934).
40. O. Heusler. Ann. Phys., 19, 155 (1934).
41. F. Hames and D. Eppelsheimer. J. Metals, 1, 8, 495 (1949).
42. B. Coles, W. Hume-Rothery, and H. Myers. Proc. Roy. Soc. A, 196, 125 (1949).
43. L. Carapella and R. Hultgren. Phys. Rev., 59, 905 (1941).
44. F. Hames and D. Eppelsheimer. J. Metals, 1, 354 (1949).
45. Liu Yi-huan and Hsu Chen-chia. Scientia sinica, 6, 6, 1013 (1957).
46. Liu Yi-huan and Hsu Chen-chia. Acta phys. sinica, 13, 6, 463 (1957).

47. P. I. Kripyakevich, Nauk. Zap. L'vivsk. Univ., Ser. Khim. 46, 5, 107 (1958).
48. D. Levinson and D. Mc.Pherson. Trans. Amer. Soc. Metals, 48, 689 (1956).
49. R. Busk, D. Leman, and J. Casey. J. Metals, 2, 7, 945 (1950).
50. P. Frost, J. Kura, and L. Eastwood. J. Metals, 2, 1277 (1950).
51. A. Bradley and H. Lipson. Proc. Roy. Soc. A, 167, 421 (1938).
52. S. Lu and T. Chang. Scientia sinica, 6, 3, 431 (1957).
53. M. Bown. Acta crystallogr., 9, 70 (1956).
54. W. Köster and K. Moeller. Z. Metallk., 34, 9, 206 (1942).
55. N. G. Boriskina and I. I. Kornilov, Zhur. Neorg. Khim. 4, 9, 2171 (1959).
56. P. I. Kripyakevich and Ya. D. Khorin, Nauch. Doklady Vysshei Shkoly, Metallurgiya, 1, 198 (1958).
57. J. McMullin, S. Reiter, and D. Ebeling. Trans. Amer. Soc. Metals, 46, 7, 799 (1954).
58. J. Kasper. Acta Metallurgica, 2, 456 (1954).
59. S. Takada and N. Yukawa. Nippon Kinzoku Gakkai-Si, 21, 4, 275 (1957).
60. H. Goldschmidt. Acta crystallogr., 10, 12, 769 (1957).
61. H. Goldschmidt. Metallurgia, 56, 333, 17 (1957).
62. E. I. Gladyshevskii, P. I. Kripyakevich, and Yu. B. Kuz'ma, Fedorov Session on Crystallography, Summaries of Papers [in Russian] (Leningrad, May 1959) p. 32.
63. H. Goldschmidt. Trans. Amer. Soc. Metals, 46, 807 (1954).
64. K. Andrews. Nature, 164, 1015 (1949).
65. D. Evans and K. Jack. Acta crystallogr., 10, 12, 769 (1957).
66. K. Kuo. J. Metals, 8, 2, 97 (1956).
67. J. Leach, G. Raynor. Proc. Roy. Soc. A, 224, 251 (1954).
68. W. Burkhardt and K. Schubert. Z. Metallk., 50, 4, 196 (1959).
69. P. Pietrokowsky and P. Duwez. J. Metals, 2, 10, 1283 (1950).
70. K. Kuo. Acta metallurgica, 1, 720 (1953).
71. I. I. Kornilov and P. B. Budberg, Trudy In-ta Metallurgii Akad. Nauk SSSR, 1, 132 (1957).
72. A. Weinberg, D. Levinson, and W. Rostoker. Trans. Amer. Soc. Metals, 48, 855 (1956).
73. G. G. Urazov and M. S. Mirgalovskaya, Izvest. Sektora Fiz.-Khim. Analiza, IONKh Akad. Nauk SSSR, 19, 514 (1949).
74. F. Laves and H. Witte. Metallwirt., 15, 1, 15 (1936).
75. F. Laves, H. Wallbaum. Z. anorgan. und allgem. Chem., 250, 110 (1942).
76. K. Lieser and H. Witte. Z. Metallk., 43, 396 (1952).
77. V. I. Mikheeva and O. N. Kryukova, Izvest. Sektora Fiz.-Khim. Analiza, IONKh Akad. Nauk SSSR, 20, 76 (1950).
78. P. I. Kripyakevich, E. I. Gladyshevskii, and I. I. Zaluts'kii, Nauk. Zap. L'vivsk. Univ. 46, 5, 118 (1958).
79. N. Baenziger, R. Rundle, A. Show, and A. Wilson. Acta crystallogr. 3, 34 (1950).
80. S. Valentiner. Z. Metallk., 44, 59 (1953).
81. P. Black. Acta crystallogr., 8, 1, 39 (1955).
82. E. I. Gladyshevskii, P. I. Kripyakevich, and M. Yu. Teslyuk, Doklady Akad. Nauk SSSR, 85, 81 (1952).
83. E. E. Cherkashin, E. I. Gladyshevskii, and M. Yu. Teslyuk, Izvest. Sektora Fiz.-Khim. Analiza, IONKh Akad. Nauk SSSR, 27, 212 (1956).
84. O. Nickel. Z. Metallk., 49, 2, 57 (1958).
85. H. Nowotny. Metallforsch., 1, 31 (1946).
86. H. Nowotny. Z. Metallk., 37, 31 (1946).
87. R. Elliott and W. Rostoker. Trans. Amer. Soc. Met., 50, 617 (1958).
88. P. M. Arzhanyi and L. N. Belyakov, Izvest. Akad. Nauk SSSR, Otdel. Tekhn. Nauk, 2, 149, (1958).
89. E. I. Gladyshevskii, P. I. Kripyakevich, and Yu. B. Kuz'ma, Dopovidi Akad. Nauk Ukr SSR, 1, 67 (1956).
90. R. Vogel and W. Schlüther. Arch. Eisenhütt., 12, 207 (1938/39).
91. H. Witte. Metallwirtschaft. Wiss. Techn., 18, 22, 459 (1939).
92. H. Witte. Z. Angew. Min., 1, 255 (1938).
93. E. I. Gladyshevskii and P. I. Kripyakevich, Nauk. Zap. L'vivsk. Univ. 34, 4, 64 (1955).
94. H. Witte. Z. angew. Min., 1, 1, 83 (1937).
95. G. Brook, G. Williams, and E. Smith. J. Inst. Metals, 83, 271 (1955).
96. K. Schubert, H. Breimer, and R. Gohle. Z. Metallk., 50, 3, 146 (1959).
97. A. Bradley and A. Taylor. J. Inst. Metals, 66, 2, 53 (1940).

98. G. Raynor and P. Pfeil. J. Inst. Metals, 73, 397 (1947).
99. W. Taylor. Acta crystallogr., 10, 12, 770 (1957).
100. G. Phragmen. J. Inst. Metals., 77, 6, 489 (1950).
101. K. Robinson. Acta crystallogr., 5, 397, (1952).
102. H. Lipson. Nature, 167, 847 (1951).
103. J. Adam and J. Rich. Acta crystallogr., 7, 813 (1954).
104. S. Samson. Acta chem. scand., 3, 809 (1949).
105. F. Laves, and St. Werner. Z. Krist., A., 95, 1/2, 114 (1936).
106. G. G. Urazov and M. S. Mirgalovskaya, Doklady Akad. Nauk SSSR, 88, 2, 247 (1952).
107. A. Bradley and H. Goldschmidt. J. Inst. Metals., 65, 2, 403 (1939).
108. M. Bown and P. Brown. Acta crystallogr., 9, 911 (1956).
109. G. Raynor and B. Ward. J. Inst. Metals., 86, 4, 182 (1957).
110. M. S. Mirgalovskaya and E. S. Makarov, Izvest. Sektora Fiz.-Khim. Analiza, IONKh Akad. Nauk SSSR, 18, 117 (1949).
111. H. Perlitz and A. Westgren. Arkiv Kemi, Min., Geol., 163, 13, 5(1943).
112. C. Brink and D. Shoemaker. Acta crystallogr., 8, 734 (1955).
113. D. Schoemaker, C. Schoemaker, and F. Wilson. Acta crystallogr., 10, 1 (1957).
114. D. Das, S. Rideout, and P. Beck. J. Metals, 4, 10, 1071 (1952).
115. H. Petri. Aluminiumarchiv, 14, 14 (1938).
116. K. Robinson. Philos. Mag., 43, 775 (1952).
117. D. Wakeman and G. Raynor. Philos. Mag., 39, 245 (1948).
118. K. Robinson. Acta crystallogr., 7, 494 (1954).
119. F. Laves, K. Löhberg, and H. Witte. Metallwirtschaft., 14, 793 (1935).
120. G. Bergmann, J. Waugh, and L. Pauling. Nature, 169, 1057 (1952).
121. G. Bergmann, J. Waugh, and L. Pauling. Acta crystallogr., 10, 4, 254 (1957).
122. S. Samson. Nature, 173, 1185 (1954).
123. S. Samson. Acta crystallogr., 11, 12, 851 (1958).
124. J. Pratt and G. Raynor. J. Inst. Metals., 79, 211 (1951).
125. K. Robinson. Acta crystallogr., 6, 667 (1953).
126. H. Nowotny and H. Huschka. Monatsh Chem., 88, 4, 494 (1957).
127. H. Nowotny and E. Scheil. Metallforsch., 2, 76 (1947).
128. C. Ransley and H. Neufeld. J. Inst. Metals., 78, 25 (1950, 1951).
129. B. Aronsson and G. Lundgren. Acta chem. scand., 13, 3, 433 (1959).
130. P. Esslinger and K. Schubert. Z. Metallk., 48, 126 (1957).
131. L. Brewer and O. Krikorian. J. Electrochem. Soc., 103, 38 (1956).
132. R. Steinitz and J. Binder. Powder Metallurgy Bull., 6, 123 (1953).
133. H. Nowotny, R. Kieffer, and F. Benesovsky. Planseeber. Pulvermetallurgie, 5, 86 (1957); H. Nowotny, E. Dimakopoulou, and H. Kudielka. Monatsh. Chem., 88, 2, 180 (1957).
134. B. Aronsson. Acta chem. scand., 12, 31 (1958).
135. F. Bertaut and P. Blum. Compt. Rend., Paris, 236, 1055 (1953).
136. E. Parthé, B. Lax, and H. Nowotny. Monatsh. Chem., 86, 859 (1955).
137. J. Nielsen, N. Baenziger. Acta crystallogr., 7, 132 (1954).
138. B. Post, E. Pipitz, and W. Herz. Powder Met. Bull., 7, 3-6, 149 (1956).
139. R. Kieffer, F. Benesovsky, and B. Lux. Planseebericte für Pulvermetallurgie, 4, 2, 30 (1956).
140. H. Nowotny, E. Piegger, R. Kieffer, and F. Benesovsky. Monatsh. Chem., 89, 4-5, 611 (1958).
141. E. Parthé, H. Schachner, and H. Nowotny. Monatsh. Chem., 86, 182 (1955).
142. H. Nowotny, E. Parthé, R. Kieffer, and P. Benesovsky. Monatsh. Chem., 85, 255 (1954).
143. S. Rundquist and F. Jellinek. Acta chem. scand., 13, 3, 425 (1959).
144. K. Robinson. Acta crystallogr., 6, 854 (1953).
145. G. Bergmann and J. Waugh. Acta crystallogr., 6, 93 (1953).
146. G. Bergmann and J. Waugh. Acta crystallogr., 9, 3, 214 (1956).
147. G. Nagorsen and H. Witte. Z. anorg. und allgem. Chem., 271, 144 (1952).
148. H. Stadelmaier and L. Huetter. Acta Metallurg. 7, 6, 415 (1959).
149. L. Huetter and H. Stadelmaier. Acta Metallurg., 6, 367 (1958).
150. E. Scheil and L. Hütter. Z. Metallk., 44, 387 (1953).

151. G. Wiener and J. Berger. J. Metals, 7, S. 2, 360 (1955).
152. R. Butters and H. Myers. Philos. Mag., 46, 132 (1955).
153. R. Butters and H. Myers. Philos. Mag., 46, 895 (1955).
154. F. Morral. J. Iron Steel Inst., 130, 419 (1934).
155. K. Löhberg and W. Schmidt. Arch. Eisenhuttenwesen, 11, 607 (1938).
156. H. Myers. Report on work done on DRB Grant. The University of British Columbia (1956).
157 L. Hütter and H. Stadelmeier. Z. Metallk., 4, 199 (1959).
158. E. Morgan. J. Metals, 6, 983 (1954).
159. N. Schönberg. Acta chem. scand., 8, 213 (1954).
160. Strukturberichte, Bd 3, 59 (1937).
161. N. Schönberg. Acta Met., 2, 427 (1954).
162. K. Kuo. J. Metalurg, 5, S. 2, 745 (1953).
163. P. Rautala and J. Norton. J. Metals, 4, 10, 1045 (1952).
164. N. Schönberg. Acta Metallurg, 2, 837 (1954).
165. K. Whitehead and L. Brownlee. Plaseeberichte für Pulvermetallurgie 4, 3, 62 (1956).
166. Ya. S. Umanskii and N. T. Chebotarev, Izvest. Akad. Nauk SSSR, Otdel. Fiz. Nauk, 15, 1, 24 (1951).
167. K. Kuo. Acta Metallurg, 1, 3, 301 (1953).
168. E. N. Kislyakova, Zhur. Fiz. Khim. 17, 108 (1934).
169. R. Kiessling. J. Metals, 5, S. 2, 745 (1953).
170. V. Adelsköld, A. Sundelin, and A. Westgren. Z. anorg. Chem., 212, 401 (1933).
171. A. Westgren. Jernkontorets ann. 117, I (1933).
172. A. Westgren and G. Phragmén. Jernkontorets ann., 111, 525 (1927).
173. V. I. Arkharov and S. T. Kiselev, Izvest. Akad. Nauk SSSR, Otdel. Tekh. Nauk, 136 (1949).
174. A. Metcalf. The iron and steel institute. London, Special report, 38, 84 (1947).
175. V. I. Arkharov and S. T. Kiselev, Izvest. Akad. Nauk SSSR, Otdel. Tekh. Nauk, 749 (1947).
176. A. Rabenau and P. Eckerlin. Naturwissenschaften., 46, 3, 106 (1959).
177. N. A. Goryunova and N. N. Fedorova, Zhur. Tekh. Fiz. 25, 1339 (1955).
178. H. Pfister. Acta crystallogr., 11, 3, 221 (1958).
179. H. Nowotny and B. Glatzl. Monatsh. Chem., 83, 237 (1952).
180. H. Hardy and J. Silcock. J. Inst. Metals, 84, 11, 423 (1955, 1956).
181. R. Juza and F. Hund. Z. anorgan. und allgem. Chem., 257, 1 (1948).
182. R. Juza and W. Schulz. Z. anorgan. und allgem. Chem. , 275, 65 (1954).
183. R. Juza and W. Uphoff. Z. anorgan. und allgem. Chem., 292, 1-3, 65 (1957).
184. H. Nowotny and K. Bachmeier. Monatsh. Chem., 80, 5, 734 (1949).
185. H. Nowotny and K. Bachmeier. Monatsh. Chem., 81, 488 (1950).
186. E. I. Gladyshevskii and P. I. Kripyakevich, Doklady Akad. Nauk SSSR, 102, 4, 743 (1955).
187. P. I. Kriypakevich, E. I. Gladyshevskii, and E. E. Cherkashin, Doklady Akad. Nauk SSSR, 75, 205 (1950).
188. H. Nowotny and W. Siebert. Z. Metallk., 33, 12, 391 (1941).
189. E. Scheil and W. Siebert. Z. Metallk., 33, 12, 389 (1941).
190. H. Nowotny. Z. Metallk., 34, 237 (1942).
191. H. Nowotny and B. Glatzl. Monatsh. Chem., 82, 720 (1951).
192. F. Laves. Kristallchemie (in the book: D'Ans, E. Lax. Taschenbuchl für Chemiker und Physiker.) 2 Aufl. Berlin (1949).
193. N. L. Smirnova, Kristallografiya, 4, 1, 20 (1959).
194. R. Juza, H. Weber, and E. Meyer-Simon. Z. anorgan. und allgem. Chem., 273, 48 (1953).
195. R. Juza and F. Hund. Z. anorgan. und allgem. Chem., 257, 13 (1948).
196. R. Juza and F. Hund. Naturwiss., 33, 121 (1946).
197. R. Juza and W. Schulz. Z. anorgan. und allgem. Chem., 269, 1 (1952).
198. R. Juza, E. Anschütz, and H. Puff. Angew. Chem., 71, 4, 161 (1959).
199. R. Juza, W. Gieren, and Y. Haug. Z. anorgan. und allgem. Chem. 300, 1/2, 611 (1959).
200. R. Juza and T. Bohmann. Angew. Chem., 71, 4, 161 (1959).
201. S. Geller, B. Matthias. Phys. Chem. Solids, 4, 1/2, 156 (1958)
202. K. Löhberg. Z. phys. Chem., (B) 27, 5/6, 381 (1934).
203. R. Thompson. Amer. Mineralogist, 35, 451 (1950).
204. K. Jack. Proc. Roy. Soc. A, 195, 41 (1948).

205. R. Bridelle and A. Michel. Rev. métallurgie, 51, 278 (1954).
206. K. Jack, in Ph D. Thesis. University of Cambridge, 1949.
207. R. Rundle, N. Baenziger, A. Wilson, and R. McDonald. J. Amer. Chem. Soc., 70, 99 (1948).
208. M. Stackelber and K. Spiess. Z. phys. Chem. A, 175, 140 (1935).
209. E. Günzel and K. Schubert. Z. Metallk., 49, 5, 234 (1958).
210. M. S. Mirgalovskaya, Doklady Akad. Nauk SSSR, 77, 2, 289 (1951).
211. C. Schram, P. Gordon, and A. Kaufmann. J. Metals, 2, 1, 195 (1950).
212. E. F. Bakhmet'ev, N. G. Sevast'yanov and N. Yu. Kotov. Acta physicochim. USSR, 2, 561 (1935).
213. R. Van Thyne and H. Kessler. Trans. Amer. Inst. Min. Met. Eng., 200, 2, 193 (1954).
214. G. Libowitz, H. Hayes, and T. Gibb. I r. J. Phys. Chem., 62, 1, 76 (1958).
215. U. Zwicker. Z. Metallk., 42, 331, (1951).
216. D. West and D. Thomas. J. Inst. Metals. , 85, 97 (1956, 1957).
217. H. Nowotny, K. Komarek, and J. Kremer. Berg. u. Hüttenman. Monatsh., 96, 161 (1951).
218. M. Armand. Compt. rend, Paris, 235, 1506 (1952).
219. Pi Ch'ing-hua and I. I. Kornilov, Zhur. Neorg. Khim. 5, 4, 902 (1960).
220. K. Robinson and P. Black. Philos. Mag., 44, 1392 (1953).
221. W. Jäniche and H. Hanemann. Aluminiumarchiv, 5, 1 (1936).
222. G. Booker, J. Norbury, and M. Howes. Nature, 184, 1311 (1959).
223. A. Saulnier and G. Cabane. Rev. métallurgie, 46, 13 (1949).
224. H. Lambot. Rev. métallurgie, 47, 709 (1959).
225. W. Gruhl, and H. Cordier. Metall, 11, 11, 928 (1957).
226. H. Wiehr. Aluminiumarchiv, 31, 14 (1940).
227. H. Nowotny. Metallforsch., 1, 38 (1946).
228. S. Konobeevskii, Izvest. Akad. Nauk SSSR, Ser. Fiz. 10, 4, 371 (1946).
229. F. Halla and W. Thury. Z. anorgan. und allgem. Chem., 249, 229 (1942).
230. D. Toman. Hutnické Listy, 10, 4, 202 (1955).
231. H. Krebs, J. Pakulla, and G. Zürn. Z. anorgan. und allgem. Chem., 278, 274 (1955).
232. M. Peacock. Trans. Roy. Soc. Canada, 38, 155 (1944).
233. H. Goldschmidt. J. Iron and Steel Inst., 163, 383 (1949).
234. R. Roof and J. Lombardo. Trans. Met. Soc. AIME, 212, 1, 50 (1958).
235. H. Beattie and W. Hagel. J. Metals, 9, 7, S. 2, 911 (1957).
236. H. Goldschmidt, Symposium on High-Temperature Steels and Alloys for Gas Turbines, Iron and Steel Inst., Special Report No. 43, 249 (1952).
237. B. G. Livshits and Ya. D. Khorin, Zhur. Neorg. Khim. 3, 3, 685 (1958).
238. G. V. Raynor and J. D. Noden. J. Inst. Metals, 86, 269 (1958).
239. P. Black. Philos. Mag., 46, 401 (1955).

All abbreviations of periodicals in the above bibliography are letter-by-letter transliterations of the abbreviations as given in the original Russian journal. *Some or all of this periodical literature may well be available in English translation.* A complete list of the cover-to-cover English translations appears at the back of this issue.

BIBLIOGRAPHY

INTERNATIONAL UNION OF CRYSTALLOGRAPHY

COMMISSION ON CRYSTAL STRUCTURE DATA

LIST OF 1956 PUBLICATIONS CONTAINING NEW DATA ON CRYSTAL STRUCTURES

Translated from Zhurnal Strukturnoi Khimii, Vol. 2, No. 1, pp. 112-128,
January-February 1961

Starting with this issue, Zhurnal Strukturnoi Khimii will regularly publish lists of publications which have appeared in the world's scientific literature during recent years and which contain new data on crystal structures. The lists will appear in every issue of the journal and will contain bibliographies covering one year in the following sections:

A) Metals.

B) Inorganic compounds.

C) Organic compounds.

The following publication schedule is planned for 1961:

Number of journal		
1	A. Metals for	1956
2	B. Inorganic compounds for	1956
3	C. Organic compounds for	1956
4	A. Metals for	1957
5	B. Inorganic compounds for	1957
6	C. Organic compounds for	1957

Subsequent volumes of the journal will contain lists for publications for 1958 and the following years.

These lists are prepared as follows. Papers published in foreign journals are taken from the lists of the Commission on Crystal Structure Data, which the Editorial Board receives from the Chairman of the Commission Dr. W. B. Pearson (Canada). The bibliography of Soviet publications is compiled by direct surveys of the latter, including abstracting journals. The selection of material is guided primarily by the requirements of the international publication Structure Reports. It must be pointed out that the range of publications in the lists for 1956 is somewhat wider owing to inclusion of some papers of a theoretical and review character, and also of papers which do not contain crystal structure data in the narrow sense but which are of definite interest from the structure aspect. Future selection will probably be more rigid, in conformity with the decisions of the Commission on Crystal Structure Data, adopted at the meetings in Cambridge on August 13 and 19, 1960. The lists are compiled and prepared for the press by V. V. Bakakin (Institute of Inorganic Chemistry, Siberian Division, Academy of Sciences USSR); the editor in chief is Corresponding Member of the Academy of Sciences USSR G. B. Bokii.

Note. The transliteration system employed for the rendering of Russian names into the Latin alphabet is known as British-American Standard and is used throughout this journal, with the following exceptions: In this bibliography, the Cyrillic letters Ю and Я will be rendered as ju and ja, respectively, rather than as the usual equivalents of yu and ya; consequently, entries translated from the Russian which bear these initial letters will be found entered alphabetically in the appropriate places with the j's of the alphabet, rather than with the y's.

The published lists consist of brief bibliographical annotations. As a rule, each annotation is given in the language of the original. The abbreviated name of the language is given in parentheses at the end of the annotation. Annotations of papers published in one of the five official languages of the International Union (English, Spanish, German, Russian, and French) are given without indication of language. Annotations of papers in languages which use neither the Russian nor the Latin alphabet are translated into one of the official languages.

Within each section the annotations are given in a single list in alphabetical order of authors' names. The order is based on the Latin alphabet.

A system of abbreviations is used in order to save space. The years of publication are not given because each list refers to one year which is given in the heading. The titles of foreign journals are abbreviated in accordance with the abbreviation systems used in Structure Reports (see Vol. 13, pp. 599-606 and Vol. 15, pp. 545-548) and Chemical Abstracts (see Vol. 50, pp. 1j-314j).

In titles of papers in German, plurals of abbreviated words are produced by repetition of the last letter, for examples, Eigg.-Eigenschaften, Verbb.-Verbindungen, etc. The ending -isch is omitted from adjectives such as chemisch. The endings -ung, -ich, -ig, -ion are omitted; the endings -keit and -heit are replaced by k. and h. Legier.-Legierung, Leitfahigk-Leitfahigkeit. In compounds words each component may be abbreviated as an independent word and hyphenated; e.g., El.-beug.-Elektronebeugung. Other German abbreviations are given in the list below.

In English titles plurals are denoted by addition of the plural form s to the abbreviation; e.g. fs.-factors. Articles are omitted from English titles; the remaining abbreviations are listed below.

In titles which are in French, and in some instances in other languages, words of similar spelling to the corresponding English words are abbreviated in accordance with the system used for English when orthography permits. In addition, the following French abbreviations are used: crist.-cristallographique, é-électronique, r. X-rayons, X.

All the abbreviated forms may be used in conjunction with prefixes such as mono-, unter-, Uber, etc.; e.g. intermet.=intermetallic; Uberstr.=Uberstruktur.

Omissions of individual papers are obviously inevitable. The Editorial Board hopes eventually to remedy this fault and will be grateful to authors of omitted papers if they would send the titles and references to the Chairman of the Commission on Crystal Structure Data Dr. W. B. Pearson (Division of Pure Physics, National Research Council, Ottawa, Canada), or to the editor in chief of these lists G. B. Bokii at the address of Zhurnal Strukturnoi Khimii.

Abbreviations of English Words

A.— and
anal.— analysis, analytical
arrgt.— arrangement
at.— atomic
char.— characteristics, characterization
chem.— chemical, chemistry
coef.— coefficient
compd.— compound
compn.—composition
const.— constant
dim.— dimension, dimensional
dislocn.— dislocation
distribn.— distribution
e.— electron, electronic
electr.— electric, electrical
estn.— estimation
evapd.— evaporated
examn.— examination
expan.— expansion
expt.— experiment
exptl.— experimental
f.— factor
formn.— formation
gr.— group
hex.— hexagon, hexagonal
identfn.— identification
inorg.— inorganic
constn.— constitution
coord.— coordinate
coordn.— coordination
cr.— crystal, crystalline
crystallogr.— crystallographic, crystallography
crystzn.— crystallization
cub.— cubic
detn.— determination
diffrn.—diffraction
opt.— optics, optical
ord.— ordered
ordg.— ordering
org.— organic
orthorh.— orthorhombic
par.— parameter
pat.— pattern
phys.—. physical
powd.— powder, powdered
prepn.—preparation
pres.— pressure
prop.— property
qual.— qualitative
quant.— quantitative
radn.— radiation
refl.— reflection
refnt.— refinement

interpretn.— interpretation
intmd.— intermediate
investn.— investigation
lat.— lattice
magn.— magnet, magnetic
measrt — measurement
mech.— mechanical
met.— metal, metallic
micr.— microscope, microscopic, microscopy
min.— mineral
modifn.— modification
mol.— molecule, molecular
monocl.— monoclinic
n.— neutron
nucl.— nucleus, nuclear
obsn.— observation
reln.— relation
relnsh.— relationship
rhomboh.— rhombohedral
scatrg.— scattering
soln.— solution
sp.— space, spacing
str.— structure, structural
suscept.— susceptibility
synth.— synthesis, synthetic
syst.— system, systematic
temp.— temperature
tetrag.— tetragonal
therm.— thermal
trans.— transition, transitional
tricl.— triclinic
trig.— trigonal
u. c.— unit cell

Abbreviations of German Words

Beob.— Beobachtung
Best.— Bestimmung
Darst.— Darstellung
d.— der, die, das usw. (Artikel)
Diagr.— Diagramme
e.— ein, eine usw. (Artikel)
Eig.— Eigenschaft
Einfl.— Einfluss
El.— Elektron
Geh. — Gehalt
Git.— Gitter
Herst — Herstellung
Koef.— Koeffizient
Konst.— Konstante
krist.— kristallinisch
Kr.-str.— Kristallstruktur
met.— metallisch
Meth.— Methode
Mikr.— Mikroskop
mikr.— mikroskopisch
Str.— Struktur
Syst.— System
Temp.— Temperatur
u.— und
Unters.— Untersuchung
v.— von, vom
Verb — Verbindung
Verf.— Verfahren

LIST OF 1956 PUBLICATIONS

A. METALS

1. Abrahamson E. P., Grant N. J., Beta-Cr. J. Metals, 8, 975.
2. Agreev, N. V., Met. compds, Izvest. Sektora Fiz.-Khim. Analiza, 27, 75.
3. Ainsworth L. Single cr. Bi-telluride. Proc. Phys. Soc., London, 69, 606.
4. Aliev N. A., Applicability of the Wiedmann-Franz law to Cu–Al alloys, Tr. In-ta Fiz. i Mat. Akad. Nauk Azerb.SSR, 8, 101.
5. Anantharaman T. R., Christian J. W. Measrt. of growth and deformn. faulting in hex. Co. Acta cryst., 9, 479.
6. Anaev B. A. Carbide phases formed in annealing of tempered steel, Doklady Akad. Nauk SSSR, 107, 685.
7. Araki T. Heat-treatment of Ti–Ni alloys. J. Mech. Lab., Tokyo, 2, 28.
8. Ariya S. M., Zaslavskii A. I., and Matveeva I. I. Chem. of compds. of variable compn. IV. Syst. Ta–Se. Zh. Obshch. Khim. 26, 2373.
9. Arkharov V. I. and Bogoslovskii V. N. Str. of magnetite in reaction diffusion layers in reduction of hematite, Fiz. Met. i Metalloved. 3, 254.
10. Arkharov V. I. and Borisov B. S. Effect of alloying elements on heat resistance of alloys and bond strengths in oxide phase lats. in scale. I. Influence of Cr on bond strengths in hematite, Fiz. Met. i Metalloved. 3, 471.
11. Arkharov V. I. and Borisov B. S. Str. of hematite in outer layer of iron scale, Fiz. Met. i Metalloved. 3, 460.
12. Arkharov V. I. and Kichigina Z. P. Texture in iron scale. VII. Nature of texture in intmd. temp. region. VIII. Investn of "intmd." oxidation stage of alloyed iron, Fiz. Met. i Metalloved. 3, 269; 468.
13. Arkharov V. I. and Noskova N. I. Effect of admixtures of Ag or Zn in Al on diffusion rate of Cu, Fiz. Met. i Metalloved. 2, 472.
14. Arnold S. M. of. Tech. Proc. Am. Electroplaters Soc., 43rd. Ann. Con., Wash., 26.
15. Authier A., Warren B. E. Variation of extinction with X-ray wavelength. J. Appl. Phys., 27, 1382.
16. Avanesyan T. G. E. density and cohesive energy of Al. Sbornik Nauchn. Tr. Erevansk. Politekhn. In-Ta, 10, 9.
17. Ayphassorho C., Viallard R. Etude radiocrist. de l'hydruration du Ce. Compt. rend., 242, 630.
18. Averbach B. L., Bever M. B., Comerford M. F., and Leach J. S. Ll. X-ray a. calorimetric investns. of cold working a. annealing of Au – Ag alloy. Acta Met., 4, 477.
19. Bagaryatskii Yu. A. and Typakin Yu. D. Str. peculiarities of Ni–Al alloys during decomposition of a supersaturated solid soln. of Al in Ni, Doklady Akad. Nauk SSSR, 108, 451.
20. Baenziger, N. C., Conant J. W. Cr. str. of $SrZn_5$ a. $BaZn_5$. Acta cryst, 9, 361.
21. Baer G. Uber e. Ordnungsphase im Syst. Ni–Cr. Naturwissenschaften, 43, 298.
22. Barrett C. S. Cr. strs. of Li–Mg alloys at low temps. Acta Met., 4, 528.
23. Barrett C. S. X-ray study of alkali mets. at low temps. Acta cryst., 9, 671.
24. Bas E. B. Uber el-emissionsmikr. Beobb. d. lamellaren Ausscheid. d. Kohlenstoffs in Mo. Optik, 13, 381.
25. Bassi G., Strom B. Martensitumwandl. im Syst. Cu–Zn. Z. Metallk., 47, 16.
26. Bassi G. Einige rontg. Beobb. bei. d. Aushart. e. Cu–Be-Legier. Z. Metallk., 47, 417.
27. Beattie H. J. jr. Ver Snyder F. L. New complex phase in high-temp. alloy. Nature, 178, 208.
28. Beck P. A., Darby J. B., and Arora O. P. Occurrence of Cs Cl type ord. strs. in certain binary systs of trans. elements. J. Metals, 8, 148.
29. Beckman G., Kiessling R. Therm. expan. coefs. for U-boride a β-U-silicide. Nature, 178, 1341.
30. Bergman, G., and Waugh, J. L. T., Cr. tr. of intermet. compd. $Mg_6Si_7Cu_{16}$. Acta cryst., 9, 214.
31. Berlaga R. Ya., Rudenok M. N., and Strakhov L. P. Surface str. of thin PbS layers made by vacuum evaporation, Zhur. Tekhn. Fiz. 26, 3.
32. Bernard R. Examen au micr. e. de la str. des alliages durs. Bull. microscop. appl., 6, 50.
33. Biedermann E., Kneller E. Gefuge u. magnet. Eigg. v. Dauermagnetlegierr. wahrend. d. isothermen Ausscheidungshart. I. Teilchenwachstum, krit. Teilchengrobe u. Koerzitivkraft. II. Vorgang d. Entmisch. u. Deut. d. magnet. Eigg Z. Metallk., 47, 289, 760.
34. Binder I. New borides of Yt. Powder Met. Bull. 7, 74.
35. Binnie W. P. Str. crystallogr. of In-bismuthide. Acta cryst., 9, 686.
36. Birtalan J., Bloom R. A. Occurrence Chi-phase in 16 Pct Cr – 15 Pct Ni – 7 Pct Mn – 6 Pct Mo alloy. J. Metals, 8, 210.

37. Black P. J. Str. relnshs. between intermet. compds. Acta Met., 4, 172.
38. Blackman M. Les stades initiaux de la formn.des couches met. minces obtenues par la vaporisation therm. sur une surface cr. J. phys. radium, 17, 176.
39. Blade J. C., Ellwood E. C. Constn. of Sn – In alloys. in the range 0–30% In. J. Inst. Met., 85, 30. (Discussion, Ibid, 535).
40. Blaise R. Potentiels de dissolution et diagrames de Debye – Scherrer des alliages Pb – Sb. Bull. soc. chim. France, 10, 1335.
41. Blin J. Diffusion centrale des r. X par les mét Publ. sci. et tech. ministère air. (France), 311.
42. Boettcher A., Thun R. Phasenumwandll. im Syst. Cu – Sb. Z. anorg. Chem., 283, 26.
43. Boettcher A., Thun R. Unterss. am Zweistoffsyst. Cu – Sb mit kinemat. El.-beug. Radex Rdsch., 4, 258.
44. Bokii G. B. Theory of daltonides and berthollides in the light of the at. theory of cr. str., Zhur. Neorg. Khim. 1, 1150.
45. Bokii G. B. Theory of daltonides and berthollides, Zhur. Neorg. Khim. 1, 1599.
46. Borie B. Independent measrt.of at. scatrg. f. a. Debye f. Acta cryst., 9, 617.
47. Borie B., Warren B. E. X-ray study of change in Cu_3Au near 600°C. J. Appl. Phys 27, 1562.
48. Boyko E. R. Str. of δ -phase in U-Zr syst. Programm. a. Abstracts, 14th Pittsburgh Diffrn. Conf., p. 47.
49. Bown M. G. Str. of rhomboh. T (NiCuAl). Acta cryst., 9, 70.
50. Bown M. G., Brown P. J. Strs. of FeCuAl a. T(CoCuAl). Acta cryst., 9, 911.
51. Bradshaw F. J., Pearson S. Quenching vacancies in Pt. Phil. Mag., 1, 812.
52. Brewer L., Krikorian O. Reactions of refractory silicides with C. a. N. J. Electrochem. Soc., 103, 38.
53. Bridge J. R., Schwartz C. M., Voughan D. A. X-ray diffrn. detn. of coef. of expan. of α-U. J. Metals, 8, 1282.
54. Bridgman P. W. High pres. polymorphism of Fe. J. Appl. Phys., 27, 659.
55. Brotzen F. R., Harmon E. L., and Troiano A. R. Nature a. decompn. kinetics of α in Ti –V-alloys. Trans. Am. Soc. Metals, 48, 774.
56. Buinov N. N., and Podrezov L. I. X-ray diffrn.and e.micr. investn.of aging of Al – Zn alloy, Izvest. Akad. Nauk SSSR, Ser. Fiz. 20, 611.
57. Buinov N. N. and Shashkov O. D. Investn.of str. of deformed Al – Cu alloy in e.micr., Fiz. Met. i Metalloved. 2, 484.
58. Buinov N. N. and Shashkov O. D. E. micr. investn.of Al – Cu after high-temp. aging and annealing, Fiz. Met. i Metalloved. 3, 83.
59. Bulow H., Buckel W. El. beug.–aufnahmen v. dunnen Metallschichten bei tiefen Tempp. Z. Phys., 145,141.
60. Burgers W. G., Kooy C. L. D., and Tiedema T. J. Therm. diffuse scatrg. by Pb single crs. Konikl Ned. Akad. Wetenschap. Proc., Ser. B., 59, 195.
61. Bur'yanova E. Z. Ferroselite, Zap. Vsesoyuz. Min. O-va, 85, 286.
62. Buschert R., Geib J. G., and Lark-Horovitz K. Str. of liquid InSb. Bull. Am. Phys. Soc. 1, 111.
63. Carlson O. N., Dickinson J. M., Lunt H. E., and Wilhelm H. A. Th–Nb a. Th–Ti alloy systs. J. Metals, 8, 132.
64. Carlson O. N., Armstrong P. E., and Wilhelm H. A. Zr–Ge alloy syst. Trans. Am. Soc. Metals, 48, 843.
65. Carpenter J. H., and Searcy A. W. Prepn., identfn. a. chem. props. of Nb–germanides. J. Am. Chem. Soc., 78, 2079.
66. Carter R. S., Hughes D. J., and Palevsky H. Measrt. of lat. vibration spectrum of V by scatrg. of cold neutrons. Bull. Am. Phys. Soc., 1, 204.
67. Catterall J. A., Grogan J. D., and Pleasance R. J. Syst. U-Pd. J. Inst. Met., 85, 63.
68. Cech R. E. Evidence for solidification of metastable phase in Fe–Ni alloys. J. Metals, 8, 585.
69. Chang R. On radn. induced irreversible changes in mets. Bull. Am. Phys. Soc. 1, 129.
70. Chatterjee G. P. X-ray diffrn. studies of α-brass on progressive dezincification in vacuum. Proc. Indian Sci. Congr., 43, 464.
71. Cherkashin E. E., Gladyshevskii E. I., and Teslyuk M. Yu. Investn. of syst. Cu–Mg–Sn in the $Cu–Cu_2Mg–$ –CuMgSn region, Izvest. Sekt. Fiz-Khim. Analiza, 27, 212.
72. Chiotti P., Tracy G. A., and Wilhelm H. A. Mn–U syst. J. Metals, 8, 562.
73. Chipman D. R. X-ray study of local at. arrgt. in partially ord. Cu_3Au. J. Appl Phys., 27, 739.
74. Christian J. W., and Jensen R. V. Dislocn. etch.a. pits on Si. Bull. Am. Phys. Soc. 1, 140.
75. Christian J. W., and Spreadborough J. Stacking faults in cold-worked Co–Ni alloys. Phil. Mag., 1, 1069.
76. Clark D., and Terry J. C. Superlat. formn. in α-Ti–Al solid solns. Bull. Inst. Metals, 3, 116.

77. Coffinberry A. S., Ellinger F. H. Intermet. compds. of Pu. Peaceful uses of at. energy. Proc. of the International Conference in Geneva, Aug. 1955. vol. 9. Reactor technology a. chem. processing. N.Y., U. N. O., 138.
78. Coffinberry A. S., and Waldron M. B. Review of phys. metallurgy of Pu. Progress in Nucl. Energy, Series V. Metallurgy a.Fuels, 1, 354.
79. Cole H., Chambers F. W., and Dunn H. M. Lat. parts. of Zn_3As_2. Acta cryst., 9, 685.
80. Coles B. R. Lat. pars. of Ni–Cu a. Pd–Ag alloys. J. Inst. Met., 84, 346.
81. Cotter P. G., Kohn J. A., and Potter R. A. Phys. a. X-ray study of disilicides of Ti, Zr. a. Hf. J. Am. Ceram. Soc., 39, 11.
82. Couling S. L., and Roberts C. S. New twinning systs. in Mg. Acta cryst., 9, 972.
83. Cruickshank D. W. J., Mendoza E., and Robertson J. H. Summarized proceedings of conf. on low temp. crystallogr.–Oxford, April, 1956. Brit. J. Appl. Phys., 7, 425.
84. Dauben C. H., Templeton, D. H., and Myers C. E. Cr. str. of Cr_5Si_3. J. Phys. Chem., 60, 443.
85. Dehlinger U., and Peleiderer H. Str.-bezieh. d. $CuAl_2$ u. d. Ausscheidungsgit. v. Al–Cu-Legierr. Z. Metallk., 47, 229.
86. Dejace J. Radiocrystallogr. study of deformn.a. polygonization of Fe single crs. Rev. univ. min., 12, 60.
87. Dekhtyar I. Ya. Diffusion pars. and x-ray absorption spectra of atoms in alloys, Doklady Akad. Nauk SSSR, 108, 1069.
88. Denney J. M. Precipitate kinetics a. str. in Cu- 2.4%. Fe alloy. Acta Met., 4, 586.
89. Diament R. Construction et mise au point d'une chambre de precision pour diagrammes de r. X. à haute temp. Métaux (Corrosion-Inds.), 31, 167.
90. Dickins G. J. Accuracy of at. coords. derived from Fourier synths. Acta cryst., 9, 201.
91. Dickins G. J., Douglas A. M. B., and Taylor W. H. Cr. str. of $CoCr_8$ phase. Acta cryst., 9, 297.
92. Domagala R. F., McPherson D. J., Hansen M. Syst. Zr–N. J. Metals, 8, 98.
93. Donnay G., Kracek F. C., and Rowland W. R., jr. Chem. formula of empressite. Am. Mineralogist, 41, 722.
94. Drechsler M. Mess. v. Kristallstufen, Gitterkonst. u. Atomradius mit Feldemissions-Mikroskopen. Z. phys. Chem., 6, 272.
95. Drechsler M. Schraubenversetz. u. Feldverdampf. v. Metall–Einkristallspitzen in Feldemissionsmikroskop. Z. Metallk., 47, 305.
96. Duncan B. J., Sworn L. Temp. behaviour of ferrimagn. resonance in ferrites located in wave guide. J. Appl. Phys., 27, 209.
97. Dunlap W. C., Jr., Marinace J. C., and Puth R. P. Props. of vapor-deposited Ge-layers. Bull. Am. Phys. Soc. 1, 294.
98. Dwight A. E. Allotropic transformns. in Ti, Zr, a. U-alloys. J. Metals, 8, 122.
99. Edwards A. R., and Johnstone S. T. M. Constitutional diagram of syst. Cr–Be from 0 to 70 at. per cent Be. J. Inst. Met., 84, 313.
100. Elagina E. I. and Abrikosov N. Kh. Investn of PbTe–PbSe syst. Doklady Akad. Nauk SSSR, 111, 353.
101. Ellinger F. H. Cr. str. of δ', Pu a. therm. expan. chars. of δ-, δ'- a. ε-Pu. J. Metals, 8, 1256.
102. Elpat'evskaya O. D., Konikova R. A., Regel' A. R. and Yavorskii I. V. Stability of the cr. str. in the HgSe–HgTe syst. of solid solns. Zhur. Tekhn. Fiz. 26, 2154.
103. Elyutin V. P. and Funke V. F. Some data on the equilibrium diagram of the Cr–Nb syst. Izvest. Akad. Nauk SSSR, Otdel. Tekhn. Nauk, 3, 68.
104. Enge E. and Margolin H. Re-examn. of Ti–Fe a. Ti–Fe–O phase relns. J. Metls, 8, 572.
105. Épel'baum V. A., Gurevich M. A., and Ormont B. F. Phase compn.of the B–C syst. Zhur. Neorg. Khim. 1, 2149.
106. Eremenko V. I. Interaction of Ti carbide with mets. of the Fe family, Zhur. Neorg. Khim. 1, 2131.
107. Farrar P. A., Stone L. P., and Margolin H. Ti–Mo–O syst. J. Metals, 8, 595.
108. Feder R., Nowick A. S. and Rosenblatt D. B. Effect of heat treatment a. n. irradn. on lat. par. of α-brass. Bull. Am. Phys. Soc., 1, 129.
109. Ferro R. Cr. strs. of Th-antimonides. Acta cryst., 9, 817.
110. Figgins B. F., Jones G. O. and Riley D. B. Therm. expan. of Al at low temps. as measured by X-ray diffrn. method. Phil. Mag., 1, 747.
111. Finlayson D. M., Greig D., Llewellyn J. P., and Smith T. Some electr. chars. of single cr. Fe-monotelluride. Proc. Phys. Soc. Long., 69, 860.

112. Flanagan W. F. and Averbach B. L. Hall effect in solid solns. Phys. Rev., 101, 1441.
113. Florio J. V., Baenziger N. C. and Rundle R. E. Compds. of Th with trans. mets. II Systs. with Fe, Co a. Ni. Acta cryst., 9, 367.
114. Franks J. Met. whiskers. Nature, 177, 984.
115. Frazer B. C. N. diffrn. study of magn. str. of Fe_4N. Progam a. Abstracts, 14th Pittsburgh Diffrn. Conf., p. 54.
116. Fridlyander I. N., Konstantinov V. A., and Zaitseva I. I. Investn. of cr. lat. pars. of Al–Mn alloys after different kinds of heat treatment, Zhur. Fiz. Khim. 30, 1623.
117. Friedmann H. D. charakterist. Energieverluste mittelschneller Elektronen in Se-Schichten verschiedener Str. Z. Naturf., A, 11, 373.
118. Fujita F. E., Watanabe D., Yamamoto M., and Ogawa S. Study of plastic deformn. in Al crs. by e. diffrn. a. e. micr. J. Phys. Soc. Japan, 11, 502.
119. Fukano J., and Ogawa S. Study on precipitation phenomena during ageing of Al–Ag alloy in thin evapd. films. Acta cryst., 9, 971.
120. Garber R. I., Gindin I. A., Kogan V. S., and Lazarev B. G. X-ray investn. of plasticity of Be single crs. Izvest. Akad. Nauk SSSR, Ser. Fiz., 20, 639.
121. Garrod R. J. Anomalous interplanar sps. in evapd. deposits of face-centered cub. mets. Proc. Phys. Soc. Lond., 69 B, 260.
122. Geller S. Set of effective coordn. number (12) radii for β-W str. elements. Acta cryst., 9, 885.
123. Gersch H. A., Shull C. G., and Wilkinson M. K. Critical magn. scatrg. of neutrons by Fe. Phys. Rev., 103, 525.
124. Gertsriken S. D., Dekhtyar I. Ya., Diffusion of Co in Co–Al alloys, Fiz. Met. i Metalloved. 3, 242.
125. Gilde D. Kr-str. d. KPb_2. Z. anorg. Chem., 284, 142.
126. Gingrich N. S., and Heaton L. R. Diffrn. of ns. by Cs a. Rb in liquid state. Program a. Abstracts, 14th Pittsburgh Diffrn. Conf., p. 57.
127. Gintsburg Ya. S., Margolin Yu. M., and Sachavskii A. F., Phys. methods for studying slow trans. in high-Al-loy steel, Zavodskaya Lab. 31, 1046.
128. Gladyshevskii E. I. and Cherkashin E. E., Solid solns. based on met compds. Zhur. Neorg. Khim. 1, 1394.
129. Gladyshevskii, I. I. and Kripyakevich, P. I., Solubility of Zn in met. compds. Cu_2Mg and Cu_2Cd, Izvest. Sekt. Fiz.-Khim. Analiza, 27, 209.
130. Gladyshevskii E. I., Kripyakevich P. I., and Kuz'ma Yu. B., Cryst. str. of ternary compds in the systs. Mn – –Ni–Si, Dopovidi Akad. Nauk Ukr SSR 1, 67 (Ukr.; Russ. summary).
131. Gladyshevskii E. I., Kripyakevich P. I., and Kuz'ma Yu. B. X-ray investn. of some alloys of trans. mets. with Si, Fiz. Met. i Metalloved. 2, 454.
132. Glagoleva V. P. and Zhdanov G. S., Str. of superconductors. I. X-ray detn of the str., of α-Bi_4Rh, Zhur. Éksp. i Teor. Fiz. 30, 248.
133. Glazov V. M., Mal'tsev M. V., and Chistyakov Yu. D. Investn. of Al–Ta phase diagram, Izvest. Akad. Nauk SSSR, Otdel. Tekhn, Nauk, 4, 131.
134. Golovchiner Ya. M., and Landa R. A. Investn. of fine cr. str. of γ-phase stabilized by reverse martensite trans. Doklady Akad. Nauk SSSR, 107, 67.
135. Golubtsova R. B. and Mashkovich L. A. Investn. of met. compds. in Ni alloys containing Al, Doklady Akad. Nauk SSSR, 111, 824.
136. Gonser U., Okkerse B. X-ray superlat. lines a. heteropolarity of InSb. Bull. Am. Phys. Soc., 1, 299.
137. Goon E. J., Mason J. T., and Gibb T. R. P. X-ray powd. diffrn. study of UH_3, UH_{11} a. UBe_{13} at elevated temps. a Hpress. Program a. Abstracts, 14th Pittsburgh Diffrn. Conf., p. 42.
138. Goryunova N. A., and Grigor'eva V. S., Ga arsenoselenides, Zhur. Tekhn. Fiz. 26, 10, 2157.
139. Goryunova N. A., Kolomiets B. T., and Mal'kova A. A., Props. and str. of ternary semiconductor systs. Zhur. Tekhn. Fiz. 26, 1625.
140. Göttsche H. Fehlordnungserscheinn. in El.-beug-diagrr. Zur. Keut. d. Kontinuierlichen Streifen u. d. Zwillingsrefexe. Acta cryst., 9, 179.
141. Graf R. Hardening phenomena in Al–4% Cu alloys. Publ. sci. et tech. ministère air (France), 315, 61
142. Graf R. Nouvelles obsns. aux r. X. sur les phénomènes de precipitation dans l'alliage Al–Zn–Mg à 7% de Zn et 3% de Mg. Compt. rend., 242, 2834.
143. Graf P., Cunningham B. B., Dauben C. H., Walimann J. C., Templeteon D. H., and Ruben H. Cr. str. a. magn. suscept. of Am met. J. Am. Chem. Soc., 78, 2340.

144. Greenfield P., Beck P. A. Intmd. phases in binary systs. of certain trans. elements. J. Metals, 8, 265.
145. Guentert O. X-ray measrts.of cold work in β-brass. Bull. Am-Phys. Soc., 1, 138.
146. Gurevich M. A. and Ormont B. F. Precision detn.of identity periods of polycr. with backrefl. exposure camera of high resolving power, Zhur. Tekhn. Fig. 26, 1106.
147. Haraldsen H., Gronvold F., and Hurlen T. X-ray a . magn. investn. of syst. Co–Te. Z. anorg. Chem., 283, 143.
148. Hardy H. K., and Silcock J. M. Phase sections at 500° a. 350°C of Al-rich Al–Cu–Li alloys. J. Inst. Met., 84, 423.
149. Hasovitsh D., Kaufman M., and Rosenthal D. Geiger-counter detns. of X-ray lat. strains in plastically deformed Al alloy. Acta Met., 4, 218.
150. Hashimoto K., and Hirakawa K. Electr. props. of Sn-telluride, Sn Te. J. Phys. Soc. Japan, 11, 716.
151. Hauk V., and Hummel C. Zur Ermittl. v. Teilchengröbe u. Gitterverzerr. aus Röntgeninterferenzen. Z. Metallk., 47, 254.
152. Hauser F. E., Landon P. R., and Dorn J. E. Deformn. a. fracture mechanisms of polycr. Mn. at low temps. Trans. Am. Soc. Metals, 48, 986.
153. Hellner E. Flusspat-Misch-Typen (mit e. Strukturbest. d. $RhSn_2$ u. $PdSn_2$). Z. Krist., 107, 99.
154. Hendus H., Knödler H. Überstr. d. γ-Hochtemp.-phase im Syst. Cu–Zn. Acta cryst., 9, 1036.
155. Henry W. G., and Rogers J. L. agn. suscepts. of some diamagn. alloys: primary solid solns. of Zn, Ga, Ge a. As in Cu. Phil. Mag., 1, 237.
156. Herbstein F. H., and Averbach B. L. On ord. str. proposed for Li_3Mg_5. Acta cryst., 9, 91.
157. Herbstein F. H., and Averbach B. L. Str. of Li–Mg solid solns. I. Measrts.on Bragg refls. II. Measrts. of diffuse X-ray scatrg. Acta Met., 4, 407, 414.
158. Herbstein F. H., Borie B. S. jr., and Averbach B. L. Local at. displacements in solid solns. Acta cryst., 9, 466.
159. Hill R. B., and Axon H. J. Lat. sps. of Ag-rich solid soln. containing Mn a. Sb. J. Inst. Met., 85, 109 (discussion, Ibid, 408).
160. Hillert M., Averbach B. L., and Cohen M. Thermodynamic props. of solid Al–Ag alloys. Acta Met., 4, 31.
161. Himmel L., and Jack R. H. Discussion on "Contribution to the Bi–Mn systo." J. Metals, 8, 1406.
162. Hurabayashi M., and Ogawa S. X-ray study of ordg. processes in CuAu single crs. J. Phys. Soc. Japan, 11, 907.
163. Hirone T., and Chiba S. Magn. props. of $FeSe_x$ with NiAs-str. J. Phys. Soc. Japan, 11, 666.
164. Hirone T., Maeda S., Tsubokawa J., and Tsuya N. Magn. props. of syst. MnSb–CrSb. J. Phys. Soc. Japan, 11, 1083.
165. Hirsch P. B., Horne R. W., and Whelan M. J. Direct obsns of arrgt. a. motion of dislocns.in Al. Phil. Mag. 1, 677.
166. Hirst R. G., King A. J., and Kauda F. A. Ba–Sr equilibrium syst. J. Phys. Chem., 60, 302.
167. Hoerni J. A. Multiple elastic-scatrg. in e. diffrn. by [I] Molecules; [II] Crs. Phys. Rev., 102, 1530, 1534.
168. Holden A. N., and Symour W. E. Intmd. phase in U-Zr syst. J. Metals, 8, 1312.
169. Hyman R. A. Epitaxial growth of crs. of hex. Se. Proc. Phys. Soc., B69, 687.
170. Hyman R. A. Electr. conductivity of hex. Se. Proc. Phys. Soc., B69, 743.
171. Hyman R. A. Bending of single crs. of Se. Proc. Phys. Soc. B69, 771.
172. Iida S. Phase diagram of Fe–Co–O syst. I Exptl. study. J. Phys. Soc. Japan, 11, 846.
173. Il'ina V. A. and Kristskaya V. K. Detn of static deformation of cr. lat. with x-ray radns.of different wave lengths, Doklady Akad. Nauk SSSR, 110, 765.
174. Iveronova V. I. and Zvyagina A. P. Intensity of x-ray scatrg.by solid solns. Izvest. Akad. Nauk SSSR, Ser. Fiz., 20, 729.
175. Jack K. H., and Wachtel M. M. Str. char. of Cs-antimonide: temp. fs. in cub. crs. Nature 178, 1408.
176. Jaffe L. D. Metallographic identfn. a. cr. symmetry of ti-hydride. J. Metals, 8, 861.
177. Jagodzinski H., and Hellner E. D. eindimensionala Phasenumwandl. d. $RhSn_2$. Z. Krist., 107, 124.
178. James W. J. Lat. par. a. coef. of therm. expan. of Th. Acta cryst., 9, 376.
179. Jaoul B., Lacombe P. Appearance of Laue spots as function of geometry of deformn. of Al single crs. Compt. rend., 242, 1994; 2164
180. Jaumot F. E., and Savatzky A. I. Isotherm anneal study of quenched a. cold-worked. Cu–Pd–alloys. II. Order-disorder a. cold-work phenomena in Cu–Pd-alloys. Acta Met., 4, 118; 127.

181. Jones W. R. D., and Hogg G. V. Stability of mech. props. of β-phase Mg–Li-alloys. J. Inst. Met., 85, 255.
182. Jordan C. B., Duwez P. Approximate phase relnshs. in Ti–V–Al-syst. at 1800 a. at 1400° F. Trans. Am. Soc. Metals, 48, 783.
183. Kahn A. H. On X-ray obsn. of vacancy-interstitital pairs in irradiated Cu. Bull. Am. Phys. Soc., 1, 129.
184. Kapustinskii A. F., Radii of eight-e. cations, Zhur. Neorg. Khim. 1, 82.
185. Kapustinskii A. F., Dims. of atoms and ions of transuranium elements in crs. Kristallografiya, 1, 382.
186. Kasper J. S. At a. magn. ordg. in trans.-met. strs. Theory of alloy Phases. Am. Soc. Met., 264.
187. Kasper, J. S., and Roberts B. W. Antiferromagn. str. of α-Mn a. magn. str. study of β-Mn. Phys. Rev., 101, 537.
188. Kasper J. S., and Waterstrat R. M. Ordg. of atoms in δ-phase. Acta cryst., 9, 289.
189. Kehoe R. B., Newman R. C., and Pashley D. W. Automation recording of e. diffrn. pats. to study of evapd. Cu layers. Brit. J. Appl. Phys., 7, 29.
190. Keith H. D. X-ray study in high vacuum of str. of evapd. Cu-films. Proc. Phys. Soc., B69, 180.
191. Kelly A. Mechanism of work softening in Al. Phil. Mag., 1, 835.
192. Kerr J. S., and Wilman H. Str. a. growth of oxide layers formed on Be. J. Inst. Met., 89, 379.
193. Khmylev B. V. Phase diagram of the syst. Fe–Ni–S, Tsvetnye Metally, 3, 89.
194. Kidin I. N., Mechanism of austenite formn. in rapid heating, Doklady Akad. Nauk SSSR, 106 1009.
195. Kieffer R., Benesovsky F., and Schmid H. Beitrag zum Aufbau d. Syst. V–Si u. Nb–Si. Z. Metallk., 47, 247.
196. Kimoto K. E. Diffrn. study of plastic deformn. of Al single crs. J. Phys. Soc. Japan, 11, 487.
197. Klemm W. Zur Frage d. Übergangs v. salzart. Verbb. zu intermet. Phase. "3eme Reunion internacion. sobre reactividad de los solidos. Resumenes." Madrid; 2-7, April 1956, Madrid. C. Bermejo, 1956, 18.
198. Knop O., and Haraldsen H. Note on syst. W–Te. Can. J. Chem., 34, 1142.
199. Koch W., Ilschner-Gensch C. Interme+. Phase mit α-Mn-Str. in e austenit. CrNi–Mo-Stahl mit erhöhtem Ti-Geh. Arch. Eisenhüttenw., 27, 453.
200. Kohara S., and Kuczynski G. C. Internal stresses during ordg. Acta Met., 4, 221.
201. Kohn J. A., Cotter P. G., and Potter R. A. Synth. of Al-nitride monocrs. Am. Minerologist. 41, 355.
202. Kohn A., Plateau J., and Pomey G. Sur les modes de croissance de la cementite des constituants de transformn. isotherme observes dans un acier hypereutectoide à 12% Mn. Compt. rend., 242, 256.
203. Kornilov I. I., Ternary and more complex solid solns. of met. compds. Doklady Akad. Nauk SSSR, 106, 476.
204. Kornilov I. I. and Boriskina N. G., Phase diagram of the Ti–Fe syst. Doklady Akad. Nauk SSSR, 108, 1083.
205. Kornilov I. I., Pylaeva E. I., and Volkova M. A., Phase diagram of binary syst. Ti–Al, Izvest. Akad. Nauk SSR, Otdel. Khim. Nauk 7, 771.
206. Korst W. L., and Warf J. C. Cr. str. of deuterides of Yb a. Eu. Acta cryst., 9, 452.
207. Kos'ko Z. K. Dim. changes of carbide crs. in annealing of tempered chrome steel, Doklady Akad. Nauk SSSR, 108, 1072.
208. Köster W., Schmid H., and Dahesh E. Über d. Aufbau u. d. Aushärt. v. Co–Ni–Zn-Letgierr. Z. Metallk., 47, 165.
209. Krebs H., Holz W., Lippert W., and Worms K. H. Neuere Ergebnisse zur Allotropie d As. Österr. Chemiker-Ztg., 57, 137.
210. Krebs H., Müller K. H., and Zurn G. Über kristallisierte Metallpolyphosphide. I. Darst. u. Str. d. CdP_4. Z. anorg. Chem., 285, 15.
211. Krebs H., and Schultze-Gebhardt F. Allotropie d. As. Z. anorg. Chem., 283, 263.
212. Krivoglaz M. A., Theory of diffuse x-ray scatrg. by solid solns. Zhur. Éksp. i Teoret. Fiz. 31, 625.
213. Kudielka H., Nowotny H. Disilizid-syst. Mh. Chem., 87, 471.
214. Kiessmann A., and Raub E. Über ferro- u. antiferromagnet. Eigg. im Syst. Au–Mn. Z. Metallk., 47, 9.
215. Kuo K. New intmd. phase in burnt W-steels. J. Metals, 8, 97.
216. Kuznetsov V. G., X-ray diffrn. analysis at high and low temps. Zhur. Neorg. Khim. 1, 1458.
217. Kurdyumov G. V., Kaminskii É. Z., and Rozenberg V. M., Influence of the inner str. of austenite grain on high-temp. strength, Doklady Akad. Nauk SSSR, 109, 85.
218. Kurdyumov G. V. and Perkas M. D., Tempering of unalloyed carbon-free iron, Doklady Akad. Nauk SSSR, 111, 818.
219. Kurov G. A. and Pinsker Z. G., Nature of amorphous Sb, Kristallografiya, 1, 407.
220. Kushta G. P. and Rybailo O. I., Str. state of the lat. of naturally aged supersaturated solid soln. based on Al. I. Investn. of initial aging stage of Al alloy by harmonic anal. of x-ray interference intensity distribn. curves, Nauchn. Ezhegodnik, Chernovits. Un-t, 1, 272.

221. Kuz'menko P. P., Trans. in No. 1 heat-resisting alloy of Fe–Cr–Al syst. Nauch. Zap. Kievsk. Un-t. 15, 135 (Ukr.).
222. Kuz'menko P. P., Reln. between maximum short-range order par. and concentration for typical met. strs. Naukovi Povidomleniya Kiivs'k. Un-tu, 1, 32 (Ukr.).
223. Ladage A. E. diffrn. from electrodeposited surfaces after cathodic spluttering. Z. Phys., 144, 354.
224. Lafourcade L., and Larroque P. Emploi de la micr. é. et de la diffrn. des électrons dans l'etude de la str. des films met. minces. "Les techniques recentes en micr. é. et corpusculaire" Paris, C. N. R. S., 271.
225. Lambot H. Study of geometric imperfections in met. single crs. Rev. univ. min., 12, 55.
226. Landa R. A., Detn. of residual austenite in steels by x-ray str. anal. Zavodskaya Lab. 31, 83.
227. Langeron G. P., and Lehr P. Sur la prépn. de gros cr. de Zr et la dém. de l'orientation des précipités d'hygrure de Zr. Compt. rend., 243, 151.
228. Lashko O. S. Str. of liquid K, Ukr. Fiz. Zhur. 1, 403 (Ukr.; Russ. summary).
229. Lawless K. R., and Gwathmey A. T. Str. of oxide films on different faces of single cr. of Cu. Acta Met., 4, 153.
230. Lee H. T., and Breck R. M. Deformn. of Be single crs. at 25 to 500°C. Trans. Am. Soc. Metals, 48, 1003.
231. Leont'ev B. A. and Palatnik L. S., Mechanism of intmd. trans. of austenite, Izvest. Akad. Nauk SSSR, Otdel. Tkehn. Nauk, 10, 28.
232. Levisnon D. W., and McPheson D. J. Phas. reens. in Mn–Li–Al alloys. Trans. Am. Soc. Metals, 48, 689.
233. Libowitz G. G., and Gibb T. R. P., Jr. Ionic character of trans. met. hybrides. J. Phys. Chem., 60, 510.
234. Liu Y. C. Martensitic transformations in binary Ti-alloys. J. Metals, 8, 1036.
235. Linchevskii B. V., and Samarin A. M., Oxidation of Mn dissolved in liquid iron, Doklady Akad. Nauk SSSR, 110, 209.
236. Livshits B. G., Molotilov B. V., Myuller N. N., and Savost'yanova N. O., Mechanism of ordg. of NisMn alloy with various additions of Mo, Fiz. Met. i Metalloved. 3, 477.
237. Logan H. L. Reensh. between cr. orientation a. stress-corrosion cracking in α- a. β-brasses. J. Res. Nat. Bur. Stand., 56, 159.
238. Lysak L. N. Anal. of stresses of 2nd kind in α-phase of annealed and quenched steel, Izvest. Akad. Nauk SSSR, Ser. Fiz. 20, 624.
239. Macherauch E. Über d. Einfl. v. Schwellasten auf d. röntg. bestimmte Biegeflie β-grenze. Z. Metallk., 47, 312.
240. McDonald B. J., Fardon J. B. Prepn. a. props. of some Pu-hydride. J. Chem. Soc. 781.
241. McQuillan M. K. Constn. of Ti–Sn syst. in region 0–25 at. per cent Sn. J. Inst Met., 84, 307 (Discussion 532).
242. Makarov E. S., Modern cr.-chem. aspects of N. S. Kurnakov's theory of daltonides and berthollides, Zhur. Neorg. Khim. 1, 2032.
243. Makarov E. S. and Gudkov L. S. X-ray diffrn. investn. of Th–Zn alloys, Kristallografiya, 1, 650.
244. Makarov E. S. and Ledvik V. A., Cr. str. of UGa and UGa_2, Kristallografiya, 1, 644.
245. Makarov E. S. and Vinogradov S. I., Cr. str. of Th_2Zn_{17} and U_2Zn_{17}, Kristallografiya, 1, 634.
246. Maksikyuk P. A. and Zhmudskii A. Z. X-ray diffrn. investn. of the effect of Ni on decomposition of Al–Cu alloys, Naukovi Povidomleniya, Kiivs'k. Un-tu, 1, 38.
247. Mamedov K. P. Investn. of temp. f. in Al cr. Izvest. Akad. Nauk Azerb. SSR, 10, 139.
248. Manenc J. Diffusion anormale des r. X au cours de la precipitation dans un alliage à base de Ni contenant 7% de Si. Compt. rend., 243, 1119.
249. Meleka A. H. A. Etchpits a. dislocns. in Zn single crs. Phil. Mag., 1, 803.
250. Melsert H., Tiedema T. J. and Burgers W. G. X-ray study of allotropic modifns. of Ca met. Acta cryst., 9, 525.
251. Mengarelli E., and Weill A. R. Orientation des étoiles de phase γ dans les laitons β-γ. Compt. rend. 242, 254.
252. Menter J. W. Direct study by e. micr. of cr. lats. a. their imperfections. Proc. Roy. Soc., Ser. A236, 1109.
253. Menzel-Kopp C., and Menzel E. Zum Temp.-einfl. auf d. El.-beug. in Reflexion u. Durch-strahl. Z. Phys., 144, 538. Optik, 13, 382.
254. Michel P. Prépn. et étude par diffrn. é d'alliages mét. en couches minces. Ann. Phys., 1, 719.
255. Michell D. Release of stored energy a. changes in line shape during annealing of deformed Ni. Phil. Mag., 1, 584.

256. Mikheeva V. I., Babyan G. G., Phase diagram of syst. Mg–Cu–Ni, Doklady Akad. Nauk SSSR, 108, 1086.
257. Mikheeva V. I. and Babyan G. G., Chem. nature of ternary intermetallic phases in the Mg–Cu–Zn and Mg–Cu–Ni, Doklady Akad. Nauk SSSR, 108, 1086.
258. Mondolfo L. F., Gjostein N. A., and Levinson D. W. Str. changes during ageing in Al–Mg–Zn alloy. J. Metals, 8, 1378.
259. Moodie A. F. Contribution to anal. of effect observed on heating Au in air. II. Acta cryst., 9, 999.
260. Morris N. P., and Preston R. P. Str. trans. a. antiferromagnetism in alloy auMn. Proc. Phys. Soc. B69, 849.
261. Moskowitz D. New V-boride of compn V_3B_4. J. Metals, 8, 1325.
262. Mourgues L. de. Etude str. d'un fil de Pt par differn. X. Bull. soc. chim. France, 6, 868.
263. Mulford R. N. R., and Sturdy G. E. Pu–H syst. II. Solid soln. of H in Pu-dihydride J. Am. Chem. Soc., 78, 3897.
264. Newman R. C. Lat. sps. of thin electrodeposits of Co a. Ni on Cu single or. Proc. Phys. Soc., B69, 432.
265. Nielsen A. Investn. on promoted Fe catalysts for synth. of ammonia. Jul. Gjellerups Forlag, Copenhagen, 233.
266. Niemiec J., and Trzebiatowski W. Existence of sigma-a. ch-phases in Re-alloys. Bull. acad. polon. sci. III, 4, 601.
267. Nikolaeva S. M. and Umanskii Ya. S., Det. of char. temps. and lat. deformations in certain refractory met. compds and solid solns based on them, Izvest. Akad. Nauk SSSR, Ser. Fiz. 20, 631.
268. Nishigaki S. Age hardening of ternary Cu–Be–Ti alloys. I. Vibration of lat. const., quenched hardness a. tempered hardness in α-phase. J. Japan Inst. Metals (Sendai), 20, 55.
269. Nishyama Z., Shimizu K. On sub-bands in martensite plate J. Electronmicroscopy (Chiba) 4, 51.
270. Noskova N. N., Pavlov V. A., and Yunikov B. A. X-ray diffrn.investn.of deformations and bond strengths in cr. lat. of alloys of α-solid soln. of Al–Mg alloy, Fiz. Met. i Metalloved. 3, 557.
271. Nowak S. K. Solid solubility in Li in Al. J. Metals, 8, 553.
272. Nowotny H., Lux B., and Kudie Ika H. Verhalten metallreicher, hochschmelzender Silizide gegenüber Bor, Kohlenstoff, Stickstoff u. Sauerstoff. Mh. Chem., 87, 447.
273. Nowotny H., Searcy A. W., and Orr J. E. Strs. of some germanides of formula M_5Ge_3 J. Phys. Chem., 60, 677.
274. Okazaki A., and Hirakawa K. Str. study of Fe-selenides, $FeSe_x$. I. Ord. arrgt. of defects of Fe atoms. J. Phys. Soc. Japan, 11, 930.
275. Okazaki A., and Ueda I. Cr. str. of SnSe. J. Phys. Soc. Japan, 11, 470.
276. Ono K. Etude par diffrn. e. des surfaces des alliages Cu–Be et Cu–Mg polies électrolytiquement avec une remarque sur une surface spéciale pour l'émission d'électrons secondaire. J. Appl. Phys. Japan, 25, 120.
277. Ono K., Oda Z. Recherche sur la str. d'une pellicule de Ni evaporée, par la méthode de diffrn. é. J. Appl. Phys. Japan, 25, 164.
278. Ormont B. F., Possible formn of deuteride (hydride) met. strs. with retention of mols. or pairs of H atoms in lat. Kristallografiya, 1, 142.
279. Ormont B. F. and Smirnova V. I., Some requirements in modern x-ray phase anal. of systs. containing phases of variable compn. Zhur. Fiz. Khim. 30, 2588.
280. Ovsienko D. E. and Sosnina E. I., X-ray diffrn.detn.of block size in cast Al single crs. Fiz. Met. i Metalloved. 3, 516.
281. Ovsienko D. E. and Sosnina E. I. Influence of the growth rate of Al single crs. on their mosaic str. Fiz. Met. i Metalloved. 3, 374.
282. Papoular M. Accélérateur linéaire avec rassemblement préliminaire des électrons. Application à la diffrn. é. entre 0.5 et 1 MeV. Ann. Phys., 1, 914.
283. Parthe E. Strs a. str. relns. of refractory met. compds. Powder Met. Bull., 7, 138.
284. Patzak I. Über d. Str. u. d. Lage d. Phasen im Syst. Cu–Te. Z. Metallk., 47, 418.
285. Pauling L., and Pauling P. On valence a. at. size of Si, Ge, As, Sb a. Bi in alloys. Acta cryst., 9, 1036.
286. Peterson D. T., Kiljak P. F., and Vold C. L. Str. of Th–Mg intermet. compds. Acta cryst., 9, 127.
287. Pfefferkorn G. E .-mikr. Unterss. zum Nadelwachstum bei d. Korrosion v. Metall. oberflächen. Angew. Chem., 68, 224.
288. Pietrokowsky P, Frink E. P., and Duwez P. Investn. of partial constn. diagram Ti–Ti Au_2. J. Metals, 8, 930.
289. Pincherle L., and Radcliffe J. M. Semiconducting intermet. compds. Advances Phys. 5, 271.
290. Pines B. Ya. and Chaikovskii E. F., X-ray diffrn.detn.of heterodiffusion coefs. in alloys forming substitutional solid solns. Doklady Akad. Nauk SSSR, 111, 1234.
291. Pinsker Z. G. and Kaverin S. V., E. diffrn.detn.of Fe_4C str. Kristallografiya, 1, 66.

292. Pinsker Z. G. and Kaverin S. V. Mechanism of phys. transs. and nondiffusional transformations in nitriding of iron, Trudy In-ta Kristallogr. 12, 3.
293. Pinsker Z. G. and Khitrova V. I., Investn.of str. of some four-component Ti–Sb–As–Se alloys, Kristallografiya, 1, 300.
294. Pinsker Z. G., Orekhov O. S., and Miller A. I., E. diffrn.investn.of Bi and Sb alloys and some oxides of these elements, Kristallografiya, 1, 239.
295. Pinsker Z. G., Semiletov S. A., and Belova E. N. E. diffrn.detn.of the str. of $Ti_2Sb_2Se_4$ Doklady Akad. Nauk SSSR, 106, 1003.
296. Pivnik E. M. Formn.of σ-phase in high-alloys austenitic alloys, Fiz. Met. i Metalloved. 2, 531.
297. Polonis D. H., and Parr J. G. Orientation relnshs. between α -a. β-phases in Ti–Ni alloys. J. Metals, 8, 892.
298. Polonis D. H., and Parr J. G. Phase transformns. in Ti-rich alloys of Ni a. Ti. J. Metals, 8, 531.
299. Post B., Pipitz E., and Herz W. H. New ternary boride Cr_4NiB_2. Powder Met. Bull., 7, 65.
300. Prasad S. C., and Wooster W. A. Anomalous X-ray background from β-Sn. Acta cryst., 9, 35.
301. Prasad S. C., and Wooster W. A. Elasticity of single crs.of Pb. Acta cryst., 9, 38.
302. Rachinger W. A., and Collrell A. H. Slip in crs. of Cs-chloride type. Acta Met., 4, 109.
303. Raub E., and Plate W. Aushärt. u. Entmisch. d. Pt–Ir-Legierr. Z. Metallk., 47, 688.
304. Rausch. J. J., Crossley F. A., and Kessler H. D. Ti-rich corner of Ti–Al–V-syst. J. Metals, 8, 211.
305. Reynolds J. and Hume-Rothery W. Equilibrium diagram of syst. Cu–Ge. J. Inst. Met., 85, 119.
306. Rieck G. D. Fragmentation in W crs. Acta Met., 4, 47.
307. Roberts B. W. N.-diffrn. study of strs. a. magn. props. of Mn-bismuthide. Phys. Rev., 104, 607.
308. Roberts B. W. Strs. of BiMn by n. diffrn. Program a. Abstracts, A. C. A., French. Lick, Indiana, 23, G-1.
309. Roberts B. W., and Vineyard G. H. Short-range order coexisting with long-range order in Cu_3Au. J. Appl. Phys., 27, 203. Bull. Am. Phys. Soc., 1, 44.
310. Robinson W. H., and Smolwchouski R. Low-angle X-ray scatrg. by surface defects. J. Appl. Phys., 27, 657.
311. Rosi F. D. Kink-bands in Ge. Acta Met., 4, 26.
312. Rothstein J. Wrong bonds vs wrong atoms in Cu_3Au Bull. Am. Phys. Soc., 1, 147.
313. Ruchkina V. D. X-ray diffrn investn of dependence of str. of a Pd catalyst on conditions of electr. production and therm. treatment, Izvest. Akad. Nauk SSSR, Ser. Fiz., 20, 761.
314. Rüdiger O., and Knorr W. Zur Kerbschlagzähighk. d. Ti. Tech. Mitt. Krupp, 14, 136.
315. Rudman P. S., and Averbach B. L. Effect of cold work on local order. Acta Met., 4, 382.
316. Rumsh M. A., and Baklagina Yu. G., E. diffrn investn of texture of layers formed by evaporation in vacuum, Zhur. Tekhn. Fiz. 26, 1497.
317. Rumsh M. A. and Zimkina T. M., Mechanism of texture formn in layers condensed on neutral supports, Izvest. Akad. Nauk SSSR, Ser. Fiz., 20, 827.
318. Rumsh M. A. and Zimkina T. M., Textures of layers formed by vacuum evaporation on solid surfaces, Vestnik Leningr. Un-ta, 4, 33.
319. Runnalls O. J. C. Cr. strs. of some intermet. compds. of Pu. Can. J. Chem., 34, 133.
320. Russel R. B. Correction to crystallogr. angles for othorh. (α) U. J. Metals, 8, 1408.
321. Rymer T. B. E. diffrn examn. of thin films of Al a. Au prepared by vacuum evaporation. Proc. Roy. Soc. A, 235, 274.
322. Rymer T. B., Fayers F. I., and Hewitt S. J. Stacking faults in vacuum evapd. crs. of Cu a. Ag. Proc. Phys. Soc., B69, 1059.
323. Salkovitz E. I. Crystallogr. angles for Bi a. Sb. J. Metals, 8, 176.
324. Samsonov G. V., Some phys.-chem. props. of compds of trans refractory mets. with B and C, and chars. of their binary alloys, Izvest. Sektora Fiz.-Khim. Analiza, 27, 97.
325. Samsonov G. V. and Grodshtein A. V., Some props. of alkali and rare-earth met. hexaborides, Zhur. Fiz. Khim. 30, 379.
326. Samsonov G. V. and Latysheva V. P. Diffusion of B, C, and N into trans. mets. of grs. IV, V, and VI of the periodic syst. Dokaldy Akad. Nauk SSSR, 109, 582.
327. Samsonov G. V. and Latysheva V. P., Investn.of diffusion of B and C into certain mets. of the trans. grs. Fiz. Met. i Metalloved. 2, 309.
328. Samsonov G. V. and Markovskii L. Ya., Chem. of borides, Usp. Khimii, 25, 190.
329. Samsonov G. V., Neshpot V. S., and Lange L. V. Relnshs. in formation of binary alloys of Ti, Metallovedenie i Obrabotka Metallov, 1, 35.

330. Samsonov G. V. and Rozinova N. S., Some phys.-chem. props. of Zr–C alloys, Izvest. Sektora Fiz.-Khim. Analiza, 27, 126.
331. Samsonov G. V., Zhuravlev N. N., and Amnuél' I. G., Phys.-chem. Props. of B–C alloys, Fiz. Met. i Metalloved, 3, 309.
332. Samuels L. E. Solid solubilities of Sn, In a . Cd in Al. J. Inst. Met., 84, 333.
333. Sandler N. I. X-ray diffrn.study of lat. distortions in cold-rolled Fe and Al, Trudy Ukr. N.-I. In-ta Metallov, 2, 284.
334. Saulnier A. Study of Al–Mn alloys. Rev. mét. 53, 285.
335. Savitskii E. M., Terekhova V. F., and Kholopov A. V., Recrystzn.diagram of Cr, Doklady Akad. Nauk SSSR, 109, 794.
336. Schneider A., and Heyamer G. Temp.-abhängigk. d. Molvolum in d. Phasen NaTl u. LiCd. Z. anorg. Chem., 286, 118.
337. Schoening F. R. L. Fourier anal. of X-ray diffrn. profiles obtained from Ta filings. Acta Met., 4, 510.
338. Schubert K. Über d. Auftreten d. Kr.-strr. C1, C16, C2, C18 u. C6 bei Phasen d. Art TB_2. Z. Krist., 108, 276.
339. Schubert K. Über einige Beziehh. zwischen Kr.-strr. I. D. chem. Elemente. II. Strr. mit Kommensurabler Ortskorrelation d. Partner (Cu_2Mg, $CaCu_5$, $NaZn_{13}$ u. Verwandte). Z. Naturf., A, 11, 920, 999.
340. Sears G. W., and Coleman R. V. Growth mechanism of Zn whiskers a. platelets. Bull. Am. Phys. Soc., 1, 204.
341. Segmüller A. Texturunterss. an dünnen Zn- u. Ge-Schichten. Z. Krist., 107, 18.
342. Semiletov S. A., E. diffrn.investn.of str. of Ge films made by vacuum evaporation, Kristallografiya, 1, 542.
343. Semiletov S. A., E. diffrn.detn.of the str. of Sb_2Te_3, Kristallografiya, 1, 403.
344. Semiletov S. A., E. diffrn.investm.of thin layers of cadmium sulfide, selenide, and telluride, Kristallografiya, 1, 306.
345. Semiletov S. A. and Pinsker Z. G., E. diffrn.investn.of degree of perfection of Ge single crs. Kristallografiya, 1, 209.
346. Seybolt A. U., Hansen H., Roberts B. W., and Yurcisin P. Contribution to Bi–Mn systs. J. Metals, 8, 606.
347. Shih-Yuan S. Rate of ordg. at const. temp. of $AuCu_3$. Acta Met. Sinica, 1, 200.
348. Shull. C. G. Magn. spin correlations in Fe at high temp. Physik Verhandl., 7, 118.
349. Sidhou S. S., Heaton L., and Zauberis D. D. N. diffrn.studies of Hf–H a. Ti–H systs. Acta cryst., 9, 607.
350. Sidhou S. S., Heaton L., Zauberis D. D., and Campos F. P. N. diffrn. study of Ti–Zr syst. J. Appl. Phys., 27, 1040.
351. Silcock J. M. Double refl. in Al–Cu alloys. Acta cryst., 9, 86.
352. Silcock J. M., and Hal T. J. θ-str. of Al–Cu alloys. Acta cryst., 9, 680.
353. Smallman R. E., and Frost B. R. T. X-ray investn. of str. of liquid Hg a. liquid Hg–Tl alloys. Acta Met., 4, 611.
354. Smirnov A. A. and Stoyanov I. A., Effect of interstitial atoms on order in alloy, Fiz. Met. i Metalloved. 2, 524.
355. Smirnova V. I. and Ormont B. F., Homogeneity boundaries and dependence of thermodynamic and certain other props. of Ta carbide phases on their compn. and str. Zhur. Fiz. Khim. 30, 1327.
356. Smith J. F., Carlson O. N., and Vest R. W. Allotropic modifns. of Ca. J. Electrochem. Soc., 103, 409.
357. Sokolova M. A., Investn of the Ni–S syst. (from 30.0 to 50.0 at. % S) Zhur. Neorg. Khim. 1, 1440; Doklady Akad. Nauk SSSR, 106, 286.
358. Sosnina E. I. and Ovsienko D. E. Influence of small additions of Cu and Zn on mosaic str. of Al crs. Fiz. Met. i Metalloved. 3, 527.
359. Spedding F. H., Daane A. H., and Herrmann K. W. Cr. strs. a. lat. pars. of high-purity Sc, Yt a. rare earth mets. Acta cryst., 9, 559.
360. Spencer C. W. and Mack D. J. Decomposition of β-phase in Cu–Ga eutectoid alloy. J. Inst. Met., 54, 461.
361. Stangler F. Beobb. an Spitzen d. Cr–Ni-Stahls 18/8 im Feldel.-mikroskop. Z. Phys. 146, 496.
362. Staritzky E. Diberyllium carbide Be_2C. Anal. Chem., 28, 915.
363. Staritzky E., and Walker D. I. Li-hydride LiH a. Li-deuteride LiD. Anal. Chem., 28, 1055.
364. Steeg M. G. van der, and Vos K. J. de. Reversibility of coercive force in Alnico 5. J. Appl. Phys., 27, 1250.
365. Steeple H., and Edmunds I. G. Formn. of order in alloy $CdMg_3$. Acta cryst., 9, 934.
366. Straumanis M. E., and Weng C. C. Absorption a. refraction corrections a. lat. const. of Cr. Am. Mineralogist, 41, 437.

367. Sturdy G. E., Mulford R. N. R. Gd–H syst. J. Am. Chem. Soc., 78, 1083.
368. Sturkey L. E. diffrn. a. micr. study of surface str. of Cu single crs. J. Phys. Soc. Japan 11, 129.
369. Suzuki T., and Willis B. T. M. Diffrn. from dislocns. Nature, 177, 712.
370. Svechnikov V. N. and Lesnik A. G., Theory of polymorphism of Fe. Fiz. Met. i Metalloved. 3, 87.
371. Swalin R. A., and Geisler A. H. N. diffrn. study of annealing textures in drawn body-centered-cub. mets. J. Metals. 8, 1259.
372. Swanson H. E., Gilfrich N. T., and Cook M. I. Standard X-ray diffrn. powd. pats. VI Data for 44 inorg. substances. Nat. Bur. Standards (U. S.), Circ. 539 VI. (Data on Cr_3Si a. GaSb).
373. Takagi M. E. diffrn. study of str. of supercooled liquid Bi. J. Phys. Soc. Japan, 11, 396.
374. Takahashi N., and Trillat J. J. Formn. de monocr. de Cu_2O et ZnO par oxidation selective d'un film de laiton α prepare par evaporation sous vide. Acta Met., 4, 201.
375. Tatarinova L. I., E. diffrn. investn. of amorphous GaSe, Kristallografiya, 1, 534.
376. Tatarinova L. I., Auleitner Yu. K., and Pinsker Z. G., E. diffrn. investn. of GaSe, Kristallografiya, 1, 537.
377. Taylor A. Constn. of Ni-rich quarternary alloys of Ni–Cr–Ti–Al syst. J. Metals, 8, 1356.
378. Taylor J. L. Beta-phase pars. in syst. Ti–V–Mo. J. Metals, 8, 959.
379. Trillat J. J., Tertian Mme. L., and Terao N. Sur la transformn. du Ni cub. en Ni hex. Compt. rend., 243, 666.
380. Trumbore F. A. Solid solubilities a. electr props. of Sn in Ge single crs. J. Electrochem. Soc., 103, 597.
381. Trzebiatowski W., Weglowski S., and Zukaswewicz K. Struktur arsenkow cyrkonu. Roczn. Cehm., 30, 353.
382. Tsobkallo S. O., New x-ray cameras for investn of fine str. of polycr. materials, Zhur. Tekhn. Fiz. 26, 213.
383. Tsubokawa I. Magn. props. of Cr–Te–Se syst. J. Phys. Soc. Japan, 11, 662.
384. Tucker C. W. jr., Senio P., Thewlis J., and Steepls H. Joint note on β-U-str. Acta cryst., 9, 472.
385. Uchida E. Note on ferromagn. of CoTe. J. Phys. Soc. Japan, 11, 465.
386. Ueno M. Studies on ball-bearing steels. VI. X-ray detns. of retained austenite by integrated intensities. Tetsu to Hagane, 42, 257.
387. Umanskii Ya. S. and Samsonov G. V., Certain cr.-chem. chars. of trans. met. silicides, Zhur. Fiz. Khim. 30, 1526.
388. Vasenin F. I. and Konovalov P. F. Ionization x-ray str. investn. of Bi_2Te_3, Zhur. Tekhn. Fiz. 26, 1406.
389. Vaughan D. A. X-ray diffrn. study of nitrides of U. J. Metals, 8, 78.
390. Vaughan D. A., and Bridge J. R. High temp. X-ray diffrn. investn. of Zr–H syst. J. Metals, 8, 528.
391. Vereshchagin L. F. and Brandt I. V., X-ray str. investn of substances under pressures up to 30,000 atm. Doklady Akad. Nauk SSSR, 108, 423.
392. Viswanathan A. Influence de l'épaisseur de couches minces sur leur str.: cas de l'alliage Cu–Be. Compt. rend., 242, 1586.
393. Vul'f B. K., Classification of ternary met. phases, Fiz. Met. i Metalloved. 3, 97.
394. Waite T. R., Wallace W. E., and Carig R. S. Strs. a. phase relnshs. in Ta–H syst. between –145 a. 70° C. J. Chem. Phys., 24, 634.
395. Walker C. B. X-ray scatrg. a. therm. vibrations in Al. Bull. Am. Phys. Soc., 1, 138.
396. Walker C. B. X-ray study of lat. vibrations in Al. Phys. Rev, 103, 547.
397. Walker C. B. X-ray Compton scatrg. for Al. Phys. Rev., 103, 558.
398. Wang C. C., and Grant N. J. Transformn. of TiO phase. J. Metals, 8, 184.
399. Washburn J. Exptl obsns. concerning collapse of dislocn. loops during annealing. J. Metals, 8, 189.
400. Watanabe D. E. diffrn. pats. from oriented Ag films. J. Phys. Soc. Japan, 11, 740.
401. Watanabe D. E. diffrn. study of thin Al–Ag alloy films. J. Phys. Soc. Japan, 11, 1072.
402. Watanabe D., and Ogawa S. On superstr. of ord. alloy Cu_3Pd. I. E. diffrn. study. Phys. Soc. Japan, 11, 226.
403. Webb M., and Beeman W. W. Small angle X-ray scatrg. from cold-worked mets. Bull Am. Phys. Soc., 1, 138.
404. Wei C. T. Zone refl. camera for studying cr. imperfections by Schulz Technique Rev. Sci. Instrum., 27, 397.
405. Wei C. T., and Beck P. A. Str. of bent Zn crs. J. Appl. Phys., 27, 1508.
406. Weill A. R. Conference annuelle du chromdur. Remarques sur l'examen par diffrn. der r. X de revêtements electrolytiques de Cr sur acier. Rev. gén. mécan., 40, 308.
407 Weinberg A. F., Levinson D. W., and Rostoker W. Phase relns. in Mg–Li–Zn alloys. Trans. Am. Soc. Metals, 48, 855.

408. Weiss R. J., de Marco J. J., Weremchuk G., Corliss L., and Hastings J. Apparent anisotropic Debye-Waller f. in cubcrs. Acta cryst., 9, 42.
409. Weissmann S. Method for study of lat. inhomogeneities combining X-ray micr. a. diffrn. anal. J. Appl. Phys., 27, 79.
410. Werner F. E., Averbach B. L., and Cohen M. Matrix phase in lower bainite a. tempered martensite. J. Metals, 8, 1484.
411. Wernick J. H., and Davis H. M. Prepn. a. inspection of high purity Cu single crs. J. Appl Phys., 27, 149.
412. West D. R. F., and Thomas D. L. Constn. of Cu-rich alloys of Cu–Mn–Al syst. J. Inst. Met., 84, 109.
413. Weyerer H. Strukturunters. an flächenhaften Proben in e. kleinen Zylinderkamera. Z. angew. Phys., 8, 135.
414. Weyerer H. Präzisionsbest. v. Gitterkonstt. Z. angew. Phys., 8, 202, 297, 553.
415. Whapham A. D. Rotational slip in Zn single crs. J. Inst. Met., 84, 109.
416. Wilkinson M. K., and Shull C. G. N. diffrn-studies on Fe at high temps. Phys. Rev., 103, 516.
417. Williamson G. K., and Smallman R. E. Dislocn. densities in some annealed a. cold-worked mets. from measrts. on X-ray Debye-Scherrer spectrum. Phil. Mag., 1, 34.
418. Winkelmann A. El.-interferenz-Unterss. an ausscheidungsfähigen Legierr. in dünner Schicht. I. Syst. Al–Ag. II. Syst. Al–Cu. Z. Metallk., 47, 621, 627.
419. Wood E. A. Question of phase trans. in Si. J. Phys. Chem., 60, 508.
420. Wood E. A. and Matthias B. T. Cr. strs. of Nb_3Au a. V_3Au. Acta cryst., 9, 534.
421. Woolley J. C., Smith B. A., and Lees D. G. Solid soln. in GaSb–ZnSb syst. Proc. Phys. Soc., London, B69, 1339.
422. Yoshida S. E. diffrn. studies of ageing in Mg alloys. Program. a. Abstracts, A. C. A., French Lick, Inidana, p. 7.
423. Young E. W. jr. Spirals developed on single crs. of Cu by heating to high temps. in high vacuums. J. Appl. Phys., 27, 554.
424. Zachariasen W. H., and Elliner F. H. Str. of α-Pu. Program. a. Abstracts, A. C. A., French Lick, Indiana, 7.
425. Zakharova M. I. and Mogarycheva I. B. Investn. of eutectoid decomposition in Cu–Sn alloy, Izvest. Akad. Nauk SSSR, Ser. Fiz., 20, 621.
426. Zakharova M. I. and Soboleva I. N. Decomposition of a solid soln. in thin plates, Doklady Akad. Nauk SSSR, 108, 841.
427. Zalkin A., and Ramsey W. J. Intermet. compds. between Li a. Pb. I. Strs. of Li_3Pb a. Li_7Pb_2. J. Phys. Chem., 60, 234.
428. Zhirnov D. F., Lashko N. F., and Sorokina K. P., Nonisomorphous character of strs. in Fe alloys containing Mo and W, Zhur. Neorg. Khim. 1, 2588.
429. Zhuravlev N. N., Micr. and x-ray diffrn. investn. of Co–Sb all ys, Kristallografiya, 1, 506.
430. Zhuravlev N. N. X-ray diffrn. detn. of SiB_6 str. Kristallografiya, 1, 666.
431. Zhuravlev N. N. and Zhdanov G. S., Metallographic and x-ray diffrn. investn. of alloys in the Ge–Rh syst. Kristallografiya, 1, 205.
432. Zhuravlev N. N. and Zhdanov G. S., X-ray diffrn. investn. of compds. in the Bi–Rh and Bi–Pd systs. in relation to superconductivity studies, Izvest. Akad. Nauk SSSR, Ser. Fiz., 20, 708.
433. Zhuravlev N. N. and Zhdanov G. S. X-ray diffrn. investn. of the strs. of $CoSB_3$, $RhSb_3$, $IrSb_3$. Kristallografiya, 1, 509.
434. Zubenko V. V. and Umanskii M. M. X-ray diffrn. detn. of coef. of therm. expansion of polycr. substances in the −50 to +100° range, Kristallografiya, 1, 436.

All abbreviations of periodicals in the above bibliography are letter-by-letter transliterations of the abbreviations as given in the original Russian journal. *Some or all of this periodical literature may well be available in English translation.* A complete list of the cover-to-cover English translations appears at the back of this issue.

SIGNIFICANCE OF ABBREVIATIONS MOST FREQUENTLY ENCOUNTERED IN SOVIET PERIODICALS

FIAN	Phys. Inst. Acad. Sci. USSR.
GDI	Water Power Inst.
GITI	State Sci.-Tech. Press
GITTL	State Tech. and Theor. Lit. Press
GONTI	State United Sci.-Tech. Press
Gosenergoizdat	State Power Press
Goskhimizdat	State Chem. Press
GOST	All-Union State Standard
GTTI	State Tech. and Theor. Lit. Press
IL	Foreign Lit. Press
ISN (Izd. Sov. Nauk)	Soviet Science Press
Izd. AN SSSR	Acad. Sci. USSR Press
Izd. MGU	Moscow State Univ. Press
LEIIZhT	Leningrad Power Inst. of Railroad Engineering
LET	Leningrad Elec. Engr. School
LETI	Leningrad Electrotechnical Inst.
LETIIZhT	Leningrad Electrical Engineering Research Inst. of Railroad Engr.
Mashgiz	State Sci.-Tech. Press for Machine Construction Lit.
MEP	Ministry of Electrical Industry
MES	Ministry of Electrical Power Plants
MESEP	Ministry of Electrical Power Plants and the Electrical Industry
MGU	Moscow State Univ.
MKhTI	Moscow Inst. Chem. Tech.
MOPI	Moscow Regional Pedagogical Inst.
MSP	Ministry of Industrial Construction
NII ZVUKSZAPIOI	Scientific Research Inst. of Sound Recording
NIKFI	Sci. Inst. of Modern Motion Picture Photography
ONTI	United Sci.-Tech. Press
OTI	Division of Technical Information
OTN	Div. Tech. Sci.
Stroiizdat	Construction Press
TOE	Association of Power Engineers
TsKTI	Central Research Inst. for Boilers and Turbines
TsNIEL	Central Scientific Research Elec. Engr. Lab.
TsNIEL-MES	Central Scientific Research Elec. Engr. Lab.– Ministry of Electric Power Plants
TsVTI	Central Office of Economic Information
UF	Ural Branch
VIESKh	All-Union Inst. of Rural Elec. Power Stations
VNIIM	All-Union Scientific Research Inst. of Metrology
VNIIZhDT	All-Union Scientific Research Inst. of Railroad Engineering
VTI	All-Union Thermotech. Inst.
VZEI	All-Union Power Correspondence Inst.

Note: Abbreviations not on this list and not explained in the translation have been transliterated, no further information about their significance being available to us. – Publisher.

Soviet Journals Available in Cover-to-Cover Translation

ABBREVIATION	RUSSIAN TITLE	TITLE OF TRANSLATION	PUBLISHER	TRANSLATION BEGAN Vol.	Issue	Year
AÉ	Atomnaya énergiya	Soviet Journal of Atomic Energy	Consultants Bureau	1	1	1956
Akust. zh.	Akusticheskii zhurnal	Soviet Physics – Acoustics	American Institute of Physics	1	1	1955
	Antibiotiki	Antibiotics	Consultants Bureau	4	1	1959
Astr(on). zh(urn).	Astronomicheskii zhurnal	Soviet Astronomy–AJ	American Institute of Physics	34	1	1957
Avto(mat). svarka	Avtomaticheskaya svarka	Automatic Welding	British Welding Research Association (London)		1	1959
	Avtomatika i Telemekhanika	Automation and Remote Control	Instrument Society of America	27	1	1956
	Biofizika	Biophysics	National Institutes of Health*		1	1957
	Biokhimiya	Biochemistry	Consultants Bureau	21	1	1956
Byull. éksp(erim). biol. i med.	Byulleten' éksperimental'noi biologii i meditsiny	Bulletin of Experimental Biology and Medicine	Consultants Bureau	41	1	1959
DAN (SSSR) / Dokl(ady) AN SSSR	Doklady Akademii Nauk SSSR	The translation of this journal is published in sections, as follows:				
		Life Sciences: Doklady Biochemistry Section	American Institute of Biological Sciences	106	1	1956
		Life Sciences: Doklady Biological Sciences Sections (Includes: Anatomy, biophysics, cytology, ecology, embryology, endocrinology, evolutionary morphology, genetics, histology, hydrobiology microbiology, morphology, parasitology, physiology, zoology sections)	American Institute of Biological Sciences	112	1	1957
		Life Sciences: Doklady Botanical Sciences Sections (Includes: Botany, phytopathology, plant anatomy, plant ecology, plant embryology, plant physiology, plant morphology sections)	American Institute of Biological Sciences	112	1	1957
		Chemical Sciences: Proceedings of the Academy of Sciences of the USSR, Section: Chemical Technology	Consultants Bureau	106	1	1956
		Chemical Sciences: Proceedings of the Academy of Sciences of the USSR, Section: Chemistry	Consultants Bureau	106	1	1956
		Chemical Sciences: Proceedings of the Academy of Sciences of the USSR, Section: Physical Chemistry	Consultants Bureau	112	1	1957
		Earth Sciences: Doklady Earth Sciences Sections (Includes: Geochemistry, geology, geophysics, hydrogeology, mineralogy, paleontology, petrography, permafrost sections)	American Geological Institute	124	1	1959
		Earth Sciences: Proceedings of the Academy of Sciences of the USSR, Section: Geochemistry	Consultants Bureau	106-123	1 6	1957- 1958
		Earth Sciences: Proceedings of the Academy of Sciences of the USSR, Sections: Geology	Consultants Bureau	106-123	1 6	1957- 1958
		Mathematics: Doklady Soviet Mathematics	The American Mathematics Society	131	1	1961
		Physics: Soviet Physics–Doklady (Includes: Aerodynamics, astronomy, crystallography, cybernetics and control theory, electrical engineering, energetics, fluid mechanics, heat engineering, hydraulics, mathematical physics, mechanics, physics, technical physics, theory of elasticity sections)	American Institute of Physics	106	1	1956
		Physics: Proceedings of the Academy of Sciences of the USSR, Applied Physics Sections (does not include mathematical physics or physics sections)	Consultants Bureau	106-117	1	1956-1957
Derevoobrabat. prom-st'.	Derevoobrabatyvayushchaya promyshlennost'	Wood Processing Industry	Timber Development Association (London)		9	1959
	Élecktrosvyaz	Telecommunications	Massachusetts Institute of Technology*		1	1957
Éntom(ol). oboz(renie)	Éntomologicheskoe obozrenie	Entomological Review	American Institute of Biological Sciences	38	1	1959
Farmakol. (i) toksikol(ogiya)	Farmakologiya i toksikologiya	Pharmacology and Toxicology	Consultants Bureau	20	1	1957
FMM	Fizika metallov i metallovedenie	Physics of Metals and Metallography	Acta Metallurgica*	5	1	1957
Fiziol. zhurn. SSSR (im. Sechenova)	Fiziologicheskii zhurnal im. I. M. Sechenova	Sechenov Physiological Journal USSR	National Institutes of Health*		1	1957
Fiziol(ogiya) rast.	Fiziologiya rastenii	Plant Physiology	American Institute of Biological Sciences	4	1	1957
	Geokhimiya	Geochemistry	The Geochemical Society		1	1958
FTT	Fizika tverdogo tela	Soviet Physics–Solid State	American Institute of Physics	1	1	1959
Izmerit. tekh(nika)	Izmeritel'naya tekhnika	Measurement Techniques	Instrument Society of America		1	1959
Izv. AN SSSR, O(td). Kh(im). N(auk)	Izvestiya Akademii Nauk SSSR: Otdelenie khimicheskikh nauk	Bulletin of the Academy of Sciences of the USSR: Division of Chemical Sciences	Consultants Bureau		1	1952

continued

Izv. AN SSSR, O(td). T(ekhn). N(auk): Met(all). i top.	(see Met. i top.)				
Izv. AN SSSR Ser. fiz(ich).	Izvestiya Akademii Nauk SSSR: Seriya fizicheskaya	Bulletin of the Academy of Sciences of the USSR: Physical Series			
Izv. AN SSSR Ser. geofiz.	Izvestiya Akademii Nauk SSSR: Seriya geofizicheskaya	Bulletin (Izvestiya) of the Academy of Sciences USSR: Geophysics Series			
Izv. AN SSSR Ser. geol.	Izvestiya Akademii Nauk SSSR: Seriya geologicheskaya	Izvestiya of the Academy of Sciences of the USSR: Geologic Series			
Kauch. i rez.	Kauchuk i rezina	Soviet Rubber Technology	Columbia Technical Translations		1 1954
	Kinetika i kataliz	Kinetics and Catalysis	American Geophysical Union		1 1954
	Koks i khimiya	Coke and Chemistry USSR	American Geological Institute		1 1958
Kolloidn. zh(urn).	Kolloidnyi zhurnal	Colloid Journal	Research Association of British Rubber Manufacturers	18	1 1959
	Kristallografiya	Soviet Physics – Crystallography	Consultants Bureau	1	3 1960
Metalov. i term. obrabot. metal.	Metallovedenie i termicheskaya obrabotka metallov	Metal Science and Heat Treatment of Metals	Coal Tar Research Association (Leeds, England)		1 1958
	Metallurg	Metallurgist	Consultants Bureau	14	1 1952
Met. i top.	Metallurgiya i topliva	Russian Metallurgy and Fuels	American Institute of Physics	2	1 1957
Mikrobiol.	Mikrobiologiya	Microbiology			
OS	Optika i spektroskopiya	Optics and Spectroscopy	Acta Metallurgica	6	1 1958
	Pochvovedenie	Soviet Soil Science	Acta Metallurgica		1 1957
	Priborostroenie	Instrument Construction	Eagle Technical Publications		1 1960
Pribory i tekhn. éks(perimenta)	Pribory i tekhnika éksperimenta	Instruments and Experimental Techniques	American Institute of Biological Sciences	26	1 1957
Prikl. matem. i mekh.	Prikladnaya matematika i mekhanika	Applied Mathematics and Mechanics	American Institute of Physics		6 1959
			American Institute of Biological Sciences		1 1958
PTÉ	(see Pribory i tekhn. éks.)		British Scientific Instrument Research Association		1 1959
	Problemy Severa	Problems of the North	Instrument Society of America		1 1957
Radiotekh.	Radiotekhnika	Radio Engineering	American Society of Mechanical Engineers		1 1958
Radiotekh. i élektronika	Radiotekhnika i élektronika	Radio Engineering and Electronics			
	Stanki i instrument	Machines and Tooling	National Research Council of Canada		
	Stal'	Stal (In English)	Massachusetts Institute of Technology*	12	1 1957
Stek. i keram.	Steklo i keramika	Glass and Ceramics	Massachusetts Institute of Technology*	2	1 1957
Svaroch. proiz-vo	Svarochnoe proizvodstvo	Welding Production	Production Engineering Research Assoc.		1 1959
Teor. veroyat. i prim.	Teoriya veroyatnostei i ee primenenie	Theory of Probability and Its Applications	Iron and Steel Institute		1 1959
			Consultants Bureau	13	1 1956
Tsvet. Metally	Tsvetnye metally	Nonferrous Metals	British Welding Research Association		4 1959
UFN	Uspekhi fizicheskikh Nauk	Soviet Physics – Uspekhi (partial translation)	Society for Industrial and Applied Mathematics		1 1956
UKh	Uspekhi khimii	Russian Chemical Reviews	Primary Sources		1 1960
UMN	Uspekhi matematicheskikh nauk	Russian Mathematical Surveys	American Institute of Physics	66	1 1958
Usp. fiz. nauk	(see UFN)		The Chemical Society (London)		1 1960
Usp. khim(ii)	(see UKh)		London Mathematical Society	15	1 1960
Usp. matem. nauk	(see UMN)				
Usp. sovr. biol.	Uspekhi sovremennoi biologii		Oliver and Boyd		48 1959
Vest. mashinostroeniya	Vestnik mashinostroeniya	Russian Review of Biology	Production Engineering Research Assoc.		4 1959
Vop. gem. i per. krovi	Voprosy gematologii i perelivaniya krovi	Russian Engineering Journal			
		Problems of Hematology and Blood Transfusion	National Institutes of Health*		1 1957
Vop. onk.	Voprosy onkologii	Problems of Oncology	National Institutes of Health*		1 1957
Vop. virusol.	Voprosy virusologii	Problems of Virology	National Institutes of Health*		1 1957
Zav(odsk). lab(oratoriya)	Zavodskaya laboratoriya	Industrial Laboratory	Instrument Society of America	25	1 1959
ZhAKh Zh. anal(it). khimii	Zhurnal analiticheskoi khimii	Journal of Analytical Chemistry USSR	Consultants Bureau	7	1 1952
ZhETF Zh. éksperim. i teor. fiz.	Zhurnal éksperimental'noi i theoreticheskoi fiziki	Soviet Physics–JETP	American Institute of Physics	28	1 1955
ZhFKh Zh. fiz. khimii	Zhurnal fizicheskoi khimii	Russian Journal of Physical Chemistry	The Chemical Society (London)		7 1959
ZhMÉI Zh(urn). mikrobiol. épidemiol. i immunobiol.	Zhurnal mikrobiologii, épidemiologii i immunobiologii	Journal of Microbiology, Epidemiology and Immunobiology	National Institutes of Health*		1 1957
ZhNKh Zh(urn). neorgan(ich). khim(ii)	Zhurnal neorganicheskoi khimii	The Russian Journal of Inorganic Chemistry	The Chemical Society (London)		1 1959
ZhOKh Zh(urn). obshch(ei) khimii	Zhurnal obshchei khimii	Journal of General Chemistry USSR	Consultants Bureau	19	1 1949
ZhPKh Zh(urn). prikl. khimii	Zhurnal prikladnoi khimii	Journal of Applied Chemistry USSR	Consultants Bureau	23	1 1950
ZhSKh Zh(urn). strukt. khimii	Zhurnal strukturnoi khimii	Journal of Structural Chemistry	Consultants Bureau	1	1 1960
ZhTF Zh(urn). tekhn. fiz.	Zhurnal teknicheskoi fiziki	Soviet Physics–Technical Physics	American Institute of Physics	26	1 1956
Zh(urn). vyssh. nervn. deyat. (im. Pavlova)	Zhurnal vysshei nervnoi deyatel'nosti (im. I. P. Pavlova)	Pavlov Journal of Higher Nervous Activity	National Institutes of Health*		1 1958

*Sponsoring organization. Translation through 1960 issues is a publication of Pergamon Press.

Published by Consultants Bureau
for the Board of Governors of Acta Metallurgica
under a grant from the National Science Foundation

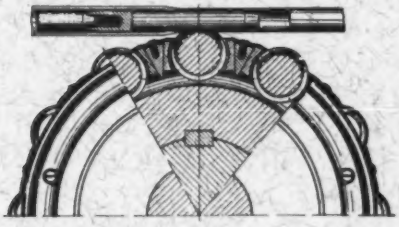

CONTEMPORARY PROBLEMS OF METALLURGY

Edited by A. M. Samarin

TRANSLATED FROM RUSSIAN

(Original published by the Academy of Sciences USSR Press)

CONTEMPORARY PROBLEMS OF METALLURGY was selected for translation into English by the Board of Governors of Acta Metallurgica since it offers Western scientists a comprehensive review of the most significant research and industrial applications in the field of metallurgy developed in the Soviet Union. This volume, in addition to detailing the recent Soviet developments in this field, contains two chapters which outline achievements in China and in East Germany.

Soviet advances in the production of steel and pig iron are discussed at length. Heat-resistant, austitic, and stainless steels have been subjected to a great deal of research in the USSR and data on various heat treatments and their effects on steel structures have been collected. These methods and the many others detailed in this book assure its value to all Western scientists and technologists concerned with metallurgical problems.

530 pages **$16.00**

CONSULTANTS BUREAU
ENTERPRISES, INC.
227 W. 17 ST., NEW YORK 11, N. Y.

МЕТАЛЛУРГИЯ ПОЛУПРОВОДНИКОВ

THE METALLURGY OF SEMICONDUCTORS

by Yu. M. Shashkov

Translated from Russian

(Original published by the State Scientific-Technical Press for Literature on Ferrous and Non-Ferrous Metallurgy, Moscow)

In this up-to-date survey of semiconductor metallurgy, the two main semiconductor materials – germanium and silicon – and their physical and chemical properties are discussed. A detailed review of chemical methods of purifying these elements is followed by a description of metallurgical methods of purification. Partition coefficients are given for many impurities and apparatus used in purification is surveyed.

Methods of growing single crystals are treated in an excellent chapter, with the method related to the type of defect to be expected in the finished crystal. Of particular interest is a discussion of alloying and doping.

The last section of the volume deals with heat treatment and diffusion of impurities, production of rectifiers and transistors, and methods of etching crystals and finished devices.

Technologists concerned with industrial processes of established value, as well as graduate students, will find this book of great value. The 293 references provide a good selective guide to the existing literature on the subject.

PARTIAL CONTENTS

Physicochemical, Electrical, and Optical Properties of Germanium and Silicon
Physicochemical Properties of Germanium and Silicon
Electrical Properties of Germanium and Silicon
Optical Properties of Germanium and Silicon
Chemical Methods of Purifying Germanium and Silicon
Production of Pure Germanium
Production of Pure Silicon
Acid Washing of Silicon
Reduction of Silicon Tetrachloride with Zinc (Beketov's Method)
Iodide Method of Producing Silicon
Silane Method of Producing Silicon
Trichlorosilane Method of Producing Silicon
Reduction of Silicon Tetrachloride with Hydrogen
Other Methods of Producing High-Purity Silicon
Metallurgical Methods of Purifying Germanium and Silicon
Zone Melting, Pulling, and Controlled Crystallization
Theory of Distribution of Impurities in Zone Melting, Pulling, and Controlled Crystallization
Distribution of Impurities in Zone Melting and Controlled Crystallization
Distribution of Impurities in Pulling and Controlled Crystallization
Distribution of Impurities in Zone Melting
Evaporation of Impurities During Fusion and Pulling Under Vacuum
The Partition Coefficient
Apparatus Used in Metallurgical Methods of Purifying Germanium and Silicon
Practical Details of Metallurgical Methods of Purifying Germanium and Silicon

208 pages **$9.50**

CONSULTANTS BUREAU ENTERPRISES, INC.
227 W. 17 ST., NEW YORK 11, N. Y.